IPP

Max-Planck-Institut
für Plasmaphysik

Annual Report 1997

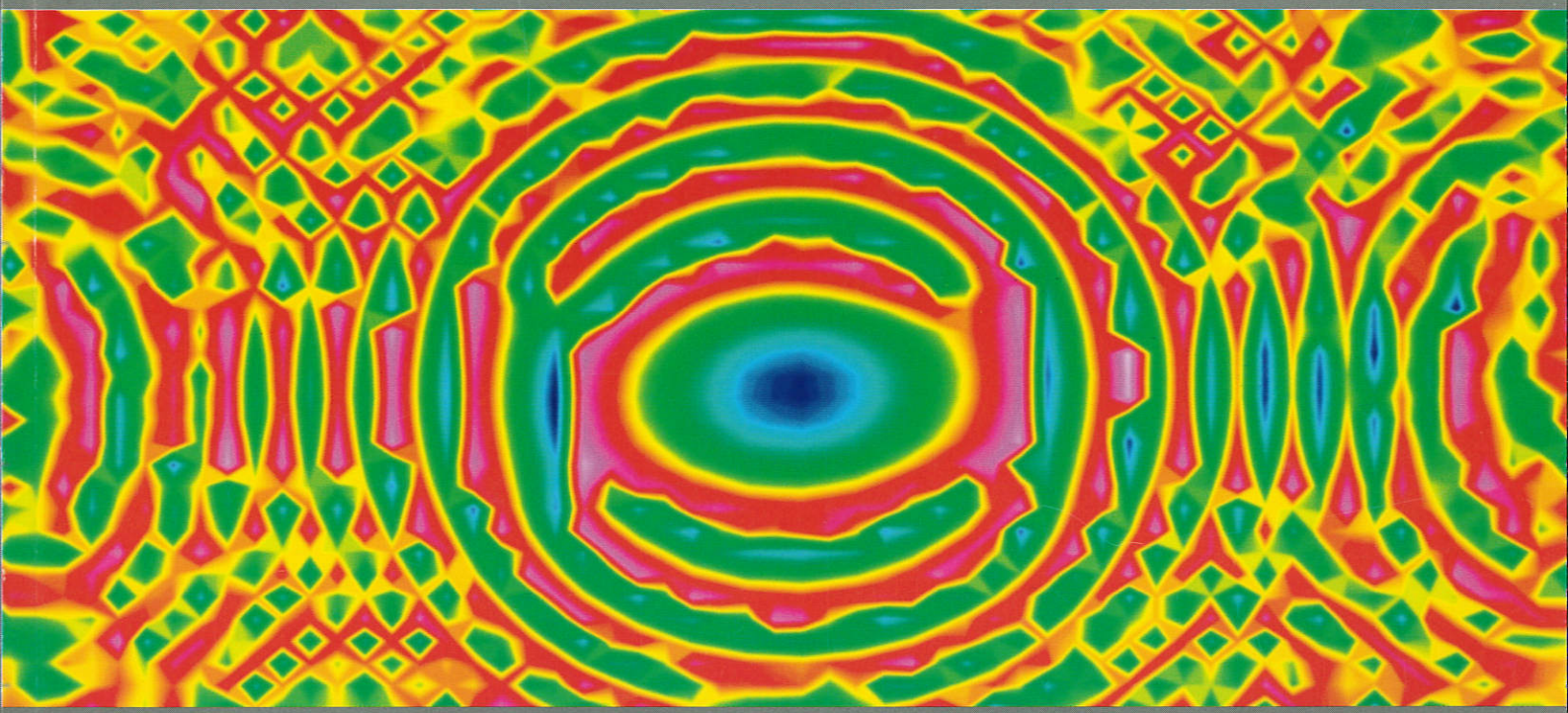

COVER ILLUSTRATION

Phase pattern of a non-imaging Winston cone flux collector originally used for measuring of the cosmic background microwave radiation (P. de Bernardis, M. de Petris, Universita di Roma). The properties of this antenna type are investigated to determine its suitability as a simple wideband antenna for radiometry of the electron cyclotron emission from the ITER plasma, which is being used to measure the electron temperature of the plasma (P. Buratti, M. Zerbini, ENEA Frascati and H. Hartfuss, IPP Garching; D. Wagner, IPF Stuttgart).

IPP Max-Planck-Institut für Plasmaphysik

EURATOM Association

Annual Report 1997

CONTENTS

PREFACE

Max-Planck-Institut für Plasmaphysik is investigating the two main types of fusion devices, the tokamak and the stellarator. The aim of the ASDEX Upgrade divertor tokamak is to realize a reactor-compatible divertor and study reactor-relevant plasma edge physics as well as particle and energy transport in the bulk plasma. Experiments are strongly focused on preparations for ITER: In 1997 the focal point of the ASDEX Upgrade activities was the installation and first operation of the new "closed" divertor, which is very similar to the proposed ITER divertor. First results show the divertor heat load to be clearly reduced in the new configuration. Installation of a second neutral particle injector doubled the available heating power for ASDEX Upgrade. The ratio of heating power to plasma radius, P_h/R_0, characterizing the reactor similarity is thus the highest among the European fusion devices and comes closer to the ITER value.

On the WENDELSTEIN 7-AS stellarator the plasma conditions leading to the development of the electron root observed last year - positive radial electric fields close to the plasma centre reducing the neoclassical electron heat transport and allowing electron temperatures of up to 4 keV - were examined in detail. Evidence was found that the transition is induced by locally trapped suprathermal electrons. Transport studies concentrated on clarifying and comparing various good confinement regimes. Preparation of the planned divertor experiments involved predictive two-dimensional plasma simulations and three-dimensional Monte Carlo calculations. The heating system of WENDELSTEIN 7-AS was further improved by installing a new 140 GHz gyrotron, extending the flexibility of the two existing ones. The advanced gyrotron is equipped with an energy recovery system leading to an energy efficiency of 50 per-cent, thus marking a milestone in the development of gyrotrons towards the needs of WENDELSTEIN 7-X. Also the ICRH system was technically improved, enabling the application of a second heating scenario on WENDELSTEIN 7-AS, second-harmonic heating of a neutral-beam heated hydrogen plasma.

The follow-up experiment for demonstrating the reactor relevance of the Advanced Stellarator principle, WENDELSTEIN 7-X, will be a 5-period Helias configuration with a helical divertor and a superconducting coil assembly. It is to be built in the new branch institute of IPP at Greifswald. Construction of the buildings was started at the beginning of 1997; by the end of the year the foundations of all buildings had been laid. Technical development concentrated on manufacture of a demonstration cryostat - which is now in its final stage - and a demonstration coil. For the original-sized superconducting demonstration coil the winding pack was finished, fully conforming to specification. Divertor elements developed for WENDELSTEIN 7-X were also successfully tested. An advanced conductor for the superconducting magnets has been made by industry and is now to be tested.

On the national level, IPP coordinates its research effort with Forschungszentrum Karlsruhe within the "Entwicklungsgemeinschaft Kernfusion" and also with Forschungszentrum Jülich. IPP also closely cooperates with a number of German universities, the collaboration with the University of Stuttgart being particularly intensive.

The research conducted at IPP is part of the European fusion programme: IPP is involved in JET, the joint European experiment. The ASDEX Upgrade tokamak and the alternative stellarator concept of the WENDELSTEIN experiments provide essential information for preparing the next steps in the overall European programme. Furthermore, IPP acts as host to NET, the European reactor study group, which has been working at Garching since 1983.

Coordination of research activities is also worldwide in extent. IPP is party to two Implementing Agreements: the one - with the USA - covering cooperation on the ASDEX Upgrade divertor tokamak; the other - with the USA, Japan, Australia and Russia - regulating cooperation in the joint stellarator programme, to which the WENDELSTEIN experiments make a major contribution. From 1988 IPP provided the technical site for the American-European-Japanese-Soviet group responsible for the conceptual design activities of ITER, the International Thermonuclear Experimental Reactor. After completion of the conceptual design, IPP was also chosen in 1992 - together with the fusion laboratories in Naka and San Diego - as site for the ITER Engineering Design Phase.

Klaus Pinkau

Projects

TOKAMAKS

A large part of the capacity at IPP is devoted to investigating confinement in the tokamak configuration. IPP pioneered the divertor principle with the ASDEX tokamak, which demonstrated the favourable impurity control capabilities of this configuration and discovered the so-called H-regime of improved energy confinement. The divertor configuration has also been adopted for ITER, and ASDEX Upgrade, IPP's successor experiment to ASDEX, closely resembles a scaled-down version of ITER.

As a consequence, experiments on ASDEX Upgrade are strongly focused on the critical R&D tasks for ITER. Originally, this implied mainly studies of divertor behaviour and control issues relating to its ITER-like configuration. With the enhancement and diversification of its heating and particle control systems and the extension of its diagnostic capabilities, ASDEX Upgrade is now also strongly contributing, however, to the basic understanding of magnetohydrodynamic instabilities and particle and energy transport in the bulk plasma. After detection of the strong correlation of the properties of the plasma edge and core this extension of the research to core physics has become even more important. In all areas the experimental work is accompanied by strong theoretical effort, with, in particular, IPP's divertor theory effort (carried out in close collaboration with KFA Jülich and New York University) also constituting the main modelling input to the ITER design. First-principle-based fluid turbulence studies for clarifying transport in the outer regions of the bulk plasma are a further area of excellence of IPP. MHD stability phenomena have become a further focal point of our theoretical efforts due to the increasing importance of high-β scenarios for ASDEX Upgrade and steady-state tokamak reactor operation.

During 1997, ASDEX Upgrade routinely operated with plasma currents between 0.8 and 1.2 MA. The NBI heating power capability P_H was extended from 10 MW to 20 MW by installing and commissioning a second injector box. With this heating power, the characteristic number P_H/R_0 is the highest in Europe and comes closer to the ITER value. ECRH was operated with heating powers of up to 1 MW and ICRH up to 4 MW. The available pellet centrifuge can reach injection velocities of up to 1200 m/s and injection rates of up to 80 pellets per second. Particularly successful was the operation with a high-field-side pellet injector system, which has achieved outstanding results. It was possible to obtain a stationary discharge with a density clearly beyond the Greenwald limit and good confinement.

The focal point of the ASDEX Upgrade activities in 1997 was the installation of and first operation with the new LYRA divertor. This divertor with its narrow "W" shape is very similar in its relative dimensions to the proposed ITER divertor. First results show a remarkable step forward in performance: the divertor heat load is clearly reduced compared with the previous open divertor under comparable conditions. The existing pumping system was augmented by the addition of powerful cryopumps, and the magnetic field power supplies were enhanced to allow better plasma shape control.

Outstanding physics results of ASDEX Upgrade in 1997 were:

- experimental proof of the requirements for the onset of neoclassical tearing modes: (i) β has to exceed a critical value, (ii) the collisionality has to be low enough, (iii) a seed island is needed, which is usually created by a sawtooth at ASDEX Upgrade;
- quantitative agreement for the growth time as well as the saturated island width between theoretical simulations and experimental results;
- identification of new MHD phenomena (cascades of high-n tearing modes, resistive interchange mode driven by locally inverted pressure profiles);
- detailed analysis of operation with the tungsten-covered divertor target plates; low-Z material seems to play an important role in reducing the core tungsten concentration;
- characterization of different edge operating conditions (L-mode, type-I and type-III ELMs) through measurement of the local edge parameters, in particular T_e and n_e; introduction of a now universally used parametric representation ("ASDEX Upgrade

diagram"), illuminating also the roles of the ballooning and density limit; this work was also accompanied by significant progress in clarifying the connection between core transport and edge behaviour;

- the facility for pellet injection from the high-field side was improved; it is now possible to inject pellets accelerated by a centrifuge from the high-field side; a controlled stationary discharge with continuous pellet injection reached good H-mode confinement at $\bar{n}$=1.2 n_{GW};
- The extended possiblity to control the currents in the poloidal field coil allows precise adjustment of the SOL inside the narrow divertor.
- Investigation of the energy balance in the new LYRA divertor showed a large fraction of divertor radiation in addition to the radiation in the main chamber. A detailed comparison with model calculations is under way.

ASDEX Upgrade maintains fruitful collaborations with the following institutions: Forschungszentrum Jülich; Inst. für Plasmaforschung, University of Stuttgart; University of Kiel; University of Magdeburg; University of Düsseldorf; University of Augsburg; Culham Lab., Abingdon, UK; Centro de Fusão Nuclear, Lisbon, Portugal; University College, Cork, Ireland; Inst. Allgemeine Physik, TU Vienna, Austria; NCSR Demokritos, Athens, Greece; IESL-FoRTH, Heraklion, Greece; CRPP, École Polytechnique, Lausanne, Switzerland; CEA Cadarache, France; Istituto di Fisica del Plasma, CNR Milano, Italy; CREATE Group, Naples, Italy; University of Strathclyde, Scotland; FOM-Inst. voor Plasmafysica, Rijnhuizen, Netherlands; VTT Energy, Helsinki, Finland; Research Inst. for Particle and Nuclear Physics, Budapest, Hungary; Inst. of Applied Physics, Nizhni Novgorod, Russia; I.V.Kurchatov Institute of Atomic Energy, Moscow, Russia; Ioffe Institute, St. Petersburg, Russia; Technical University of Applied Physics, St. Petersburg, Russia; Landau Institute, Moscow, Russia; St.P.T.U., St. Petersburg, Russia; PPPL, Princeton, USA; GA, San Diego, USA; MIT, Cambridge, USA; Oak Ridge National Lab., Oak Ridge, USA; Sandia Labs, Livermore and Albuquerque, USA; N.Y. University, Courant Institute, USA; University of Toronto, Canada; Institute for Plasma Research, BHAT, Gandhinagar, India; Institute of Plasma Physics, Hefei, China; Korea Basic Science Institute, Yusung, Korea.

Besides operating its own tokamak, ASDEX Upgrade, IPP has been involved in JET, the Joint European Torus at Culham (UK) for many years. IPP participates in the scientific exploitation of the JET experiment and gives advice and support for the design and operation of many JET plasma diagnostic systems. The cooperation with JET is organized within three Task Agreements. Especially Task Agreement No. 5, "Support of ITER Design Activities", has gained more and more importance during the last year, because it coordinates investigations on both tokamaks with the aim of discovering an optimized plasma discharge scenario for the next-step device, ITER. Within the frame of this Task Agreement there are regular informal meetings dealing with divertor and edge physics related questions as well as the interrelation of plasma edge conditions and global discharge behaviour.

In 1997 the experimental programme of JET concentrated on the preparation and execution of experiments where mixtures of deuterium and tritium were used as the plasma fuel. In contrast to the 11% tritium concentration used in each of the two discharges of the preliminary tritium experiment (PTE) of 1991, tritium concentrations of up to nearly 100% were used in the 1997 deuterium/tritium experiments (DTE1), allowing optimization of the plasma fuel mixture for maximum fusion power as well as enabling studies of isotope effects on plasma performance. The total amount of tritium on site was 20g compared with 0.2g in 1991. The DTE1 campaign was limited to a total number of $2.4 \cdot 10^{20}$ neutrons in order to restrict machine activation and the time ($\sim$1 year) during which manual intervention inside the machine is prevented. Results exceeded expectations. The highest fusion power was achieved in a hot-ion ELM-free H-mode discharge yielding 16.1 MW (>10 MW for 0.7) of fusion power and a ratio of $P_{fusion}/P_{absorbed}$ of 0.66 with a transient Q of 0.9. The fusion energy reached a value of 13.8 MJ. The DTE1 campaign at JET has produced a wealth of new and ITER-relevant data and has also proven to be a considerable technical success, with the machine, diagnostics, heating, and gas-handling system working at a very satisfactory level of reliability.

The results of JET, IPP and, in general, the world-wide tokamak programme formed the groundwork for planning an experimental reactor as a next step. The European Union, Japan, the USA and Russia have agreed to prepare this next step as a joint venture. The engineering design study (EDA) of this ITER experimental reactor is being carried out by a joint team of the four partners, working at three sites (San Diego/USA, Naka/Japan, Garching/EU). IPP has directed the major part of its experimental and theoretical effort to the scientific support of the ITER design. The results are fed into the system through three major channels: (i) direct participation of IPP scientists in the numerous expert meetings called together by ITER to deal with special subjects, (ii) handling of special tasks in support of NET/ITER, and (iii) participating in various NET/ITER committees. Important contributions included the analysis of the confinement data base and contributions to the development of a divertor model and to the design of diagnostic systems. In 1997 this work culminated in the compilation of the final design report (FDR) for submission to the ITER Council and the evaluation by the four partners early in 1998. With this report the ITER project has been brought to a status of technical preparation quite adequate for a construction decision, requiring essentially only further site-specific design efforts to become ready for construction.

ASDEX UPGRADE PROJECT

(Head of Project: Dr. Otto Gruber)

Experimental Plasma Physics Division E1: M. Alexander, Ch. Aubanel, K. Behler, M. Bessenrodt-Weberpals, H. Blank, H. deBlank, H.-S. Bosch, R. Brückner, B. Brüsehaber, E. Buchelt, A. Buhler, Ch. Dorn, R. Drube, J. Ernesti, U. Fahrbach, P. Franzen, J.C. Fuchs, O. Gehre, J. Gernhardt, O. Gruber, E. Gubanka, A. Gude, G. Haas, Th. Härtl, G. Herppich, W. Herrmann, M. Hoek, H. Hohenöcker, H. Hupfloher, D. Jacobi, E. Kaplan, Th. Kass, M. Kaufmann, G. Klement, G. Kölbl, H. Kollotzek, P. Krüger, B. Kurzan, P.T. Lang, R.S. Lang, A. Lorenz, H. Maier, M. Maraschek, F. Mast, K. Mattes, D. Meisel, R. Merkel, V. Mertens, H.W. Müller, M. Münch, H. Murmann, G. Neu, Ch. Niemann, E. Oberlander, M. Pflug, G. Raupp, G. Reichert, H. Röhr, V. Rohde, H.-B. Schilling, D. Schleußner, H. Schneider, G. Schramm, G. Schrembs, S. Schweizer, U. Seidel, S. Sesnic, Ch. Sihler, M. Sokoll, K.-H. Steuer, A. Stimmelmayer, J. Stober, B. Streibl, W. Suttrop, W. Treutterer, M. Troppmann, M. Ulrich, W. Ullrich, G. Weber, R. Wolf, D. Zasche, Th. Zehetbauer, G. Zimmermann,

Guests in Division E1: S.M. Egorov, I. Miroshnikov, Technical University, Plasma Physics Department, St. Petersburg, CIS;
G. Serebrianyj, IOFFE Technical Institute, St. Petersburg, CIS
L. Hu, Academia Sinica, Hefei, China
M. Warrier, Institute for Plasma Physics, Gandhinagar, Indien
Q. Yu, Academia Sinica, Hefei, China

Tokamak Physics Division: G. Becker, A. Bergmann, K. Borrass, M. Brambilla, K. Büchl, A. Carlson, D. Coster, O. Gruber, S. Günter, O. Kardaun, K. Lackner, P. Martin, J. Neuhauser, G. Pautasso, A.G. Peeters, G. Pereverzev, K. Reinmüller, W. Sandmann, R. Schneider, W. Schneider, J. Schweinzer, B. Scott, M. Weinlich, R. Wunderlich, H.-P. Zehrfeld

Guests in Tokamak Physics Division: B. Braams, New York University, N.Y., USA;
G. Petravich, S. Kalvin, G. Veres, KFKI, Budapest, Hungary;
I. Veselova, V. Rozhansky, A. Ushakov, LPI, St. Petersburg, CIS;
P. Lalousis, IESL.Forth, Heraklion, Greece
S. Khirwadkar, IPP, Gandhinagar, Indien
R. Brandenburg, IAP, Wien

Technology Division: W. Becker, R. Beckmann, F. Braun, H. Brinkschulte, H. Faugel, R. Fritsch, D. Hartmann, B. Heinemann, F. Hofmeister, W. Kraus, F. Leuterer, F. Monaco, M. Münich, J.-M. Noterdaeme, S. Obermayer, F. Probst, S. Puri, R. Riedl, F. Ryter, W. Schärich, E. Speth, A. Stäbler, O. Vollmer, F. Wesner, R. Wilhelm, K. Wittenbecher

Experimental Plasma Physics Division E4: K. Asmussen, A. Bard, K. Behringer, S. de Peña Hempel, R. Dux, W. Engelhardt, J. Fink, A. Geier, F. Huber, A. Kallenbach, T. Madeira, H. Meister, B. Napiontek, R. Neu, H. Salzmann, D. Schlögl, K. Schmidtmann, A. Thoma

Berlin Division: G. Fussmann, A. Herrmann, H. Kastelewicz, M. Laux, E. Pasch, U. Wenzel

Computer Science Division:G. Gzapski, H. Friedrich, P. Heimann, F. Hertweck, J. Maier, M. Pacco-Düchs, U. Schneider-Maxon, C. Tichmann, R. Tisma, M. Zilker, H. Richter

Surface Physics Division: R. Behrisch, E. Berger, V. Dose, K. Krieger, J. Roth, G. Venus, H. Verbeek

Stellarator Division: H. Greuner

Central Technical Services:S. Kötterl, R. Goihl, F. Gresser, D. Grois, S. Kamm, M. Kluger, H. Kosniowski, H.-J. Kutsch, R. Kutzner, H. Lohnert, W. Melkus, S.B. Mukherjee, J. Perchermeier, R. Zickert, H. Eixenberger, J. Simon-Weidner

University of Cork, Ireland: P. McCarthy H. Callaghan

IPF University of Stuttgart: G. Dodel, W. Förster, J. Gafert, G. Gantenbein, K. Hirsch, E. Holzhauer, W. Jentschke, P.G. Schüller, K. Schmidtmann, U. Schumacher, H. Zohm

IPP Kernforschungszentrum Jülich: H. Euringer, J. Linke, M. Sauer, M. Scherer, R. Uhlemann

Centro de Fusão Nuclear, Lisbon, Portugal: E.-M. Manso, L. Meneses, I. Nunes, L. Cupido, J. Santos, F. Serra, A. Silva, P. Varela, S. Vergamota

NCSR Demokritos, Athens, Greece: N. Tsois, G. Kyriakakis, M. Markoulaki, P. Theodoropoulos, N. Xantopoulos

TEKES (HUT and VTT), Finland: J.A. Heikkinen, T. Kiviniemi, T. Kurki-Suonio

University of Augsburg: U. Fantz

1. OVERVIEW

The experimental program of the non-circular Tokamak ASDEX Upgrade was and still is focused to a large extent on edge and divertor physics in high power, high confinement regimes, with the aim to identify and optimise ways for safe power exhaust and particle control for next generation divertor tokamaks. During the last year the focal point in the ASDEX Upgrade program was progressively shifted towards core physics, confinement and performance related questions and especially the edge-core interplay, where ASDEX Upgrade has already done pioneering work. The introduced edge operational diagram characterises different edge operating conditions for L- and H-mode in connection with the ballooning and density limits. MHD stability and limits and the avoidance and mitigation of disruptions are further main items.

Thereby the similarity to ITER in plasma shape, in relative distance of the plasma to poloidal field coils and in the divertor and performance studies, makes ASDEX Upgrade particularly suited to test control strategies for shape, plasma performance (including profile control) and mode stabilisation. Additionally, the similarity in cross-section with the European divertor tokamaks, Compass-D and JET, and the US devices, Alcator C-MOD and DIII-D, is important to determine size scalings for core and edge physics. This collaborative work including the extrapolation to ITER parameters has continued.

The physics program of 1997 was based on the results of the last years with the DV-I and the ITER requirements. Four months of successful operation with the DV-II allowed comparisons with the previous DV-I configuration (Section II). Emphasis was placed on issues which, according to common knowledge, should be related to edge/divertor geometry, in particular upper density limits in H- and L-mode with gas-puffing and pellet injection from the high field side, H-mode characteristics, particle control and impurity behaviour. Besides the relevance for ITER, these informations are also important for the divertor programme of JET. In conclusion, after an initial conditioning and learning phase, the experiments with DV-II have reached machine performance in terms of confinement quality and operational limits comparable to the DV-I phase. Thereby the maximum heating power was increased to 14 MW (compared to <12 MW before), while an enhanced divertor radiation fraction (<40% of the heating power) leads still to reduced heat flux to the target plates below 4 MW/m^2.

Finally, the ASDEX Upgrade program is imbedded in a framework of national (IPF Stuttgart, University of Augsburg, see also Section University contributions to IPP program) and international collaborations (see Section International Cooperation) including mainly support of diagnostic and theoretical developments.

1.1 Operation and Technical Systems

In the divertor physics program, the DV-II phase with the LYRA version (including a roof baffle), which is rather similar to the present ITER reference design, started in June this year. The installation of this new divertor hardware and the new cryo-pump was finished in April 97. Thereby the time delay compared with the proposed end at the beginning of the work (August 96) was just one week. But the beginning of the plasma experiments with the new divertor was delayed by nearly two months due to problems with new control systems for the power generators and thyristor bridges. These power supply circuits had been updated due to the enhanced demands of DV-II geometry for precise adjustment of the SOL inside the narrow divertor slits. This refined control of the plasma shape and the strike points -despite being aggravated by the very distant poloidal field coils - was successfully demonstrated. The divertor diagnostics were adapted to a large extent to the new geometry and additional new diagnostics (like the motional Stark effect spectroscopy for measuring the current density) in the divertor and main chamber have also been installed.

In the shut down period from mid August to end October, the second neutral beam injector (see Section 6) and connected vessel installations were finally mounted allowing now heating powers P_h up to 20 MW with deuterium injection. The equivalent lower level of 14 MW with hydrogen injection was already used for heating ASDEX Upgrade plasmas. With 20 MW heating power the power density in ASDEX Upgrade is the highest world-wide and the characteristic number P_h/R_0 is only a factor three below the ITER value.

The ICRH system was fully equipped with 3 db couplers for a better coupling to the plasma, which should allow the use of the full installed ICRH power. The upgrading of the ECRH system to 2 MW is somewhat delayed due to problems with the gyratrons. Presently 2 gyratrons with 0.4 MW each and 2 s pulse length are running. This might be just enough for feedback stabilisation of neo-classical MHD modes limiting β.

The pumping system with 14 turbomolecular pumps was improved by the addition of the much more powerful cryopump, which was successfully tested at LHe temperature, but not used in plasma experiments up to now.

The routine operation with the new divertor was restricted to plasma currents between 0.6 and 1.2 MA with toroidal fields up to 3 T. Flexible use of the auxiliary heating power was provided by the availability of the three different heating methods.

1.2 Summary of the Main Results

The following evident conclusions can be drawn from the comparison between the more closed DV-II and the more open DV-I configurations (Section II). No major changes occurred in the typical high power density ramp-up scenarios including similar values for the upper density limits in H-mode and the ultimate L-mode density limit. But, as expected, the divertor neutral density is higher in the more closed DV-II. This observed invariance of the density limit is in agreement with B2-Eirene modelling calculations. Also in agreement with these simulations a strong improvement of the helium pumping capability has been reached achieving a ratio $\tau^*(He)/\tau_E \approx 4$ at limited pumping. A small increase in the L-H transition power threshold was observed. This needs further consideration especially

of the decisive power flux across the separatrix which couldn't be determined reliably enough. Typical CDH scenarios were reestablished using Neon puffing, but no evidence for enhanced divertor radiation has been observed using nitrogen puffing in DV-II. The confinement times in discharges without strong core MHD activity have remained virtually unchanged.

One very important observation in the DV II geometry is a strongly reduced power flux density to the surrounding structures both during ELM and ELM-free phases. The origin of this reduction by about a factor of three compared with DV I is presumably a larger fraction of divertor radiation in addition to the main chamber radiation. A detailed comparison with B2-Eirene simulations is underway to clarify the influence of hydrogen and impurity radiation. The observed fact might have strong influence on future divertor designs.

Additionally remarkable results have been achieved in the characterisation of the L-H transition in terms of local edge parameters, in the power dependence of the temperature profile and for stationary H-mode discharges at a density 20% above the Greenwald density and at a high confinement level using pellet refuelling from the high field side (Section III).

Changes have been observed in the central MHD behaviour (sawteeth, fishbones) influencing the neo-classical MHD modes at high β_N by the creation of seed islands. At low plasma densities and therefore reduced collisionality not only m=3, n=2 neo-classical modes occur as observed previously, but also m=2, n=1 start to limit β. The measured saturated island widths agree with the theoretical MHD calculations. New MHD phenomena were observed as resistive interchange modes with centrally inverted pressure profiles and cascades of high-n tearing modes in flat shear regions (Section 4).

The experiments of the final DV-I phase in 1996 with tungsten-clad target tiles in the inner and outer strike point regions were finally analysed (Section 5). As reported last year no deleterious effects from tungsten were found; even in high power operating conditions only tolerable core tungsten concentrations occurred. This is partly explained by a neo-classical outward drift of tungsten caused by low-Z impurities. By post-mortem analyses new results are obtained on the long-term migration of tungsten, the coating of the tungsten tiles with low Z materials and their deuterium inventory.

1.3 ASDEX-Upgrade Progamme in 1998

Next year the DV-II will be investigated with only minor modifications (e.g. baffle length) using additional diagnostics and extended explorations in parameter space (1.4 MA plasma currents, 20 MW heating power). Core physics studies will continue with the investigation of plasma performance (energy and particle transport, MHD-instabilities and their stabilisation using ECRH and ECCD). Regarding energy transport the relation between core and edge and their reciprocal influences, profile resilience, transport barrier physics, dimensionless scalings (mainly in connection with JET) and heat wave studies are envisaged. The studies on MHD modes like the neoclassical tearing modes close to the β-limit or transport induced toroidal Alfvén waves will be continued. Particle transport and density limit remain a substantial part of our effort, including the promising refuelling by pellet injection from the high field side.

Additionally scenarios and physics of advanced tokamak plasma concepts leading to stationary operation and enhanced performance will be investigated. These 'advanced tokamak' concepts are characterised by a high fraction of bootstrap current and external current drive. The compatibility of these new ideas with stationary operation at high power and, simultaneously, cold divertor should be one of the key elements of the ASDEX Upgrade program. To achieve high confinement and plasma pressures stationary flat or reversed shear profiles with $q_0>1$ are needed which can be produced with early heating during current ramp-up and require an off-axis current drive capability for sustainment. This can be achieved in a flexible way by mode conversion CD (available at the end of 1998 with our ICRH system) and NBCD using tangential injection (preferential support for turning one of the existing injectors will be applied for in 1998). NBCD with the existing nearly perpendicular beams, ECCD and fast wave CD can provide central CD to maintain a seed current. To get stationarity on the transport and MHD time scales and to approach the skin time a flattop time of 10 s should be sufficient for 1 MA plasma current and an additional heating of 20 MW. Present flattop times of 4-5 s are feasible but longer pulses require a reactive power compensation for the generator EZ3 (preferential support will be applied for in 1998, see Section 7).

Both for conventional (higher confinement) and advanced scenarios (higher β s) plasma shapes with higher triangularities up to 0.5 are advantageous . They can be run already in the DV-II with the outer strike point on the roof baffle, but this requires a modification of the ICRH antennae in summer next year. In these configurations plasma currents up to 1 MA are possible according to poloidal field and power supply capabilities.

This programmatic evolution has been mainly carried out by the IPP tokamak study group, which has also looked for the IPP interests and contributions to ITER and a possible role of a complementary experiment.

In the following Sections 2 - 6 the topics LYRA DV-II, transport and H-mode studies, MHD stability, tungsten DV-I and neutral beam injection are presented. In Section 7 the ASDEX Upgrade technical systems, preparation of long pulse operation, control, data processing and wave heating systems are described. Section 8 deals with additional results concerning the plasma core, while Section 9 is particularly devoted to the edge operating conditions. The progress in diagnostic development and adaptation to the DV-II is given in Section 10.

2. THE LYRA DIVERTOR

2.1 Status and Effect on Global Plasma Performance

Construction of the new LYRA divertor (DV-II), including a number of new or modified divertor diagnostics, was completed

in spring 1997. The LYRA design, characterized by inward inclined target plates, a dome baffle in the private flux region and strong baffling towards the main chamber (Fig. 2.1), was the result of extensive numerical studies with the B2-EIRENE edge simulation code. Besides the beneficial effects for the ASDEX Upgrade performance, the LYRA divertor activity is a key element of the voluntary ITER R&D programme at IPP.

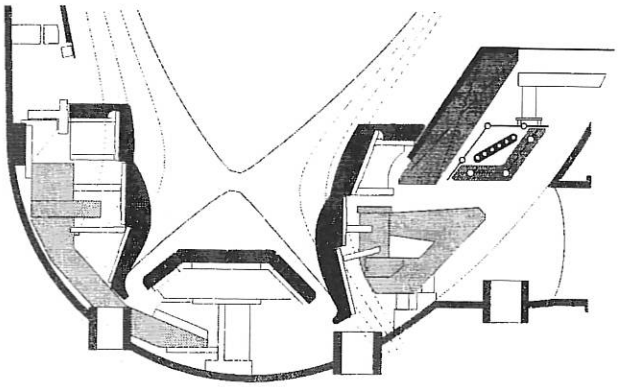

FIG. 2.1: Poloidal cross-section of the LYRA divertor.

Preliminary data analysis and comparison with the previous divertor shows that overall there is no dramatic influence of the detailed divertor configuration on the global plasma performance and operational limits. In fact, essentially the same global density limit is obtained with the old and new divertors. Also, the H-mode power threshold is the same for DV-I and DV-II within the experimental uncertainties (for details see Sections 3 and 8, resp.). On the other hand, there are significant differences with respect to the detailed divertor behaviour and power handling capability, as expected. A selection of preliminary results is given in the following.

2.2 Density Limit in DV-I and DV-II

Ohmic, L- and H-mode density limits were explored with the LYRA divertor to reveal advantageous or disadvantageous influences of the closed new divertor geometry on the density operational window. It was found that the same density limits and heating power dependences are obtained with the LYRA divertor as with DV-I. Furthermore, the same basic physical phenomena (e.g. Marfe evolution) are observed. The Greenwald limit can be reached or slightly exceeded with gas puffing. An overview of the first density scans is shown in Fig. 2.2. Data of discharges in H^+ and in D^+ are shown. The solid curves represent the behaviour of the corresponding scans in DV-I. The L-mode density limit is clearly sensitive to the quality of the wall boronization state, but rather insensitive to the location of the gas puff (main chamber vs. divertor). The reduction of the hydrogen density limit data (triangles) in relation to the DV-I data (dashed curve) reflects such an old boronization state. In DV-I the H^+ scan is performed with a fresh boronization. Divertor detachment starts at comparable $\overline{n}_e$. Also the edge density behaviour represented by $n_e^{sep}, n_e^{sep}/\overline{n}_e, \overline{n}_e^{SOL}$ (line-averaged SOL density in the midplane) and λ_e^{SOL} (SOL density profile decay length) is similar. The maximum divertor neutral particle pressure immediately before the disruption seems to be significantly higher with LYRA. Moreover, a significant increase of $\overline{n}_e$ beyond the Greenwald limit was again obtained with pellet injection (see Sect. 8.4).

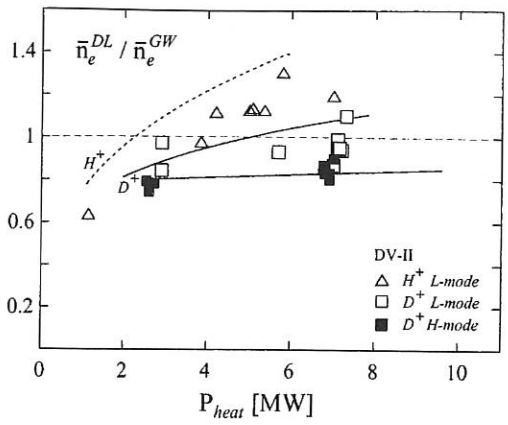

FIG. 2.2: Comparison of the global density limit in DV-I (curves) and DV-II (data points) . The significant reduction of the H^+ L-mode densities in DV-II compared to the dashed curve representing DV-I is caused by an old boronization.

2.3 Particle Balance and Impurity Behaviour

2.3.1 Hydrogen neutral gas and intrinsic impurities

No dramatic change in the core plasma impurity composition is observed when DV-I and II are compared. Carbon is the dominant impurity, followed by boron, fluorine and oxygen. Low-field-side limiter erosion in the main chamber by beam ions is, under some conditions, an effective source for the core carbon inventory. The actual contribution to the plasma carbon inventory depends sensitively on the density, plasma position, shape and choice of NBI sources.

Noteworthy was the very long conditioning time of the machine in terms of the H/D ratio. A possible reason may be water from the new CFC tiles, which were not baked before installation. The hydrogen content at the end of the deuterium campaign was still about 20% (in a state of aged boronization). Fresh boronization leads only to temporary reduction of the hydrogen content.

The distribution of the neutral gas in the divertor region is substantially changed. Whereas in DV-I the neutral flux density outside the outer strike zone was usually larger than in the private flux region, except under low-recycling conditions, it is now always higher in the private flux region. The neutral flux there also rises more steeply with increasing main plasma density .

2.3.2 Pumping of noble gases

As in DV-I, the divertor compression and pumping of noble gases exhibit a pronounced increase with the neutral deuterium flux density in the divertor. The most evident difference to DV-I is the considerable improvement of helium pumping for H-mode conditions with moderate or high neutral flux levels. Helium removal 1/e times as short as 0.2 s have been measured

for H-mode conditions with high neutral flux level, pointing to very long neutral helium retention times in the divertor. The corresponding value of τ_{HE}^{*}/τ_E is about 4.

Figure 2.3 compares for the two configurations the global helium recycling flux after a short helium puff during ELMy H-mode. The faster decay rate with DV-II points to a much longer ($\sim$ factor 4) effective helium retention time, on the basis of a simple particle balance analysis. Preliminary analysis of neon pumping reveals a moderate degradation of the pumping time: while in DV-I neon pumping was more efficient than helium pumping under most conditions, the opposite is the case in DV-II.

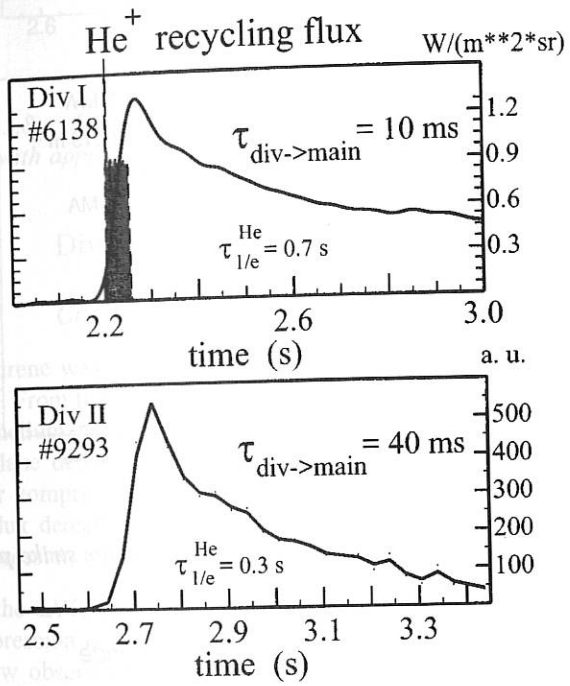

FIG. 2.3: Comparison of the global helium recycling flux after a short helium puff during ELMy H-mode. The faster decay rate with DV-II points to a much longer (factor 4) effective helium retention time.

2.3.3 Impurity seeding and divertor detachment

The typical CDH-mode scenario (characterized by type-III ELMs, divertor detachment, electron density profile peaking in conjunction with moderate confinement improvement and final loss of sawtooth activity, reduction of central transport) was achieved in DV-II by neon injection (so far only in feed-forward mode) and feedback control of the divertor hydrogen neutral flux at intermediate levels (Fig. 2.4 shows time traces for a case without pronounced peaking, but with continuing sawtooth activity).

A strong reduction of CIII emission in the outer divertor indicates detachment in the lower part of the divertor (Fig. 2.5) due to the neon puff. The inner divertor is detached even without impurity seeding, which is typical of DV-II except for low-density cases. No evidence of enhanced divertor radiation compared with DV-I has been observed so far in the LYRA divertor, using nitrogen puffing at 4 toroidally distributed divertor positions. As in DV-I, nitrogen appears in the main chamber, and again detachment seems to be caused primarily by main chamber radiation. However, analysis of the total divertor radiation distribution was not yet possible in 1997.

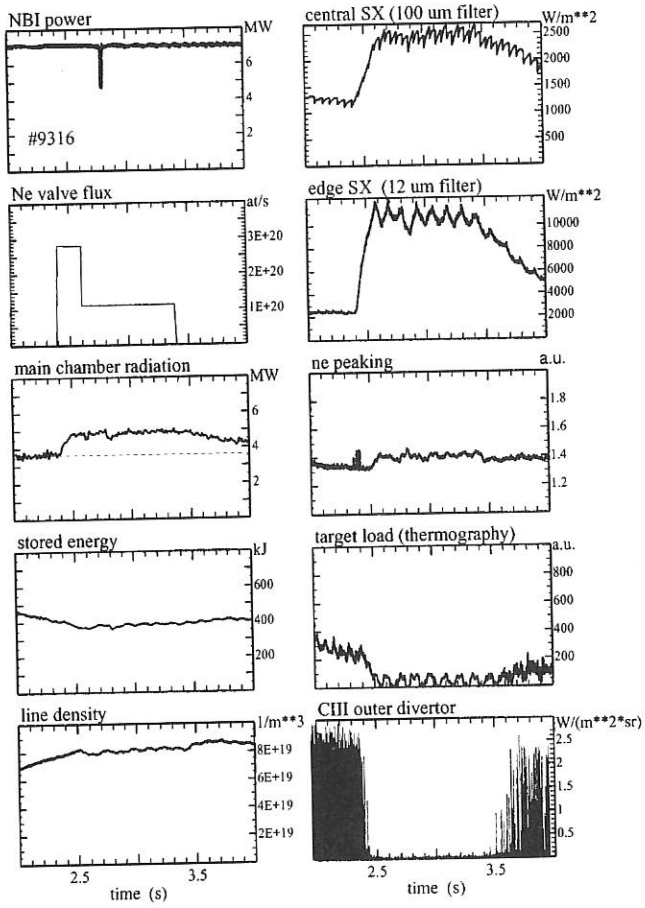

FIG. 2.4: Time traces of a CDH-mode discharge without density peaking. Sawteeth are preserved, central particle transport is fast and confinement is low (due to high divertor neutral flux); $f_{H,ITER89p}$=1.2, I_p=0.8 MA, P_{heat}=7 MW, $\Gamma_{o,div}$= 6•10^{22} m^{-2} s^{-1}.

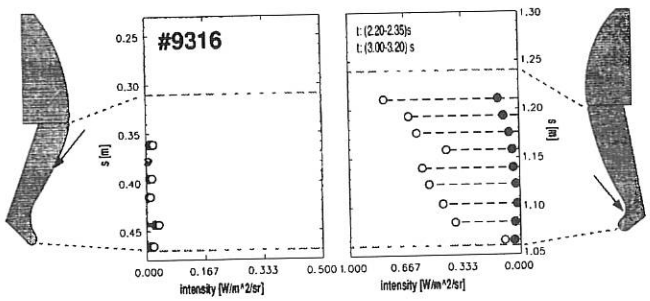

FIG. 2.5: CIII emission profiles along the target plates in the inner and outer divertor during the type-I ELMy and the type-III ELMy-CDH phases of the discharges shown in Fig. 2.4.

2.3.4 Hydrogen volume recombination

At high line-averaged density a divertor temperature below 1 eV was spectroscopically measured by the method of the Balmer-Paschen continuum ratio and by Lyman continuum analysis. Simultaneously, the plasma density in the low-temperature re-

gion ranges between $4 \cdot 10^{20}$ and $8 \cdot 10^{20}$ m^{-3} , as found from the Stark broadening and the absolute intensity of the Balmer series terms. Under such plasma conditions volume recombination ($\approx 8 \cdot 10^{22}$ s^{-1}) exceeds the ion collection at the target plate ($\approx 2 \cdot 10^{22}$ s^{-1}).

In DV-II the volume recombination already sets in at lower density due to the different geometry. The plasma parameters, however, are of the same order of magnitude as determined in the DV-I configuration. The in-out asymmetry is observed as before. The occurrence of both a recombination region and an ionization front was directly measured for the first time. Their existence had already been predicted by the Braams-Eirene simulation. Figure 2.6 shows different spectral lines of hydrogen from the inner divertor over the deflection angle of the spectrometer mirror proportional to a linear poloidal coordinate. The emission of n=3 (L_β) originates mainly from the recombination region. In contrast, L_α is emitted over a much broader spatial region. In the recombination region the collision limit is between 2 and 3, i.e. the line ratio L_α /L_β is determined by recombination alone (about 2). Outside this region n=2 and n=3 are occupied by electron collisions from the ground state. Here the ratio L_α/L_β takes much greater values.

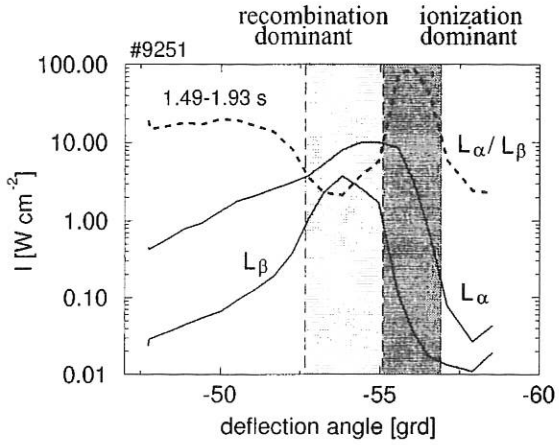

FIG. 2.6: From the line ratio L_α/L_β in the inner divertor the recombination zone may be distinguished from the ionization zone.

2.4 Radiation and Power Deposition

2.4.1 Heat load distribution in the divertor

A new high-resolution IR system was installed at ASDEX Upgrade to allow measurement of the surface temperature of the strike point modules. The system consists of a fast IR line camera viewing from the bottom of the machine via an IR endoscope and stainless-steel mirrors behind the outer divertor and roof baffle, respectively, onto the strike point modules. Together with the existing system, this allows nearly complete monitoring of the divertor surface temperature. The measured temperature evolution is used to calculate the heat flux. It is found that the inner strike point module is largely detached and the heat flux is deposited on the inner part of the roof baffle as well as on the inner transition and retention module with a maximum heat flux below 1 MW/m^2. This is compatible with the high radiation in the inner divertor leg, as measured with the bolometer. Broad heat flux profiles with decay lengths of a few centimetres are measured at the outer strike point module. The maximum heat flux detected by thermography in an H-mode discharge is only 4 MW/m^2 or below for a total input power of 12.5 MW without radiating mantle, except for some ELMs showing a moderately higher heat flux. The reduction of the heat flux at the divertor plates is also found for the parallel heat flux calculated from the measured data using the poloidal and toroidal pitch angles. First investigations show that under comparable discharge conditions the maximum parallel heat flux at the divertor plates is reduced by a factor of 2-3 and the decay length becomes broader (Fig. 2.7).

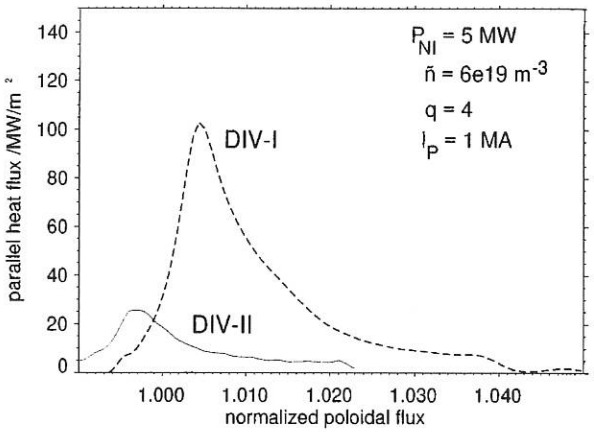

FIG. 2.7: Parallel heat flux profiles at the outer strike point module.

2.4.2 Radiation pattern and power balance

The measured line integrals of the 22 divertor bolometers were unfolded together with the other 72 bolometers of ASDEX Upgrade in order to reconstruct the radiation distributions in the divertor region and main chamber. Integrating over the whole plasma, one finds that the total radiated power is about 60% - 80% of the input power (Fig. 2.8), which is similar to discharges with the old DV-I configuration. However, radiation from the divertor and X-point region has now increased to about 40% - 50% of the input power, which is clearly higher than the radiated fraction in DV-I, thus also reducing the power load on the divertor plates. Also, the radiation distribution in the inner and outer divertor is more symmetric than in DV-I. A large part of the radiation measured in DV-II for shots with additional heating is located in the inner divertor, both for L and H-mode plasmas. This is in contrast to the old DV-I, where a significant amount of radiation over the inner divertor plate was found only during ELMY H-mode plasmas.

The total power balance for ohmic, L and H-mode discharges, taking into account input power, radiation measured by bolometers, power load on the divertor plates measured by thermography and change of the MHD energy tends to be overcompensated. However, considering that parts of the divertor radiation are recorded by both the bolometer and thermographic cameras, one arrives at a reasonably good power balance.

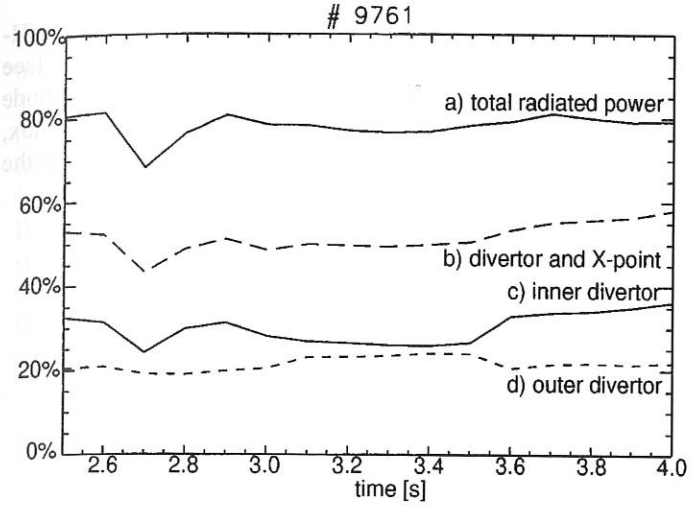

FIG. 2.8: Fraction of radiated power to heating power for a shot with approx. 8 MW neutral beam injection.

2.5 Divertor Modelling with B2-Eirene

2.5.1 Compression of recycling impurities

B2-Eirene was used to simulate density ramp-up scenarios for DV-I. From these runs, one can derive the compression of neon and helium at the position of the pump duct relative to the midplane density. Compression of neon and helium (neon is better compressed than helium) increases with higher neutral gas flux density in the divertor. The basic mechanism for the compression is the recycling cycle in the outer scrape-off layer.

For the LYRA configuration modelling predicts much better compression of helium (a enrichment of helium of typically 2 is now observed in the pumping duct location) than for DV-I (enrichment factors for helium between 0.1 and 0.4). The very good compression of neon in the outside tilted DV-I (enrichment of 1 to 6) is reduced to practically the same as that of hydrogen (enrichment 1 to 1.5), but is still large enough for effective feedback control. In LYRA the pumping duct recycling is now concentrated in the dome region close to the separatrix hit point. Due to the higher electron densities there, creation of impurity neutrals at the plate and reionization of colder neutrals from the dome occur at practically the same position. The better compression of helium in LYRA is then due to the fact that the helium neutral atoms have longer mean free paths than neon and can therefore escape more easily from the inclined target plate region into the dome and from there into the pump.

2.5.2 Divertor detachment and L-mode separatrix density limit

B2-Eirene had previously reproduced well the experimental findings regarding the L-mode separatrix density limit in both ASDEX Upgrade DV-I and JET. Apparently, different trends with heating power could be reconciled by the detailed modelling. ASDEX Upgrade showed practically a square-root power dependence of the density limit for relatively low net input powers. For a typical LYRA equilibrium configuration, B2-Eirene simulations predict for DV-II a much earlier onset of detachment at the separatrix ($2 \cdot 10^{19}$ m^{-3}) than for DV-I ($3.9 \cdot 10^{19}$ m^{-3}), both for divertor and midplane gas puff and with reasonable pumping, transport and C-impurity production (physical and chemical sputtering). The predicted earlier detachment of the separatrix region compared with the global detachment in DV-I is due to the geometry of LYRA, where neutrals are preferentially reflected towards this hot part of the plasma at the separatrix, whereas in DV-I the inner divertor (usually the first to detach) was practically orthogonal. The change of divertor profiles due to this change of geometry (with a much sooner cold separatrix for DV-II and a hotter outer scrape-off layer part trying to keep attached much longer with respect to midplane density) seems to be confirmed by thermography and Langmuir divertor profiles from LYRA (Fig. 2.9).

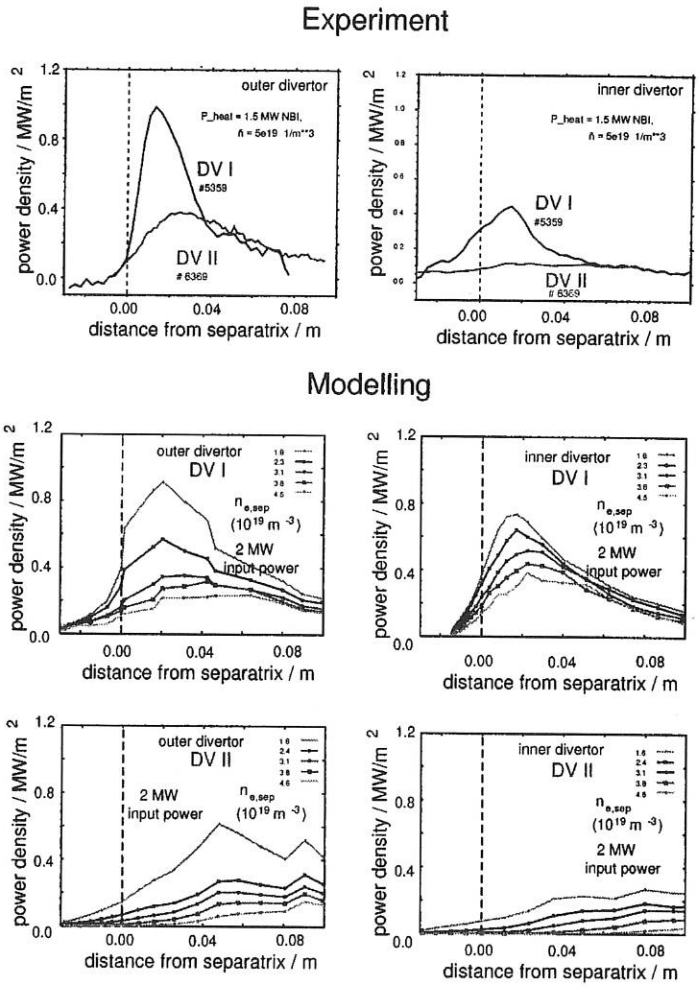

FIG. 2.9: Comparison of experimental and modelling results for the divertor power loads for DV-I and DV-II.

Therefore, this geometry effect does not affect the scrape-off layer density limit due to complete detachment, which is indicated by a large drop of the integral ion saturation current by at least one order of magnitude. This complete detachment limit is not changed for LYRA in comparison with DV-I as long as the impurity production of carbon is assumed to be equal in DV-I and LYRA, in agreement with experiment.

3. TRANSPORT AND H-MODE STUDIES

3.1 H-mode Threshold

With the new, second neutral beam injector installed at ASDEX Upgrade, it has become possible to study the H-mode threshold at higher heating powers. Especially in hydrogen plasmas the H-mode threshold power is considerably higher than in deuterium, whereas the available neutral beam power is lower with hydrogen injection than with deuterium injection. With the hydrogen neutral beam power now up to $P_{NBI,H}$ = 14 MW, it was possible to extend the range of threshold studies up to densities of 10^{20} m^{-3}, for magnetic fields at and above B_t = 2.5 T.

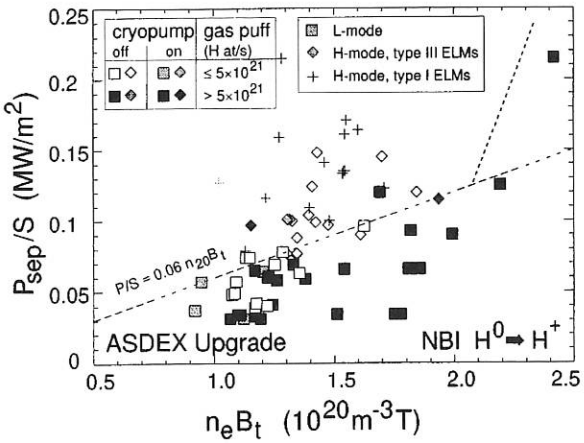

FIG. 3.1: $\overline{n}_e \times B_t$ scaling of the H-mode power threshold in hydrogen plasmas with DV-II with active/inactive cryopump and for different levels of hydrogen gas puff. At high gas puff levels the H-mode threshold is considerably increased.

Figure 3.1 shows the power flux across the separatrix P_{sep} = P_{heat} - dW/dt - $P_{rad,sep}$ as a function of the product $\overline{n}_e \times B_t$. The magnetic field was in the range of B_t = 2.0 ... 2.7 T, with the majority of cases at B_t = 2.5 T, and with ion-∇B drift towards the X-point (favourable ∇B direction). The threshold power rises linearly with ($\overline{n}_e \times B_t$) up to $\overline{n}_e \times B_t \approx 2.0 \times 10^{20} m^{-3} T$ and can be described by the expression $P_{thresh}/S = 0.06\, \overline{n}_e \times B_t$, as indicated by the lower dashed line. In order to reach densities near the Greenwald density limit ($\overline{n}_{GW}$ = 1.2 × 10^{20} m^{-3} at I_p = 1 MA) strong gas puffing is used, in which case the H-mode is not reached even at the highest heating power (P_{NBI} = 14 MW) considerably above the H-mode threshold scaling obtained for densities far below the Greenwald limit. This deviation is marked by the upper dashed line in Fig. 3.1.

A similar observation is made in deuterium, as demonstrated for a large data set from the measurements in DV-I shown in Figs. 3.2a) and b). The separatrix power (Fig. 3.2a) is plotted as a function of the neutral gas flux measured by an ''ASDEX-type'' ionization gauge located near the midplane in the main chamber. At neutral gas fluxes above $10^{21} m^{-2} s^{-1}$ the heating power necessary to maintain H-modes sharply increases. Edge temperature measurements (Fig. 3.2b) reveal that the critical edge temperature necessary to maintain H-mode remains unchanged (dashed line). The critical edge temperature for H-mode still follows the same scaling as for low neutral flux (see Annual Report 1996). This observation indicates that H-mode transition physics is not affected by the increased neutral flux, but transport deterioration and/or additional losses lead to the increased H-mode power threshold. .

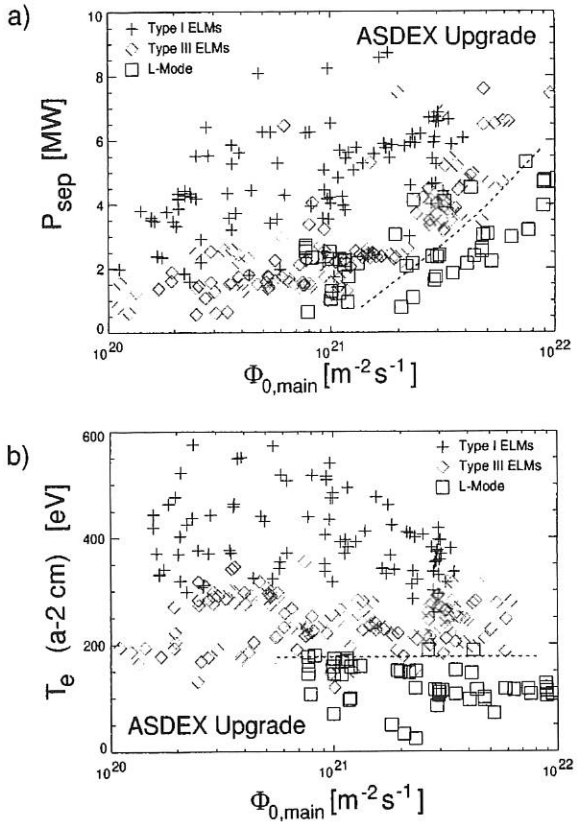

FIG. 3.2: Separatrix power (a) and edge electron temperature (b) vs. main chamber neutral gas flux. At high neutral gas flux, the power needed to maintain H-mode increases, whereas the edge temperature at the H-mode threshold remains unchanged.

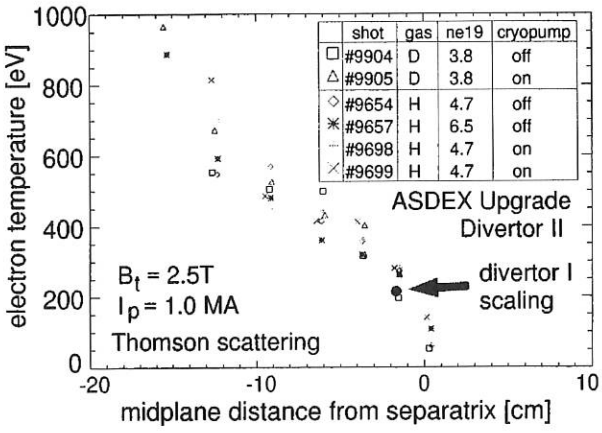

FIG. 3.3: Edge electron temperature profiles just before the L-mode to H-mode transition in DV-II. Deuterium plasmas show transition temperatures close to the scaling derived for DV-I. Transition temperatures in hydrogen are slightly (20-30%) higher than in deuterium.

Edge temperature measurements at the L-H transition were made to compare the edge conditions in DV-I and DV-II (Fig. 3.3). The transition temperatures in deuterium are found to be very close to the scaling derived for DV-I, whereas transition temperatures for hydrogen appear slightly (20% to 30%) increased over the scaling. More edge measurements in DV-II are needed in order to establish whether this difference is statistically significant. However, as shown above, the power threshold in hydrogen is considerably increased over the power threshold in deuterium in line with the observation of reduced confinement in hydrogen.

3.2 Relation between Plasma Edge and Core Transport

It has already been reported (Annual Report 1996, p. 27 ff., and /309/) that there is a correlation between the edge and core temperatures for discharges with an edge pressure gradient near the ballooning limit. Together with the essentially flat density profiles in gas-puff-fuelled type-I ELMy H-mode discharges, this results in a relation between the stored energy and edge pressure gradient.

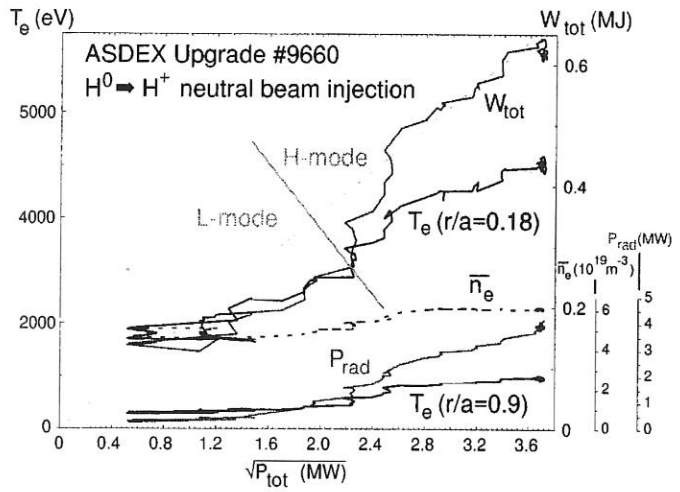

FIG. 3.4: Heating power dependence of total stored energy, central and edge electron temperatures for an H-mode discharge in hydrogen with constant electron density and low radiated power. In H-mode, T_e saturates with increasing heating power.

These studies have hitherto been conducted exclusively in deuterium, where sufficient heating power in excess of the H-mode threshold was available to study the power dependence of type-I ELMy H-mode confinement. With the installation of a second neutral beam injector box, it is also possible to conduct scans of P_{heat} in type-I ELMy H-mode hydrogen discharges. Figure 3.4 shows an example of a discharge where the neutral beam power is ramped up in steps to the full number of eight neutral beam sources (total injected power $P_{NBI,H}$ = 14 MW). At total heating powers P_{tot} (neutral beams plus ohmic heating) just above the H-mode threshold, small type-III ELMs are obtained, whereas for all heating powers above P_{tot} = 6 MW, type-I ELMs appear. At these high values of P_{tot}, the central electron temperature (taken at the innermost ECE channel resonant at r/a = 0.18) increases only weakly with heating power and is approximately proportional to the electron temperature at all other radial locations (the edge temperature trace at r/a=0.9 is shown in Fig. 3.4). A similar observation is made with charge exchange recombination spectroscopy, indicating that $T_i = T_e$ and that T_i exhibits the same saturation effect and invariance of profiles. At the same time, the plasma density was constant over the entire type-I ELMy H-mode phase.

Consequently, the stored thermal energy can be increased only very weakly in type-I ELMy H-modes if high heating power flux is applied (in this case up to P_{tot}/S = 0.27 MW/m^2). Expressed in terms of a heat-diffusive model, this observation means that the heat diffusivity $\chi_\perp$ increases almost linearly with heating power. Note that in contrast the total stored energy W_{MHD} (thermal plus fast particles), obtained from the reconstruction of the magnetic equilibrium, continues to increase proportionally to $P_{tot}^{1/2}$ in H-mode. This difference indicates that the confinement of the fast particles produced by neutral beam injection does not deteriorate in the same way as that of the thermal particles.

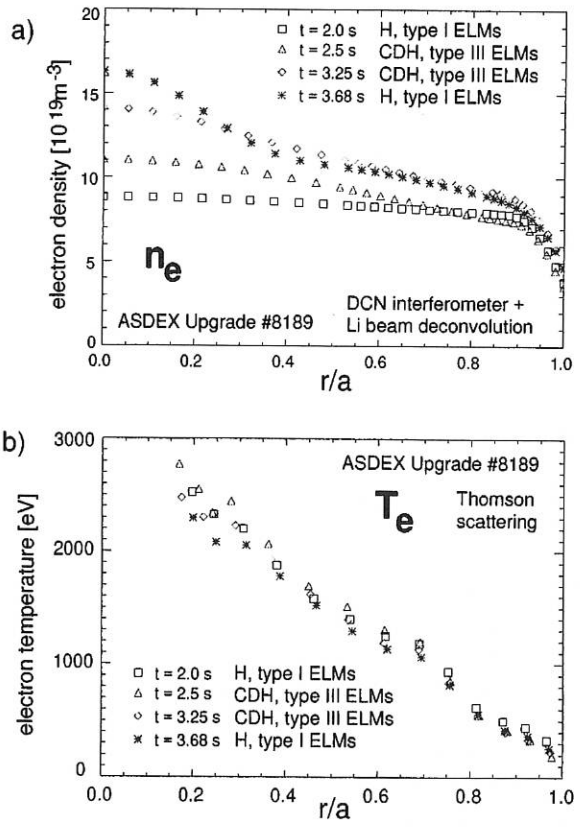

FIG. 3.5: Electron density (a) and electron temperature (b) profiles at the transition from type-I ELMy H-mode to Completely Detached H-mode (CDH). The density peaks in the plasma core, while the core temperature remains invariant. The input heating power is constant during the time interval shown.

The invariance or "stiffness" of temperature profiles with respect to perturbations in situations with high heating power flux is demonstrated for the transition from type-I ELMy H-mode to Completely Detached H-mode (CDH) by adding a radiating mantle at the plasma edge by means of controlled impurity

gas puff of neon. At high fractions of radiated power (>85%) the density profile begins to increase in the plasma centre as shown in Fig. 3.5a). This peaking occurs on a time scale considerably slower than the confinement time ($\tau_E \approx 90$ ms in this case). While the density profile peaks, the core temperature profile (electrons and ions) remains unchanged (Fig. 3.5b), even though the same heat flux is now carried by more particles. The stored thermal energy in the CDH phase increases slightly (≈10%) over that of the type-I ELMy H-mode phase, an effect which can be attributed to the central density peaking.

A high fraction of the heating power is radiated from the plasma edge, resulting in not only complete divertor detachment but also a reduction of the edge temperature sufficiently great to reduce the edge pressure gradient below the ideal ballooning limit (avoiding large type-I ELMs) and permit the occurrence of type-III ELMs. The divertor remains detached even during the small peak power flux associated with this favourable type of ELMs.

It should be noted that the core temperature profile is not affected by the reduction of the H-mode edge pedestal temperature. This indicates that the critical boundary condition for core confinement may be inside the pedestal region and not at the very plasma edge. Also, although the temperature profile is stiff at large heating power flux, the density profile can apparently be modified in the plasma core and possibly lead a way to improved confinement. Such density profile modification is achieved by peaking in CDH-mode or can be attempted by bulk fuelling with pellet injection (see next section).

3.3 Pellet Injection and Core Particle Transport

In the previous section it is stated that in the case of stiff core temperature profiles confinement improvement mainly relies on modifications of the density profile. One solution is to enhance the core density. This is not possible by gas puffing, since increased edge fuelling in H-modes near the ideal ballooning limit at the plasma edge can only increase the density at the expense of edge temperature reduction. Consequently, no confinement improvement is found, but a significant deterioration at high gas puff levels. A successful method to raise the core density to values significantly above the Greenwald density limit is the injection of deuterium pellets into the plasma. High fuelling efficiency is found in H-mode, especially for injection from the high-field side. This result was presented in the Annual Report 1996.

The effect of the increased particle flux in the core on particle transport is illustrated in Fig.3.6 for a discharge with large pellets injected at v = 240 m/s from the high-field side. Density profiles (Fig. 3.6a) are taken in the initial ohmic phase (1), and in H-mode before pellet injection (2), as well as during pellet injection (3) and at some time after a pellet (4). Traces of the line-averaged density $\overline{n}_e$ and edge density gradient $(-\nabla n_e)$ are shown in Fig. 3.6b). The density gradient is calculated from the finite difference of Thomson scattering viewing channels 14 and 15 located at the positions indicated in Fig. 3.6a). The vertical lines indicate the times at which the profiles are taken. It is seen that while the line-averaged density is increased significantly above the Greenwald density, the edge density gradient cannot be increased by pellet injection. The highest value of the edge density gradient essentially builds up already shortly after the L-mode to H-mode transition at t=1.85 s. With additional particle flux due to pellets, the edge density gradient is not increased. Instead the higher particle inventory is countered by extending the width of the edge gradient region further inward into the core plasma. The central part of the density profile remains essentially flat.

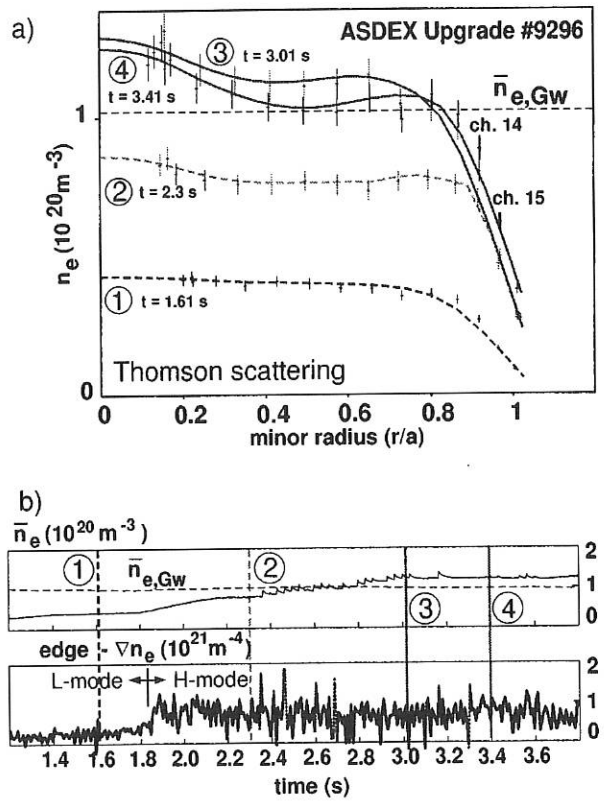

FIG. 3.6: Effect of pellet injection on edge and core densities: a) density profiles before and during repetitive pellet injection, b) line averaged density and edge density gradient as a function of time. The profiles (a) are taken at the time points marked in the traces (b): 1. L-mode, 2. H-mode before pellet injection, 3. and 4. H-mode during pellet injection. While with pellets the core density builds up strongly and $\overline{n}_e$ can be raised significantly over the Greenwald density, the edge density gradient (taken from the finite difference of Thomson channels 14 and 15) is not increased over the gradient obtained right after the L-H transition.

It should be noted that the high core densities are obtained by pellet injection only with a certain amount of additional gas puff. On the other hand, strong gas puff is known to cause severe deterioration of confinement. It is hence an important objective to find an optimum level of gas puff that allows high-density operation combined with good energy confinement. To date it is not entirely clear which parameters affect this optimum level of gas puff. Further experimental work on ASDEX Upgrade will be devoted to studying this effect in more detail.

4. MHD STABILITY

4.1 Neoclassical Tearing Modes

In long-pulse discharges the maximum achievable β is often limited by the onset of neoclassical tearing modes. These modes are driven by a helical hole in the bootstrap current resulting from the pressure flattening across magnetic islands. Since the β limit given by these resistive modes is well below the ideal MHD limit, neoclassical tearing modes are expected to constitute a serious problem in a tokamak fusion reactor.

Besides the destabilizing effect of the perturbed bootstrap current, there are at least three stabilizing effects: (i) the Glasser effect resulting from toroidicity and shaping of the poloidal cross-section, (ii) the finite perpendicular transport, which prevents the pressure from flattening across small magnetic islands, and (iii) the ion polarization current. Since all of these stabilizing contributions are most effective for small islands, they lead to an onset condition for the neoclassical modes, the so-called seed island. From error field measurements at COMPASS-D it has been concluded that the ion polarization current should be the essential stabilizing effect.

This current is a consequence of the time-varying radial electric field felt by the plasma due to the island's rotation in the plasma frame. Since in the collisionless regime only the trapped particles are affected by the electric field, the stabilizing effect should be less important compared with the collisional case, where the polarization current is a factor of $\epsilon^{-3/2}$ larger. It is therefore usually expected from the theory that only if the mode can move completely around the torus before the average ion is affected by collsions ($\bar{\nu_{ii}} = \nu_{ii}/\epsilon\omega_{*,e} \ll 1$), neoclassical tearing modes may occur.

This assumption was tested by studying the variation in the collisionality during the shots. The onset of a neoclassical mode was found to require not only a high pressure but also small enough collisionalities. As can be seen in Fig. 4.1, only if the normalized collisionality ($\bar{\nu_{ii}}$) falls below a critical value and the pressure is high enough does the following sawtooth crash provide the necessary seed island to enable the mode to grow. It can thus be concluded that it is the polarization current, rather than the finite perpendicular transport that determines the so-called seed island, which is necessary to drive the modes unstable.

Besides the onset conditions for the neoclassical modes, its growth time and its size on saturation are of importance. To investigate the nonlinear growth of neoclassical islands, numerical simulations using the large-aspect-ratio tokamak approximation were carried out. In these simulations Ohm's law and the equation of motion are solved nonlinearly, taking into account the non-inductively driven bootstrap current. Since the transport across the island and polarization current effects are not included, no predictions about the size of the seed islands are possible. One expects, however, reliable growth times for the modes considered as well as saturated island widths.

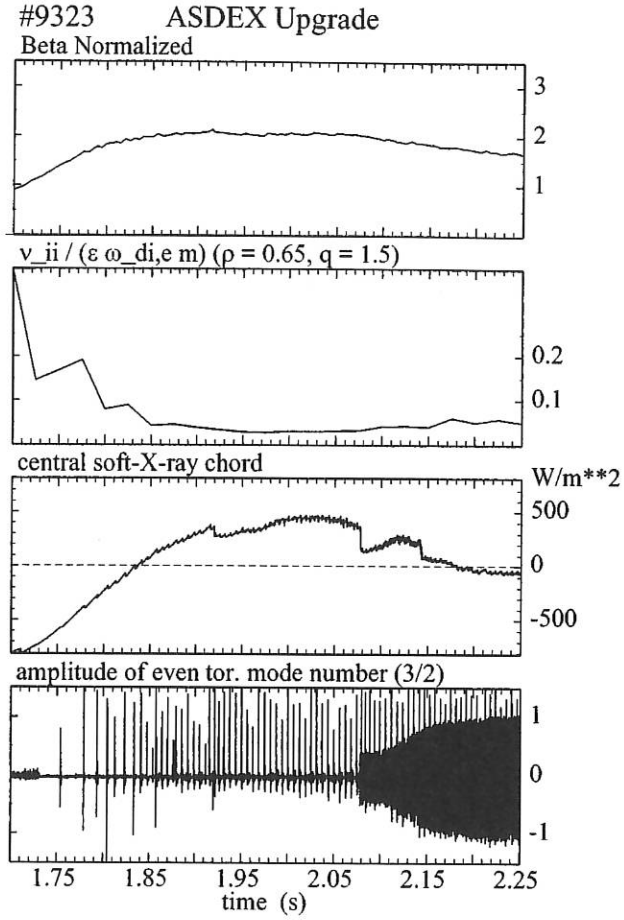

FIG. 4.1: The onset of the neoclassical (3,2) mode requires a high enough pressure (characterized by $\beta_N = \frac{\beta}{I/(aB)}, \beta = 2\mu_0\langle p\rangle/B^2$) as well as low enough collisionality. If both conditions are fulfilled, the seed island provided by the following sawtooth can be driven unstable by neoclassical effects.

Although the basic equations solved in the simulation are essentially the same as those of the corresponding analytical theories, some assumptions associated with these theories were avoided. The perturbed flux is not considered to be constant across the island and the nonlinear coupling between different toroidal harmonics is accounted for. As a consequence, for example the nonlinear change in the current profile due to the island growth was taken into account.

In Fig. 4.2 the simulated growth of an (m,n)=(3,2) island is shown for ASDEX Upgrade shot 8216. The equilibrium bootstrap current density was found from a transport analysis using the ASTRA code to be about 11 per cent of the total plasma current density at the q = 3/2 surface. After a growth time of about 25 ms the island reaches its saturated size of approximately 8.5 cm. These results are in excellent agreement with the experimental observations.

Since the driving mechanism of the neoclassical tearing modes is the vanishing bootstrap current within the island, replacing this amount of current by external current drive should be able to stabilize the modes. It is therefore planned to use phased electron cyclotron current drive for mode stabilization. The results of corresponding simulations are seen in Fig. 4.2.

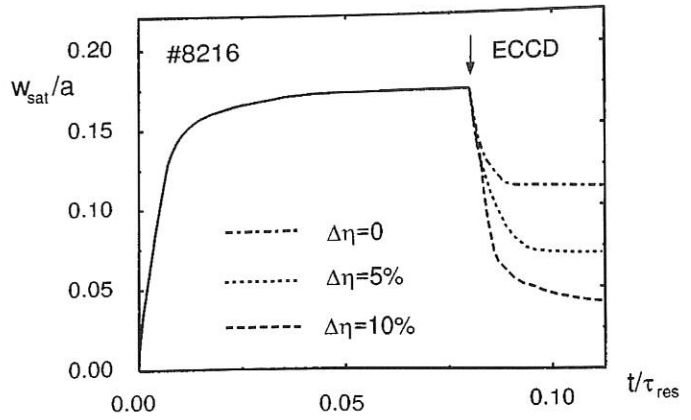

FIG. 4.2: Neoclasical growth as well as stabilisation by ECCD/ECRH of a (3,2) mode simulated for ASDEX Upgrade shot 8216. The effect of heating is taken into account by a change in the resistivity. The resistive time τ_{res} for this shot is 4.3 s.

Besides driving current, the ECRH changes the resistivity inside the island, leading to an additional stabilizing current. Under ASDEX Upgrade conditions this current can easily exceed the current driven by ECCD. The profile of the driven current is assumed here to be Gaussian with a deposition width of about 2 cm. The total driven current is 5 kA. If one neglects the change in resistivity, the island size is reduced by about 30%. The saturated island size corresponds approximately to the ECCD current width. The change in the resistivity reduces the saturated island width further.

4.2 New MHD Phenomena

In shots with strong impurity accumulation some new MHD phenomena were found which could be identified via a stability analysis. The excellent agreement between the experimental observations and the theoretical results can be regarded as a successful test of the validity of the CASTOR resistive MHD code.

The impurity accumulation, especially of high-Z elements, leads to significant central radiation. This causes a strong and fast reduction in temperature and, thereby, an increase in resistivity in the plasma centre. Consideration of the current diffusion leads to a flat shear region first developing in the vicinity of the q = 1 surface and moving towards larger q-values with time.

When the low-shear region is in the vicinity of the q = 1 surface, cascades of modes with high toroidal mode numbers, typically up to 20, were observed. In Fig. 4.3, a wavelet analysis of the soft X-ray (SXR) data of some of these cascades is given.

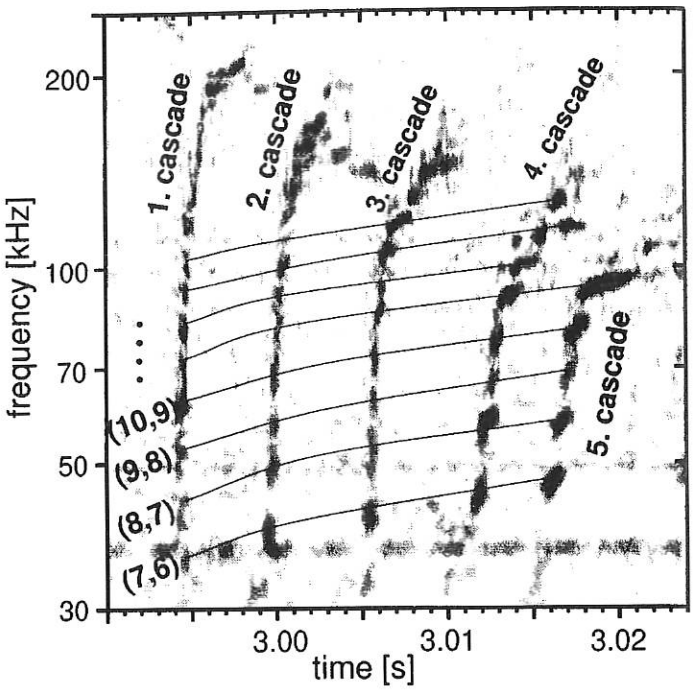

FIG. 4.3: Modes observed in wavelet spectrum of the soft X-ray radiation.

Whereas the lower (m,n) modes, not shown in Fig.4.3, can be continuously observed, one finds a series of short bursts with one mode following another in order of increasing n. The relation between the poloidal and toroidal mode numbers is given by m = n + 1. Knowing the mode numbers and the location of the modes from SXR measurements, one may infer the q-profile. In the vicinity of the q = 1 surface one finds a large current gradient together with small shear, which according to the theory drives high-n tearing modes with m = n+1 unstable in a circular cylinder. Although high-n tearing modes are usually believed to be very stable, they are also found to be unstable in a torus, where small islands are stabilized by the well-known Glasser effect. It has been shown that the coupling between different poloidal mode numbers due to toroidicity and plasma shaping is sufficient to overcome the Glasser effect.

The cascading process is generated by nonlinear interaction of the different modes via fast local changes of the equilibrium current and pressure profiles. Quasilinear cylindrical code calculations reveal that each mode excites the next higher mode and stabilizes the previous mode.

Considering the same shots at later times, one finds a temperature profile which has a positive gradient within the low shear region, now located at higher q-values, where modes with lower mode numbers become resonant. As seen in Fig. 4.4, the positive pressure gradient drives a (4,3) mode unstable. The mode's amplitude is large for a positive pressure gradient and appreciably weakens when the pressure gradient becomes negative. Furthermore, the mode's frequency changes in the same way as the pressure gradient varies. This frequency change is in quantitative agreement with the expected variations in the electron diamagnetic drift frequency with the pressure gradient.

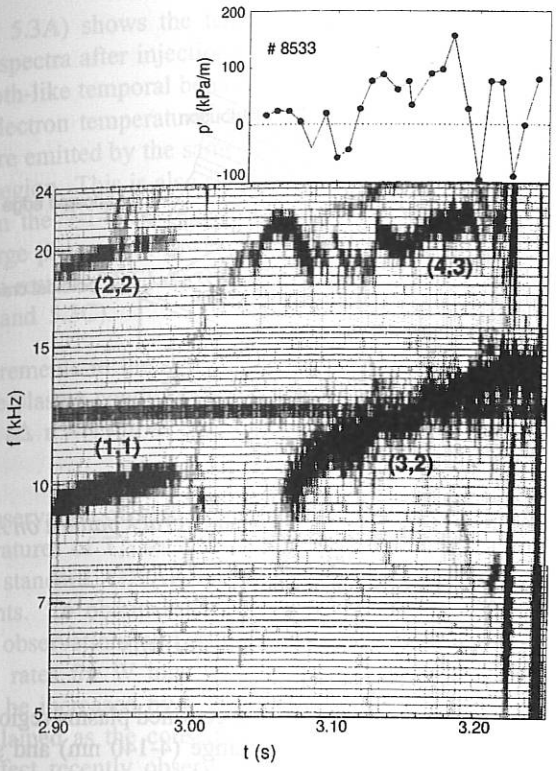

FIG. 4.4: Pressure gradient at r=27 cm together with a wavelet amplitude plot.

From a stability analysis performed with the CASTOR code, the unstable mode was identified to be a resistive interchange mode coupled to two (m = 4,n = 3) tearing modes. This coupling is possible since the strong radiation in the plasma centre causes a non-monotonic q-profile leading to three q = 4/3 surfaces at early times.

Resistive interchange modes have been found in advanced tokamak scenarios, where they are driven by the large pressure gradient in negative shear regions. An interchange mode driven by a positive pressure gradient was observed in ASDEX Upgrade for the first time.

The results of the stability analysis are in excellent agreement with the experimental observations. They are able to explain the pressure dependence of the mode's amplitude and frequency as well as the time development of its radial location.

4.3 TAE Modes Driven by Fast Particles

The transport of fast particles across the equilibrium magnetic field is generally negligible on the time scale for thermalization. However, resonant interaction between a spectrum of toroidal Alfvén eigenmodes (TAE) and suprathermal particles (such as those generated by the neutral beam injection system) may take place, leading to significant anomalous transport of the particles.

The HAGIS nonlinear self-consistent δf code was used to investigate this nonlinear resonant interaction of fast particle distributions with linear MHD eigenmodes in realistic ASDEX Upgrade geometry. The HAGIS code accurately resolves the linear and nonlinearly saturated phases of the wave growth and reactive frequency shifts. There are no restrictions on the form of the guiding-centre fast-particle distribution function, which is simultaneously and self-consistently evolved along with the spectrum of linear modes present in the system.

In ASDEX Upgrade TAE are routinely observed in NBI-heated plasmas and the HAGIS code was used to study the interaction between the population of energetic deuterons arising from the NBI system and a single TAE in a shaped ASDEX Upgrade plasma (#7692). The plasma parameters were chosen to simulate the injection of 60 keV deuterons into a pure D plasma. The radial fast-particle distribution was matched to the NBI deposition profile with an isotropic slowing-down distribution assumed in velocity space. The results indicate that the fast particle drive is comparable to the damping mechanisms present, and that for more quantitative results a better description of the fast particle distribution is necessary.

The HAGIS code has many natural areas of applicability beyond the study of Alfvén eigenmode instabilities, such as the study of fishbone and sawtooth oscillations. Furthermore, HAGIS provides a means of accurately modelling the distribution for such particles in a variety of additional heating scenarios, affording the possibility of investigating sawtooth suppression by particle heating.

5. THE TUNGSTEN DIVERTOR EXPERIMENT

5.1 Introduction and General Behavior

Tungsten-coated divertor tiles (thickness of the coating: 500 μm) were mounted at the position of the strike zone in the ASDEX Upgrade during the last experimental campaign with the DV-I configuration in 1996.

As reported earlier, there was no influence of the tungsten divertor on the other intrinsic impurities and global plasma behaviour.

Tungsten erosion was measured by spectroscopic observation of line radiation of neutral tungsten in the visible range and by exposing test tiles for one or several successive discharges using a manipulator system. As expected, significant tungsten erosion occurred only under discharge conditions with high divertor plasma temperatures, such as low-density ohmic discharges or H-mode discharges with ELMs. Using sputtering yields of carbon impacting on tungsten from laboratory ion beam experiments and adopting a 1% fraction of C^{3+} ions, one obtains good agreement with the spectroscopically measured erosion fluxes. The difference in the observed gross erosion (spectroscopy) and the measured net erosion (probes), especially for low-temperature, high-density divertor operation, could be quantitatively explained in terms of prompt redeposition of W.

Tungsten concentrations in the plasma centre were monitored spectroscopically throughout the campaign. In the majority of

H mode discharges (80%, all monitored discharges 85%), the maximum W concentration was found to be clearly below the maximum tolerable level ($\approx 2 \cdot 10^{-5}$) for ITER. Figure 5.1 shows a strong decrease of the W concentration with increasing $\bar{n}_e$ and also the beneficial effect of higher heating power. Neon seeded discharges showed only slightly enhanced W concentrations. Due to the strong influence of the bulk transport on the concentration (see Sec. 5.4) only a weak correlation with the tungsten tile erosion flux is observed.

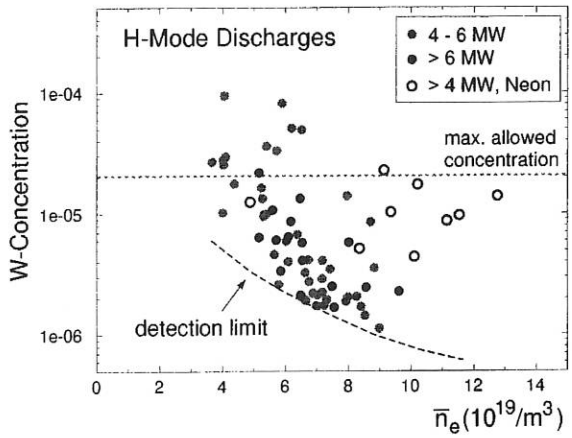

FIG. 5.1: Maximum tungsten concentrations in H mode discharges as a function of the line-averaged density.

The results of post mortem analyses and refined studies are presented in the following sections.

5.2 Technical Performance

Approximately 800 plasma discharges with varying average heat fluxes of up to 6 MW/m^2 were performed during the campaign. The measured surface temperatures were in the same range as in electron beam tests at comparable heat fluxes and pulse lengths. Throughout the discharge period the surface temperature stayed below 700° C. After termination of the discharge period, cracks were detected on almost all tiles. This is in accordance with the results found on tiles with identical coating in electron beam tests conducted concurrently. Despite the formation of cracks in the divertor tiles, no influence on plasma performance and the measured W concentrations in the plasma was found.

In Figure 5.2, the heat load distribution on the divertor tiles and the crack pattern are shown schematically. Toroidal cracks always started from the thicker edge of the tapered tiles, which was exposed to the maximum heat load, and propagated through the bulk of the graphite. Surface analysis of the cracks revealed that the failure started at the rounded edge within the graphite near the interface between the graphite and W coating. In that region, the rounded edge gives rise to stress concentration. Further major cracks in the coating had poloidal orientation. It can be assumed that they originate from the mismatch in thermal expansion. At the interface between the graphite and coating no carbide formation due to the thermal loading was found, as could be expected from the relatively low temperatures on these tiles during operation.

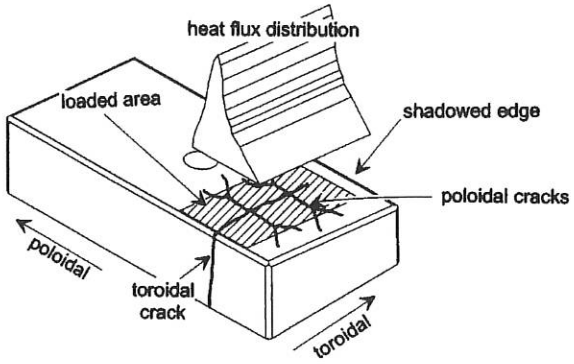

FIG. 5.2: Heat load distribution and crack pattern on ASDEX Upgrade divertor tiles.

5.3 Spectroscopic Investigations

Spectroscopic investigations in the confined plasma region were performed in the VUV spectral range (4-140 nm) and soft X-ray range. The well-known quasicontinuum structure at ≈5 nm emitted by W ions around W^{27+} was used for the determination of the W concentrations during the tungsten divertor campaign. Apart from this structure, isolated lines of tungsten were observed in the same spectral region, in the range from 12-14 nm and around 0.7 nm. The observed single spectral lines are all emitted by tungsten ions around charge state W^{42+}, which have a relatively simple electron configuration and therefore exhibit fewer resonant spectral lines. The spectral lines were identified by comparison with *ab initio* calculations of level energies and predictions of collisional-radiative calculations, made by K. Fournier of Lawrence Livermore National Laboratory as part of a collaboration.

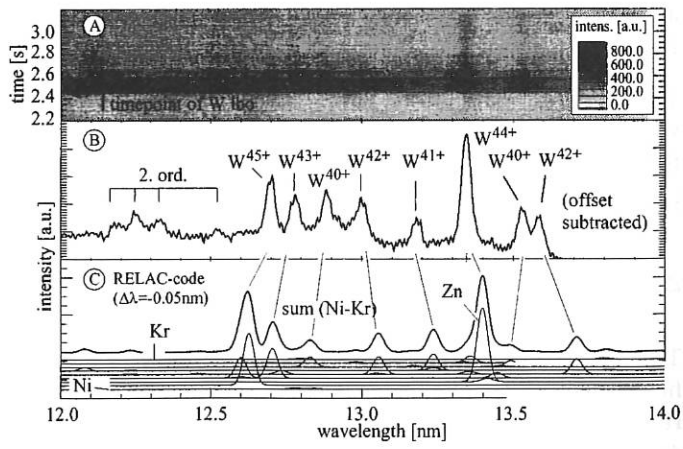

FIG. 5.3: VUV spectrum of highly charged tungsten ions in the additionally heated discharge #7470 (I_P=1.0 MA, $\bar{n}_e$=6.0·10^{19}/m^3 and P_{NBI}=5.2 MW). A) Temporal behaviour of the lines after W-LBO at t=2.45 s. B) Time-integrated spectrum (t_{integ}=100 ms, 200 ms after injection). C) Spectra from RELAC code calculations.

Figure 5.3A) shows the temporal behaviour of grazing incidence spectra after injection of tungsten by laser ablation. The sawtooth-like temporal behaviour of the line intensities and the high electron temperature ($T_{e0} \approx 2.6$ keV) suggest that these lines are emitted by the same W ions as the spectral lines in the 5 nm region. This is also supported by the absence of tungsten lines in the 7-14 nm region after W injection into an ohmic discharge phase with lower T_{e0}. The time-averaged spectrum and the result of RELAC code calculations are shown in Figs. 5.3B) and 5.3C).

Measurements in the soft X-ray region at 0.7 nm under comparable plasma conditions, also reveal spectral lines from transitions (Δ n = 1) in Br-like (W^{39+}) to Ni-like (W^{46+}) tungsten ions.

The observation of such highly ionized tungsten ions at plasma temperatures of $T_{e0} \approx 2.5$ keV cannot be explained, however, by the standard ADPAK ionization and recombination rate coefficients. To obtain satisfactory agreement between spectroscopic observations and impurity transport predictions, the ionization rates for W ions with charge numbers larger than 30 had to be increased by a factor of up to 3. This increase can be explained as the consequence of the excitation autoionization effect recently observed in the case of the molybdenum ionization equilibrium in Alcator C-Mod discharges.

5.4 Observation of Neoclassical Outward Drift

The influence of light impurities on the tungsten transport in the main plasma due to collisional transport effects was investigated by studying a type-I ELMy H-mode discharge with a strongly varying carbon concentration. Figure 5.4 shows the temporal behaviour of the tungsten flux in the divertor and at the midplane, and of the carbon and tungsten densities in the plasma bulk, as derived from spectroscopic measurements and a rotatable deposition probe. The net influx in the divertor amounts to ≈10% of the total influx because of the prompt redeposition.

Towards the end of the NBI-heated phase the carbon density rises due to sublimation from overheated parts of the ICRH antenna limiters. Correspondingly the WI influx increased by a factor of ≈2, as expected from the dominance of impurity impact on the sputtering of tungsten. Despite the increased erosion flux the tungsten flux onto the mid-plane deposition probe remains constant. However, the most prominent effect is seen from the time trace of the W density in the plasma bulk, which shows a strong decrease even below the detection limit at t = 4.0 s.

Calculations were performed with the STRAHL impurity transport code using measured electron density and temperature profiles. The anomalous diffusion coefficient (assumed equal for C and W) was taken from an analysis of the impurity density evolution after gas puffing of helium and neon in similar H-mode discharges. The drift velocity of carbon (v^C) was determined from the measured density profiles of C^{6+}. It is directed inward over the whole plasma cross-section.

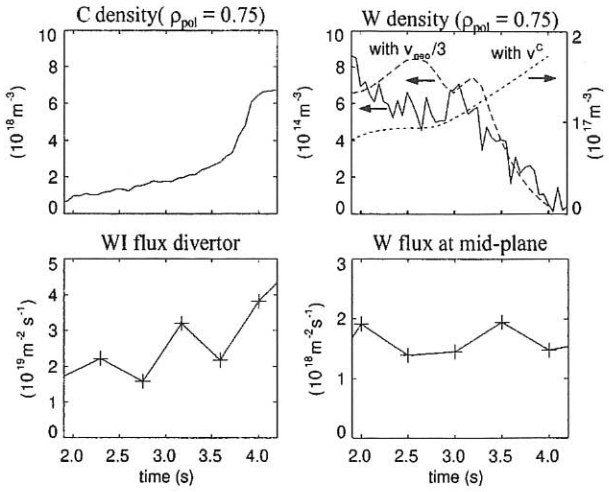

FIG. 5.4: Temporal evolution of C and W densities in the plasma bulk and of tungsten flux densities in the divertor and midplane. The dashed and dotted lines show results of transport simulations using a neoclassical drift velocity or anomallous drift as in the case of carbon.

Two transport calculations for tungsten were made: one with $D^W = D_{an}+D_{neo}$ and $v^W = v_{neo}$ and another one with a purely anomalous ansatz $D^W = D_{an}$ and $v^W = v^C$. The source flux was taken according to the WI flux density in the divertor. With carbon transport parameters, the calculated tungsten density at ρ_{pol} = 0.75 (dotted line in Fig. 5.4) is about an order of magnitude too high and the time dependence simply reflects the increasing source flux. In contrast, the neo-classical calculation shows the observed decrease, but the absolute values can only be fitted when the neo-classical drift is multiplied by a factor of 0.3.

5.5 Long-term Migration of Tungsten

By measuring the poloidal distribution of deposited tungsten atoms it was possible to obtain a global long-term migration pattern of W. All main chamber components exhibited roughly the same low level of tungsten contamination (see Fig. 5.5a)). By comparing the measured values with previous results, where some tungsten test tiles had already been installed in the divertor, one obtains an upper limit of 10^{15} W atoms/cm^2 deposited within a total plasma discharge time of ≈3000 s. The tungsten deposition on the lower divertor plates exceeds the main chamber results by a factor of up to 50-80. Figures 5.5b) and 5.5c) display the radial distribution of the tungsten deposition for the inner and outer target plate, respectively. The peak positions coincide with the maxima of the deuterium fluence to the target plates, as determined from Langmuir probe measurements.

The overall W redeposition maximum was found at the deposition-dominated inner divertor plate (Fig. 5.5b)), with a less pronounced broader maximum on the erosion-dominated outer target plate (Fig. 5.5c)).

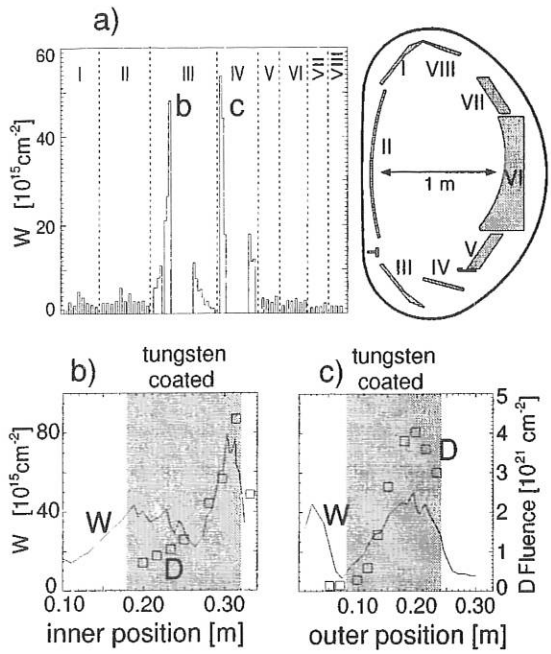

FIG. 5.5: a) Poloidal distribution of tungsten deposition on plasma facing vessel components. The data in the tungsten coated area were obtained from graphite thermography tiles (b) and c) solid line; the squares show the integrated D-fluence).

5.6 Deposition of Low Z Elements

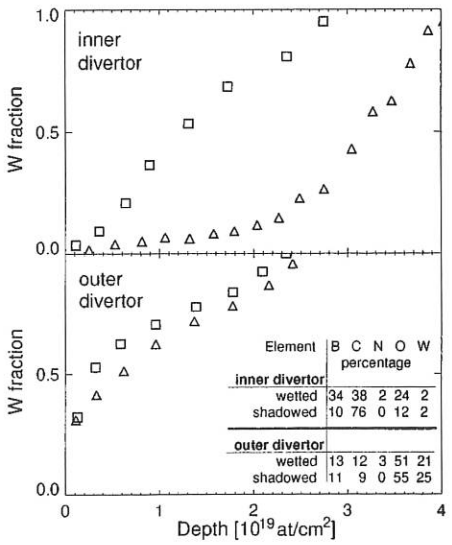

FIG. 5.6: Depth profiles of the tungsten coating in the strike point area of the inner and outer divertor as measured in the plasma-wetted zone (triangles) and shadowed region (squares) of the tilted tiles. The table shows the near-surface amounts of low-Z material and tungsten determined by XPS measurements.

Apart from sputtering tungsten, the carbon impurity ions impacting on the W-coated target tiles will also cause long-term surface modifications. The composition of the target surface was determined by X-ray Photoelectron Spectroscopy (XPS) and found to consist of, besides tungsten, mainly boron, carbon and oxygen with varying percentages (see table in Fig. 5.6). Rutherford backscattering (RBS) was used to determine the depth distribution of tungsten within the deposited layers. Figure 5.6 shows tungsten depth profiles from strike point samples of the inner (a) and outer (b) divertor, respectively. At the inner target area, we find deposited layers of low-Z material up to several μm thick with only a few per cent of tungsten remaining at the surface. In contrast to this deposition pattern, erosion dominates the outer target area, where the fraction of tungsten was found to be close to the initial level originating from the manufacturing process.

Shadowing effects due to the tilted surface geometry of the tungsten tiles could be observed by both analysis methods. In particular, it was found for the inner divertor that the layer in the plasma-wetted zone of the tungsten tiles is significantly thicker than in the shaded area. In contrast, the dominance of erosion in the outer divertor inhibits any formation of deposited layers.

5.7 Deuterium Inventories

Figure 5.7 shows the deuterium inventories for the different regions of the inner and outer divertor as measured by Thermal Desorption Spectroscopy (TDS) and Nuclear Reaction Analysis (NRA).

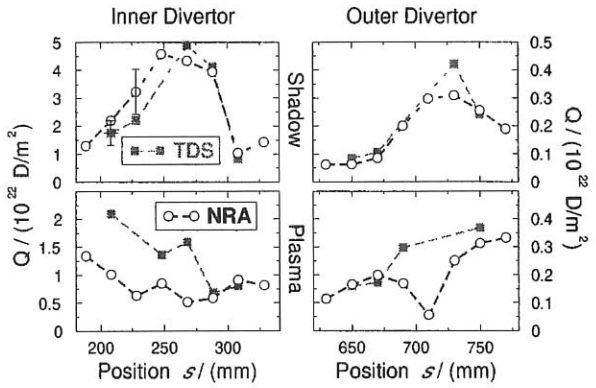

FIG. 5.7: Distribution of the total D inventories (Q), measured by NRA and TDS, at the shadowed and the wetted regions of the tungsten coated tiles, respectively.

The highest deuterium inventories (about $5 \cdot 10^{22}$ D/m^2) are measured in the shadowed region of the inner divertor outside the separatrix. At the position of the separatrix (s $\approx$ 310 mm), the inventory shows a minimum, although the amount of deposited carbon shows only minor poloidal variations. The inventories of the outer divertor samples are generally a factor of 10 smaller than the inner divertor inventories; here the total inventories, measured by TDS, show a maximum at the separatrix position (s $\approx$ 725 mm), whereas the inventories in the near-surface region, measured by NRA, show a minimum at the separatrix. The results indicate that deuterium retention on the tungsten-coated tiles in the inner divertor is governed by co-deposition of deuterium with carbon ions from the plasma, whereas retention in the outer divertor is due to implantation. The deuterium inventories in the co-deposited layers are of the same order of magnitude as those in the graphite divertor

tiles $< 2 \cdot 10^{23}$ D/m^2, considering the shorter exposure time of the tungsten-coated tiles (about 700 compared to about 2,000 discharges).

The total inventory in the tungsten-coated divertor samples differs from the near-surface inventory by only a factor of less than 2, except for the separatrix region of the outer divertor. This is in contrast to the graphite divertor samples, where the total inventory exceeds the near-surface inventory by a factor of up to 100, indicating diffusion of large amounts of hydrogen from the co-deposited/implanted layer into the graphite bulk to depths of a few 100 μm. This indicates that diffusion from the co-deposited layer into the underlying tungsten layer (inner divertor) is inhibited by the tungsten/carbon interface. The observation of total inventories in the separatrix region of the outer divertor exceeding the near-surface inventories suggests that deuterium diffuses into the bulk of tungsten with ranges of just a few μm (hence exceeding the implantation range by a factor of more than 1,000), as assumed in models describing the behaviour of hydrogen in tungsten.

6. NEUTRAL BEAM INJECTION

6.1 Summary

Neutral beam injection (NBI) into ASDEX Upgrade has been the major work horse throughout the year, with the first injector operating reliably and routinely at 7 MW (55 keV H^0) or 10 MW (60 keV D^0). A major step forward was achieved at the beginning of December when the second injector became operational . The total NBI heating power available has been doubled, now reaching 14 MW in H^0 (55 keV) or 20 MW in D^0 (60 keV). The RF sources of the second injector have proved to be as reliable and efficient as the arc discharge sources of the first injector.

6.2 Teststand Results

Work at the teststand was devoted to optimizating the mechanical components and power supplies of the RF plasma sources, which are used in the second injector. In this type of source (Fig. 6.1) an RF power of max. 125 kW is inductively coupled to the discharge by an external coil. The coil is separated from the source plasma by a quartz wall protected against plasma erosion by an internal copper Faraday shield. The entire source is mounted inside a stainless-steel vacuum chamber. In order to prevent breakdowns between the windings, the RF coil is coated with Teflon. To avoid having an auxiliary power supply on high voltage, the starter filament and the transmitters of the diagnostic signals are powered by batteries. The matching components, including a compact ferrite-core transformer, are placed on an insulator plate close to the backplate of the vacuum vessel. Because of the large distance between the second injector and the RF generators, an RF transmission line of the required length (135 m) was used at the teststand too.

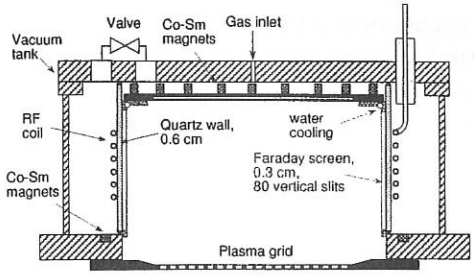

FIG. 6.1: RF plasma source for the second injector.

Assembly of the four series sources and a fifth spare source was followed by conditioning with hydrogen up to 55kV/90A in a duty cycle with a 3 s pulse every 4 min. Concerning matching characteristics and power efficiency, the differences between the series sources are negligibly small (Fig. 6.2). Some slight differences in the power transmission to the calorimeter can probably be attributed to differences in the PINI extraction systems. During reliabilty tests and conditioning no operational problems occurred.

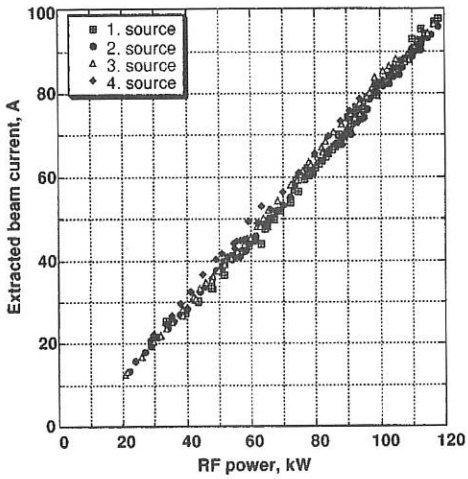

FIG. 6.2: Extracted beam current vs. RF power for the four series sources (teststand results).

6.3 Commissioning of the Second Injector

This new injector is the first in the world to replace conventional arc discharge ion sources by powerful RF ion sources. Apart from the application of RF ion sources, the second injector is almost a one-to-one copy of the first injector, wich has been operating very reliably with high availability for many years. The power supplies, SIMATIC-based control system and data acquisition and diagnostic systems were duplicated as well for the second injector and no major problems occurred during commissioning of the injector components.

The RF ion sources were conditioned on the testbed to full performance with hydrogen beams and operated on the injector up to the full power level without further adjustment of the RF-matching circuits and HV conditioning. In addition, commissioning was already supported in its early stage by nearly

complete diagnostics: calorimetry showed that the power loading of beamline components is as expected and the magnetic shielding turned out to be sufficient for the operation of the RF sources in the tokamak stray fields.

7 MW hydrogen beams were provided by the second injector in December 1997, as scheduled, and routine heating experiments have been possible from the first day of injection into the tokamak, achieving a total heating power of 14 MW with hydrogen beams at a beam energy of 55 kV. Meanwhile, internal shots onto the calorimeter have confirmed that the second injector operates as reliably as the first one and also delivers 10 MW deuterium, yielding a total power of 20 MW.

Comparison of the tokamak plasma successively heated by an ion source of the first injector and then by one of the second injector proved the equivalence of the two source types and the correct calibration for measuring the injected beam power (see FIG. 6.3). Doppler shift spectroscopy shows a 10% increase of the power in the full-energy beam component compared with the values of the first injector. This holds for both hydrogen and deuterium.

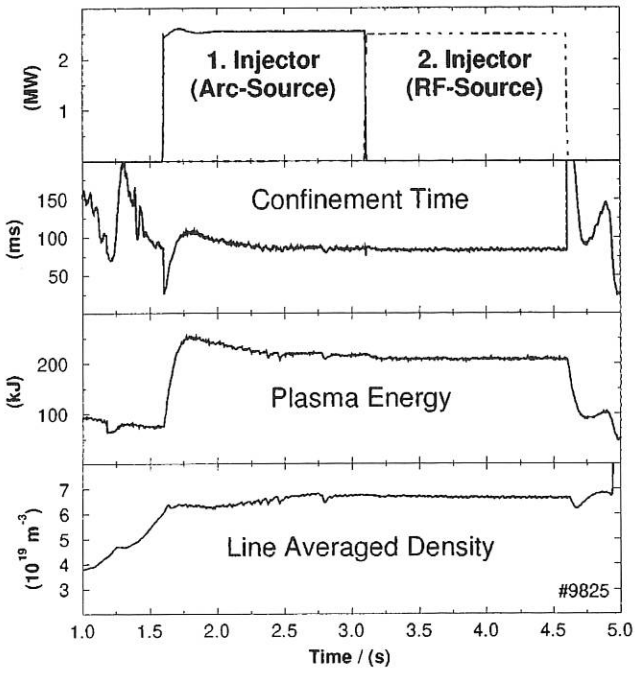

FIG. 6.3: ASDEX Upgrade plasma successively heated by the first and second injectors.

6.4 Tangential NB Injection for Off-axis Current Drive

The medium-term plans of the ASDEX Upgrade physics programme include investigation of advanced tokamak scenarios with quasi-stationary flat or reversed shear profiles. It has been shown that this requires a non-inductive current drive of about 250 kA with a rather broad current density profile peaked off-axis around $\rho \approx 0.5$. This section illustrates how this requirement could be met with neutral beams, which have hitherto not been considered as a suitable candidate for off-axis current drive. This calls for only moderate changes of the existing NBI system and ASDEX Upgrade vessel.

At present, each of the ASDEX Upgrade injectors is equipped with four ions sources arranged in a rectangle. One pair of beams is aiming at a radius of tangency R_T= 0.53 m and the other one at R_T = 0.93 m with the consequence that a considerable fraction of the fast ions are born on trapped orbits. The inclination of the beam axes $\pm 4.9^\circ$ with respect to horizontal and their crossover are such that central beam deposition is obtained. However, off-axis current drive by NBI requires, on the one hand, tangential injection in order to avoid trapping of fast ions and, on the other, off-axis deposition of the fast ions. This requires a change in beam geometry. Within the technical boundary conditions in ASDEX Upgrade, one of the present injectors can be re-directed so that almost all fast ions from the two more tangential beams (R_T = 1.29 m) are born on passing orbits. In addition, the orientation of the individual axes of these two beams has to be changed so that the beams miss the plasma centre. This involves increasing the vertical distance between the two sources by 0.2 m, further inclining the beam axes to $\pm 6.7^\circ$ and moving the sources about 0.5 m further from the plasma.

Particle deposition profiles H(r) for various beam geometries which can be realized within the ASDEX Upgrade boundary conditions were calculated with the FAFNER code in order to establish the above-mentioned geometrical changes. For some specific cases the total NBI-driven current (I_{NBCD}) as well as its radial distribution (j_{NBCD}) were determined with the ASTRA code. The results can be summarized as follows:

(i) For the modifications indicated above an H(r) peaked off-axis around $\rho \approx 0.5$ is obtained; this deposition profile is rather independent of the plasma density and beam energy over a reasonable range.

(ii) The radial profiles of $j_{NBCD}(r)$ and H(r) are similar over most of the plasma cross-section, but the total driven current depends on the radius of the maximum beam deposition. This is illustrated in Fig. 6.4, where these two (normalized) profiles are compared for a deposition maximum at ρ = 0, 0.3 and 0.5, respectively. The higher driven current for on-axis deposition is due to the higher electron temperature in the plasma centre.

(iii) For electron temperatures of $T_e(\rho=0.5) \approx 2$ keV a beam energy of 100 keV(D^0) is close to the optimum CD energy. 100 kV D^0 beams will be available on the second injector in 1998. Higher beam energies, which would then require transition to negative-ion beams, are only beneficial for significantly higher electron temperatures.

(iv) The two tangentially injecting 100 keV D^0 beams with 2.5 MW each will drive the required 250 kA in a plasma with $n_e(\rho=0.5) \approx 4 \cdot 10^{19}$ m^{-3} and $T_e(\rho=0.5) \approx 2$ keV.

(v) The radial deposition for one of the two tangential beams strongly changes if the plasma is shifted vertically with respect to the injector. However, the superposed deposition profiles of both beams (arranged symmetrically with respect to the equatorial plane) are insensitive over a wide range to the vertical position of the plasma. This is shown in Fig. 6.5, where H(r)

profiles are given for different positions of the plasma centre between -2 cm and +12 cm with respect to the midplane.

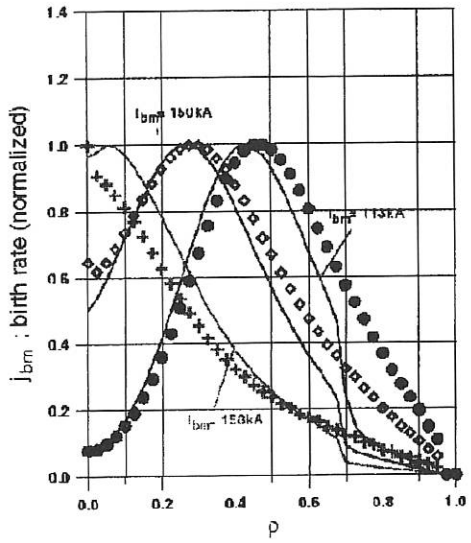

FIG. 6.4: Comparision of H(ρ) (symbols) and $j_{NBCD}(\rho)$ (solid lines) for tangential NBI with a deposition maximum at $\rho \approx 0$, 0.3 and 0.5, respectively.

In summary, modifying the geometry of the second ASDEX Upgrade injector as specified above leads to an NBI system which could be used flexibly for off-axis heating and current drive using two tangential 100 kV D^0 beams with 2.5 MW each, while the two remaining, more perpendicular beams of this injector are still available for central heating.

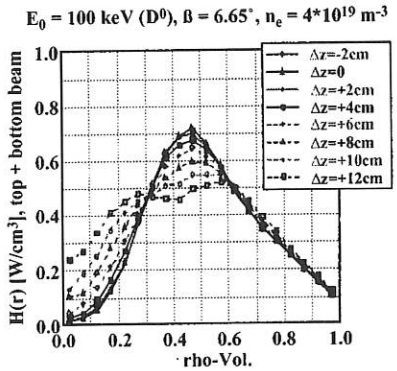

FIG. 6.5: H(r) profiles of both beams for different vertical plasma positions Δz (= -2 cm to +12 cm).

The realization of this new beam geometry calls for modifications which are related to, on the one hand, the re-orientation of the injector as a whole and, on the other, the change in beam inclination. Conceptual design studies of all the necessary modifications were conducted in order to ensure that they can be done.

Re-orientation of the injector as a whole means changing its position with respect to the plasma by less than 1 m. This of course requires modifying the injector support, moving the high-voltage cage and external magnetic screening together with the injector, and adapting all connections to the injector to its new position. In addition, the duct region connecting the beam line to the ASDEX Upgrade vessel has to be newly designed. The most critical part in this respect is the modification of the vessel port, which means cutting out the existing radial A-port and welding in a new more tangentially oriented new port.

Internal modifications of the injector are required in order to incorporate the proposed changes in orientation of the two more tangential beams. The new position of the ion sources as well as the modified inclination angle call for a new ion source flange on which to mount the sources. Ion orbit calculations show that no change of the magnet is necessary and that it is sufficient to move the ion dumps vertically as a whole by a few centimetres, which can be realized within the present boundary conditions. The calorimeter, however, has to be redesigned so that the individual V-shaped panel arrangements are correctly adapted to the new position of the beam axes. This requires that a completely new central calorimeter assembly be built.

It is estimated that all the modifications detailed above will take three years to complete. At present, an application for EURATOM preferential support for this proposal is being prepared.

7. TECHNICAL SYSTEMS

After mounting the new LYRA divertor together with a cryo pump the vacuum vessel was closed on schedule in April. The supply and control of the cryo pump was then moved from the testing area to the experiment.

Parallel to mounting LYRA, the protective limiters of the ICRH antenna were hardened by substituting wider CFC tiles for the fine-grain graphite tiles. In the same way the 2 additional protective limiters between the NBI port and ICRH antenna were hardened. The heat load of these limiters depends sensitively on their clearance to the plasma boundary and on the density decay length. Under unfavourable experimental conditions it could even become necessary to cool these limiters actively in the future.

Before the end of the year the new second neutral beam injector, NI2, was commissioned up to the full power of 10 MW. ICRH commissioned the new 3 dB couplers and has hitherto achieved powers of 1 MW/antenna. ECRH now has 2 of the planned 4 gyrotrons in operation. Each gyrotron delivers 0.5 MW for as long as 2 s.

7.1 Machine

The heating power delivered into the AUG vessel has meanwhile reached 15 MW. The heat flow ratio into the divertor is comparable to that of the open DV-I, but distributed over a considerably larger area. As a result the maximum strike point heat flux density has not become higher than 5 MW/m^2. The

edge shading on the strike point region works perfectly. No hot spots are encountered. On the transition and retention modules, both without edge shading, the heat load is larger than expected. This is, on the one hand favourable since it relieves the strike point module, but, on the other, minor hot spots evolve there.

The cool-down of the cryo pump reduces the vacuum vessel pressure by almost a factor of 10. The cold-He-circulating pump with magnetic bearings works well. It permits highly flexible adjustment of the He throughput of the He panel to all operating conditions. Up to now there are still 5 minutes of helium glowing between consecutive discharges. The resulting increased heat flux to the He panel is used for regenerating it. The following cool-down to LHe temperature (4.2 K) is finished after less than 3 minutes.

7.2 Preparations of Long-pulse Operation

At a full additional heating power of P_{add} = 20 MW, long-pulse operation of 10 s can be achieved in ASDEX Upgrade by reducing the plasma current from the nominal short-pulse value IpN = 1.4 MA to the long-pulse value IpL = 1 MA. However, this requires extensive compensation of reactive power for the EZ3 generator. Although present operational experience with LYRA indicates that it can also take up adiabatically the heat load of full-power long-pulse operation, first steps were initiated to develop a simple non-brazed steady-state target.

7.2.1 Reactive power compensation

In contrast to IpN short-pulse operation of 4-5 s, IpL long-pulse operation requires the full exploitation of the fly-wheel energy of the two poloidal field (PF) generators, EZ3 and EZ4. This constraint considerably increases the demand of reactive power compensation. Satisfactory conditions for long-pulse operation can only be achieved with a reactive power compensation plant consisting of four modules with 30 MVAr each. A prototype module was ordered in late 1997 from SIEMENS.

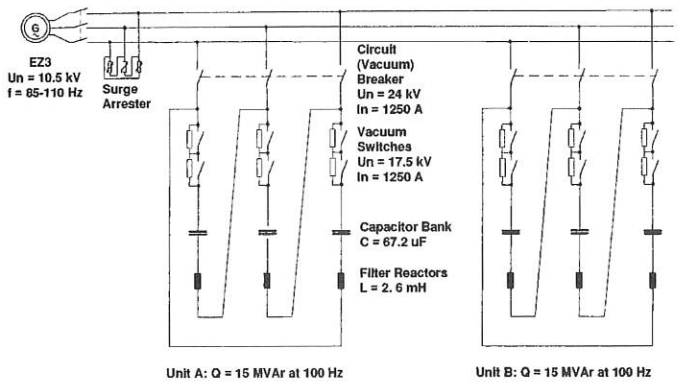

FIG. 7.1: 30 MVAr pilot module for reactive power compensation under construction.

The prototype module is shown in Fig. 7.1 together with the ratings for the capacitor bank and filter reactor. It consists of two capacitor units switched on and off by vacuum breakers. SIEMENS had already manufactured a similar plant for JET. They were therefore given a study contract which included the general plant layout and numerical computations of the switching surges. Accordingly, the unit size to be switched as a whole was chosen as 15 MVAr at 100 Hz in order to keep the voltage surges for the EZ3 insulation at a low value. The capacitors and reactors were dimensioned for 20,000 worst-case switching actions and for an effective pulse duration of 20 s.

7.2.2 Non-brazed steady-state target

In summer activities were started to develop a robust and simple steady-state divertor target of the monoblock type. A brazed joint between the cooling tube and CFC tile should be avoided and the cooling tube should be able to support unaided the eddy current forces originating in a tokamak during plasma disruption.

The main uncertainty initially was whether sufficiently good heat contact between the cooling tube and CFC block could be achieved just by clamping. To improve the heat transfer, an interlayer of soft copper and a high contact pressure were chosen. The annular geometry favoured this concept since the high machining precision achievable guaranteed good contact mating. The Cu interlayer was realized by a 0.5 mm thick galvanic coating of the cooling tube, subsequent machining and heat treatment to re-soften the Cu. To achieve a high contact pressure, the CFC block was slotted and clamped with bolts against the Cu surface. Changes of the bolt forces due to thermal cycling were reduced by adding disk springs (Fig. 7.2).

A copper-coated steel tube with inner diameter 20 mm and wall thickness 1 mm was chosen for the first heat flux tests, dedicated mainly to the properties of the clamped thermal contact. The CFC blocks were SEP N11.

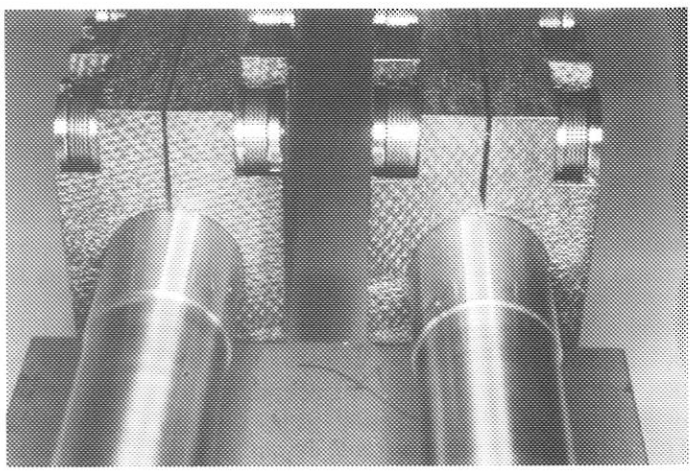

FIG. 7.2: Non-brazed CFC target (heat incidence on bottom surface).

Figure 7.3 shows the results of the irradiation tests carried out by FZ Jülich in the MARION ion beam facility. After 20 s irradiation with 10 MW/m^2 the CFC surface reaches a temperature of only 1400 °C despite the fact that about half of the temperature rise already originates in the steel tube. The surface temperature was measured with a pyrometer. Apart from the pyrometer, there were thermocouples measuring the temperature 5 mm underneath the surface of heat incidence.

Figure 7.3 also shows computational results (white points) for an ideal heat joint. The results are sensitively dependent on the assumptions for the heat conductivity of the CFC material. At the values warranted by SEP (220 W/m_K at ambient, 80 W/m_K at 1000 °C), the surface temperatures are about 40% too high. Inserting the 20% better values, which correspond to the expectations for good production conditions, yield good agreement with the measurements. In any case there is no indication that the non-brazed heat joint has any deteriorating influence.

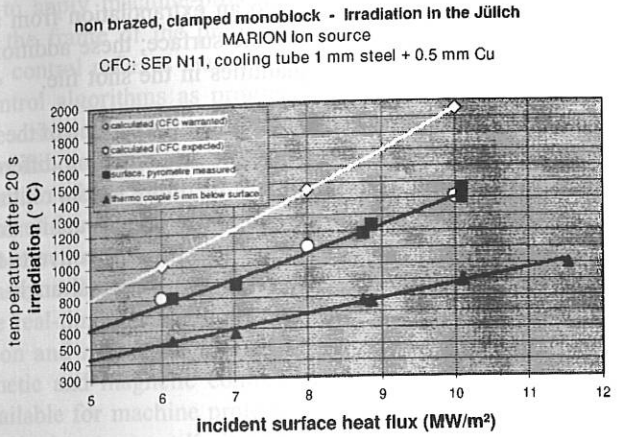

FIG. 7.3: Test results obtained with the non-brazed tiles after 20 s irradiation time.

7.3 Data Processing

New diagnostics and extensions of existing diagnostics were set up to meet special measuring requirements concerning the DV-II configuration, the machine security and other topics.

1. A new Rogowskii coil system beyond the divertor with 24 channels addresses halo currents in the vacuum vessel. Other halo current diagnostics with shunt resistors have also been extended.
2. The CAMAC equipment of the Langmuir probes was replaced by a complete set of Jorway modules having less channel crosstalk and allowing higher time resolution than before. This diagnostic now samples up to 70 MBytes per shot.
3. Two 20–channel recording systems for a novel optical diagnostics with spectral, spatial and very high temporal (1–2 μs) resolution were put into operation for investigating fast transport processes following pellet particle deposition.

By the end of the year the total amount of data acquired in a single shot was 500 MBytes.

Soft X-ray, Mirnov probes and some other multichannel diagnostics require higher sampling rates and doubling of channels. This increasing amount of data is not manageable without reducing the final storage requirements. For immediate data reduction by processing or filtering some effort has therefore been concentrated on systems doing data acquisition from the analog inputs directly into the main memory of conventional workstations or PCs. The intention is to use for this purpose commercially available systems with (multiple) powerful processors, large and cheap memories (of the order of several GBytes), and fast I/O channels. Two designs for PCI bus platforms were made:

1. A PCI compliant interface with eight "hotlink" input channels was developed and tested. Each input link is expected to have a minimum data rate of about 10 MBytes/s. This allows one to build up efficiently high-speed, point-to-point interconnects to the analog-digital converters with twisted pair, coax or fibre technology. In this configuration the analog channels can be well isolated from each other.
2. An S-Link [http://www.cern.ch/HSI/s-link/] project was launched to achieve a most cost effective DAQ system for a renewed ECE diagnostic at ASDEX Upgrade. Having the S-Link PCI interfaces and definitions available from the CERN HSI group made it possible to restrict the home-work required to a multiplexed ADC frontend [http://www.ipp.mpg.de/~Wolfgang.Suttrop/daq/].

7.4 Ion Cyclotron Resonance Heating

On the basis of the favourable results of the tests with a 3 dB hybrid circuitry, completed in 1997 and partly reported in Annual Report 1996, the ICRF system of ASDEX Upgrade was modified, the principle of the test setup being applied to the whole system: A first hybrid combined the power of two generators that have to be operated with a feedback-controlled phase difference of 90°, the second one splits this power to two antennas. The 4 generators and antennas of ASDEX Upgrade have thus been combined to two double systems with two generators, two hybrids and two antennas each. The hybrids, specifically developed for ASDEX Upgrade, can be operated within a frequency band between 30 and 60 MHz, corresponding to the fundamental cyclotron frequency O_c of hydrogen at a magnetic field >2 T and to the second harmonic 2 O_c at <2 T. Their length can be modified by shifting the frequency range to 37.5 - 75 MHz, corresponding to O_c at >2.5 T and 2 O_c at <2.5 T. The first experimental experience with the modified system showed that the whole ICRF operation is much more stable and much less sensitive to antenna coupling variations, and that a larger heating power can be achieved more reliably. Especially power reflections due to ELMs are largely compensated by the hybrids.

The further programme of ASDEX Upgrade calls for more triangular plasmas, which will interfere with the lower half of the present antenna. Antenna modifications were therefore developed to allow plasmas of moderate triangularity as well as the hitherto used Single Null plasma. The deterioration of the antenna coupling, unavoidable due to the larger average distance of the antenna to all plasmas, could be limited to about 30% by an increased antenna depth, made possible by some vessel modifications. The redesign of the antenna has nearly been completed; the antennas are to be modified in the summer shut-down 1998.

The technical conditions for Ion Cyclotron Current Drive at ASDEX Upgrade were investigated for application in the planned

advanced tokamak programme. The required phase difference between antenna loops can be achieved by adequate feeding connections between the hybrids and antenna loops by making use of the 90° between the hybrid outputs. In addition, the mutual coupling between the antenna loops must be compensated to avoid phase variations and asymmetries of the power launched from the loops.

7.5 Electron Cyclotron Resonance Heating

An ECRH system with f = 140 GHz, P = 2 MW (4 gyrotrons), T = 2 s is under construction. Details of this system can be found in previous annual reports.

Two gyrotrons are now installed and have already been used in the experiments. They were successfully operated via one modulator with cw pulses and with on/off modulation up to 1 kHz, both with 2 s pulses into loads and into the plasma. Higher modulation frequencies of up to 30 kHz, synchronized by Mirnov signals as necessary for the stabilization of MHD modes, were realized by reducing the beam voltage only partly so that the oscillation in the gyrotrons continues at a very low level. However, if both gyrotrons are connected simultaneously, this leads to severe loading of the modulator tube anode, restricting the useful time for this mode of modulation to 100 ms.

The available power is transmitted via two transmission lines with 8 quasi-optical mirrors and oversized waveguides with ≤3 mitre bends. The transmission loss determined by calorimetric measurements was 16%, which is compatible with the 11% estimated for the components. The power available in the plasma is further reduced by the losses incurred by the vacuum window and the two mirrors inside the torus, estimated together at 9%.

The microwave beams are highly focused in the plasma and result in a power deposition profile 5 cm wide at half power, even when the beams are obliquely launched for off-axis deposition. This allows one to investigate local electron heat transport and the impact of very localized power deposition on global confinement (/197,274/).

By means of two corrugated mirrors the polarization of the microwave beams can be changed to practically any linear or elliptical polarization. This is necessary to excite the proper second-harmonic X-mode, which has practically complete single-pass absorption, in order to achieve a narrow power deposition profile, particularly in the case of non-radial launching.

The two gyrotrons for the second part of the system were considerably delayed and are now expected to be delivered in spring 1998 and to be available for experiments in autumn 1998. The modulator unit for these tubes is ready, the launching mirrors are installed in the torus, and the transmission lines are under construction. This second part of the system can be operated independently of the first part, in particular with respect to modulation. In experiments on the stabilization of MHD modes we can thus launch the waves with the proper phase of the modulation determined by the toroidal location of the mirrors and the rotating MHD mode.

7.6 MHD Equilibrium Identification

For the DV-II configuraton the FP algorithm had to be changed: 48 magnetic measurements are now taken into account and the procedure was extended to the regression of 88 scalar quantities. In particular, the regression of the strike points on the new DV-II target plates had to be entirely new: besides the regression of z along the curved target plate surface, there is also regression of virtual strike points along two vertical and one horizontal lines. It turned out that the regression along the curved surface was less accurate; therefore, we do an extrapolation from the virtual strike points to the target plate surface; these additional variables are added to the 88 quantities in the shot file.

It turned out that a unique coordinate along the surface of the divertor plates is an appropriate platform for comparing different diagnostics. The libKK public library therefore stocks routines which deliver this coordinate as well as the other graphite contour data (kkGCdd). Another routine (kkGCSrza) converts the above-mentioned s-coordinate to (R,z) and a normal angle on the surface.

8. CORE PLASMA PHYSICS

8.1 Plasma Control

With the new DV-II installed, control of the strike point position had to be adapted to the new geometry. While the former - open - divertor was made up from two planar plates more or less perpendicular to the plasma legs, the new closed V-shaped divertor design is an assembly of curved modules spreading almost tangentially to the plasma legs.
The tangential alignment makes the strike point position very sensitive to small plasma displacements. A further problem is the curved shape of the divertor surface, which gives rise to strongly varying, position-dependent gains of the controlled circuit. The solution was to define the target coordinates for strike point control as straight vertical lines approximating the divertor shape instead of using the actual local curved coordinate . Strike point control is realized as part of the multivariable plasma shape control with a matrix PI-controller where the integral component ensures stationary accuracy. Adjustment of the two strike point positions is decoupled and the tracking behaviour is that of a first-order lag with a time constant of 100 ms.
In addition to standard plasma position and strike point control, shape control was recently augmented with control of the inner plasma radius utilizing an additional coil (V1o) in the control loop. Tracking, decoupling and disturbance rejection showed very good performance with transient deviations of less than 1 cm in the presence of β_{pol} steps of 0.2 and a radial shift of the outer plasma radius of 1 cm. In order to relieve the V2o and OH2u coils, which operate close to their operational limits, from current variations due to β_{pol} and l_i changes, partial disturbance compensation using the V3o and V3u coils was added in an experiment. Since the operational window of the PF coil system is a permanent problem, this method is destined to be

used more frequently in future. Note that for the first time all available active coils of the ASDEX Upgrade experiment were engaged in the feedback control loop.

Moreover, the kinetic controller was extended by an additional control reflex layer. Control reflexes are single or multi feedforward or feedback processes. Reflexes are started automatically on the occurrence of technical or physical events or states and also terminated automatically after completion of the control action at given times or states. The purpose of control reflexes is to apply machine-protecting or plasma- stabilizing actions in the frame of the programmed discharge schedule. To do so, control reflexes may override any feedforward or feedback control algorithms as programmed by the experimentalist for the discharge. However, depending on the discharge goal, in specific discharge phases the experimentalist may have to select specific sets of control reflexes waiting for execution. A reflex control layer was introduced to manage transitions. If reflex processes realize that attempts to re-stabilize the machine or plasma will not be successful, the reflex control layer informs the real-time discharge supervisor of the loss-of-stability situation and requests a change in the overall discharge goal for kinetic and magnetic control. Currently, control reflexes are available for machine protection when approaching or exceeding the input energy limit, or for plasma stabilization to prevent radiation collapse situations or suppress Marfes occurring.

8.2 Global Energy Confinement at High Density

The global confinement time of the H-mode degrades when the density increases by gas puffing. It was shown in the Annual Report 1996 that the degradation with increasing neutral density (n_0) in the main chamber or divertor occurs according to $\tau_{th} \propto n_0^{\approx -0.1}$. For high values of n_0, corresponding to a density of about 90% of the Greenwald limit, the H-mode confinement time takes values close to those of the L-mode. This is a dramatic expression of the influence of edge parameters on the core. It must be stressed that we do not attribute this effect directly to the neutrals but to the values of the edge density and temperature under such conditions, as documented in another section.

Recent analysis of the database yields the following scaling expression for type-I ELMy H-mode in ASDEX Upgrade:

$$\tau_{th} \propto I_P^{0.67} P_{heat}^{-0.56} \bar{n}_e^{+0.48} n_0^{-0.12}$$

where P_{heat} is the net heating power. The B_T dependence is not significant. The positive density dependence is compensated at high densities by the negative dependence of the neutral density. This is illustrated in Fig. 8.1, in which we also indicated type-III ELMs and results with radiative mantle (CDH mode). It must be sressed here that the increase of τ_{th} with density in the low-density region does not occur in situations in which the density is controlled, but results from the widely observed coupling between energy and particle confinement. In contrast, the degradation with neutrals occurs under conditions where the density is controlled by gas puffing, causing the increase of n_0. Figure 8.1 also indicates that type-I ELMs could not be sustained at densities above $\approx$ 70% of the Greenwald limit. High densities with good confinement can only be achieved with highly radiative mantle, which means type-III ELMs or CDH mode. As discussed earlier, the good CDH-mode confinement comes partly from the density peaking occurring under such conditions.

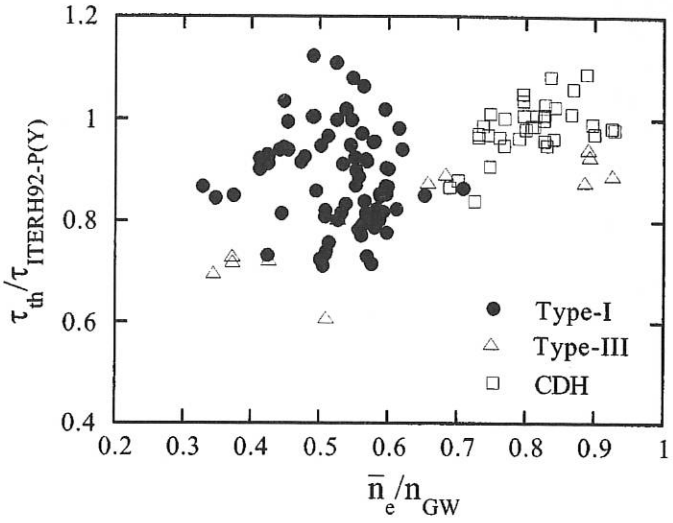

FIG. 8.1: Thermal energy confinement time normalized by an ELMy H-mode scaling (ITERH92-P(Y)) versus density normalized to the Greenwald limit. Data from discharges in deuterium with I_p = 1 MA, 2T $\leq B_T \leq$ 2.5 T and 2 MW $\leq P_{heat} \leq$ 9 MW.

8.3 H-mode Density Limit

While the L-mode density limit is believed to be well understood at least qualitatively as an edge thermal instability limit (Marfe), the H-mode limit is still not completely clarified. One explanation, recently proposed by F.W. Perkins connects the H-mode limit (i.e. the H→L-mode back transition) with the attainment of the ballooning limit, i.e. critical pressure gradients at the edge. Another attempt is discussed by K. Borrass, who correlates the limit in both the L- and H-mode with the achievement of full divertor detachment. During density increase by means of gas puff H-mode discharges exhibit type-I ELMs well above the L→H threshold. At higher densities, the phases between the ELMs detach and, as recycling continues to increase, the ELMs change to type-III before the H→L back transitions happen. In the approach to the type-III phase the edge densities n_e^{sep} and $\bar{n}_e^{SOL}$ saturate. In parallel, the edge electron pressure and pressure gradients decrease smoothly, reaching values at the H→L back transition significantly below the ballooning limit. In general, the edge data show a stronger correlation of the density limit characteristics with divertor detachment than with attainment of the critical edge pressure gradient.

8.4 High-field-side Pellet Injection

The development of high-density, high-performance scenarios is still a key element of the ASDEX Upgrade programme. Experimentally, the most direct method to achieve high line-averaged densities beyond the Greenwald limit is the injection

of cryogenic hydrogen pellets. In this way stationary H-mode operation was demonstrated, albeit with reduced H-mode quality. A disadvantage of the standard pellet injection scheme relying on pellet launch from the (easily accessible) torus outside (LFS) is that with increasing heating power the fuelling efficiency drops significantly, this being accompanied by a confinement drop. Fortunately, this deficiency can be removed to a large extent by high-field-side (HFS) injection, as recently shown on ASDEX Upgrade.
In this scheme the ablatant acceleration, directed towards the plasma centre, was expected to inhibit particle losses and even allow deeper penetration. During HFS injection, fuelling efficiencies were high and showed no degradation with increasing heating power. Moreover, deeper penetration of the frozen pellet was observed for HFS injection with respect to LFS pellets. This was attributed to precooling in front of the slowly travelling pellet resulting from the high-β plasmoid moving ahead of the pellet.

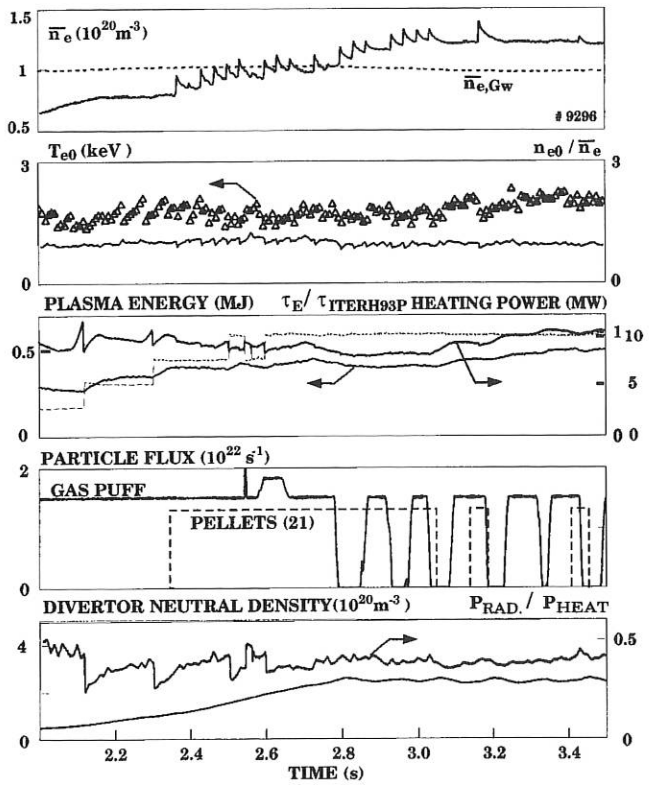

FIG. 8.2: Density control by HFS pellet refuelling. The line-averaged density (upper trace) is adjusted to a value of 1.2 x 10^{20} m^{-3} by pellet injection. The pellet particle flux had to be supported by gas puffing in order to allow the required density build-up on time. No significant degradation of the energy confinement occurs during the pellet sequences.

A discharge with HFS pellet injection, performed to demonstrate feedback-controlled operation beyond the Greenwald limit, is shown in Fig. 8.2. Thus, the original scheme injecting pellets in the horizontal plane was altered, causing the injection path to incline 44° to the horizontal plane towards the plasma centre. Due to technical limitations (240 m/s, 30 Hz), the pellet repetition rate and hence the pellet particle flux injected were less than half the values available during the LFS injection scheme.

HFS pellet injection was not yet sufficient to realize the required density increase (to $\bar{n}_e$ = 1.2 x 10^{20} m^{-3}, approximately 1.2 x $\bar{n}_{e,Gw}$ for the plasma configuration used), making additional gas puffing necessary. However, strong gas puffing causes degradation of the energy confinement, the detailed physical origin of which is not well known. Consequently, minimization of the additional gas puffing was tried in order to achieve maximum energy confinement. Thus, in a first attempt $\bar{n}_e$ was increased and feedback-controlled at a high level beyond the Greenwald limit by pellet injection, while a constant gas puff was maintained. With increasing plasma density and recycling fluxes, the energy confinement gradually degrades as with gas puff only. In an alternative approach, the divertor neutral pressure was raised and then kept constant by feedback-controlling the external gas puff. In a second, independent control loop the line density was controlled at a high level beyond the Greenwald limit by interrupting the pellet train as required. Again, the energy confinement gradually degrades with increasing neutral pressure, whereas at too low gas puff rates the required density level could not be reached. In the discharge shown, #9296, the optimum condition at the available pellet rate was realized with a neutral pressure just sufficient to allow the required density increase while retaining the best available energy confinement. During the pellet sequence, no central cooling and also no significant density profile peaking occurred; a constant deposition profile was also maintained. However, it should be noted that the discharge shown in Fig. 8.2 was contaminated by a strong influx of carbon after t = 2.7 s, causing an increase in Z_{eff} of approx. 1.
Advances are being made to improve the injection setup with respect to the maximum available pellet repetition rate and hence pellet particle flux. The aim is to enhance the pellet particle rate further in order to gain greater headroom for a decrease in gas puff and hence still better confinement.

8.5 Central Impurity Transport in ASDEX Upgrade H-mode Discharges

In earlier investigations of the radial impurity transport in the confined plasma the diffusion coefficient was found to decrease towards the plasma centre. The central D was in in the range of 0.3–0.6 m^2/s for H-,CDH- and L-mode discharges. These measurements were time-averaged and did not distinguish between 'undisturbed' radial diffusion and the additional transport caused by sawtooth instabilities. Here, the central impurity transport of intrinsic low-Z and injected high-Z impurities (tungsten) in the time interval between sawtooth crashes and the effect of the sawtooth crashes were treated separately. Three soft X-ray cameras served as the main diagnostic tool, with up to 90 line-of-sight measurements being made to get defolded radiation profiles. Using time-averaged data with a time resolution of $\Delta t \approx 1$ ms, the measured line-of-sight radiation fluxes could be described by an emissivity profile that is constant on flux surfaces. With the measured n_e and T_e, the emissivity profiles could be transformed into impurity profiles for poloidal flux labels $\rho_{pol} \leq 0.5$ by using the corona equilibrium radiative power coefficient in the soft X-ray range.

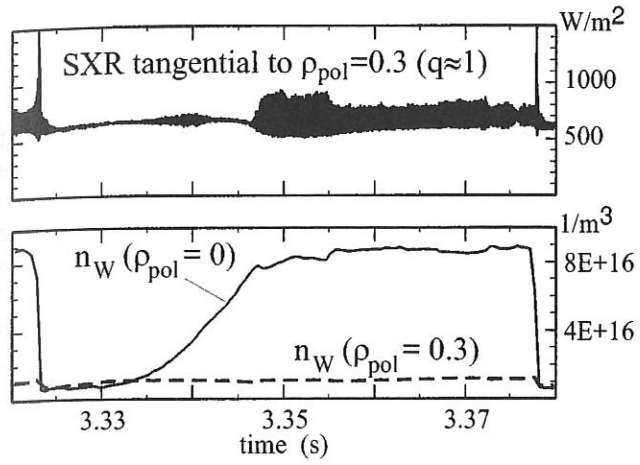

FIG. 8.3: Between two sawtooth collapses the tungsten profile inside the q=1-surface becomes strongly peaked. The peaking stops with the onset of an m=1,n=1-mode.

From the temporal evolution of the impurity profile after a sawtooth crash we evaluated the central diffusion coefficient D and the drift velocity V. In H-mode discharges with high heating power the impurity profile reaches equilibrium long before the next crash. This equilibrium profile could be used to get another measure of the ratio of V/D. The central D was found to be ≈ 0.1 $m^2 s^{-1}$ for low- and high-Z impurities. The drift velocity was always directed inward and for low-Z impurities a value of V/D ≈ 6 m^{-1} at $\rho_{pol} = 0.2$ was extracted from the temporal evolution and equilibrium profile. In the investigated discharges with continuous tungsten laser blow-off the tungsten profiles were strongly peaked for $\rho_{pol} \leq 0.3$, i.e. approximately inside the q = 1 surface, with values of V/D in the range of 50 m^{-1} at $\rho_{pol} = 0.2$. This value, however, depends on the mode activity at the q=1 surface (see Fig. 8.3). Since the sawtooth period is long in relation to the equilibration time of the impurity profile, the mean impurity profile is only weakly influenced by sawtooth collapses. Each crash expels the impurities from the plasma centre and leads to a flat or slightly hollow profile directly after the crash. However, tungsten is mainly expelled to the low-field side, resulting in profiles with a high poloidal asymmetry after the crash.

8.6 Variation of Sawtooth Activity with ICRF Heating

In large plasma experiments, ion cyclotron resonance frequency (ICRF) heating provides a quite localized power source for ions and/or electrons. By judiciously choosing the frequency, magnetic field and plasma composition, it is possible to select the repartition of the power between electrons and ions, and the location of the heating. The influence of these effects (repartition of the power and its location) on sawtooth activity was investigated. It is usually observed that increasing the central electron temperature lengthens the sawtooth period, whereas fast ions in the centre can lead to complete stabilization of the sawteeth. Minority current drive near q =1 has been used on JET to exert a strong effect on the sawteeth.
In ASDEX Upgrade, in ICRF-heated discharges using H in D minority heating (H in D) the sawtooth period is changed 50% by a displacement of the resonance by only 5% of the major radius. More central heating results in larger temperature excursions and a longer sawtooth period. Experiments with He3 in H in which the concentration of He3 was varied covered the range from mode conversion heating to minority heating, thereby changing the share of power between electrons and ions. The location of the power deposition also changes. Both shortening and lengthening of the sawtooth period were achieved, modifying the sawtooth period by a factor of over 4. Fig 8.4 shows the time traces for a discharge with 1.7 MW of NI heating and 2 MW of ICRF heating at 30 MHz. The magnetic field at R = 1.65 m is 2.7 T. The majority gas is H. At t = 2.4 s, a He3 pulse of 1.35×10^{20} He3 atoms is added, after which the concentration is allowed to decay. Prior to the He3 pulse, the heating is direct e-heating through the fast wave. After the pulse the sawtooth period shortens from 38 ms to 22 ms, but then it lengthens again to 48 ms. Figure 8.5 shows the change of the sawtooth period for this discharge and for a different discharge with a larger He3 pulse (2.7×10^{20} atoms). In the latter case the shortened sawtooth period is maintained up to the change in ICRF power.

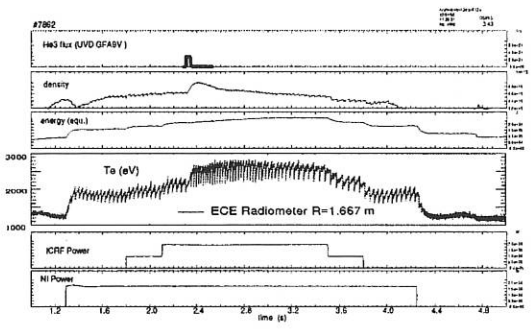

FIG. 8.4: Time traces for the flux of He^3, line-averaged density, electron temperature, ICRF power and NI power.

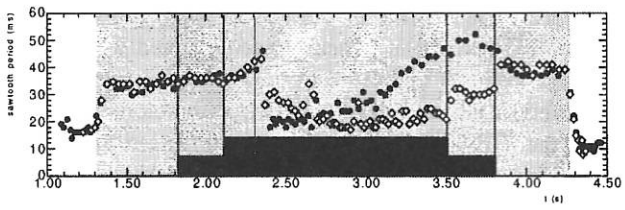

FIG. 8.5: Variation of the sawtooth period, for low (closed symbol) and high (open symbol) He^3 gas puff.

The He3 concentration is estimated to vary from 12% to 6% for the first discharge, and from 6% to 3% for the second. At high He3 concentration, the heating scenario is mode conversion heating leading predominantly to direct heating of the electrons, whereas at low concentration minority heating dominates.

8.7 Disruption Investigation

A large number of disruptions in flat-top were analyzed to find the technical causes, physical mechanisms and precursors of the

disruptions. This analysis is being used to develop avoidance strategies, recognition algorithms and mitigation techniques (killer pellet).
We identified an initiating cause of all the disruptions analyzed; in addition, most of the disruptions were found to be attributable to some external technical or operational causes (as "planned density limit, with and without NI" or "density limit after NI turned off") and could be regarded as avoidable. The result of this analysis is summarized in Fig. 8.6:
Several detailed causes were idendified (indicated by code numbers) and subdivided into five major groups. Procedures were set up to avoid specific kinds of disruptions.

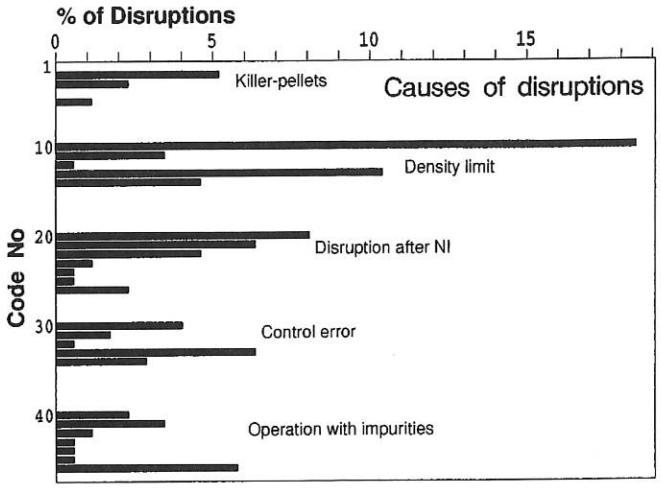

FIG. 8.6: The disruptions are subdivided into five major groups according to their cause. Each specific cause is indicated by a code number (not further described in this report).

The better known chain of mechanisms leading to disruption is triggered by cooling of the plasma edge: the increased resistivity of the edge causes peaking of the current profile (increase of l_i) and growth of the m = 2/n = 1 islands at the q = 2 surface. The cooling of the plasma edge can be achieved in different ways and is typically accompanied by a Marfe in the X-point region. The onset of the cold-edge regime leading to a disruption can easily be identified with bolometer channels viewing the X-point region and with information from the $l_i(q)$ stability diagram. The majority of our disruptions (90%) can be interpreted according to this mechanism and automatically recognized. The remaining 10% of disruptions are mainly discharges with planned or accidental impurity accumulation, or disruptions after density control with pellets which also have an easily detectable predisruption phase.

9. SOL and DIVERTOR PHYSICS

The major subject of SOL and divertor physics in 1997 was concerned with the initial operation of Divertor II and comparison with Divertor I, described in Chapter 2. Here those items are described which are of general interest.

9.1 Interaction of Charge Exchange Neutrals with the Main Chamber Walls

The fluxes and energy distributions of the charge exchange (CX) neutrals are measured at specific locations in the tokamak ASDEX Upgrade as functions of the discharge conditions. Evaluation of the plasma-wall interaction calls for a knowledge of the energetic neutral fluxes and their energy and angular distributions at all poloidal and toroidal locations. For ASDEX Upgrade these are obtained from B2–EIRENE computer simulations taking the experimental results into account. The CX fluxes Γ_{cx} and the shapes of the spectra vary strongly around a poloidal cross-section. This strongly affects wall erosion by sputtering and hydrogen isotope implantation into the vessel walls.

The sputtering of the actual carbon wall and the effect on possible wall materials such as tungsten, beryllium, TiC and SiC are expressed by an effective erosion yield Y_{eff} obtained by multiplication of the energy-dependent CX fluxes by the appropriate energy-dependent sputtering yields. For carbon walls the formula by Roth and Garcia-Rosales including chemical erosion was used, while for the other materials the Bohdansky formula for physical sputtering was applied. Integration over all energies yields the sputtered flux Γ_{sp} and $Y_{eff} = \Gamma_{sp}/\Gamma_{cx}$.

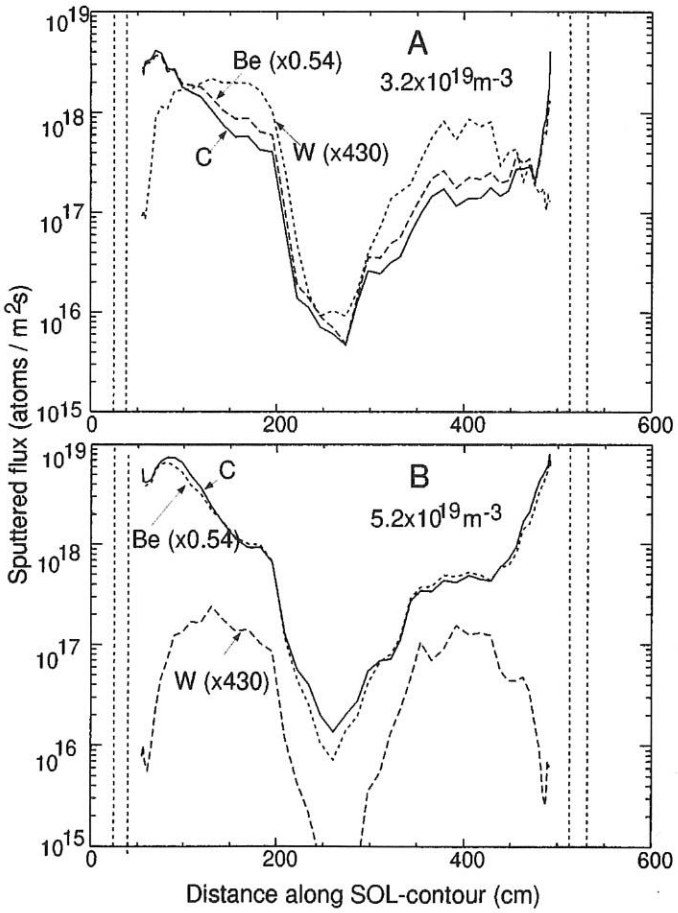

FIG. 9.1: Hydrogen discharge #7888: sputtered flux Γ_{sp} versus distance along the SOL contour for C (solid), W (dashed) and Be walls (dotted) for (A) $n_e^{sep}=3.2\times10^{19}$ m^{-3} (attached plasma) and (B) $n_e^{sep}=5.2\times10^{19}$ m^{-3} (detached plasma).

In Fig. 9.1 the sputtered fluxes for a carbon wall are compared with those for assumed W and Be walls at two different densities. The sputtered fluxes are shown along the SOL contour around the plasma cross-section from inside to outside, starting at the divertor X-point. In order to facilitate material comparison the sputtered fluxes in Fig. 9.1 were multiplied by factors given by the tolerable impurity concentration in the plasma with respect to carbon.

For low density and high mean energies of the CX fluxes the normalized W fluxes are very similar to those of carbon and beryllium. While the sputtered fluxes of carbon and beryllium increase with increasing density, the integrated W flux decreases by almost an order of magnitude. This is due to the decrease of the mean energy of the CX fluxes at higher densities combined with the high threshold energy for W sputtering. Concerning erosion and impurity production, W walls should be considerated, especially as cladding of the area just above the divertor. Be, from this point of view, offers no advantage over carbon.

9.2 Separatrix Position Tested by SOL Model

A 1.5–D model assuming electron heat conduction along field lines to be the dominant mechanism for the power flow in the Scrape-Off Layer predicts the temperature at the separatrix ($T_{e,mod}$) and the exponential fall-off length λ_{Te} for the temperature profile in the SOL. The following formula for the separatrix temperature $T_{e,mod}$ can be derived:

$$T_{e,mod}\,[eV] = \alpha \left[\frac{P_{SOL}\,[W] q_{95}^2}{\lambda_{T_e}\,[cm]} \right]^{2/7}$$

where P_{SOL} denotes the power crossing the separatrix. The parameter α involves geometric factors and is determined by a linear regression fit. Such a fit ($R^2 = 0.93$) applied to a set of discharges covering almost the complete operational space of ASDEX Upgrade delivers $\alpha = 0.5$, where the approximation $P_{SOL}=P_{heat}-P_{rad}$ was used.

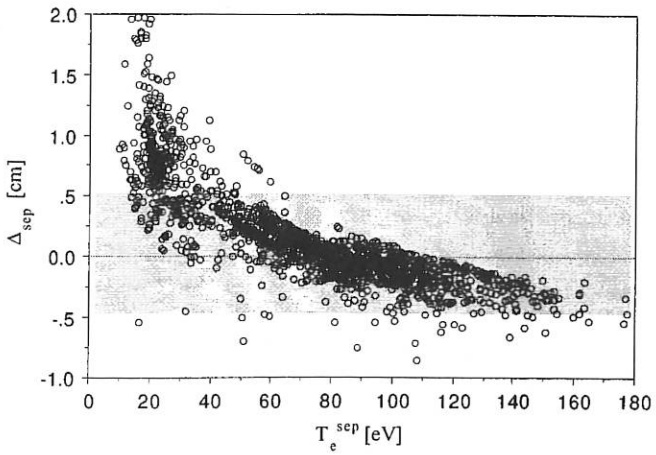

FIG. 9.2: Necessary shift Δsep in separatrix position to achieve $T_{e,sep} = T_{e,mod}$. The grey area indicates a reasonable error in the magnetically determined separatrix position.

The $T_{e,mod}$ values cover a range from 30 - 115 eV, whereas the measured $T_{e,sep}$ values occur between 20 and 180 eV (Fig. 9.2). Assuming the difference in the two T_e values to be due to an inaccurate, magnetically defined separatrix position, one can estimate a shift D_{sep} of the latter by $\Delta_{sep} = \lambda_{Te} \cdot [\ln(T_{e,mod}) - \ln(T_{e,sep})]$. Most Δ_{sep} values are located within 5 mm (see grey area in Fig. 9.2) in the high-temperature range ($T_{e,sep} > 40$ eV), which corresponds to the error in the magnetic separatrix position. For lower temperatures, however, shifts of up to 1.5 cm would be necessary to identify the $T_{e,mod}$ value in the measured T_e profile. This systematic increase of an inside shift of the separatrix position for lower T_e indicates the limit of applicability of the assumed model.

10. DIAGNOSTICS

10.1 Spectroscopy System in DV-II

In the course of replacement of DV-I by the new DV-II in 1997 the entire divertor spectroscopy was also reconstructed to a large degree. On the one hand, the line-of-sight arrangement was adapted to the changed geometry of the divertor plates. With the new sets of poloidally and toroidally viewing lines of sight it was possible for the first time to investigate the outer and the inner divertor of ASDEX Upgrade separately. On the other hand, a complete glass fibre coupling system offers the flexibility of connecting each line of sight to any of the spectrometers, providing different temporal, spectral and spatial resolutions. The overall number of 160 lines of sight used to investigate the divertor plasma can be divided into the poloidal (Fig. 10.1) and toroidal groups.

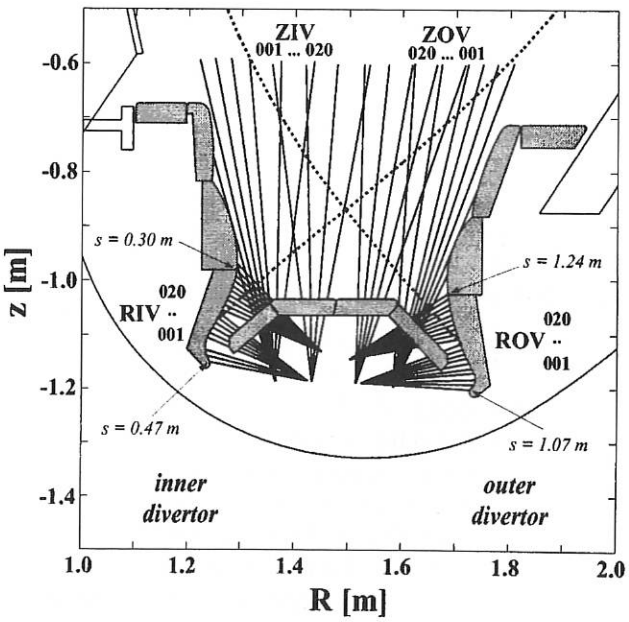

FIG. 10.1: Poloidal lines of sight in DV-II; for orientation a separatrix and the s-coordinates of some relevant points are included.

For more clarity the s-coordinate at some points and a 'typical' separatrix (dashed) are added. The toroidal chords and their applications are described in the contribution of the IPF Stuttgart. The poloidal system (10.1) consists of chords directed vertically (ZIV, ZOV) and horizontally (RIV, ROV) in the poloidal plane. With the latter, the strike-point regions of the inner (RIV) and of the outer (ROV) divertor tiles are observed. They are mainly used for measuring spatial emissivity profiles, ion temperatures and electron densities and temperatures near the surfaces. In addition, the Z-chords cover the region from the outer to the inner plates, including the X-point.

10.2 Bragg Crystal Spectrometer

As impurities emit line radiation and therefore cool the plasma, measurements of impurity concentrations are necessary. Due to central plasma temperatures of several keV, plasma impurities are highly ionized and emit line radiation with wavelengths in the X-ray region below 0.2 nm.

A Bragg crystal spectrometer is mounted on ASDEX Upgrade as shown in Fig. 10.2.

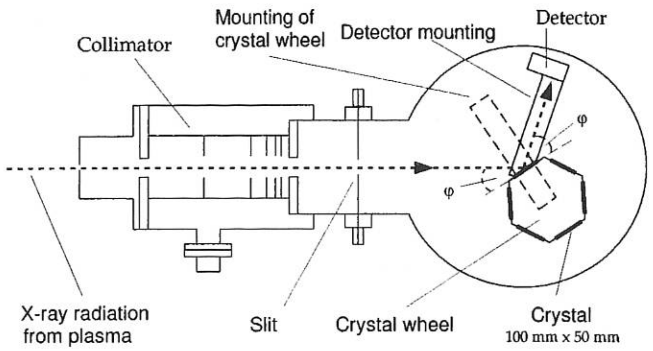

FIG. 10.2: Scematic view of the Bragg spectrometer.

It makes use of the fact that crystals irradiated with polychromatic X-rays reflect only the fraction which satisfies the Bragg equation. By rotating the crystal during a plasma shot with angular velocity ω and the detector with angular velocity 2ω X-ray spectra are obtained. To observe the temporal evolution of specific emission lines, both, the crystal and detector are kept fixed at angles ω_0 and 2 ω_0, respectively.

In order to obtain measurements of impurity concentrations, the spectrometer was absolutely calibrated. With this aim in view, the efficiencies of all components were determined by means of integrated reflection efficiencies and mass absorption coefficients from the literature. The result of this calculation was compared with the already calibrated oxygen monitor and a semiconductor detector of the Si(Li) type. From absolute intensity measurements of ionic lines impurity concentrations of fluorine and oxygen were calculated by comparison with results of the STRAHL code.

10.3 Motional Stark Effect Diagnostic

The motional Stark effect (MSE) diagnostic for determining the current density profile of ASDEX Upgrade is nearing completion. Ten spatial channels measure the local pitch angle near the magnetic midplane between the plasma centre and edge using one of the 2.5 MW heating beams. Several measures were taken to maximize the signal-to-noise ratio, which include large apertures, optical fibres with a high numerical aperture, and low-noise current amplifiers for the photo multiplier tubes. First measurements of the beam emission spectrum show that sufficiently high signal levels can be achieved (Fig. 10.3).

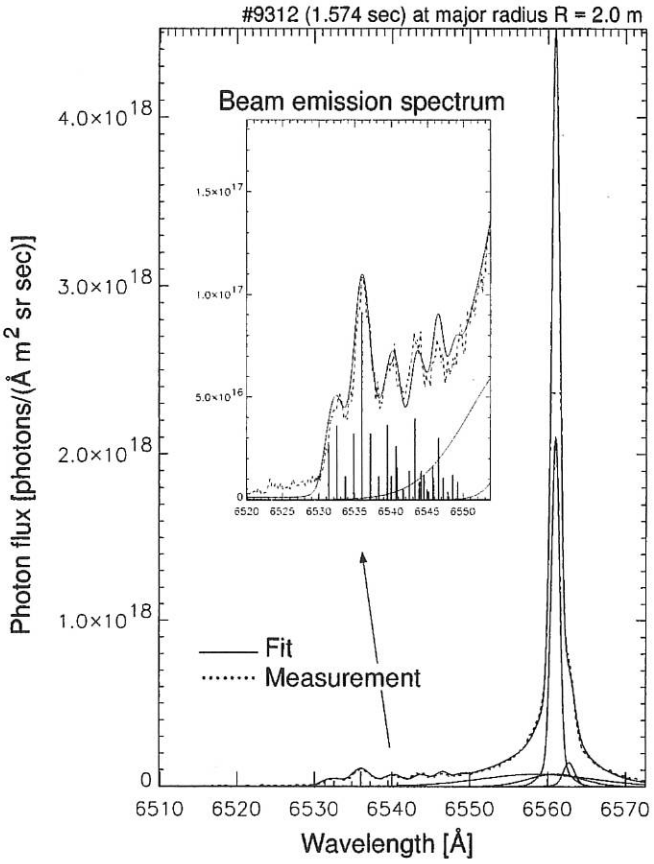

FIG. 10.3: *Spectrum of the Doppler shifted Balmer-α beam emission. The strong spectral line at the right is a superposition of D_α and H_α radiation from the plasma edge and passive and active charge exchange emission mainly from deuterium. The σ-lines of the full energy component, which is the most prominent peak in the insert, is used for the MSE diagnostic.*

The current profile is derived from the measured MSE polarization angle with the equilibrium code CLISTE. First simulations have shown that, including ten MSE channels, the number of shape parameters of the current profile can be increased from two to eight.

INTERNATIONAL COOPERATION

The collaboration with other international institutes and universities was considerably extended. Besides the below-mentioned collaborations there was cooperation with the following institutions: Istituto de Fisica del Plasma, CNR (Italy); Ecole Polytechnique Fédérale, Lausanne (Switzerland); University of Strathclyde (Scottland); FOM-Institute voor Plasmafysica, Rijnhuizen (Netherlands); Centre Canadien de Fusion Magnétique, Varennes (Canada); University of Toronto (Canada); Institute of Applied Physics, Nishni Nowgorod (Russia); I.V. Kurchatov Institute of Atomic Energy, Moskau (Russia); IOFFE Institute, St. Petersburg (Russia); Institute for Plasma Research, Bhat, Gandhinagar (India); Southwestern Institute of Physics, Chengdu (China); Institute of Plasma Physics, Academia Sinica, Hefei (China); Korea Basic Science Institute, Yusung (Korea); NIFS, Nagoya (Japan); Kuo University, Yokohama (Japan).

1. DOE – ASDEX Upgrade Activities

The collaborative activities within the IEA ASDEX Upgrade Implementing Agreement have continued effectively in 1997. This year the collaboration was primarily through personnel exchanges in several areas of tokamak research including spectroscopy of high-Z impurities and divertors, energy transport, ICRF, and materials. These exchanges involved scientists from MIT (Alcator C-MOD), General Atomics (DIII-D), University of Maryland, Oak Ridge National Laboratory, Lawrence Livermore National laboratory, Sandia Albuquerque Laboratory in the U.S. and IPP Garching (ASDEX Upgrade) from Germany. The exchanges were in both directions on a wide range of activities including coordinated experiments, theory, materials testing, and hardware development.

This year the Executive Committee (E.C.) decided not to hold a technical workshop associated with the annual meeting of the E.C. since a part of the collaborative experiments was discussed at the IAEA Technical Committee Meeting (TCM) on H-Mode. The Executive Committee was held at the occasion of this IAEA TCM at Kloster Seeon, Germany on September 22, 1997. Among the topics of discussion was a suggestion for possible realignment of the IEA Large Tokamak Agreement with the shutdown of TFTR which would also include ASDEX Upgrade, DIII-D, and C-MOD together with JET and JT-60U to create a family of divertor tokamaks. The Executive Committee also discussed the participation of non-member countries (Mexico, South Korea, and China) in the IEA ASDEX Upgrade Agreement.

The IEA ASDEX Upgrade collaboration continues to be beneficial to both sides, bringing together scientists from many institutions working together on common scientific and technical issues. This year a coordinated data analysis was initiated between Alcator C-MOD, ASDEX Upgrade, and DIII-D to further our understanding on transport. IPP scientists participated in the DIII-D operation through remote operations.ORNL, IPP Garching and GA shared information on testing of hardware for the ICRF systems used on DIII-D and ASDEX Upgrade. In addition to these, there is extensive interaction between the ASDEX Upgrade and the U.S. programs through the ITER Physics Expert Group activities, especially in the area of divertor and edge physics. These type of collaborations are expected to increase next year and contribute to the world fusion program.

2. CEA, Cadarache

Six working groups were established where ASDEX Upgrade, W7X and CEA Cadarache collaborate: confinement and turbulence, plasma-wall interaction, control and data acquisition for long pulse discharges, ECRH physics and technology, negative ions and ITER satellite.

3. University of Cork, Ireland

The collaboration with the University of Cork concerning MHD equilibrium identification using magnetic measurements was continued. Detailed studies between the different versions of FP and an interpretative equilibrium package "CLISTE" were started. The latter includes information from the presently installed MSE diagnostics and from rational q-values from SXR measurements.

4. DEMOKRITOS, Greece

The reciprocating Langmuir probe system (LPS) for the ASDEX Upgrade divertor had to be modified to access the new Divertor II-LYRA configuration. Radial scans in ohmic discharges have revealed profiles of plasma parameters (n_e, p_e) strongly shifted inward (5–10 cm) from the separatrix location in the inner divertor. These results are in good agreement with B2–EIRENE modelling calculations.

At medium-power NI-heated discharges a large difference between the parallel power flow recorded at the probe position and at the divertor tiles was observed. The reasons for this difference are still unclear.

The fluid equations for multispecies plasma including drifts and currents were derived and implemented into B2. A test scenario calculation for ohmic plasmas in Divertor II configuration has been performed.

5. Centro de Fusão Nuclear, EURATOM IST Association, Lisbon, Portugal

The goal of this cooperation is to operate and extend the FM reflectometry diagnostic system on ASDEX Upgrade. A focus of recent work has been to complete the diagnostics hardware and to develop data analysis techniques for density profile evaluation in presence of background plasma fluctuations.

Three new ADC boards with 4 channels at 250 Msamples/s have been developed and are tested under normal diagnostics operation conditions. The extension of the system with a W-band heterodyne reflectometer has started to extend the accessible density range. The existing V-band channels are being modified for heterodyne detection in order to increase the immunity of the system against signal loss due to scattering losses. A fixed frequency reflectometer has been installed to routinely monitor density fluctuations at the plasma edge. This system has the option to detect the L-mode to H-mode transition in real time which will be used for the plasma control system on ASDEX Upgrade.

6. UKAEA Culham, United Kingdom

The topics of collaboration were the H-mode threshold at low densities, the ideal and resistive MHD stability and the preparation of ECRH/ECCD stabilization experiments of magnetic islands.

7. Institut für Allgemeine Physik, TU Wien and Friedrich Schiedel Foundation

Collaboration with the Austrian Institut für Allgemeine Physik concerns the development and operation of the lithium beam diagnostic. These activities are made possible by financial support of the Austrian Friedrich Schiedel Foundation für Energietechnik. The current project contributes to the extension of the diagnostic potential by improving necessary atomic data bases for accurate raw data interpretation.

8. TEKES (HUT and VTT), Finland

The Finnish group are concerned with modeling by Monte Carlo and Fokker-Planck techniques the energetic ion behaviour in the plasma under the influence of electromagnetic fields. In a first step the confinement of ripple-trapped ions by a radial electric field, as observed in the experiments, was verified and fast time constants were demonstrated to be possible in this measurement. Investigations were started to model ion loss orbits under the influence of radial electric fields.

9. Inst. of Electronics, Res. Found. Hellas, Heraklion, Greece

1.5-D and 2-D Vapour Shield Modelling - IESL.FORTH, Heraklion, Greece (EURATOM Cost Sharing Action). Parametric studies were performed with the help of the 1.5-D code aimed at the effect of such factors as particle energy spectrum, drift, lateral expansion, and magnetic field strength on the erosion rate of divertor plates subjected to a disrupting plasma. The development of a self-consistent 2-D code was continued.

10. KFKI RMKI, Budapest, Hunbary

One guest scientist contributed considerably to the improvement and extension of the optical observation systems of the Lithium beam diagnostic. While an improved photomultiplier system records the Li(2p->2s) light emission for determination of density profiles, the new spectrometer-CCD-camera system detects local impurity ion emission profiles activated by charge exchange of ions with neutral lithium atoms.

Radiation of Light Impurities – Centr. Res. Inst. of Physics (KFKI), DFG Project 436 UNG 113/118
The collisional (non-equilibrium) radiation loss model was extended to include local reabsorption effects. The numerical model developed for computing the ablation rate of carbon pellets reproduced the penetration depths of carbon pellets measured in Stellarator W7-AS.

11. Cooperation with Russian Institutes

Pellet Ablation, Surface Erosion Phenomena - Technical University
St. Petersburg (WTZ Project Russ. 554-96): Electrostatic shielding phenomena with non-vanishing currents along the magnetic field lines were studied in a 1-D approximation. Results of impurity (neon) pellet shots in Asdex-Upgrade were reproduced by a quasi-three-dimensional code developed in the framework of this project.

Cooperation outside WTZ:
Technical University, St. Petersburg: Pellet injection – A fast framing camera system was adapted for installation at ASDEX Upgrade by a scientist from SPU. For an improved pellet detection system in the novel injection scheme from the magnetic high field side a concept was worked out at SPU.

Killer-pellet injector. A pellet injector, to be used for impurity pellets of 1-2.4 mm of diameter, was designed and constructed by a scientist from SPU.

12. CREATE Group, Napoli, Italy

The collaboration with the CREATE team concentrated on equilibrium identification for ITER using neural networks and function parametrization.

JET COOPERATION

(Head of Project: Prof. Dr. Michael Kaufmann)

In 1997 the experimental programme of JET concentrated on the preparation and execution of experiments where mixtures of deuterium and tritium were used as the plasma fuel. In contrast to the 11% tritium concentration used in each of the two discharges of the preliminary tritium experiment (PTE) of 1991, tritium concentrations of up to nearly 100% were used in the 1997 deuterium/tritium experiments (DTE1), allowing optimization of the plasma fuel mixture for maximum fusion power as well as enabling studies of isotope effects on plasma performance. The total amount of tritium on site was 20 g (compared with 0.2 g in 1991), and recirculation of the tritium through the tritium-processing plant allowed 99.3 g of tritium to be introduced into the neutral beam injector and torus. The DTE1 campaign was limited to a total number of 2.4×10^{20} neutrons in order to restrict machine activation and the time (1 year) during which manual intervention inside the machine is prevented.
The highest fusion power was achieved in a hot-ion ELM-free H-mode discharge yielding 16.1 MW of fusion power and a ratio of $P_{fusion}/P_{absorbed}$ of 0.66. The fusion energy reached a value of 13.8 MJ. The performance in these hot-ion H-mode discharges was limited by MHD events.
The high fusion power discharges provided about 3 MW of α-particle heating power. In a separate set of D/T experiments with constant heating power (10 MW) but varying concentrations of tritium, plasma heating by α-particles was demonstrated by observing that the largest increase of the electron temperature occurred in the plasmas which had the optimum tritium concentration (50%). No indications were found of α-particle-induced energy losses by driving toroidal Alfvén wave eigenmodes unstable.
Whereas hot-ion ELM-free H-modes exhibit an energy transport barrier at the plasma edge, discharges with optimized q-profiles can exhibit an internal plasma transport barrier (ITB). Application of a combination of lower hybrid frequency heating (LH) and ion cyclotron resonance frequency heating (ICRH) during the plasma current rise phase produces the ITB close to the q=2 surface, which can move radially outwards with time. The maximum D/T fusion power achieved in these discharges when heated with up to 19 MW of neutral beams and up to 6 MW of ICRF was 8.2 MW, with the plasma core being close to the β-limit; the central pressure is in excess of 3 bar at 3.45 T. ITB discharges show a high degree (50%) of non-inductively driven plasma current potentially opening new paths for high-performance steady-state operation in a tokamak. High steady-state fusion power was created in ELMy H-mode discharges. 4 MW of fusion power was sustained for 3.5 s corresponding to 8 times the energy confinement time and limited only by the duration of the heating power. A total of 21.7 MJ of fusion energy was produced. A clearly lower power threshold for the H-mode was observed in tritium discharges compared with deuterium discharges and this inverse mass scaling suggests that the ITER H-mode power threshold is about 70 MW, 25% lower than predicted earlier. The energy confinement, however, appears to be independent of or only weakly dependent on the isotope, this being quite different to the ITER scaling, which assumes a $M^{0.4}$ dependence. ELMs were also studied in D/T discharges. Differences from pure deuterium discharges were found to be small, although the frequency was somewhat lower in D/T. In general, ELMs are more benign (less power loss per ELM) when induced by ICRF heating as compared with NB heating.
So called ITER similarity pulses were carried out with the normalized plasma collisionality (n*) and pressure (β) kept constant and the normalized ion gyro radius (ρ*) varied to investigate the confinement scaling. Results indicate that core confinement exhibits gyro-Bohm-type scaling, whereas the plasma edge is more like Bohm scaling. Scaling to ITER suggests that ITER as it is designed would ignite.
Overall the DTE1 campaign at JET has produced a wealth of new and ITER-relevant data addressing many questions that need to be answered before the next-step machine can be constructed. It has also proved to be a considerable technical success, with the machine, diagnostics, heating, and gas-handling system working at a very satisfactory level of reliability. Further experience and progress will be made during the remote divertor tile exchange programme scheduled for the beginning of 1998 and in which the JET divertor will be modified to become an even more ITER-like device. For many years IPP has been contributing to the exploitation of JET scientific results as well as supporting the development and operation of JET diagnostic systems. The cooperation between IPP and JET has been intensified with the aims of finding an optimized discharge scenario for ITER and providing accurate predictions for the ITER design. Activities covered by three Task Agreements are presented in the following.

1. TASK AGREEMENT NO. 1

In 1997, IPP supported further optimization of pellet performance and diagnostics and contributed to considerations to improve fuelling efficiency on JET by providing pellet tracks for the inboard launch. However, the installation of the latter will be postponed to 1999 because of the high tritium levels in the torus after the DTE1 phase.
Before the DTE1 phase, first systematic attempts at injection of 4 mm pellets at 5 Hz and 250 m/s were made in order to raise the plasma density close to the Greenwald limit in type-I ELMy H-mode discharges with and without additional gas puffing. These discharges are compared with similar investigations using gas fuelling only. Pellet injection with penetration depths exceeding many times the recycling layer thickness did not succeed in producing higher plasma densities, but mitigates the ELM event in the divertor as judged from the carbon spectroscopy signal.
A gas gun lithium injector was developed at IPP, which is capable of performing wall conditioning at ASDEX Upgrade and flexible enough for easy adaptation to JET requirements. Laboratory tests dedicated to JET-like scenarios were also performed and inspected by JET personnel. The injector is capable of delivering lithium pellets at a rate of up to 3 Hz in the velocity range from 300 to 1000 m/s. The injector performance with respect to reliability, angular scatter and velocity precision was found to be well within JET requirements.

2. TASK AGREEMENT NO. 2

For spectroscopic plasma diagnostics mirrors are needed inside the vessel. However, the mirror surfaces are modified by erosion, deposition and hydrogen implantation from the plasma. These modifications result in a decrease of the reflectivity of the mirror surfaces, which will be even more pronounced in next-step fusion devices with long-pulse operation such as ITER and W7-X. Mirror surfaces are eroded by sputtering due to bombardment with neutral hydrogen atoms. The reflectivity change of carbon, aluminium and nickel long-term samples (LTS) mounted at the vessel walls of JET and exposed to about 50.000 plasma seconds was measured at a wavelength of 670 nm before installation and after removal. The optical reflectivity of eroded samples decreased by a factor of about 2-3. This is mainly due to surface roughening caused by erosion and, in addition, to a change of the chemical composition in the near-surface region. The mean surface roughness of non-eroded samples determined with a mechanical profiler was about 20 nm and increased linearly with the amount of eroded material. The chemical composition of the near-surface region was investigated by ion beam analysis methods. Implanted hydrogen isotopes and oxygen are present at the surface of all materials, but also other impurities such as Be, C, Ni, Fe, Cr, P, S, Cl are present. The concentrations of these impurities depend on the mirror material. From the flux of neutrals expected in ITER one can predict the reflectivity change of different mirror materials.
The midplane Penning gauge calibration and the determination of the pumping speed of the divertor cryopump in JET were continued. JET is not equipped with absolutely calibrated pressure gauges. For calibration pulses the pressure in the vessel has to be derived from both the amount of puffed gas and the vessel volume. This method suffers at low D_2 pressures from adsorption effects, as experiments with a temporarily installed capacity pressure gauge have shown. This leads for low pressures to overestimation of the pressure after short gas puffs and therefore to underestimation of the pumping speed. Other investigations were devoted to the impact of the poloidal field on the Penning gauge output.

3. TASK AGREEMENT NO. 5

During a density ramp-up JET ELMy H-modes typically show a saturation of the core density which may even be followed by a decrease (density limit). At the limit the discharge detaches between ELMs and a recently proposed edge-based detachment limit for the separatrix density applies. A simple picture has been proposed for the relation between the separatrix and core densities which allows derivation of the corresponding limit for the core density. The empirical evidence from JET was discussed and compared with the model predictions. It was shown that the resulting limit for the line-averaged density n_e coincides in size and scaling with the empirical Greenwald limit.
The impact of divertor closure on detachment was studied with the B2-EIRENE code package. The main focus was the observation that detachment occurs at unexpectedly low core densities in the closed MARK-II divertor. JET MARK-I and II horizontal plate configurations were adopted as study points. Effects of the observed magnitude are reproduced. While the increase of ion-neutral interaction, expected for closed configurations, is found in the simulations, the main impact on the detachment upstream density is due to volume recombination, which is significantly enhanced in cold, dense plasma corners, forming as a consequence of the specific plate inclination and divertor chamber shape of the horizontal configuration. Recent simulations of MARK-II vertical cases, where this particular effect is absent, confirm that closure-induced enhanced ion-neutral interaction has in general little impact on the upstream operation window.

NET/ITER COOPERATION PROJECT

(Head of Project: Prof. Dr. Karl Lackner)

Since its foundation IPP has hosted the NET Team, a group of scientists and engineers from the European countries participating in the EURATOM programme. They were called together to prepare the design of NET, the Next European Torus. Since the initiation of the ITER (International Thermonuclear Experimental Reactor) project, the primary function of the NET Team has been to carry out and coordinate the European contribution to the ITER design effort in the areas of physics and, particularly, technology. IPP contributes to the NET activities both by direct secondment of personnel to the NET team and by performing NET supporting work.

Work on ITER started in 1988 as a joint project between EURATOM, Japan, Russia and USA. ITER aims at demonstrating the physical and technological feasibility of a fusion-based power station. IPP hosted the full ITER Team during the conceptual design activity (CDA) phase till the end of 1990. Since the initiation of the engineering design (EDA) phase, the strongly increased ITER Team resides at three locations (San Diego/USA, Naka/Japan, Garching/Germany). The work of the Garching branch covers the design of the in-vessel components and therefore fits in very well with the scientific interests of IPP.

Through its scientific work, IPP Garching makes extensive and essential contributions to the ITER design activity. In particular, the programme of ASDEX Upgrade is directly aimed at scientific support of ITER. The stellarator experiments at IPP also make significant contributions to ITER. The results of these efforts are described in the sections dealing with the ASDEX Upgrade and W7-AS projects. The following sections therefore describe only additional, specific design effort projects.

1. MODEL CALCULATIONS IN SUPPORT OF ITER DESIGN

1.1 Analyses of the ITER Divertor

A. Kukushkin, H. Pacher (ITER JCT), D. Reiter (Forschungszentrum Jülich), D. Coster, R. Schneider

The B2-Eirene code package was used to study the performance of the ITER divertor in the presence of radiating impurities, both seeded and sputtered. In these calculations, the total power coming to the edge of the plasma was fixed at 200 MW (with allowance for 100 MW radiated from the core). The particle balance is determined by the densities of D, He and Ne ions at the core boundary, together with the efficiency pumping rate (albedo surface in the private flux region). The helium concentration at the core was always kept at 10%, and the neon density there was varied in order to see the trends. Carbon was assumed to be sputtered from the targets and walls due to both physical and chemical sputtering mechanisms. Exploration of the operational space is done in terms of the neon seeding level, the upstream plasma density, the cross-field transport, the chemical sputtering yield, the carbon-covered area, and the "dome" shape. Given the high dimensionality, no regular coverage of the operational space could be provided, and 1 D and 2 D parameter scans were done instead. The following intermediate conclusions were drawn from the current results [1, 2]. Radiation from intrinsic and seeded impurities in ITER can spread the exhausted power over a larger area for values of $Z_{eff} < 1.8$ at the core (the design criterion). Partially attached operation provides little edge radiation in the main chamber, thus avoiding excessive edge cooling with its potentially detrimental effect on plasma confinement. The radiation deposited on the targets is peaked, producing significant power loads. However, these loads remain acceptable, 5 to $10 MW/m^2$, for a reasonable upstream plasma density at the separatrix ($3.5 \times 10^{19} m^{-3}$) and not very low cross-field diffusivities. Reduction of the upstream density and/or the cross-field transport causes strong peaking of the plasma profiles with a corresponding increase of the peak loads onto the target. Reduction of the cross-field transport by a factor of 2 or of the upstream density to $3.0 \times 10^{19} m^{-3}$ seems marginally acceptable. Mechanisms that increase radiation far from the targets, e.g. charge-exchange recombination of impurities, may modify the result and should be incorporated in the model. Helium removal poses a less severe problem than power loading. The primary optimization can therefore be performed with respect to power handling. Momentum transfer to the side walls by neutrals is not dominant in the overall momentum balance for the partially attached divertor plasmas.

Nonetheless, neutrals can play an important role in the momentum balance by redistributing the plasma pressure across the divertor plasma. The divertor geometry should allow easy access of neutrals from the private flux region to the upstream plasma in the divertor in order to expand the zone where they can penetrate the hot part of the divertor plasma. In particular, a longer "dome" can be detrimental to divertor performance.

1.2 Global Confinement Time and Threshold Analyses

O. Kardaun, in cooperation with the ITER Database Group

The ITER databases oriented towards the empirical global confinement time and H-mode power threshold were expanded during the year. Further analyses yielded a consolidation of the (rather large) interval estimates produced by the ITER Expert Group Meeting at Naka (1995). The present version of the ITERH.DB3 confinement database contains contributions from 12 tokamaks from Europe, Japan, and the USA, with several heating schemes (NBI, ECRH, ICRH and ohmic H-mode). The analysis of various working subsets of the ELMy database, yields a log-linear scaling not unlike ITERH-92P(y), while three different log non-linear scalings determine to a large extent the prediction range of the energy confinement time. During the year, the practical and methodological details of statistical interval estimation were further developed and are described in several documents. The L-mode database work, organized by S. Kaye, came this year to a temporary conclusion by a Nuclear Fusion article and a new (log-linear) thermal L-mode scaling. The threshold database activities, organized by F. Ryter, led to an extension of the database and orientation towards the plasma edge parameters. Results of analyses by the working group can be found in joint publications by T. Takizuka (IAEA), F J Cordey (EPS), J. Snipes (EPS), and E. Righi (H-mode Workshop). At the invitation of the Japanese Society for the Promotion of Science investigations were made towards a unifying statistical approach in this area.

1.3 Surface Vaporization and Pellet Ablation Phenomena

L. Lengyel in cooperation with IESL.FORTH , Heraklion, Tech. Univ. of St. Petersburg, and RMKI.KFKI Budapest

During hard disruptions, the divertor plates are subjected to three kinds of energy fluxes: corpuscular (energetic ions and electrons), thermal (vapour particles), and radiative (vapour particles). The balance of these fluxes with the conductive losses into the solid determines the erosion rate of the plates. A significant fraction of the energy flux transported by the plasma particles is dissipated by radiation emanating from the vapour layer, which consists of impurity (eroded divertor plate) particles. The evolution of this radiative shielding vapour layer was simulated by means of 1-D (1.5-D) and 2-D resistive MHD codes. The 1-D (1.5-D) code is used for analyzing the effects of fundamental physical phenomena such as the energy spectrum of the incident particles, electrostatic fields and sheaths evolving in the vapour layer and at the vapour plasma and vapour solid interfaces, applied magnetic field, and the lateral motion (expansion or drift) of the erosion products. The major objective of 2-D calculations is to investigate geometrical and boundary condition effects. Results of numerous scenario calculations performed for graphite-coated divertor plates show that, for the same thermal energy flux emanating from the disrupting plasma, the erosion rates may differ by an order of magnitude, depending upon the temperature (energy) of the incident plasma particles. Electrostatic shielding may reduce the erosion rate by an order of magnitude. Both collisional and electrostatic shielding, and thus the incident particle and energy fluxes incident at the solid surface, are considerably affected by the lateral motion - expansion and drift - of the vapour across the SOL. Drift may be substantially reduced if internally closed current loops evolve in the vapour shield. Also the Hall effect seems to play a significant role in determining the shielding characteristics of the vapour layer. Electrostatic phenomena, lateral drift, lateral expansion, radiation transport, and the Hall effect strongly call for at least two-dimensional treatment of the problem. The computations performed with up-to-date carbon opacities show that a fraction of the radiation emitted by the C particles is reabsorbed in the vapour layer. Nevertheless, the fraction escaping through the lateral SOL surfaces (1.5-D model) seems to be sufficient for effective radiative damping of the disruptive plasma energy.

The basic physical processes that define surface erosion during plasma-wall contact and during pellet ablation associated with the injection of solid pellets into fusion plasmas are identical. For this reason, the development of the vapour shield model was paralleled by the development of a quasi-three-D up-to-date radiative ablation code (another resistive MHD code), based on the same physical principles as the vapour shield model discussed, for modelling the ablation of impurity ('killer') pellets. Killer pellets are envisaged for rapid disposal of the thermal plasma energy prior to major disruptions by means of a radiation burst produced by injecting impurity pellet(s) into the plasma interior. The pellet material deposited between two successive flux surfaces (i.e. in a flux tube bounded by two flux surfaces) becomes ionized, begins to radiate, and continues to expand along the (helical) magnetic field lines even after its expansion perpendicular to B is stopped. The emission of radiation first rapidly increases with increasing ablatant temperature, and then, after reaching a maximum, decreases to negligible values. With this radiative ablation model, neon pellet ablation data measured in ASDEX Upgrade and carbon pellet data measured in the W7-AS stellarator were successfully reproduced. Note, furthermore, that electric potential differences of the order of magnitude of keV were measured in the vicinity of pellets in the JIPP T-11U tokamak, the value being in agreement with the field strengths and potential drops monitored in our calculations.

1.4 Runaway Generation by Disruptions in ITER

M. Schittenhelm

Following the thermal quench phase of a strong disruption, the high resulting loop voltage can lead to significant generation of

runaways, posing a potential wall damage problem. In the expected parameter regime, runaway multiplication will primarily result from secondary generation, where new runaways are born with a predominantly perpendicular energy distribution. In the outer plasma region this corresponds to banana-trapped orbits, which excludes them from acceleration by the loop voltage. Pitch-angle scattering can again bring them onto transiting orbits, but detailed calculations show that through this effect the resulting growth rate of the runaway avalanche at the plasma edge is reduced with respect to the core by a factor of two to three. As the runaway current production proceeds over many generations, this difference can lead to a huge difference in local current density. A complete simulation of this situation has to include the local response of the electric field to the changing current distribution. Numerical modelling was therefore done with an appropriately modified version of the ASTRA transport code and included situations in which a killer pellet was injected into a disruption-prone discharge to attenuate the thermal power load and the mechanical loads due to halo currents. The full simulations show the predicted effect of current peaking, leading to a drop of the central q-value to 0.23. Due to the large area with q<1 (extending over 20% of the plasma radius), MHD instabilities are expected to play a significant part in determining the final fraction of runaways and will have to be considered in the future.

1.5 Transport Simulations for ITER

G. Becker

A comprehensive scaling relation for the effective heat diffusivity in high-density ELMy H-mode plasmas was applied in simulations of radiative mantle scenarios of the ITER EDA device. For the case of argon puffing, the sensitivity of transport to the density profile shape was studied. It was found that the required thermal energy confinement time remains almost unchanged (varying between 4.5 and 4.8 s), which is explained by an analytical expression for the thermal energy. Peaking of the electron and impurity densities does not alter the required argon concentration but peaks the radiation profiles and reduces the temperatures. Sufficiently narrow fuel ion densities were shown to cause inward-directed neoclassical drift velocities of argon in the collisionless plasma. The minimum volume average density for steady-state operation at the designed alpha particle heating power, still compatible with the transport predicted by the heat diffusivity scaling, was found to be $< n_e >= 9.1 \times 10^{19}\ m^{-3}$.

2. DIAGNOSTICS DEVELOPMENT AND MATERIAL TESTS FOR ITER

H. Salzmann, A. Herrmann, F. Mast, H.-J. Hartfuss, G. Haas, Plasma Diagnostics Division

The activities in this field were governed by the fact that the diagnostic design descriptions (DDD), which are part of the ITER final design report, had to be prepared by the end of '97. 1. LIDAR Thomson scattering for the core plasma: Work on the key problem of the front optical element directly viewing the plasma was continued. Baking properties, sputtering properties and the laser damage threshold of metal-coated metal mirrors were examined experimentally. Finite-element calculations for evaluating thermal stresses and deformations due to heat deposition by both nuclear and laser radiation were started. 2. Thermography for the target plates: A wavelength-multiplexing front optic was fitted into the latest design of the diagnostic divertor cassette. The SNR estimates for this setup and calculations for the attainable spatial resolution along the target plates were done. 3. Pressure gauges: The limitation of the attainable electron emission (see Annual Report 1996) was identified as an impurity problem and can be avoided by proper design of the gauge box. 4. Bolometry of core and divertor region: Nuclear irradiation of a pure 20 mm thick Mica bolometer substrate with a dose equivalent to 10^{-5} dpa yielded no visible degradation. The irradiation test will be continued in 1998 with an increased dose equivalent to 10^{-4} dpa. 5. ECE: The characteristics of flux collectors based on non-imaging optical elements (Winston cones with circular aperture) were tested in the laboratory in order to check the possibility of employing these elements for Electron Cyclotron Emission (ECE) diagnostics on ITER. In particular, the effects of diffraction on the achievable spatial resolution and on the concentrator light pipe coupling were verified by antenna pattern measurements at microwave frequencies. While the directivity properties were found to be compatible with the spatial resolution required for the ECE spectral survey, cross-polarization measurements pointed to the need to develop Winston cones with square or rectangular aperture which might keep polarization.

The joint effort of the Plasma Diagnostics Division and PTB in Berlin to establish a diagnostic method for determining the hydrogen isotope ratio was successfully terminated in 1997. As could be demonstrated by measurements in the PSI device, sufficient fluorescent light is obtained from a single laser pulse (two anti-parallel beams at $\lambda = 243nm$) for neutral densities in the range $n_H \approx 10^{17} m^{-3}$. Estimates show that the method may be improved to give reliable information on the n_D/n_T ratio down to $n_D \approx 10^{14} m^{-3}$; it is thus one important possibility to measure this crucial parameter in ITER. Discussions are continuing to check possible application on one of the current tokamaks in order to consolidate the usefulness of the method for ITER.

In the low-temperature and high-flux regime in ITER the chemical erosion of graphite is a critical plasma-wall interaction mechanism. To assess the importance of this process, an experimental investigation of various graphites was started at the PSI-1 plasma generator in IPP-Berlin. The erosion yields were measured as a function of the ion flux, ion energy and temperature of target in the flux range 10^{21} to $10^{22} m^2 s^1$ (more information is given under ''Plasma Diagnostics Division'' in this report). Measurements with respect to the fluence dependence of the chemical erosion yield are planned for 1998.

STELLARATORS

IPP's activities in the stellarator field are concentrated on developing the next-step facility in the WENDELSTEIN line, WENDELSTEIN 7-X, and on exploiting the WENDELSTEIN 7-AS facility, and on stellarator theory. Work on the first topic is split between the W7-X Construction projects, headed by M. Wanner, for construction of the W7-X facility, and Experimental Division 2, headed by G. Grieger, for the scientific part. G. Grieger is also responsible for setting up of the new institute at Greifswald to house the Greifswald branch of IPP. Work on the second topic is done by Experimental Division 3, headed by F. Wagner, and work on the third topic is done by the newly formed Stellartor Theory Division, headed by J. Nührenberg.

The work of the W7-X Construction project is focused on the design, manufacture and assembly of the stellarator, the in-vessel components, the heating systems and the machine control system. The project is closely cooperating with the diagnostics projects for W7-X and the construction project of the Greifswald Branch to agree on the various interfaces between the machine, the building, the infrastructure and the experiments.

With the beginning of 1997, construction of the new Greifswald Branch of IPP was started and by the end of 1997 the foundations of all buildings were laid.

Development of divertor elements for W7-X proceeded well. Two elements were tested and demonstrated their capability of withstanding reliably a power density of 10 MW/m^2.

On W7-AS a new 140 GHz gyrotron provided by the Institute of Applied Physics, Russia, was successfully installed in 1997. This advanced gyrotron is equipped with an energy recovery system and consequently has an electrical efficiency of about 50 %. It increases the available heating power up to 1.5 MW and extends the flexibility of the two existing 140 GHz gyrotrons. The ICRH heating system was technically improved. It was thus possible to condition the system to higher voltage stand-offs. This enabled the application of a second heating scenario for the first time on W7-AS, i.e. the second-harmonic heating of a neutral-beam-heated hydrogen plasma.

Plasma edge studies were continued by investigating the role of edge parameters on the density limit. It was found in almost stationary discharges that the onset condition for the density limit is determined by plasma detachment from the limiters. The plasma conditions which lead to the development of the electron root observed for the first time in 1996 were examined in more detail. Further evidence was found that the transition into the electron root is induced by locally trapped suprathermal electrons and not by thermal radial fluxes. Transport studies concentrated on understanding and comparing various good confinement regimes and on the influence of magnetic shear on confinement. Degraded confinement in the presence of low-order magnetic field resonances can be improved to good confinement by applying positive or negative ohmic currents to increase the magnetic shear.

A newly developed diagnostic for measuring the line-integrated density based on the Cotton-Mouton effect was successfully applied to W7-AS. This diagnostic is especially suited for measuring high densities in stationary discharges. First results are in good agreement with other line-integrated density measurements.

Preparation of the divertor experiments involved extension of predictive 2D simulations of island divertor plasmas and a 3D Monte Carlo edge transport code. Further theoretical work relating to experimental results on W7-AS dealt with, for example, ECRH power absorption at high power levels, production of suprathermal electrons, neoclassical impurity transport and the neoclassical bootstrap current.

Theoretical investigations in the Stellarator Theory Division being built up in Greifswald concern four major areas of research: i) further development of the stellarator concept, ii) equilibrium and stability investigations with advanced computational tools, iii) development of a stellarator-specific basis of anomalous-transport theory, iv) development of 3D plasma edge theory.

WENDELSTEIN 7-X Construction

(Head of Project: Dr. Manfred Wanner)

Members of the W7-X team and contributors to the project: see section "Divisions and Groups, WENDELSTEIN 7-X Construction"

1. INTRODUCTION

The W7-X Construction Division is responsible for engineering, design, manufacture and installation of the W7-X device. The W7-X device comprises the plasma vessel, the in-vessel components, the superconducting magnet system, the cryostat, the ECR, ICR and NBI heating systems as well as the monitoring and control system.

The appointment of staff for the project team has been continued and tools for project control and quality management are being introduced.

The work is still focussed on the completion of the R&D activities. This development work was requested by the ad hoc group of the EU Commission as necessary input for constructing the W7-X machine. An advanced conductor which will feature a higher current capability during operation has been built by industry. An original-sized DEMO coil will demonstrate that the winding pack with 120 windings and representative bending radii can be manufactured and integrated into a steel casing while complying with the narrow geometrical tolerances required for the magnetic field topology. Finally, a DEMO cryostat featuring all mechanical and cryogenic aspects of a sector of the W7-X cryostat is being manufactured by industry.

Detailed planning shows that manufacture of the superconducting coils constitutes the critical path of the project. Progress with the manufacture of the DEMO coil has meanwhile bred a degree of confidence allowing the coils to be specified and calls for tender to be issued.

The interfaces between the machine and both the experimental building and diagnostics are being defined and installation planning has started.

Cooperation is being negotiated with Forschungszentrum Karlsruhe (FZK) and the Low Temperature Laboratory of Commissariat à L'Énergie Atomique (CEA) at Saclay. FZK is to provide the complete ECRH system and support W7-X by performing tests with the conductor and DEMO coil. CEA has shown interest and demonstrated its capability to take over the cryogenic acceptance tests of the 70 coils.

2. R & D WORK

2.1 Superconductor

In May 1997, 200 metres of the "advanced conductor" was delivered by SWISS METAL. This conductor was used to manufacture the STAR IV test coil by the TESLA company. The coil was delivered after major delay at the end of the year. IPP has prepared the coil for the tests at FZK, now scheduled for the first half of 1998. Prior to the winding of the test coil, strands were taken from the ends of the conductor and subjected to the same hardening process as the test coil. Measurements of the critical currents at a number of triplets, extrapolated to the full bundle current, clearly show the expected increase of current capability of the advanced conductor. This will give a safety factor of 2 for the critical current at the nominal induction of 6 tesla.

Minor problems involved in the CONFORM method of cladding the superconducting cable showed that the aluminium rods have to be scrupulously cleaned during series production of the conductor. This will be demonstrated on a further length of conductor ordered in 1997 from the Finnish company, OUTOKUMPU, which will use the same CONFORM technology.

2.2 DEMO coil

The winding pack for the DEMO coil was finished at ANSALDO at the end of 1997 after a total delay of eighteen months (see FIG.1). The quality of the winding pack fully conforms to the specification, i.e. dimensional tolerances as well as

dielectric and hydraulic requirements were fulfilled. The winding pack successfully passed an integral vacuum leak test prior to delivery to the main contractor, NOELL.

At NOELL's each of the two half-shells of the coil casing were precisely assembled from eight cast steel segments by welding. A first dimensional check demonstrated that the winding pack fits into the shells well. Final assembly of the coil will start in January 1998.

The schedule for the remaining work appears realistic and indicates delivery of the complete DEMO coil by the end of June 1998.

At FZK, the intermediate frame for matching the DEMO coil with the EU - LCT coil in the TOSKA plant was preliminarily assembled. NOELL will deliver the DEMO coil mounted on the frame. In this way, the whole assembly can be inserted in the TOSKA test facility within a short time in July 1998. After installation of the instrumentation, current leads and all electrical and cryogenic supplies has been completed, cooldown can start. This is planned for the end of 1998.

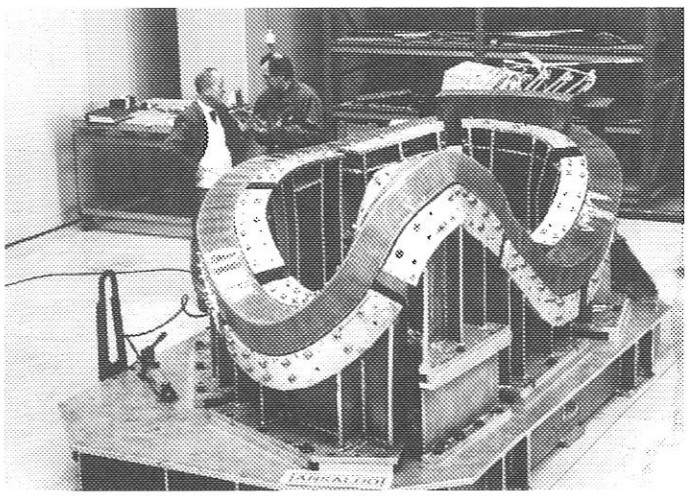

FIG. 1: Winding pack of the DEMO coil for W7-X at ANSALDO's, ready for delivery

2.3 DEMO cryostat

The DEMO cryostat construction is in its final stage. The plasma vessel was finished, with the geometry conforming to specification. In this way, it was demonstrated that manufacture of this complex-shaped component of W7-X can be realized economically with the required geometric tolerances. At the end of 1997, mounting of the thermal insulation and 80 K shield as well as assembly of the coils on the plasma vessel were well advanced. The coil vault and weight support structures are ready for assembly; the surface of the support structure was covered with copper sheets to allow more rapid cooldown to 4 K and better temperature uniformity. All 8 model coils were pre-mounted in their final position and all structure elements were adjusted accordingly (see FIG. 2). No further adjustments are thus required during final assembly of the coils and vault structure. Work is now concentrated on routing the piping and conductor. A new electrical insulation for the conductor connections was developed for use in the DEMO cryostat. All ports were leak-tested prior to delivery. They are partly equipped with electrical heaters and thermal insulation. The instrumentation is ready and attached.

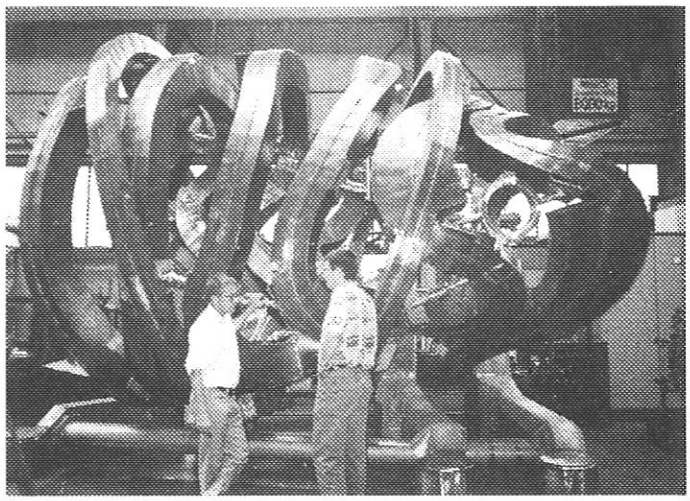

FIG. 2: Pre-mounted model coils of the DEMO cryostat

The helium refrigerator for supplying the DEMO cryostat with 110 W of refrigeration is now working routinely. The gas storage system was partly renewed.

3. W7-X BASIC MACHINE

3.1 Magnet system

The completed final design of the non-planar coils for the W7-X magnet took into account the experience gained during manufacture of the DEMO coil. CAD drawings were produced of the winding packs and casings for all of the ten different types of coil. The arrangement of the coils was checked with respect to potential collision areas between neighbouring coils. Design of the vault elements for the coil set assembly has started.

A fundamental finite-element analysis of the stresses and strains in the coil set was carried out for the maximum magnetic load. The results show that stresses are within the material yield limits.

The detailed technical specification for the 50 non-planar coils and the associated procurement documents were worked on. Calls for tender for the coil system will be issued in spring 1998.

3.2 W7-X cryostat

A first layout of the plasma vessel has been completed. Design of the plasma vessel has to be done in an iterative way taking into account all constraints imposed by the position of the magnet coils and the requirements of the divertor. A particular design problem arises from the thermal contraction of the superconducting coil system during cooldown with respect to the position of the plasma vessel and thermal movements of the plasma vessel during operation. Possible support concepts for the plasma vessel were therefore studied.

Most of the ports for diagnostics and heating were roughly designed. A discussion was started within the project to keep the total number of ports within limits.

The forces exerted on the plasma vessel by eddy currents from a fast coil discharge were calculated, and estimates of the forces induced by externally produced plasma quenches have begun. Mathematical programs were developed for studies on different types of superconducting current leads. A finite-element analysis has been started for the design of the coil housing cooling.

3.3 W7-X Helium refrigerator

Two industrial studies for the helium refrigerator system were finished. They resulted in two different layouts with several variants. These proposals are now under evaluation.

4. HEATING SYSTEMS

4.1 ECRH for W7-X

The ECRH system for W7-X will consist of 10 gyrotrons with 1 MW of power per unit at 140 GHz and will have CW capability.

Major achievements in gyrotron development were made in 1997 with respect to the high-efficiency operation envisaged for W7-X. A gyrotron with 0.8 MW of output power and depressed collector technology, which yields an electrical efficiency of 50 %, was developed by the Russian company, GYCOM, and installed at the W7-AS stellarator. The gyrotron is running routinely in the experimental environment. Operation is still limited to a pulse duration of 1 s due to the window.

Industrial development of CW-compatible diamond windows made significant progress and a diamond disk with the required performance for 1 MW CW transmission is now available at FZK. On the basis of these results there is great confidence that the gyrotrons for W7-X will be made available in time.

The design of the optical transmission system, which is based on the concept of a multi-beam waveguide, i.e. single mirrors are used for the transmission of many individual RF beams, is making good progress. IPF Stuttgart has taken full responsibility for designing this system and is preparing a prototype transmission line at Stuttgart which allows testing of the optical and thermomechanical properties of the system. The materials technology for the transmission mirrors with efficient cooling for CW operation with low losses was successfully developed together with industry.

There were major changes in the organizational structure of the ECRH division: FZK declared its readiness to assume the responsibility for the entire ECRH project and co-ordinate the various partners contributing. FZK is willing to set up the necessary project organization. The sharing of responsibilitiy for the various tasks between IPP, IPF and FZK is being negotiated. The conceptual design, engineering design and supervision of the construction of the entire transmission system will be handled by IPF Stuttgart. The development of the gyrotrons and the manufacture, installation and testing of the ECRH system, including all subsystems required, will be handled by FZK. IPP will contribute with respect to the in-vessel components and the related plasma diagnostics.

4.2 Neutral beam injection

Neutral beam injection is envisaged in W7-X for bulk heating of the plasma in the high-density, high-ß regime. The ultimate neutral beam power (stage II heating) will attain 20 MW, delivered by two injector boxes of the ASDEX Upgrade type (55 keV H^0 or 60 keV D^0). However, so far only a quarter of this power (stage I heating) has been approved.

Each of the two beam lines (in principle, capable of housing four PINIs = plug-in neutral injectors) will therefore be equipped with one PINI only in stage I, thereby delivering a total of up to 5 MW for pulse lengths of up to 10 s.

The two beam lines will make use of the newly developed RF sources, as recently put into operation on the second injector of ASDEX Upgrade. These RF sources offer higher availability and significant cost savings compared with conventional arc discharge sources.

The main progress in 1997 was the delivery of the RF generators and vacuum boxes, whereas the manufacture of the PINIs is still under way. It was decided to postpone procurement of further components to a later phase, when timing of the stage II heating becomes clearer. Furthermore, a number of interfaces with respect to water cooling, buildings, low and high voltage supplies have been defined.

In view of the highest densities conceivable in W7-X (i.e. $\geq 3 \times 10^{20}\,m^{-3}$), penetration of beams with an energy of ≤ 55 keV/nucleon to the plasma centre is unsatisfactory. The later application (stage III) of high-energy beams with energies of around 350 keV, based on negative ions, may therefore be an interesting alternative. In order not to preclude later use of this new technology, the necessary tangential portholes have been designed conceptually (see FIG. 3).

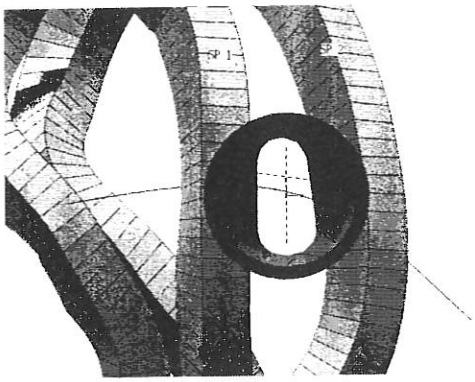

FIG. 3: Three-dimensional view of the tangential porthole for neutral beam injection

A modification proposal was submitted to the project to provide these tangential portholes in addition to the near-perpendicular portholes for stages I/II. Approval of these tangential portholes by the "Scientific Advisory Committee" is being deliberated.

WENDELSTEIN 7-X

(Head of Project: Prof. Dr. Günter Grieger)

1. W7-X DIVERTOR STUDIES

H. Greuner, H. Grote+, F.W. Hoffmann, J. Kisslinger, H. Renner, E. Strumberger, H. Bitter*, O. Jandl*

(+W7-X Construction Division,
*Central Technical Services of IPP)

1.1 Physics and Modelling

1.1.1 Definition of divertor components

For lack of an elaborated 3D code, at present essentially several methods deduced and calibrated from tokomak data banks have been applied to define the specifications and shape the geometry of W7-X divertor components.

- The results of 3D ray tracing of the vacuum configuration, including finite <ß> equilibrium cases at the boundary[1], are used to define the interacting divertor surface pattern. The power load was estimated in combination with simulation of perp. transport (a typical transport coefficient is 1 m^2/s, values of up to 10 m^2/s were investigated) by Monte Carlo code. Fig. 1 shows the deposition pattern on the target area as adapted to the HS5V10U configuration for various magnetic parameters, including variation of <ß> by up to 4%.

- The B2 multi-fluid code[2] was adapted to describe the SOL parameters. Since B2 is a 2D code, the geometry of the boundary was averaged (distances) and integrated (areas and volumes) in the toroidal direction. Significant unloading of the target plates is predicted by radiation losses of C impurities /264/. A high-recycling mode seems possible for relatively low separatrix densities above $2*10^{19}m^{-3}$.

- Simplified 3D SOL models were evaluated to get information about the temperature and density distributions. For this purpose, the 3D flux topology was combined with 1D fluid models. This method benefits from the ordering of the open flux bundles outside the separatrix region, where only field lines with a long connection length approach close to the LCMS and get significant loading from the confinement area by perpendicular transport[3]. The 1D treatment of the bundles of different length and power and particle flows delivers the plasma parameters along the field lines. Finally, superpositioning in 3D geometry allows the 3D temperature and density profiles to be approximated.

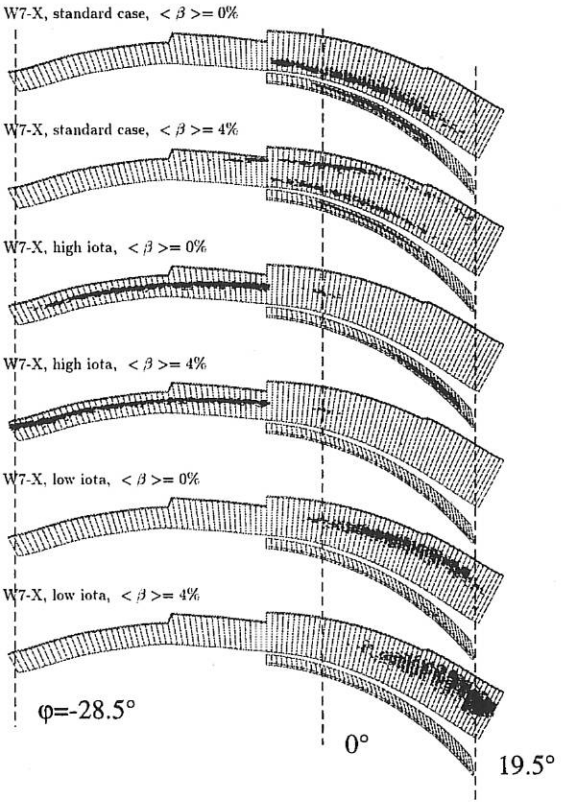

FIG. 1: Intersection pattern on the target area of one divertor unit. The variation of the deposition as a function of the rotational transform for <β> = 0 and 4% (D = 1 m^2/s). The two target plates are approximated combining target elements with a width of 5 cm and lengths of 27 to 57 cm. Note, target plates are projected as seen from the magnetic axis.

- The position of the pumping gap and the geometry of the baffle plates were optimized on the basis of 3D neutral particle studies by means of the EIRENE code[4]. The intention was to concentrate the neutral particles close to the target plates and improve the pumping efficiency.

---

[1] E. Strumberger, Lab.Rep. IPP2/339, Garching 1997
[2] B.J. Braams, Ph.D. Thesis, Rijksuniversiteit Utrecht (1986)
[3] E. Strumberger, Nucl. Fusion 36 (1996), 891-908
[4] D. Reiter, Jülich Report 1947, Jülich (1984)

1.1.2 *The stochastic edge region of W7-X*

Magnetic stochasticity is characterized by a random, diffusion-like walk of a magnetic field line with respect to the unperturbed magnetic surface and the exponential scattering of close magnetic field lines. The topology of stochastic magnetic fields in the edge region of W7-X was investigated for fields with volume-averaged ß-values of <ß> = 0, 2 and 4 % inside the last closed magnetic surface and rotational transform values of $\iota > 1$ in the edge region. The edge region of these fields is characterized by remnants of four islands surrounded by stochastic field lines. In order to quantify the stochasticity of these fields, bundles of field lines forming flux tubes were traced in the region of interest. Because of the exponential scattering of close field lines in a stochastic field, the circumference of the area enclosed by a flux tube increases exponentially. Calculating this as a function of the length of the flux tube yields the Kolmogorov length L_K, which measures the stochasticity. Furthermore, the Kolmogorov lengths of flux tubes were compared with the corresponding connection lengths L_C to an outer limiting surface. The computations show that the mean Kolmogorov length L_K (averaged over all flux tubes traced) decreases with increasing ß ($L_K \cong 57$ m for the vacuum field, $L_K \cong 44$ m for <ß> = 2% and $L_K \cong 37$ m for <ß> = 4%), and that stochastic layers ($L_K < L_C$) exist.[5]

1.2 Divertor Engineering

Only basic solutions are as yet available for the additional cryo panels inside the vessel and the wall protection. The present studies are concentrated on design of the target and integration inside the vessel. In view of geometrical restrictions (the typical distance between the vessel and LCMS in the divertor region is 30 - 50 cm, and between the target surface and LCMS 10 cm) the design of the components and their arrangement must be very compact.

The most critical component is the target area. Therefore, a R&D programme has been started to examine several cooling concepts and material combinations (CFC tiles combined with TZM, CuCrZr, Glidcop). Recently, such prototypes were successfully tested. In co-operation with the CEA Cadarache team investigations, including 1000-cycle exposure, were performed with the electron beam facility of FRAMATOME at le Creusot. Results of the pyrometric surface temperature on elements made of CFC tiles with a thickness of 6 mm are summarized in Fig. 2 for heat load of up to 12 MW/m^2 (Δt = 2 min). Material data of the heat conduction coefficients and FE analysis of the heat transfer to the coolant serve as a basis to give calculated temperatures for comparison. Except for the case with the CFC material, CX2002, for which the real data of heat conduction of the charge used must be significantly lower than the reported ones, good agreement was found:

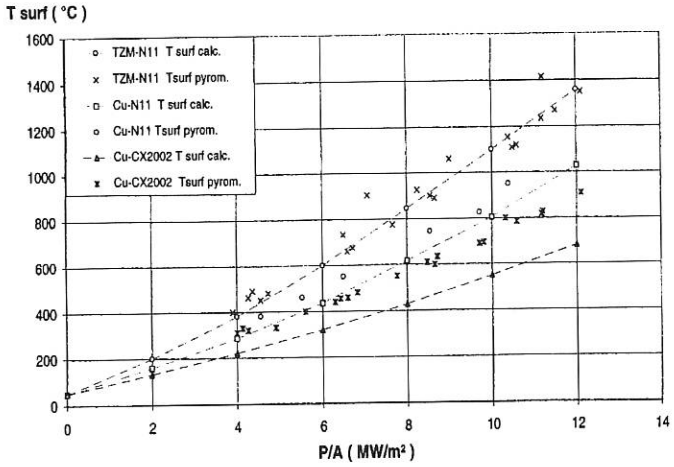

FIG. 2: Results of the HHLT (high heat load test) on various prototype target elements: The measured and calculated surface temperatures are given as function of the heat load under stationary conditions.

The data base of extensive nondestructive testing by means of thermographic measurements will allow fault detection.

The geometry of the target plates was redesigned for the new HS5V10U configuration selected, according to following criteria:

- Maximum heat load 10 MW/ m^2 during stationary operation.
- For easy maintenance and repair and to provide flexibility for the experimental programme and diagnostics, the optimized 3D target surfaces are approximated by 2D target elements with the dimensions: width 5 cm, length 27 - 57 cm.
- Arrangement of a set of 10 - 15 elements and water manifolds as modules for prefabrication and testing outside the vessel. The target area of one divertor unit divided into two parts for effective pumping will be composed of 14 individual modules. Finally, 145 elements have to be combined for one divertor unit. By standardization the number of different types could be reduced to 4. The flat elements are mounted on the supporting framework of the modules approximating the calculated 3D surface. Finally, the surface is smoothed by 3D machining to eliminate steps.

Depending on the progress with the physical understanding and control of the boundary during experiments, it is expected that the divertor system will be modified (vented targets, "closed divertor", change of material etc.). Component design, the supporting and alignment structure of the target and baffle plates, the cooling circuits and the interfaces of the vessel must be flexible for future needs.

[5] E. Strumberger, Contr. Plas. Phys. (1998), in print

2. CONTRIBUTIONS OF THE PLASMA DIAGNOSTICS DIVISION TO THE W7-X PROJECT

D. Hildebrandt, P. Bachmann, W. Bohmeyer, B. Jüttner*, M. Laux, D. Naujoks, R. Radtke, J. Sachtleben, D. Sünder, U. Wenzel

(*Humboldt University, Berlin)

The activities of Plasma Diagnostics Division can be divided into three parts

- development of machine control and plasma diagnostics methods,
- investigation of material behaviour under high heat and particle flux conditions,
- theoretical studies of transport phenomena including impurity ions.

In cooperation with the W7-X divertor and diagnostics groups the following contributions to machine control and plasma diagnostics were proposed:

- flow and temperature measurements of the cooling water for power exhaust of the target plates and heat shield in front of the vessel wall
- surface temperature measurements of the target plates with CCD cameras.
- measurements of the electric current through the target plates.

In addition, possibilities for optical and acoustic observation of the target plates will be checked. To check the possible use of Specle interferometry for in situ observation of the divertor plates, first experiments were conducted at the PSI-1 plasma generator in close cooperation with the University of Saarbrücken. The results indicate that the optical measurements are strongly influenced by diffusive reflection of the windows and mechanical vibrations. Further investigations are necessary to draw definite conclusions concerning the application of this method on W7-X.

The proposals on the development and construction of plasma diagnostics cover the following topics:

- thermography of the target plates
- target-integrated Langmuir probes
- manipulator for exposing special probe heads
- divertor spectroscopy in the visible spectral range
- determination of Z_{eff} by spectroscopy in the visible spectral range.

The material investigations on the the PSI-1 plasma generator were concentrated on erosion measurements at elevated temperatures. It was proved that the chemical erosion yield of different graphites strongly decreases with increasing ion flux density (for detailed information see Sec. Plasma Diagnostics Division). These results are of importance for estimating the erosion rate and lifetime of target plates under W7-X divertor conditions.

The theoretical studies are focused on bifurcation and time evolution of temperature profiles along the magnetic field lines between two target plates. The solutions of the one-dimensional heat conduction equation show that the nonlinear dependence of the thermal conductivity and radiative losses on temperature results in multiple solutions and bifurcations (see Fig. 3). Further studies are planned to investigate solutions of the corresponding 3D problem. These investigations are important for understanding the basic heat transport processes in the edge plasma of the W7-X stellarator.

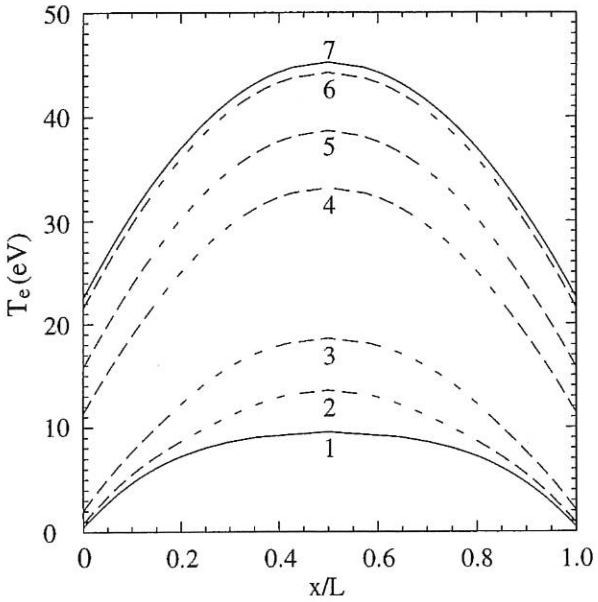

FIG. 3: Temperature profiles in a plasma with a binary impurity mixture; profiles 1, 3, 5, 7 are stable, the three remaining ones 2, 4, 6 unstable.

3. STELLARATOR SYSTEMS STUDIES

C.D. Beidler, E. Harmeyer, F. Herrnegger, J. Junker, A. Kendl, J. Kißlinger, I.N. Sidorenko, E. Strumberger, H. Wobig, A.V. Zolotukhin

3.1 Wendelstein 7–X Studies

In 1997 the work of the Stellarator Systems Study Group was focussed on special questions of the Wendelstein 7-X configuration and some aspects of the Helias reactor design. Issues relating to the mechanical load on the plasma vessel in W 7-X, caused by eddy currents induced during the deloading phase of the coil system or by time-dependent plasma currents, were considered. Some work was done on the issues of the divertor design and target plate development.

3.1.1 Magnetic field calculations of the plasma vessel

Magnetic field calculations at the location of the vacuum vessel were made in order to estimate the mechanical loads on the vessel during magnetic field variation, particularly during the deloading phase. Eddy current calculations were made by members of the University of Karlsruhe, using the EMAS computer code. The distributions of the vector potential and the magnetic field were needed as input values for these computations. The interaction of the eddy currents and the magnetic field results in the magnetic force distribution of the plasma vessel. The magnetic force distribution of the plasma vessel, caused by time-dependent currents in the plasma, was also investigated. A total toroidal plasma current of 100 kA and a total poloidal one of 2 MA were introduced. The results of the computations show that the vacuum vessel is subjected to additional pressure values of up to about 70 kPa (0.7 bar).

3.1.2 Target plate development for W 7-X

The change of the magnetic configuration of W 7-X from HS5V10N to HS5V10U made it necessary to adapt the geometries of the target and baffle plates, mainly the part which is in action in the high-iota case. It was possible to design the plates such that only straight target element are needed; this facilitates fabrication. The width of the elements is about 5 cm and their length is graduated so that the number of types is reduced.

3.2 Helias Reactor Studies

The investigations on a Helias Reactor (HSR) were continued. Particular attention was devoted to the coil system, the α-particle behaviour, the drift waves, the neutron load on the target plates, the temperature profile and its bifurcation, and the energy balance in such a device. The results of the investigations were presented at the EPS Conference in Berchtesgaden and at the Toki Conference on Plasma Physics and Controlled Nuclear Fusion, in Toki City, Japan.

A Web site, located at

`http://www.ipp.mpg.de/E2/hsr/hsr.html`

has been prepared to give an overview and detailed data of the Helias reactor configuration.

3.2.1 Coil system of HSR

The HSR coil system is a scaled-up version of the magnetic configuration of Wendelstein 7-X. It comprises a single set of 50 modular non-planar coils arranged toroidally in 5 field periods with a major radius of 22 m.

In order to reduce the maximum magnetic field at the coils, various methods were investigated. Current layering and winding pack splitting were considered. The latter was applied for the HSR-B version, which led to a maximum magnetic field at the coils of 10 T, at a reduced axis magnetic field of 4.75 T. This value allows one to remain within existing NbTi-technology. Furthermore, in HSR-B the minimum distance between the coils was considerably extended in relation to the former HSR-A version. This offers more free space for design purposes. Figure 2.1 shows the cross-section of a split modular coil, and the main data of the two versions considered are listed in Table I.

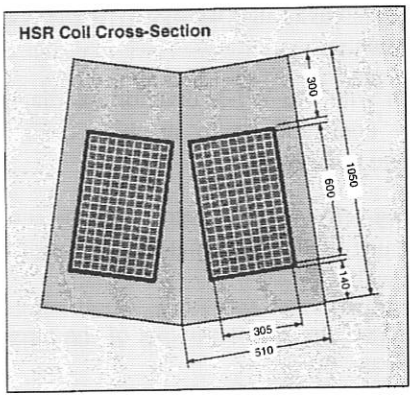

FIG. 2.1: HSR-B coil cross-section, showing the split winding pack, the insulation and the housing.

		HSR-A	HSR-B
Average major radius	[m]	22.	22.
Average coil radius	[m]	5.0	5.0
Average plasma radius	[m]	1.8	1.8
Plasma volume	[m^3]	1400	1400
Number of coils		50	50
Induction on axis	[T]	5.0	4.75
Max. induction on coils	[T]	10.6	10.0
Ov. current density	[MA/m^2]	27.1	29.5
Winding pack cross-section	[m^2]	0.42	0.37
Min. distance between coils	[m]	0.08	0.22
Current in winding	[kA]	40.0	37.5
Total magnetic energy	[GJ]	110	100
Virial stress	[MPa]	153	158
Maximum net coil force	[MN]	140	128

TABLE I: Main data of the Helias reactor.

3.2.2 *Alpha-particle orbits in Helias configurations*

Confinement of trapped α-particles is a critical issue in HSR, but finite plasma pressure produces a true minimum-B configuration in which the majority of reflected α-particles are confined for at least one slowing-down time (W. Lotz, et al., Pl. Phys. Contr. Fusion, **34**, (1992), 1037). Nevertheless, modular-coil ripple leads to a small fraction of "very prompt" losses (with confinement times less of than 10^{-3} s), potentially resulting in "hot spots" on the first wall. To estimate the severity of the problem, the α-particle birth profile is combined with the fraction of phase space in which the birth takes place in a modular ripple. For $< \beta >= 5\%$, the total heat load on the first wall due to very prompt losses is estimated to be ≤ 2.2 MW.

The effect of electric field fluctuations associated with drift wave turbulence on α-particle orbits was studied in a Helias configuration with $\beta(0) = 0.03$. For this reason trapped α-particles with two values of the initial energy, $W = 3520$ keV ("hot" α-particles) and $W = 352$ keV ("cold" α-particles), were investigated under the influence of an electric wave propagating perpendicularly to the magnetic field, for which condition $B \cdot grad(\Phi) = 0$ is fulfilled. It was shown that resonance phenomena occurs for the "cold" trapped α-particles, which have a bounce frequency ω_b of the same order as the drift wave frequency $\omega_\star$. Electric perturbation with $|E_{max}| = |grad(\Phi)| = 30$ V/cm significantly affects helically trapped "cold" α-particles and causes strong distortion of orbits, but does not significantly perturb "hot" α-particle orbits and does not increase "hot" α-particles losses. Such difference in behaviour of "hot" and "cold" α-particles under electric perturbation shows that drift wave perturbation may be useful for controlling the selective energy transport of α-particles because it does not deteriorate confinement of the "hot" α-particles, but may increase losses of the thermalized α-particles from the plasma and thus reduce the accumulation of ash.

3.2.3 *Drift waves in HSR*

Drift waves in Helias type configurations are studied. Particular attention was devoted to the effect of geometry and stellarator optimization on drift waves and anomalous transport. As a first step, the linear stability of drift waves is treated in an electrostatic model. Stellarator-specific influences of helical ripple shear, localization and particle trapping are discussed with respect to increasing optimization on Helias type devices (W 7-AS, W 7-X, HSR).

3.2.4 *Neutron load on the first wall of HSR*

A new code has been developed to calculate the wall load due to the 14 MeV neutrons generated in the plasma. The code integrates for each wall element the neutron irradiation from all visible elements of the plasma volume. The reference case of the calculation uses an average beta of the plasma of 4.6%. The total neutron power in this case was 2.4 GW, the peak neutron wall load 1.6 MWm^{-2} and the average value 0.8 MWm^{-2}. The maximum value and also the largest variation in the poloidal direction occur in the neighbourhood of the indented cross-section and reflects the variation of the distance between the plasma centre and wall. The load on the divertor plates of about 0.6 MWm^{-2} is rather weak.

3.2.5 *Finite-β calculations for HSR*

Equilibria calculations were made with average beta values up to 5%. In order to compensate the Shafranov shift at the plama edge, a vertical magetic field (0.05T at 5%-β) is superposed. The effective plasma radius shrinks slightly at finite β and the rotational transform is reduced (0.05 at 5%-β on the axis), leading to a modification of the island region at the boundary. The finite beta plasma at $< \beta >= 5\%$ is stable according to both the Mercier and resistive interchange criteria.

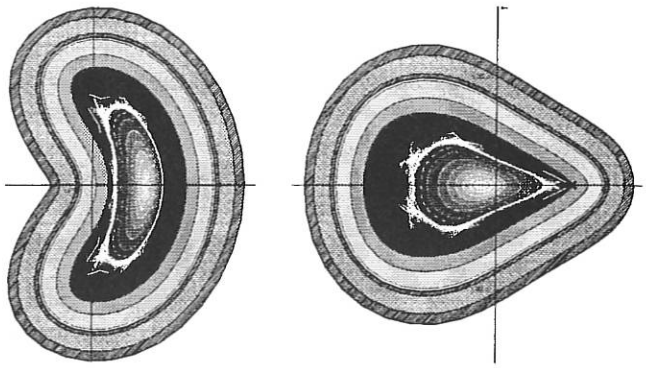

FIG. 2.2: Cross-section of plasma, blanket, shield and coils for $< \beta >= 5\%$ at $\varphi = 0^o$ and $\varphi = 36^o$.

3.2.6 *Bifurcation of the temperature profile in HSR*

The temperature profile of a fusion plasma in a Helias configuration was computed with the one-dimensional heat conduction equation. Heating of the plasma is provided by external heating and α-particle heating. The heat conduction is the sum of the neoclassical and anomalous thermal conductivities. Due to the non-linearity of α-particle heating bifurcation of the temperature profile occurs. In general several solutions exist. It can be shown that neoclassical heat conduction stabilizes the temperature profile at a temperature below 20 keV.

3.2.7 *Energy balance in the Helias reactor*

Empirical scalings of energy confinement (U. Stroth, et al., Nucl. Fusion, **36**, (1996), 1063) are used to predict ignition parameters in a Helias reactor. These scaling laws are: Lackner-Gottardi scaling (LGS), ISS95 scaling and ISS95W7 scaling. For comparison, tokamak scaling laws (ITER89, ELMYH92y and H-mode scaling) are also taken into account. LGS and ISS95W7 scaling, which represents the results of the Wendelstein line of stellarators, are sufficient for ignition: The Helias reactor requires a confinement time $\tau_E = 1.7$ s; LGS-scaling yields 1.8 s, and ISS95W7-scaling 2.2 s. An isotope factor or any improvement by H-mode confinement has not been taken into account. The ISS95 scaling, which includes the results of all existing stellarator experiments, yields a confinement time which is a bit too small for the Helias reactor under consideration.

WENDELSTEIN 7-AS

(Head of Project: Prof. Dr. Friedrich Wagner)

Members of the W7-AS group: see section "Divisions and Groups, Experimental Plasma Physics Division 3".

1. OVERVIEW

In 1997 work on W7-AS started with a two-month shutdown period for installing additional diagnostics and for some maintenance work. Experiments were resumed at the end of February. About 500 field pulses were needed for commissioning the new digital control and regulation system of the 1.45 GJ flywheel generator. Late in 1997 a new 140 GHz gyrotron provided by the Institute of Applied Physics, Russia, in continuation of a collaboration contract was successfully installed. This advanced gyrotron marks a milestone in the development of gyrotrons towards the needs of W7-X because it is equipped with an energy recovery system and consequently has an electrical efficiency of about 50%. It extends the flexibility of the two existing 140 GHz gyrotrons and allows simultaneous on and off axis heating at high power levels.

The ICRH heating system was technically further improved. Thus it was possible to condition the system to even higher voltage stand-offs. This allowed us to radiate about 500 kW of ICRH power from the antenna in another heating scenario on W7-AS, i.e. second-harmonic heating of a neutral-beam-heated hydrogen plasma. A 50% increase of the energy content at constant density was achieved, and it was possible to sustain the plasma solely with ICRH for up to 250 ms.

Plasma edge studies were continued by investigating the role of edge parameters in density limit discharges to get a better understanding of the very high density limit in W7-AS. It was found in almost stationary discharges that the onset condition for the density limit is determined by plasma detachment from the limiters.

Transport studies concentrated on the understanding and comparison of various good confinement regimes and on the role of magnetic shear in confinement. Good confinement is found for low shear in the absence of low-order magnetic field resonances. Degraded confinement in the presence of such resonances can be improved to the good confinement level by applying substantial positive or negative ohmic currents to increase the shear. The plasma conditions which lead to the development of the neoclassically predicted electron root of the radial electric field were examined in detail. Variations of the magnetic field configuration and the observation of suprathermal electrons by vertical ECE observation gave further evidence that the transition into the electron root is induced by locally trapped suprathermal electrons and not by thermal radial fluxes.

A new diagnostic for measuring the line-integrated density based on the Cotton-Mouton effect was successfully applied to W7-AS. This diagnostic is especially suited to measuring high densities in stationary discharges. First results are in good agreement with other line-integrated density measurements.

In preparing the divertor experiments predictive 2D simulations of island divertor plasmas and a 3D Monte Carlo edge transport code were extended. Further theoretical work relating to experimental results on W7-AS dealt with, for example, electron cyclotron resonance heating (ECRH) power absorption at high power levels, production of suprathermal electrons, neoclassical impurity transport and the neoclassical bootstrap current.

2. EXPERIMENTAL AND THEORETICAL RESULTS

2.1 Boundary Layer and Plasma-Wall Interaction Studies

2.1.1 Edge density limit study

In currentless W7-AS discharges, the maximum achievable plasma density is limited by an impurity-radiation-induced thermal instability (density limit, DL). The analysis includes limiter-bounded NBI (0.35 - 1.2 MW) discharges at B = 1.25 T and 2.5 T and $\iota = 0.34$. The density was slowly ramped up until the discharges collapsed.

The DL onset condition is found to be determined by detachment from limiters, as indicated by a significant drop of the

down-stream ion saturation current I_{sat} (from limiter-integrated Langmuir probes). Detached scenarios could not yet be stably maintained in W7-AS. The LCMS upstream density (from the Li beam) relating to the onset of detachment scales as $n_{es}^{det} \propto P_s^{0.5} B^{0.8}$ (Fig. 1), with P_s being the net power flow across the LCMS. This result is well consistent with a SOL two-point estimate including the power balance along field lines, momentum balance and sheath boundary condition. The B dependence needs further confirmation because the low-field discharges were less close to the quasi-steady state than those at high field.

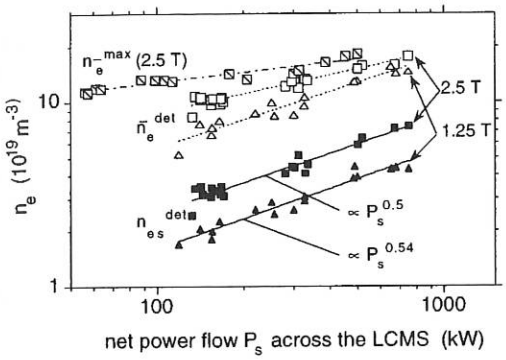

FIG. 1: Threshold densities for the onset of detachment from limiters indicated by an I_{sat} drop. n_e^{max} indicates maximum densities transiently achieved during detachment.

2.1.2 *Plasma radiation with nitrogen injection*

Nitrogen injection into separatrix-dominated discharges with magnetic islands at the plasma edge or limiter-dominated discharges with smooth open flux surfaces caused a considerable increase of the plasma radiation. The change of the plasma parameters at the edge and the spatial distribution of radiation were studied in detail.

Despite the quite different magnetic configurations and injection methods (erosion probe and gas puffing; see Annual Report 1996) the radiation pattern during strong impurity injection was found to be quite similar. In particular, enhanced radiation from island regions has not been observed even after injecting nitrogen into a magnetic island.

Strong injection caused radial plasma shrinking and pronounced poloidal asymmetries of the radiation inside the separatrix or last closed flux surface (LCFS) with a higher radiation level on the inboard side. Both effects appeared when the electron temperature at the plasma edge decreased to values lower than 40 eV. They are more strongly pronounced with increasing plasma density and decreasing temperature. When the electron temperature near the LCFS decreased to values lower than 20 eV, radiative instabilities were observed with the present gas injection control system. Pulsed nitrogen injection caused strongly localized radiation zones (MARFE's) on the inboard side at plasma densities of 1.6×10^{20} m^{-3}. The electron temperature measured on the outboard side decreased transiently to about 10 eV. In contrast to tokamaks, the radiating region is not toroidally symmetric but seems to follow a helical line within a modular section similar to the helical edge observed earlier on the outboard side.

It remains to investigate the possibilities and limitations of stabilizing plasma conditions with edge temperatures lower than 30 eV with a more sophisticated control system.

2.1.3 *Sniffer probe measurements*

The hydrogen-to-deuterium isotope ratio in the W7-AS stellarator was studied with the help of the sniffer probe during discharges with deuterium neutral beam injection. The results were compared with measurements during discharges with hydrogen neutral beam injection and also with discharges with only ECRH heating. Comparison with hydrogen NBI shows that the ratio of H in the plasma can be lowered from above 35% to the range of 14 to 27% by injection of D instead of H. Comparison with discharges without any NBI shows a lower H ratio for the latter of only 11 to 17% although in both cases only deuterium is introduced into the vessel. This is clear evidence that the hydrogen content in the plasma is largely determined by plasma-wall interaction, which itself depends on the type of the discharge.

In order to investigate the varying influence of the vessel walls, the correlations and partial correlations of the hydrogen contents in the plasma with other parameters such as energy content, rotational transform, line density and deposited neutral beam energy were studied. The result shows that particularly the energy content influences the ratio of hydrogen in the plasma, but also a correlation of the power deposited by NBI with the isotope ratio remains. It can be concluded that the limiters are not the main reason for the observed higher fraction of hydrogen in the plasma. The reason is a change in particle and energy charge onto the vessel wall (or parts of it) due to a change in plasma configuration during NBI heating.

2.1.4 *Edge transport code development and applications*

B2/EIRENE code, W7-AS version. In view on the planned installation of an island divertor in W7-AS, predictive 2D simulations of plasma scenarios in an island divertor configuration with "natural" 5/9 boundary islands were extended to higher densities and to self-consistent treatment of carbon (sputtered from the targets) as edge-dominating impurity. Volume recombination effects were considered. The power flowing across the separatrix was kept fixed at 600 kW. The main result is that - in this approach - stable, partial detachment is predicted at upstream separatrix densities $2 \times 10^{19} \leq n_{es} \leq 8 \times 10^{19}$ m^{-3}. The radiation zone is concentrated at the power-carrying layer around the island separatrix and shifts with increasing density from the target vicinity towards the x-points. At maximum stable density, about 90% of the input power is radiated off by carbon from the SOL.

EMC3/EIRENE code. The first simplified version of the EMC3 /EIRENE 3D Monte Carlo edge transport code was substantially extended. Implementation of the ion parallel momentum

equation was completed by including the cross-B viscous and convective transport of parallel momentum. The convective energy fluxes were introduced into the heat balance equations and the energy transports for ions and electrons were decoupled to allow application of the code to low-density plasmas, for which the ion and electron temperatures may significantly differ. The balance equations for mass, momentum and energies are treated with a common Monte Carlo algorithm, which solves both the diffusive and convective terms. Additionally, the code was parallelized on the Cray-T3E, leading to a drastic speed-up of the computations with 95% linear efficiency.

Drift effects. In W7-AS, with the islands deeply cut by the target plates, the poloidal electric drift fluxes associated with radial temperature gradients inside the islands can be larger than the poloidal component of the parallel particle fluxes, due to the small poloidal length of the separatrix and the very small field line pitch in the island reference frame. For W7-AS low-density ECRH discharges, higher densities (from Langmuir probe array data) were measured for the lower or upper island fans, depending on the B-field direction (Fig. 2).

The drift velocities resulting from estimated radial temperature gradients were inserted in the EMC3/EIRENE code, leading to the same asymmetry of the density contours as observed. The poloidal density gradient also implies an imbalance of the power and particle fluxes to the plates, which is consistent with calorimetric and H_α measurements.

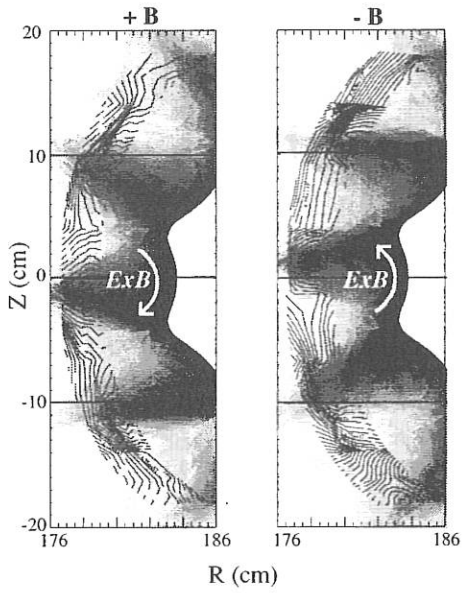

FIG. 2: Density contours from the probe array (curves) compared with EMC3/EIRENE results for positive and negative B-field.

2.2 Confinement and Transport

2.2.1 *Improved confinement NBI discharges*

The confinement time of ECRH and high-density ($n_e > 10^{20}$ m^{-3}) NBI discharges in W7-AS is rather well described by the $ISS95_{W7}$ scaling, which roughly represents the ISS95 expression multiplied by a factor of 1.25. Density control of NBI discharges at values of $n_e \leq 10^{20}$ m^{-3} turned out to be the crucial element for obtaining high-confinement NBI (H-NBI) discharges with confinement times which are enhanced by a factor of 2 above the W7-AS L-mode level, i.e. up to a factor of 2.5 above the ISS95 scaling. For NBI discharges at higher power with additional ECRH improved confinement of up to 100% was observed, too (Fig. 3). During the gradual transition to good confinement, the density profile becomes narrower, whereas the temperature profile broadens. In all discharges with optimum confinement the measured density profiles at outer radii are very similar for all central densities from 5 to 11 $\times 10^{19}$ m^{-3} and heating powers between 0.4 and 1.3 MW.

From NBI discharges at the low confinement level, the H-NBI discharges can be distinguished by the low edge density and less steep density gradient which extends further into the plasma core. This distinguishes them from H-mode discharges, which have a steep density gradient concentrated at the edge of the plasma. The confinement improvement is independent of the horizontal shift of the magnetic configuration (see Fig. 4).

As relevant physics parameters to obtain H-NBI discharges, magnetic and E×B velocity shear were investigated. The ι profiles in ECRH and H-NBI discharges are not very different, while the confinement was up to a factor of two different. Since the ι profiles are rather flat in both cases, it was concluded that magnetic shear is not the parameter to access the H-NBI regime.

On the other hand, the strong radial electric field gradients observed in the region of the transport barrier could play an important role. It was shown that neoclassical theory can account for the measured electric field. Furthermore, the theory indicates what is essential for obtaining the strong fields: The necessary condition is to have high ion temperatures in the radial region where considerable ion density and temperature gradients are present. Neutral beam heating is favourable to achieve this condition since it provides ion particle and energy sources in the core and hence the necessary gradients. Density control is the second condition needed to obtain high temperatures. In high-density NBI discharges, the central ion temperature is

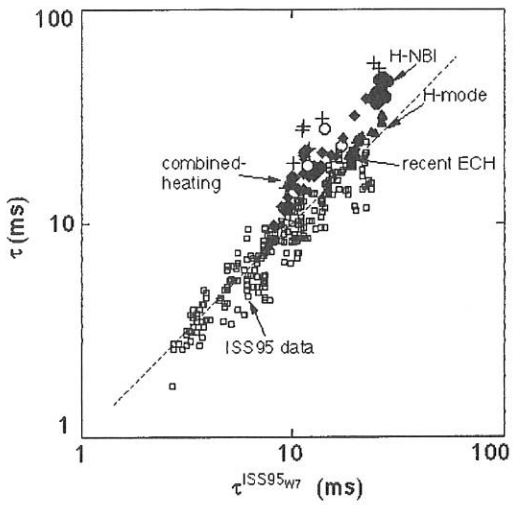

FIG. 3: Diamagnetic energy confinement time for different confinement regions compared on the basis of the $ISS95_{W7}$ scaling. Crosses indicate kinetic values.

only 300 eV compared with 800 eV in the H-NBI case. In ECRH discharges, on the other hand, the lack of a density source limits the density gradients to the plasma edge.

Nevertheless, the radial field gradients of ECRH and H-NBI discharges are not very different. If shear in the E×B flow is considered to be the stabilizing parameter, the conclusion would be that the turbulence-driving term must be stronger in discharges with ECRH than in NBI discharges. A reason for that could be that ECRH strongly heats the electron channel with very high power densities, while NBI heats electron and ion channels more gently with a rather broad deposition profile.

The fact that confinement improves gradually rather than through a fast transition could point to a causality loop where turbulent transport is reduced by sheared flow generated by the neoclassical electric field. The reduced anomalous transport leads to steepening of the gradients and increasing temperatures, which in turn again increases the neoclassical electric field etc. This loop would be interrupted when anomalous transport is suppressed and transport is, as observed, on the neoclassical level.

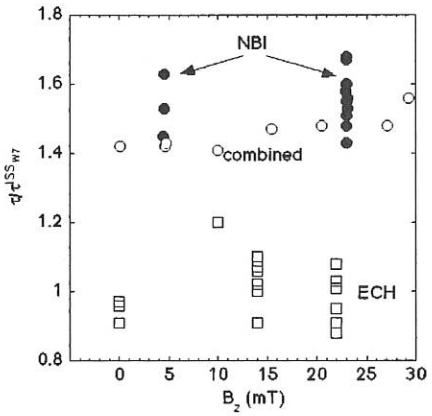

FIG. 4: Ratio of the diamagnetic confinement time and the predicted one for combined heating (blank circles), H-NBI (solid circles) and ECRH discharges (blank squares) as a function of the vertical magnetic field strength.

2.2.2 *Impurity transport in high-confinement discharges*

Aluminium laser blow-off experiments were performed in order to study the impurity transport in H-NBI discharges (see Sec. 2.2.1). Nearly stationary phases of 100 ms were used for the investigation.

Transport coefficients were derived by analysis of radially and temporally resolved radiation measured by the soft-X camera behind 25 μm beryllium filters during the penetration process of the injected aluminium into the plasma centre. The impurity density profiles were reconstructed for each time point, assuming coronal equilibrium in a first step, which is considered to be applicable in the high-density, low-transport discharges under investigation. The transport coefficients were then derived from the analysis of impurity density fluxes which are calculated from the temporal and radial behaviour of the reconstructed impurity density profiles. Deviations from the coronal equilibrium due to non-negligible transport were taken into account by additional transport code calculations.

The transport coefficients could be measured only in the central half of the plasma and were linearly extrapolated to the plasma edge. A rather low diffusion coefficient $D(r) = 0.07$ m^2/s and an inward convection velocity of $v(r) = 4(r/a)$ m/s were derived. With these values, the temporal evolution of spectral lines of Al X (33.3 nm) (measured by a grating spectrometer), of Al XII (0.778 nm) (measured by a crystal spectrometer) and of the radial soft-X profile itself could be simulated well by the SITAR transport code.

2.2.3 *Optimum confinement discharges under limiter and separatrix conditions*

All of the above-described discharges were performed at $\iota \approx 1/3$ and $B = 2.5$ T. During the recent experimental campaigns the question of achieving optimum confinement under separatrix conditions around $\iota \approx 1/2$ was one of the topics of investigation. First results at densities of about 0.7×10^{19} m^{-3} show an increase of τ_E by a factor roughly similar to that with the ISS95 scaling as in the case of $\iota \approx 1/3$ (see Sec. 2.2.1). Differences in the central electron and ion temperatures with similar heating scenarios - T_e is higher and T_i lower than at $\iota \approx 1/3$ - may be due to the smaller plasma radius at $\iota \approx 1/2$ and the modified NBI injection energy from 45 to 50 keV. Both effects change the NBI power deposition. Density and temperature profiles show the same features as found at $\iota \approx 1/3$, such as narrow density profiles and steep density and temperature gradients. Reducing the vertical magnetic field from $B_z = 22$ mT to $B_z = 0$, thus removing the plasma from the inboard limiters, does not significantly change the energy content of the discharge but increases the radiated power.

2.2.4 *The isotopic effect*

Investigations of the isotopic effect were extended to high-density ECRH discharges and the H-NBI confinement regime. Previous experiments with ECRH plasmas indicated a weak or absent effect.

The ECRH discharges of the recent campaign were carried out at $B_0 = 2.5$ T, $\iota \approx 1/3$, $P_{ECRH} = 460$ kW and $n_e \approx 5 \times 10^{19}$ m^{-3}. Both profiles and the diamagnetic energy content indicate an improvement of 20 to 30% in the deuterium case. This effect is stronger than in the previous experiments. An analysis of power modulation experiments, however, did not show a difference in the electron thermal diffusivity. This would indicate that the ion channel improves, which is in contradiction to the experience that the ion diffusivity is consistent with neoclassical theory.

In the case of the H-NBI discharges no isotopic effect could be detected. Discharges with H-into-H and D-into-D NBI were compared. About 80% of the 500 kW of injected power was absorbed in the plasma. The discharge parameters were $B_0 = 2.5$ T, $\iota \approx 1/3$ and $n_e \approx 9 \times 10^{19}$ m^{-3}. Both the diamagnetic and

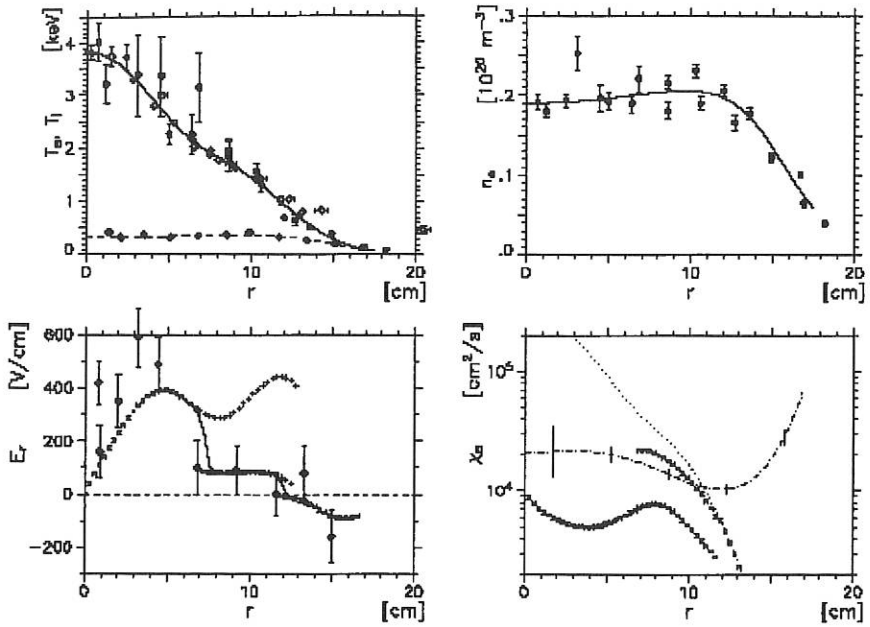

FIG. 5: Upper: electron temperature (solid line), ion temperature (dashed line) (left) and electron density (right). Lower: radial electric field from spectroscopy (dots) and neoclassical calculation (crosses: stable roots, for r < 6 cm the thermal electron root, points: unstable solution) (left) and χ_e from experimental data (dot-dashed), for stable roots (crosses), for unstable solution (points) (right).

the observations, it must be assumed that the transition into the electron root is induced by locally trapped suprathermal electrons created in the local magnetic field minimum in the ECRH launching plane. These electrons are subject to a vertical drift and thus increased electron losses from the plasma centre. This assumption is confirmed by an initially much faster decay time of the central electron temperature in comparison with the temperature outside the region of the electron root solution after the ECRH power is switched off. Additionally, the strong positive E_r disappears when the local magnetic field minimum is removed by slight modifications of the magnetic configuration. Heating power and density scans indicate the existence of power and density thresholds. Power balance analyses reveal strongly reduced electron heat conductivity in the central region of the plasma as a consequence of the strong E_r. Thus, extremely high electron temperatures of up to 4 keV were observed (Fig. 5).

the kinetic energy content where 10 to 20% higher for the deuterium discharges. Taking into account the higher absorbed power with D injection, the isotopic effect ranges between 0 and 10%, depending on which of the co NBI sources was used.

To summarize the bulk of all experiments relating to the isotopic effect, it must be stressed that confinement of deuterium discharges was never inferior to that of the hydrogen ones. Statistically, an isotopic effect can thus be detected in W7-AS. However, its magnitude is only of the order of 10%.

For the H-NBI discharges, which are on the neoclassical transport level over the major range of the plasma radius, an inverse effect might be expected due to increased neoclassical losses in the deuterium case. Predictive transport analyses indicate, however, that this need not be the case since the radial electric field increases in the case of deuterium, leaving the transport almost unchanged. This is understandable since the neoclassical electron transport is independent of isotopic mass and the electric field has to reduce the ion particle transport to the level of the electron transport.

2.2.5 *The non-thermal electron root*

In W7-AS, the electron-root solution is expected to lead to strong positive values of the neoclassical radial electric field E_r in the close vicinity of the magnetic axis. It should appear at low central electron densities, preferably with ECRH heating.

Recently, strong positive E_r were observed in W7-AS with 140 GHz ECRH in 2nd harmonic X-mode. However, the experiments indicate that the neoclassical electron root, which is driven by thermal radial fluxes, was not achieved. To describe

2.2.6 *The role of magnetic shear*

Confinement in W7-AS is found to be strongly related to magnetic shear in the presence of high-order rational values of the rotational transform ι. Shear was applied by inductive current drive to ECRH discharges at moderate β ($\beta_0 < 1\%$, $n_e \approx 4 \times 10^{19}\ m^{-3}$, $B_0 = 2.5$ T, $P_{ECRH} = 450$ kW at 140 GHz). With a small net plasma current ($I_p \leq 5$ kA), the well-known strong dependence of energy confinement on the boundary value ι_a is observed (Fig. 6), which, however, is smoothed by increasing the current (to +15 kA) and disappears at the highest current (+25 kA). Here, the level of optimum confinement in the current-free case is reached. (An increase of the effective plasma radius from 0.15 m at $I_p = 0$ kA to 0.165 m at $I_p = 25$ kA should be noted.)

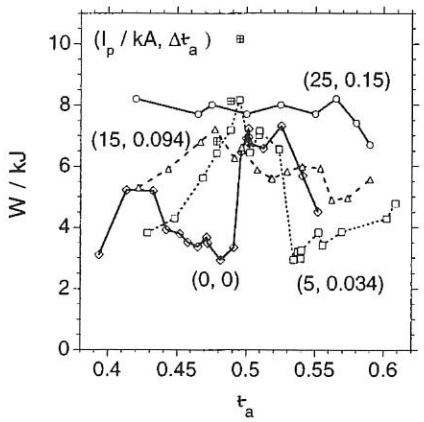

FIG. 6: Dependence of the plasma energy on the boundary rotational transform for various plasma currents. For three discharges at $I_p = 5$ kA density control was lost and the measured energy (crossed squares) was scaled by $n^{1/2}$ (squares).

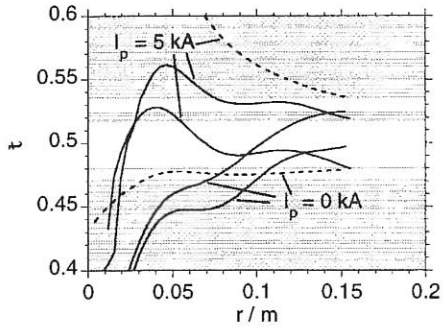

FIG. 7: Calculated ι profiles for discharges with net plasma current as indicated (solid lines: optimum confinement; dashed lines: degraded confinement). Rational n/m, m ≤ 30, are given for reference (horizontal lines; the shaded area covers the range of rationals with m ≤ 15).

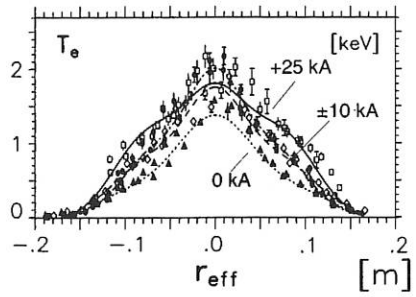

FIG. 8: T_e profiles for discharges at ι_a = 0.42 and various plasma currents.

For the discharges of Fig. 6, degraded confinement is associated with a very flat T_e profile at larger radii (r > 5 cm), whereas for good confinement a strong T_e gradient extends to the edge. The density profiles are similar for all discharges. ι-profiles are calculated by the NEMEC equilibrium code, with inductive and bootstrap current profiles from the DKES code. Figure 7 shows ι-profiles for low-current discharges (I_p = 0 and 5 kA) at selected ι_a-values close to 1/2, where the sensitivity of confinement to ι_a is strongest. The close vicinity of ι = 1/2 is free from rational values ι = n/m. For degraded confinement with small bootstrap current (~ 2 kA), shear is basically determined by the inductive current, i.e. remains low if no net current is imposed. For good confinement, both low or moderate shear may result from the combination of inductive and bootstrap current (about 7 kA) density profiles

The analysis indicates that the confinement essentially depends on magnetic shear and resonant ι-values in the outer plasma region: for optimum confinement, ι(r) has to be in the "resonance-free" region (e.g. ι_a = 0.48 at I_p = 5 kA), or shear has to be sufficiently large in the presence of high-order n/m resonances (e.g. ι_a = 0.495 at I_p = 0). Degraded confinement is associated with low shear in the presence of such resonances (e.g. ι_a = 0.48 at I_p = 0). With respect to the maximum m number, which determines the width of the "resonance-free" region, the calculated ι_a values for the onset of confinement degradation below ($\iota_a \approx 0.49$) and above ($\iota_a \approx 0.53$) ι_a = 1/2 are not consistent. However, since at present we do not know which specific perturbations at the high-order rational surfaces enhance transport, there is no a priori reason for such symmetry. Furthermore, magnetic boundary islands due to the rather strong "natural" 5/9 perturbation will be important as well for $\iota_a \geq 0.53$.

Figure 8 shows the radial profiles of the electron temperature for discharges with plasma currents of up to +25 kA at ι_a = 0.42, which is in the resonance region. With increasing shear, continuous steepening of the T_e gradient is observed at the boundary independently of the sign of the shear. In this region (0.08 to 0.14 m) the heat conductivity (from power balance analysis) decreases by a factor of up to 5. As compared with neoclassical transport, the experimental χ_e is anomalous over the whole plasma cross-section for I_p = 0, neoclassical in the very centre for ±10 kA, and neoclassical up to r/a ≤ 0.7 for +25 kA. Only at the very plasma edge does transport remain strongly anomalous. Thus, with increasing shear, the region dominated by neoclassical transport continuously expands towards the boundary due to the increase of neoclassical transport with temperature and a simultaneous strong reduction of anomalous transport.

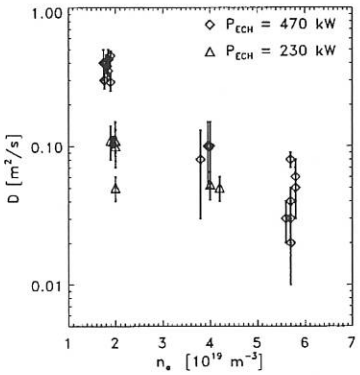

FIG. 9: Diffusion coefficient D from perturbative density transport experiments as a function of density and heating power.

2.2.7 *Perturbative particle transport studies*

In perturbative particle transport experiments, an oscillating gas feed was used to produce a harmonic density perturbation propagating from the plasma edge to the centre. The experiments were carried out at different plasma densities, heating powers and magnetic field strengths.

The amplitude and the phase of the propagating density perturbation were measured with the multi-channel microwave interferometer. The electron transport was modelled with the radial density transport equation where the electron flux was composed of diffusive and convective contributions. The diffusion coefficient was always well defined and the value is independent of whether a convective velocity was fitted simultaneously or taken as zero. The diffusion coefficients determined agree well with the equilibrium transport coefficients analyzed without a convective contribution.

The results are summarized in Fig. 9. The diffusivity decreases with increasing density and increases with increasing ECRH power. At a magnetic field of B = 2.5 T the diffusion coefficients were smaller than at 1.25 T. To determine the convective velocity more accurately, it was fitted to data obtained

from experiments at the same plasma parameters but with different gas feed modulation frequencies. With $n = 2 \times 10^{19}$ m^{-3}, $P_{ECRH} = 500$ kW, B = 2.5 T and $t_a \approx 1/3$ no indications of a convection contribution were found.

2.2.8 *Cold-pulse experiments*

In order to determine the transient energy transport coefficient, cold-pulse experiments were carried out in W7-AS. The plasma edge was perturbed by carbon injected with a laser-blow-off system. The ablated carbon leads to a fast electron density increase in the plasma edge. This causes an edge electron temperature drop during 1 - 2 ms. Radiation and ionization energy losses are only of minor importance for this initial perturbation. The propagation of the pulse to the centre is compared with model calculations.

The cold pulses were analyzed with ASTRA the time-dependent transport code. The electron heat transport equation is solved with electron-ion coupling taken into account. The radiation losses (Fig. 10, left) are prescribed in the calculation. For each discharge, the electron heat diffusivity profile under stationary plasma conditions, χ_e^{PB}, is calculated and then used in the models to simulate the transient response to the cold pulse.

The simulated and measured electron temperature evolutions for a large cold pulse, with a temperature decrease at the edge of 50%, are shown in Fig. 10 (right). In the simulation χ_e^{PB} had to be transiently increased by a factor of 2.7 during 1.183-1.184 s at r > 10 cm and reduced back to χ_e^{PB} within 3 ms. This increase could not be modelled with local plasma parameters. Nevertheless, this cannot be considered as a nonlocal effect. Within this very short time interval the local density at the edge is doubled by introducing cold electrons. This drastically changes the electron distribution function. This distortion could very well lead to a local enhancement of the local turbulence level. For the long-term evolution of the temperature, a weak local dependence of the diffusivity was assumed. In the case of small, cold-pulses, with an edge temperature perturbation of 20%, the propagation of the pulse could be modelled by using the steady-state diffusivity modified by a term $\sim n^{-0.5} T^{1.0}$.

With respect to all examined small and large, cold pulses, the transient response of the plasma to a perturbation at the plasma edge can be modelled with local models for the electron heat diffusivity. Nonlocal effects such as an increase of the central temperature were never observed in W7-AS.

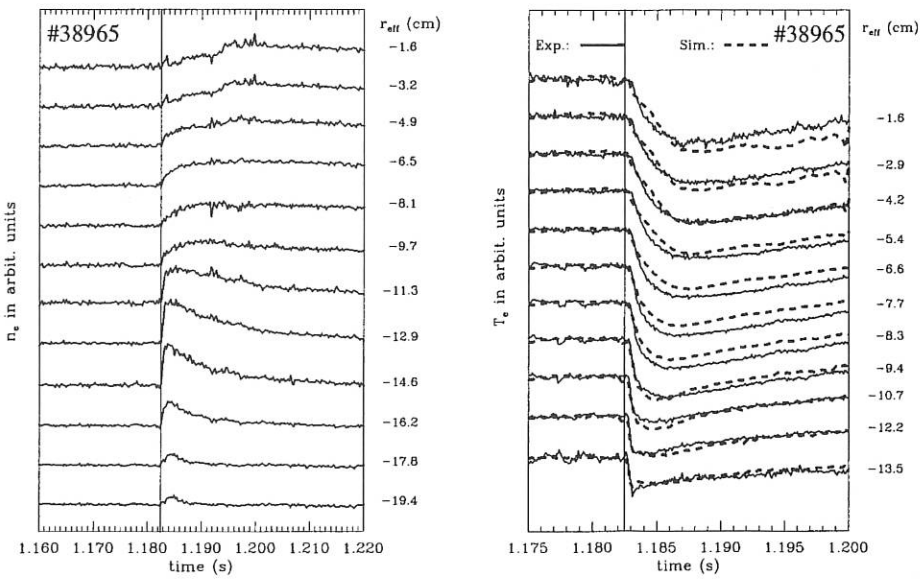

FIG. 10: Electron density and temperature evolutions at different radii for a large, cold pulse. On the right-hand side, the simulated and ECE electron temperatures are compared.

2.3 Ion Cyclotron Resonance Heating (ICRH)

During the 1997 experimental campaign the copper inner conductors of 8 m long section of transmission line between the RF generator and the stub tuners were replaced with iron inner conductors. This greatly reduced the tendency of the generator to self-oscillate as a consequence of arcs. Thus it was possible to condition the transmission lines, the antenna feeder lines and the antenna itself to higher voltage stand-offs. For 2nd harmonic hydrogen heating maximum power levels of 1.1 MW for up to 400 ms were successfully applied to the antenna. For minority hydrogen in deuterium heating only maximum power levels of 700 kW could be applied to the antenna due to the lower antenna plasma loading.

Neutral beam (NBI) generated hydrogen start-up plasmas were successfully sustained solely with ICRH for up to 250 ms with 2nd hydrogen harmonic heating. This was sufficient to reach steady-state values of the electron density ($n_e(0) = 5 \times 10^{19}$ m^{-3}), the electron temperature ($T_e(0) = 300$ eV) and the hydrogen energy spectrum ($T_H(0) = 400$ eV and $T_H^{tail} = 2$ keV) measured with active charge exchange. About 500 kW of ICRH power was radiated from the antenna. At higher densities the plasma eventually suffered from thermal collapse. The pulse duration was limited by arcs in the RF transmission lines.

ICRH at the 2nd harmonic hydrogen frequency was applied to NBI target plasmas. With typical plasma parameters ($n_e(0) = 5 \times 10^{19}$ m^{-3}, $T_e(0) \approx T_H(0) = 450$ eV, NBI = 400 kW) both the electron and ion temperatures rose by about 200 eV. A typical shot is shown in Fig. 11. The power at the antenna was about 1.1 MW for up to 300 ms. From the change in the antenna loading resistance it is estimated that about half of this power is radiated into the plasma. The antenna was operated in 0- and in π-phasing. No substantial difference was found either in the antenna coupling resistance or in the bolometric signal. By comparison of the increases in diamagnetic energy with established W7-AS confinement time scaling and by evaluation of ICRH modulation experiments it was found that more than 70% of the ICRH power radiated from the antenna was absorbed in the plasma.

Conditioning of the double-strap antenna located on the high-field side in the region of triangular-shaped plasma was begun. With NI-heated target plasma, an RF power of up to 100 kW for 10 ms could be applied to the antenna. Reasonable antenna plasma loading of ~ 3 Ω was observed, but no heating effects.

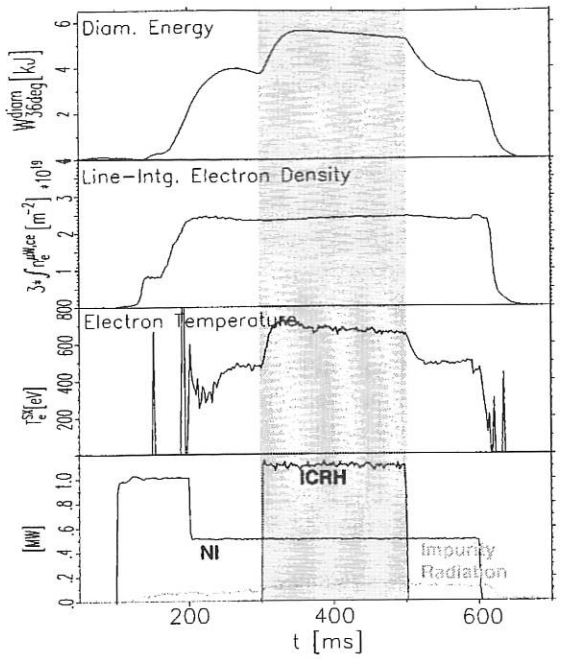

FIG. 11: 2nd harmonic hydrogen heating in shot 41912.

2.4 Electron Cyclotron Resonance Heating (ECRH)

2.4.1 The ECRH system

The W7-AS stellarator is equipped with a two-frequency ECRH system operating at 70 GHz and 140 GHz. The 70 GHz system allows plasma start-up and heating with 0.4 MW at a resonant magnetic field of 1.25 T at the 2nd harmonic X-mode, and 2.5 T at 1st harmonic O-mode. The 140 GHz system (3 gyrotrons) operates at a resonant field of 2.5 T in 2nd harmonic X-mode with a power of 1.8 MW. The year 1997 saw the completion of the installation and successful operation of an advanced 140 GHz gyrotron with energy recovery (collector voltage depression) and an output power of 0.8 MW at 50 % electrical efficiency and pulse length 1 s. The gyrotron marks a milestone in the development of gyrotrons towards the needs for W7-X and was provided by the Institute of Applied Physics, Russia, in the frame of a collaboration contract. All five gyrotrons are operating routinely and provide high flexibility for the physics experiments, because each RF beam can be steered independently to the plasma by an optical launching system with arbitrary polarization. The poloidal and toroidal launch angle of each individual beam can be chosen for on- and off-axis heating and current drive, respectively. Power modulation at arbitrary amplitudes of up to 10 kHz is possible for perturbation experiments and studies of transient phenomena. This sophisticated system was used to investigate mode conversion heating above the cut-off density, with both ECRH frequencies.

2.4.2 ECRH with electron Bernstein waves

The accessible plasma density for electron cyclotron heating (ECH) with electromagnetic waves is limited by the plasma cut-off. For the electrostatic electron Bernstein wave (EBW), the third EC mode able to propagate in a hot plasma, no such limit exists. However, since EBW's cannot be excited from the outside, they have to be generated via mode conversion from the electromagnetic waves. This can be performed by the O-X-B process at the plasma edge. The EBW's then propagate towards the dense plasma centre, where they are absorbed by cyclotron damping at the EC resonance layer.

At W7-AS EBW's were generated via the O-X-B-mode conversion of two 70 GHz microwave beams with 180 kW of power each. The central density of the neutral beam injection (NBI 360 kW) sustained target plasma was up to 1.5×10^{20} m^{-3}, which is more than twice the 70 GHz O-mode cut-off density. The central magnetic field was varied between 2.0 and 2.5 T to show resonant absorption of the EBW's. At the ECRH launch position the magnetic field increases from the outside to the inside and is approximately given by the following relation: $B(r_{eff}) = B_0\, A / (A + r_{eff} / a)$ with A = 10.5. The power deposition was estimated from the change of the temperature profile at the power switch-off, which was calculated from the soft-X emission and the Thomson scattering diagnostic. The central temperature was 500 eV. To obtain the radial X-ray emission profile the signals were inverted to the magnetic flux co-ordinates. The time and radial resolution were 0.1 ms and ~ 1 cm respectively. In Fig. 12 the absorption profiles for different magnetic fields are shown. The absorption is strongly Doppler-shifted due to the oblique launch and moves from the high-field side at 2.0 T through the centre (2.2 T) to the low-field

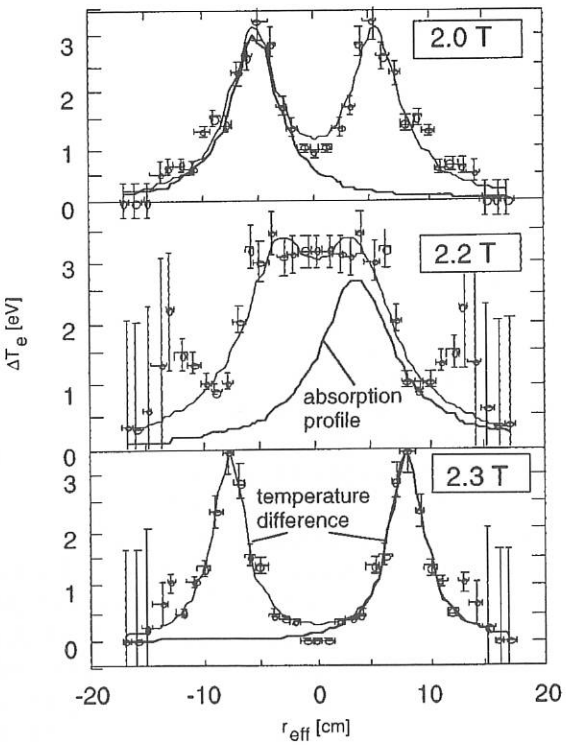

FIG. 12: Changes of temperature 3 ms after O-X-B heating switch-off and the related ECRH absorption profiles for different central magnetic fields.

side at 2.3 T with increasing magnetic field, which clearly demonstrates the propagation and local cyclotron absorption of the EBW's for the first time.

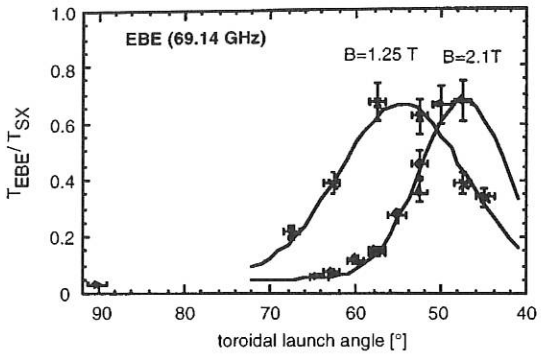

FIG. 13: Angular dependence of EBE for different central magnetic fields, a central density of 1×10^{20} m^{-3} and temperature of 600 eV. The signal is normalized to the central soft-X temperature.

2.4.3 *Detection of electron Bernstein wave emission (EBE)*

Since at the cyclotron resonance the plasma is optically thick to the EBW's, it is a black-body emitter for EBW's the same as it is for electromagnetic EC waves below the cut-off density. But in contrast to the electromagnetic waves for the EBW's it is generally not possible to leave the plasma, since they have a density threshold for propagation at the upper hybrid resonance (UHR), which totally encloses the inner part of the plasma. The EBW radiation is trapped inside the plasma as in a "hohlraum". Except for those EBW's born with an optimal $N_{||}$ (parallel to the magnetic field) for the inverse O-X-B process or for those EBW's which had achieved such an $N_{||}$ component on their way in the plasma by scattering or magnetic configuration effects such as the field line curvature. A non-vanishing $N_{||}$ component is equivalent to an oblique viewing angle of the receiving antenna. The ECE radiometers were connected with an unused movable ECRH launch antenna. After calibration with thermal ECE the receiving mirror was turned to the optimum viewing angle of 47° with respect to the magnetic field and the plasma density was ramped up to above the cut-off density. The plasma was sustained by two neutral beam injectors. The central magnetic field was lowered to 2.1 T to compensate the Doppler shift of the EBE spectrum. When the central density reaches the cut-off density of the emitting frequency, the B-X-O window opens and EBE appears. Scans of the viewing angle were performed for the 1st and 2nd harmonic EBE as shown in Fig. 13, and the predicted angular windows at 47° for 2.1 T and 55° for the 2nd harmonic EBE (69.14 GHz) at 1.25 T could be experimentally reproduced. The radiation temperature was up to 70% of the temperature measured by soft-X emission and Thomson scattering. This might be due to reduced X-O conversion caused by density fluctuations at the cut-off surface. The EBE spectrum is about 6 GHz Doppler-shifted in respect of the ECE spectrum and consists of two parts. The thermal part reflects the local thermal emission of EBW and, in principle, a radial temperature can be reconstructed from this radiation. The high-frequency part represents nonlocal "hohlraum" radiation as has already been discussed. Both the local and nonlocal characters of the EBE spectrum were demonstrated by cold-wave propagation with laser blow-off. The EBE opens a new operational window for EC diagnostics beyond the cut-off for fusion as well as for ionospheric research.

2.4.4 *Non-thermal electron energy distribution from ECE measurements*

ECRH heating at high power density results in a distortion of the Maxwellian electron distribution function located near the resonance zone with the creation of a suprathermal tail. This may affect the confinement properties, especially in stellarators, where ripple-trapped electrons are only poorly confined. Vertical ECE observation provides a tool for analyzing the down-shifted radiation emitted by the suprathermal electrons with little reabsorption. The vertically viewing Gaussian antenna system is arranged in the ECRH deposition plane. From a radial scan of the antenna it is demonstrated that the population of the suprathermal electrons is restricted to the power deposition zone (radial extent 3 - 5 cm).

Measured spectra are simulated with a ray-tracing code which assumes a bi-Maxwellian electron distribution function. Due to the presence of a local maximum of B along the vertical viewing path two peaks appear in the calculated ECE spectrum. This double-peaked structure is also found in the measured spectra (see constant part in Fig. 14). Heating a low-density plasma by high-power ECRH in O-mode polarization leads to much higher radiation temperatures than in the X-mode case. Calculations result in a much higher central density at O-mode polarization, whereas only a weak variation of the energy of the suprathermal electrons can be observed (O-mode: $n_{e0,suprath} = 6\%\ n_{e0}$, $T_{e,suprath} = 7.5$ keV; X-mode: $n_{e0,suprath} = 0.5\%\ n_{e0}$, $T_{e,suprath} = 6$ keV). By switch-off experiments it is shown that the suprathermal radiation disappears on a time scale of about 1 ms, which is attributed to the loss mechanism or at least to the collisional slowing-down.

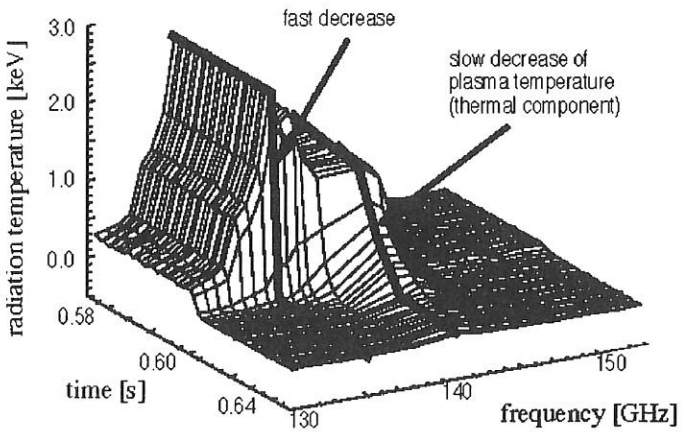

FIG. 14: Time behaviour of the ECE spectrum after the ECRH power is switched-off. Vertical observation with line of sight through the plasma centre (B = 2.5 T, $\iota \sim 1/3$, P = 800 kW, X-mode polarization).

2.5 Stability and Fluctuations

2.5.1 *Analysis of magnetic fluctuations*

Linear analysis of magnetic fluctuations measured with Mirnov probes was further developed. The normalized Lomb peri odogram, a generalization of Fourier analysis for nonevenly sampled data, was used in order to extract the poloidal mode number from spatial eigenfunctions as yielded by the SVD or from the cross-correlation function.

Nonlinear methods of analysis from dynamical systems theory were applied to Mirnov data from selected ECR-heated discharges, in collaboration with Th. Klinger (Univ. of Kiel). From a time series of Mirnov data the underlying phase space is reconstructed by a time-delay approach based on a theorem of Takens. An estimate of the dimensionality of the dynamics underlying the observed magnetic fluctuations is obtained from the correlation integral of the phase space attractor. The results indicate that the mode-like structures observed in ECR-heated plasmas (Fig. 15b) are **not** due to low-dimensional dynamics, i.e. their character is weakly turbulent.

2.5.2 *Correlated fluctuations of core temperature and density*

Temperature fluctuations were measured by correlation radiometry of ECE in purely ECRH-heated plasmas. The fluctuation spectra are composed of a low-frequency part, extending up to about 10 kHz, and a broadband component extending into the 100 kHz range of frequencies. The low-frequency component is connected with temperature perturbations of large radial scale length which propagate on a diffusive time scale from the edge into the plasma core. The high-frequency turbulent spectral component propagates on a ten to hundred times faster time scale in the opposite direction. The radial scale length is between 1.5 and 3 cm. This broadband component disappears in the case of zero temperature gradient, whereas density fluctuations as measured by reflectometry are still present. The behaviour can be explained by a turbulent mixing model.

A common antenna system is shared by the crossed-sightline correlation radiometer and a two-antenna reflectometry system. This allows simultaneous measurement of fluctuations in electron temperature and density within the same plasma volume with a poloidal width of 3 cm. A significant in-phase correlation with 10-30% coherency is observed for the high-frequency spectral component if the measured positions coincide (Fig. 16). The actual coherency may be even higher since part of the phase fluctuations measured by the reflectometer do not display the amplitude of the density fluctuations directly but arise from the 2-dimensionality of the perturbed reflecting surface. With increasing radial distance between the ECE emitting and reflecting layers, the coherency decreases. The phase difference between ECE and reflectometry signals corresponds to a phase velocity of the turbulent structures of several km/s directed radially outward in agreement with the value obtained from a correlation of the different ECE channels.

2.5.3 *Fluctuations at the plasma edge*

Fluctuations in the outer confinement zone and scrape-off layer (SOL) are investigated using Langmuir probe arrays to understand the mechanisms causing plasma turbulence in this region. At least a major fraction of the anomalous radial transport observed is due to this turbulence.

Fast sweeping of the probe characteristic with a sweep frequency >1 MHz was used to measure fluctuations of the plasma density, electron temperature and plasma potential simultaneously with each probe tip of a poloidal array (see Sec. 3). Density and electron temperature fluctuations are found to be approximately in phase in the spectral region of significant fluctu-

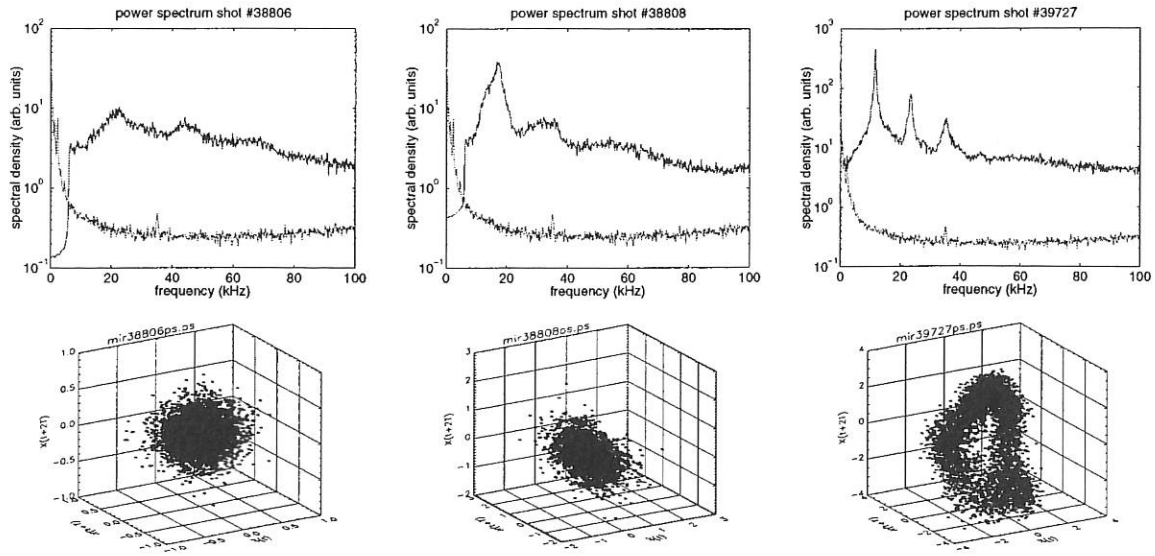

FIG. 15: Power spectra of Mirnov signals and noise (first row) and phase space diagrams for three discharges. (a) left: #38806, turbulence, (b) middle: #38808, weakly developed turbulence, (c) right: #39727, mode.

ation power. Plasma potential fluctuations are shifted in phase to result in an average outward E×B transport of particles and energy. The neglect of temperature fluctuations when calculating the fluctuation-induced particle flux is shown to result in an overestimate of the particle flux by 10 - 40%. The relative fluctuation level of the electron temperature is approximately 60% of the relative density fluctuation level.

The results of linear drift wave models and nonlinear turbulence code simulations (collaboration with B. Scott, Tokamak Phys. Division) were compared with Langmuir probe measurements. As input for the code calculations, the experimental values of the plasma density and electron temperature as well as the radial particle and energy fluxes at the last closed magnetic surface (LCMS) were used. Excellent agreement for many properties of the fluctuations was obtained, e.g., for the typical poloidal wavelength and correlation length, fluctuation amplitude and the probability density distribution function, as shown in Fig. 17 for the ion saturation current fluctuations.

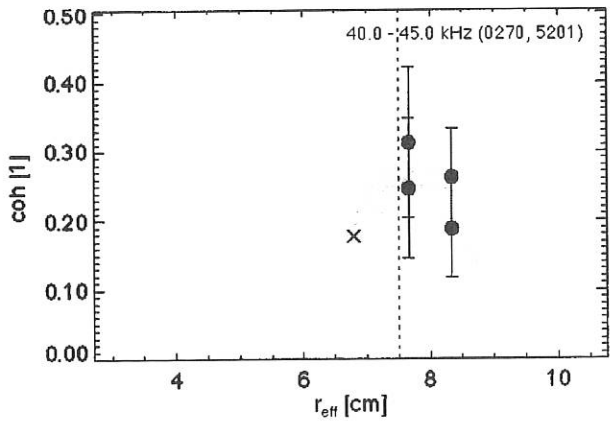

FIG. 16: Correlation between a reflectometry signal with reflecting layer at r_{eff} = 7.4 cm (vertical dashed line) and ECE measurements. By moving the reflecting layer the correlation maximum is shifted in the same way.

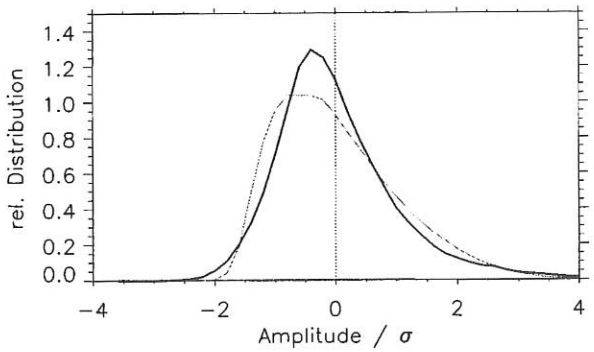

FIG. 17: Comparison of probability density distribution function of the ion saturation current from experiment (solid line) and non-local code simulation (dashed).

2.5.4 *Soft-X tomography of MHD modes*

The MiniSoX camera system with 320 channels (Miniature Soft X-ray cameras) can provide details of MHD-mode structures. Plasma discharges with strong tearing mode activity in the presence of ohmic current drive were used for tests of the tomographic reconstruction methods. Effects of mode-coupling and mode-locking phenomena similar to those in tokamaks were seen. The poloidal position of locked modes is in agreement with the (m = 2) error field in W7-AS as deduced from vacuum flux surface measurements.

New features of NBI-driven global Alfvén eigenmodes (GAE) could be revealed by SX tomography. SVD was used as a tool to separate mode structures from the equilibrium background

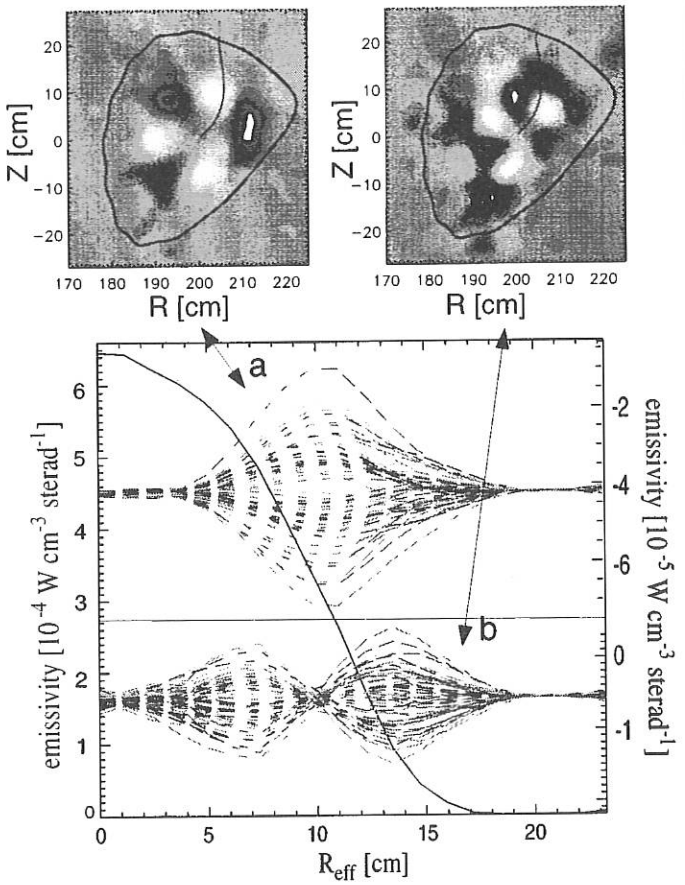

FIG. 18: Reconstructed mode structures (#35982) of an m=3 GAE with and without radial node (solid contour corresponds to a normalized radius of 0.75). The lower graph shows equilibrium and fluctuating emissivities along a magnetic angle of 40° (solid line in the upper two images) for both cases.

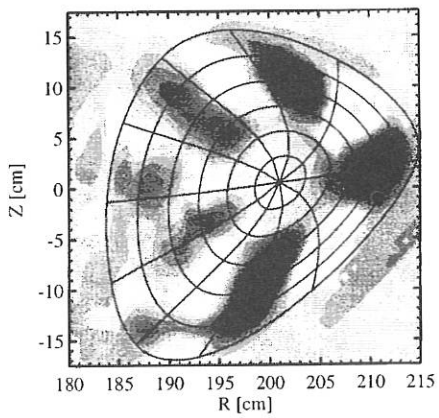

FIG. 19: X-ray tomogram of an n=2 TAE dominated by m = 5 in the inner part and by m = 6 in the outer part. (#39042, B = 2.5 T, I_p = 5 kA).

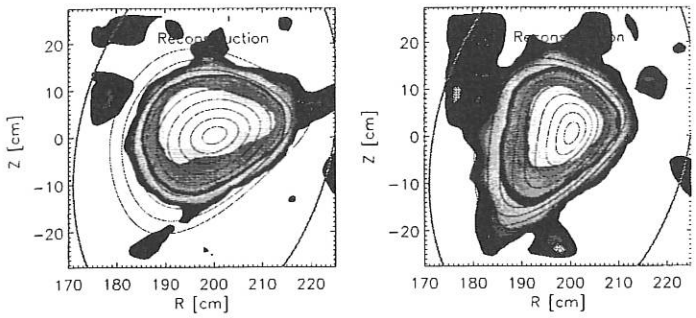

FIG. 20: Comparison of SX emissivity and flux surface contours calculated with NEMEC for large toroidal net currents (left : +30 kA, right: -30 kA).

emissivity. In Fig. 18 two GAE modes with the same poloidal mode number but different radial eigenfunctions are simultaneously observed in a plasma discharge with NBI heating. In the second example (Fig. 19), the poloidal mode structure is more complicated and consists of a dominant m = 5 component in the inner part and an m = 6 component further out. In this case OH current drive was used to increase shear, and therefore TAE gaps become accessible as in tokamaks. The observed structure is very likely due to an n = 2 toroidal Alfvén eigenmode (TAE) and is in agreement with gyrofluid code calculations (D.A. Spong, ORNL).

2.5.5 *Equilibrium and stability*

The reliability of the equilibrium calculations with NEMEC was successfully shown for discharges with large toroidal net currents by comparing the calculated flux surfaces with the contours of constant SX emissivity as reconstructed from the new MiniSoX system (Fig. 20). The agreement in the gradient region is quite good, whereas the central regions are dominated by flat profiles. The changes in the calculated flux surface shapes, i.e. more oblate for positive currents and more elongated for negative currents, are confirmed experimentally.

Resistive Ballooning Mode calculations for W7-AS were resumed for configurations at $\iota \approx 1/3$. The newly available C++ version of Garbo was successfully tested against the older F77 one. The numerical codes were tested to show the scaling of real growth rates with resistivity ($\gamma \sim \eta^{1/3}$) known from analytical theory. It was also shown that for small resistivity the scaling pertains to an increase in the mode's extension along the field line in accordance with the analytical theory. A second investigation concerned the method of scaling the equilibrium pressure gradient as a driving term in the ballooning equations to check the limitations of this method.

2.5.6 *Analysis of high-β experiments*

The high-β experiments of the last campaign showed the power limitation of the achievable β values, which is partly due to the decreasing heating efficiency of the counter NBI with both increasing β and decreasing magnetic field strength. The previously given β values had to be reconsidered since finite-β magnetic field components due to the stellarators three-dimensionality were picked up by the compensation coils of the diamagnetic coil system. This led to a reduction in the measurement of the energy content by the diamagnetic coil system by 10 to 15%, depending on the configuration. The highest β values achieved so far are between 1.8 and 2%, as evaluated from a comparison of the magnetic measurements and calculations with the NEMEC/DIAGNO package. Also, the plasma energy determined from magnetic and kinetic data are seemingly consistent.

2.6 Theory

2.6.1 *Kinetic modelling of ECRH*

Several numerical developments were finished or started in '97.

The δf Monte Carlo technique was formulated as an initial value problem for simulating the ECRH power absorption in 5D phase space. With a convolution algorithm, the suprathermal electron distribution generated by the ECRH can be calculated, although the volume of the quasilinear diffusion term in phase space is extremely small. This method will be extended to include also quasilinear degradation effects for higher ECRH power levels. The δf Monte Carlo technique was used to simulate the "effective" ECRH power deposition profile as derived experimentally from the electron heat wave propagation analysis. Several scenarios of X- and O-mode absorption for different magnetic field configurations are treated and compared with the experimental findings. (with Dr. S. Murakami, NIFS)

An interface for the bounce-averaged Fokker Planck code (FPTM) and the Garching ray-tracing code was installed. With this combination, the ECE emission as well as the ECRH absorption are estimated self-consistently in a first step (convective transport effects are not included, so far). (WTZ collaboration with Dr. N. Marushchenko, IPP-Kharkov.)

A preliminary analysis for the development of a 4D bounce-averaged Fokker-Planck code was carried out. In a fully conservative scheme, the Fokker-Planck equation with linearized Coulomb term and quasi-linear diffusion term can be solved for simplified magnetic field configurations. (This WTZ collaboration with Dr. N. Marushchenko, IPP-Kharkov, started in 1997 will continue to at least 1999.)

2.6.2 *ECRH-driven "electron role" feature*

The experimental observation of an "electron root" feature as predicted from neoclassical theory in the very lmfp regime with strongly positive radial electric fields (see Sec. 2.2) was also theoretically investigated.

The δf Monte Carlo simulation was used to calculate the convective suprathermal electron fluxes driven by the ECRH for various magnetic field configurations and with the radial electric field taken into account. The simulated electron fluxes are of the order of the ambipolar neoclassical ones for the "ion

root", but significantly exceed the prediction for the "electron root". It was clearly shown, that these ECRH-driven electron fluxes are responsible for establishing the "electron root" feature. Furthermore, the violation the usual neoclassical ordering in the ion drift-kinetic equation is strongly indicated for these very strong radial electric fields. (with Dr. S. Murakami, NIFS)

The viscous damping of the strong poloidal plasma rotation in the "electron root" region and of the parallel flows (equivalent to the Pfirsch-Schlüter currents) driven by $\underline{\nabla} \cdot \underline{v}_{E\times B} \neq 0$ as well as by the shear viscosity within the transition layer of the "electron" to the "ion root" region were analyzed. The dissipation of the rotation energy indicates the important effect of the convective radial flux of ripple-trapped suprathermal electrons generated by the ECRH. The experimental finding that the "electron feature" disappears within less 1 ms after the ECRH is switched off supports this picture. (Collaboration with Dr. K.S. Dyabilin, High Energy Density Research Center, Moscow)

2.6.3 *Self-consistent neoclassical theory*

The strong poloidal plasma rotation drives density disturbances and potential variations on the flux surfaces, which are neglected in the traditional neoclassical theory. In a self-consistent approach, the 1st order electron and ion drift-kinetic equations can be solved for various energies (allowing for the energy convolution) iteratively with the first-order potentials determined from the quasi-neutrality condition. A first step for developing a self-consistent drift-kinetic equation solver (a fully new DKES code) was performed. This approach seems to be mandatory to describe also the neoclassical impurity transport at least in a "tracer" modelling.

2.6.4 *Neoclassical bootstrap current with momentum conservation*

The simple pitch angle collision term used in the DKES or in Monte Carlo codes violates the condition of parallel momentum conservation. So far, a simple correction based on an energy convolution including Spitzer's function was used to simulate the bootstrap current for the W7-AS discharges. In a new approach with a momentum-conserving collision operator [M. Taguchi, Phys. Fluids B4 (1992) 3638], the corrections were implemented. Compared with the old simple approach, the ion friction can reduce the (electron) bootstrap current by about 20 to 30%.

2.6.5 *Effect of 3D geometry on mode structure*

Stellarator equilibria lack the continuous symmetry of their tokamak counterparts. The effect of this lack on the modes in the Alfvén continuum was studied, by means of recently obtained exact (straight) 3D MHD equilibria. The continuous spectrum familiar from the symmetric case was recovered. However, a discrete spectrum of modes, which is absent in the symmetric case, was also obtained. This new phenomenon, the nonsymmetry-induced Alfvén eigenmodes, was found analytically. It is conceivable that these modes play an important role in the interaction of externally applied waves or fast particles with the plasma. (with Dr. J. Tataronis, University of Wisconsin).

2.6.6 *Cut-offs and mode conversions in a Vlasov plasma*

A consistent method to deal with a succession of cut-offs and mode conversions in a Vlasov plasma - as can be found in ICRH situations - was developed. It avoids the inconsistencies of the usual methods, e.g. the substitution $ik_x \rightarrow d/dx$, which is definitely incorrect in the neighbourhood of cut-offs and mode conversions. Whereas the quantitative description confirms some qualitative expectations, the results for the transmitted energy are less obvious. In particular, the transmitted energy is larger when the direction of the incident wave is such that the cut-off is encountered first than it is for the opposite direction. Moreover, the transmission coefficients for forward and backward waves strongly depend on the plasma parameters.

2.6.7 *Density control problems with neoclassical transport*

With respect to the particle flux, the off-diagonal term in the neoclassical transport matrix becomes crucial in the stellarator lmfp regime. Central heating with peaked temperature profiles can make active density profile control by central particle refuelling mandatory. Depending on the magnetic configuration, a neoclassical particle transport barrier at outer radii may develop, leading to the loss of global density control. Both analytical and numerical modellings predict the appearance of this transport barrier at higher densities, especially for the W7-X "high-mirror" configuration.

2.6.8 *ECRH and ECCD in W7-X*

Two heating schemes for W7-X were investigated by means of a 3D ray-tracing code: launching of X- or O-mode polarized waves from the low magnetic field side at the 2nd harmonic of the electron cyclotron frequency. For X-mode on-axis heating, total single-pass absorption is obtained up to densities close to the cut-off density. Current drive calculations were also performed, determining the conditions of optimum launch. Significant absorption over a wide density range was also found for the O-mode. The validity of the results is confirmed by the time-dependent modelling of the heat transport by means of the ASTRA code. From these results, a successful transition from X2- to O2-mode heating is predicted for W7-X, and an increase of the operational density towards the cut-off density of the O2-mode should therefore be possible with the available heating power.

2.6.9 *High-harmonic ECRH in LHD*

During the initial experimental phase, LHD will operate at a magnetic field lower than the nominal one. In this scenario, the

gyrotrons chosen in view of 2nd harmonic heating at full-field operation will be resonant at the 3rd or 4th harmonic. Owing to the magnetic field properties of LHD (presence of a saddle point) considerable absorption is predicted for the 3rd harmonic and, in a low-density, high-temperature operational window, even for the 4th harmonic. The strong temperature dependence of absorption at higher harmonics presents some peculiar characteristics: quasilinear effects are found to improve the absorption properties, and bifurcation phenomena as well as a critical power threshold might appear.

2.6.10 Generation of "secondary ECRH-driven heat waves"

ECRH modulation experiments are used to extract information on radial transport from the analysis of the propagation of the induced temperature perturbation (heat wave). As the ECRH absorption coefficient itself depends on temperature, a propagating heat wave can modulate the absorption of stationary injected ECRH power generating a "secondary heat wave". A model was developed and compared with experimental results obtained in discharges where two gyrotrons, one resonant on- and the other off-axis, were modulated. The inclusion of the "secondary heat waves" can explain the experimental data. If, however, this phenomenon is neglected (as usually done in literature), an "obscure" transport is required in order to explain the experimental findings.

3. DIAGNOSTIC DEVELOPMENT

3.1 Periodic Multichannel Thomson Scattering

The periodic multichannel Thomson scattering diagnostic at W7-AS enables simultaneous measurement of electron temperature and density profiles along the entire plasma diameter every 50 ms. For technical details of the diagnostic see Röhr et al. (IPP III/121) and Annual Reports 1992 to 1996.

During 1997 an automatic system was installed to calibrate and control the relative spectral sensitivities of all channels. The most important component of the system is a Pockels cell which provides light pulses of variable duration. It is to be investigated whether the spectral sensitivities measured with continuous light are different from those measured with light pulses of 60 ns. A LabView program was developed in order to control the whole system by PC. All components were separately tested. Preliminary measurements were successfully performed. The relative spectral sensitivities will be used to determine electron temperature and density profiles for most of the discharges performed since the diagnostic went into operation, i.e. backdated to #32000.

Since discharge #39000 the intensity of bremsstrahlung has been measured in the near-infrared region in the same manner as before at ASDEX (see IPP III/157). It is planned to check the contribution of line radiation in the spectral region under consideration. If line radiation can be neglected Z_{eff} profiles may be derived from the intensity of bremsstrahlung.

3.2 Ruby Thomson Scattering System with High Spatial Resolution

A new Thomson scattering diagnostic with high spatial resolution for plasma edge investigation on the high-field side in the triangular plane was developed. The detection system consists of an intensified two-dimensional CCD camera and a self-developed Littrow-type spectrometer. It will replace the 5 inner channels of the existing 20-channel system, which uses interference filter polychromators for spectral analysis of the scattering distribution.

The scattered light of the ruby laser (λ = 694.3 nm, 15 J energy per pulse, one pulse per discharge) is imaged by two optical systems onto guide arrays, which transfer the light to the detection systems. For the high-resolution system a new fibre guide array was developed. At the output it forms the "entrance slit" (85 × 2 mm) of the Littrow-type spectrometer. 30 spatial channels allow the scattered radiation to be detected along a 120 mm long horizontal chord near the inner side of the torus. The spatial resolution is thus improved by a factor of 5, compared with the existing polychromator system.

The Littrow-type spectrometer has a focal length of 500 mm and uses a plane grating with 1800 ll/mm for wavelength separation. Taking into account the rather large width of the entrance slit (2 mm), the spatial resolution $d\lambda$ of this spectrometer is 1.8 nm. A total wavelength range of 60 nm can be detected by 512 vertical CCD camera pixels. Measurements of electron temperatures between 10 and 1000 eV are possible for investigation of the plasma edge and 5/9-island studies. The new system will be installed and tested after opening of W7-AS in 1998.

3.3 Collective Thomson Scattering with 140 GHz Gyrotron Radiation

In continuation of the "proof-of-principle" experiments on collective Thomson scattering with powerful gyrotron radiation, experiments in the 90° scattering geometry were performed in collaboration with IAP Nizhny Novgorod. In some shots, the EC resonance zone was shifted through the scattering volume by varying the magnetic field B. If the absorbing resonance is behind the scattering volume, a thermal ion feature is measured. The calculated ion temperature is in accordance with the value measured by independent diagnostics. In the evaluation procedure, it is assumed that cold plasma theory is valid. When the resonance zone is shifted into the scattering volume (B = 2.42 T), a strong peaking of the spectrum at the ion acoustic frequency is observed. If we assume a Maxwellian distribution of the electrons, this peak indicates a local electron temperature of at least 4 keV (as compared with the bulk temperature of 0.8 keV). The discrepancy can be explained by adding to the bulk electrons 4% of electrons with an energy of 40 keV. The experiments showed that the 90° scattering geometry allows localized measurements with a spatial resolution of $\leq$ 4 cm.

The investigations of the LH waves excited by fast transversely propagating ions from the CX diagnostic beam were continued with backscattering experiments (angle about 160 deg)

and an orientation of the scattering vector perpendicular to B. The growth of the instability was quenched if the ion temperature was increased above a threshold ion temperature of about 0.6 keV. This finding is in agreement with theoretical predictions.

During this experimental campaign, we observed for the first time excitation of these waves with strong NBI heating without using the CX diagnostic injector. Further investigations are necessary to decide if this feature can be used to diagnose fast-ion distributions.

3.4 Reflectometry System for Fast Density Profile Measurements

Density profiles and density perturbations are measured with a broadband reflectometer with heterodyne detection allowing the reflected signals to be followed despite their large amplitude fluctuations. Heterodyne detection is accomplished by a balanced feedforward tracking scheme allowing free-running independent RF- and LO-signal sources. Their frequency difference is controlled with an accuracy of $\Delta f = \pm 400$ MHz during the sweep with a slow analog circuit which limits the sweep time to about 1 ms.

The temporal resolution can be improved by two techniques: (1) The free-running RF- and LO-oscillators are PC-controlled with a fast DA converter. (2) Both frequencies, LO and RF, are derived from a single source by single-sideband modulation of one of those with the required frequency difference. In case (2) no further frequency stabilization is required.

Both techniques are tested in the laboratory. The sweeping speed is only limited by the voltage-to-frequency characteristics of the fast tunable solid-state oscillators thus allowing one profile measurement within less than 50 µs.

3.5 Line-integrated Electron Density Measurements with Cotton-Mouton Effect

Polarimetry can be used to measure the line-integrated electron density in a magnetized plasma. Depending on the propagation direction of the probing waves, two basic effects can be observed: the Faraday and the Cotton-Mouton effect (circular and linear birefringency).

At W7-AS a diagnostic for measuring the Cotton-Mouton effect was constructed by using sub-mm waves from 535 to 627 GHz. At the line of sight chosen there is no component of the magnetic field in the propagation direction, so that the Faraday effect has no influence on the measurements. First measurements are in good agreement with line-integrated densities from the microwave interferometer at W7-AS and show the good properties of the diagnostic. The dependence of the effect on the magnetic field ($\sim B^2$) and the frequency ($\sim f^{-3}$) could be shown.

3.6 Lithium Beam Activated Charge Exchange Spectroscopy on W7-AS

To allow Li-beam activated charge exchange spectroscopy (Li-CXS) on the W7-AS stellarator, the existing Li-beam diagnostic layout was extended by a 14-channel observation system, with a radial resolution of $\delta r \sim 6$ mm and extending ~13 cm along the beam, corresponding to an effective plasma radius of 3 - 17 cm. Two achromats in series ($\Omega/4\pi \sim 2.9 \times 10^{-4}$ sr) image the light onto 14 bundles, each consisting of a 2×4 array of 400 µm quartz fibres. Each bundle can be coupled either into a photomultiplier in conjunction with an interference filter ($\lambda = 529.0$ nm for C^{6+}, $\delta\lambda_{1/2} \sim 5$ Å), or into the entrance slit of an ACTON spectrometer (f = 0.75 m, blazing for 500 nm, 1200/1800 lines/mm). A 2D Proscan CCD camera with 512×512 pixels then permits spectral resolution of Li-CXS and Li I lines.

First measurements of C^{6+} spectral lines with the upgraded Li injector (2 mA, 50 keV) have proved the viability of Li-CXS on W7-AS: For purely ECRH-heated plasmas a C^{6+} concentration of about 0.5% could be measured in the plasma edge region ($r_{eff} > 10$ cm) in good agreement with H-CXS measurements. This confirms the high sensitivity of the Li-CXS diagnostic. Temperature values found for C^{6+} are similar to proton / deuterium and electron temperatures. An outstanding feature of this diagnostic is that an absolute calibration of the detection systems is not necessary for determining either electron density profiles or impurity profiles.

3.7 Measurement of Electron Density Fluctuations with Lithium Beam BES

Density fluctuations in the plasma of W7-AS induce fluctuations in the light emission of the 48 keV diagnostic lithium beam. By calculating the correlation function of beam light fluctuations, the correlation function of electron density fluctuations can be reconstructed on a newly developed numerical method. The calculation technique is generally applicable to all kinds of neutral beams, provided an appropriate model for beam light emission is available and the beam penetration time through the observation volume is shorter than the characteristic times of the plasma turbulence.

Typically, this technique can resolve electron density fluctuations in the scrape-off layer (SOL) and in the outer third of the plasma minor radius. However, at low plasma densities the beam penetrates deeper into the plasma, and as a consequence electron density fluctuations can be measured in the core region as well. In the SOL measured fluctuation levels, correlation times and correlation lengths are in agreement with Langmuir probe measurements. Around the Last Closed Flux Surface the fluctuation characteristics change. The relative fluctuation level drops from the several ten per cent level observed in the SOL to a few per cent and autocorrelation functions tend to be burst-like. In addition to these phenomena, ELM-like phenomena and density fluctuations due to GAE activity are also observed in some shots.

3.8 A PC-driven Bolometer Calibration System

A PC-driven bolometer calibration and measurement system for the laboratory based on a DC strain gauge system was developed (Measurements Group, Munich). An 8-channel system automatically measures the resistor thermally coupled to the absorber foil, so that a known ohmic heating power pulse can be applied. The data is recorded by a 12-bit AT plug-in card with a sampling rate of up to 300 kHz for one channel. From the time evolution of the foil's temperature due to its self-heating, the cooling time constant and sensitivity of the foil can be derived. A DOS-based data acquisition and control program allows the setting of the gain and magnitude of the voltage step for the ohmic heating power pulse. Post-processing of the raw data with a Bessel filter to recover the power flux to the foil from the measurement of the foil temperature was implemented. The aim is to investigate in detail the linearity of the calibration method and the pressure and temperature dependences of the calibration constants, which may compromise performance in the long-pulse discharges on W7-X. In a series where the bolometer head was heated in the range from 25° C to 80° C, preliminary measurements show that the cooling time constant increased by 6%. In the measurement mode, the offset of the full bridge is automatically corrected so that gains of up to 2000 for the differential output of the bridge can be chosen. The noise level for measurements with a sampling frequency of 1 kHz, an amplifier gain of 500 and a fifth-order Bessel filter with a 3 dB point of 30 Hz is 0.5 W/m^2.

3.9 Novel Langmuir Probe Technique for Measuring Plasma Potential and Electron Temperature Fluctuations

Simultaneous measurement of the plasma density, electron temperature and poloidal electric field fluctuations is important to calculate the radial particle and energy transports due to electrostatic fluctuations, believed to contribute a major fraction of the anomalous transport observed in tokamaks and stellarators. Furthermore, knowledge of these fluctuations and their relative phase is important for comparison with predictions of theories and numerical turbulence simulations. Langmuir probes afford the potential to yield this information if a periodic voltage is applied to them and the resulting current through the Debye sheath into the plasma is recorded. The applied voltage must be swept with frequencies well above the fastest fluctuation frequency components, i.e. in the MHz range. The required current measurement is best achieved with miniaturized amplifiers close to the Langmuir probe tips. The amplifiers must have a high common mode rejection up into the MHz range. First tests of this technique were performed on W7-AS, giving very promising results, reported in Sec. 2.5.3.

A second way to measure plasma potential fluctuations directly without the uncertainties of Langmuir probe theory entering the analysis of the data taken with the above technique could be the use of emissive probes. The development of a heatable graphite tip, coated to reduce the work function, was started in collaboration with the University of Kiel.

4. MACHINE OPERATION AND TECHNICAL ACTIVITIES OF W7-AS AND THE AUXILIARY SYSTEMS

4.1 Main Activities of W7-AS

In 1997 the W7-AS experiment was operational for about 5,000 pulses in the range of 0.6 - 2.5 T and different rotational transforms. More than 10% of the pulses were used for commissioning the new digital control and regulation system of the 1.45 GJ flywheel generator. To improve the regulation, a hybrid regulation system is being developed by IPP and will be installed in cooperation with SIEMENS AG in 1998.

To support nonresonant plasma start-up by NBI, two 900 MHz magnetron transmitters with 10 kW RF output each are now available. Three different types of antennas are installed inside the torus vessel: a quad antenna, a sleeve antenna and a skeleton slot antenna. The most successful for nonresonant plasma start-up was the quad antenna.

4.2 Neutral Injection into W7-AS

4.2.1 Existing injectors

The deposition of beam power and particles in any neutral beam heated plasma has never been measured. A method of measuring heating profiles, established for ECRH, is to modulate the heating power and measure the resulting modulation of the electron temperature. There is, however, a complication in connection with neutral beams in W7-AS: The slowing-down time of the injected particles is of the order of transport time constants and hence it is difficult to separate effects of deposition and transport. The damping of the power modulation by the finite slowing-down time of the ions was investigated by Fourier methods in a laboratory report. On the experimental side it was demonstrated that beams of all four kinds (co, counter, inner, outer) can be modulated. Injection of modulated beams into the W7-AS plasma has led to modulations of the electron temperature and density. The evaluation of these measurements is under way.

The current drive by neutral beam injection is now accessible to calculation by the NBCD code, which has radial resolution in velocity space, delivering the contribution of the fast ions to the current and the profiles of iota and beta.

4.2.2 Radial injector

The design of the coupling elements of the radial injector on the W7-AS torus was continued. One of the two existing injector boxes of the former ASDEX experiment is being revised. The high-voltage installations for the radial injector have already been completed.

STELLARATOR THEORY

(Prof. Dr. Jürgen Nührenberg)

S. Arndt, M. Drevlak, S. Gori, R. Hatzky, Ch. Hennig, R. Kleiber, A. Könies, C. Nührenberg, J. Nührenberg, P. Merkel, S. Weber, R. Zille.
Guests: A. Boozer,[1] S. Hirshman,[2] M. Fivaz,[3] T. M. Tran,[3] A. Iiyoshi,[4] N. Nakajima,[4] S. Okamura,[4] L. P. Ku,[5] D. Monticello.[5]

1. Introduction

In 1997, the work of the Stellarator Physics Group was concentrated on widening the scope of the theoretical work at the Greifswald Branch Institute and on further development of the stellarator concept, notably for quasi-axisymmetric and quasi-isodynamic configurations /92, 462, 518, 675-677/.

2. Free-Boundary Stellarator Equilibria using the FREE-BOUNDARY PIES

The synthesis of the fixed-boundary PIES code by A. H. Reiman and H. S. Greenside and the vacuum code NESTOR by P. Merkel results in the FREE-BOUNDARY PIES code. This code solves the 3-dimensional MHD equilibrium problem in a magnetic field generated by external coils without any assumptions about the flux surface geometry in contrast to the free-boundary NEMEC code which presumes the existence of nested magnetic surfaces.

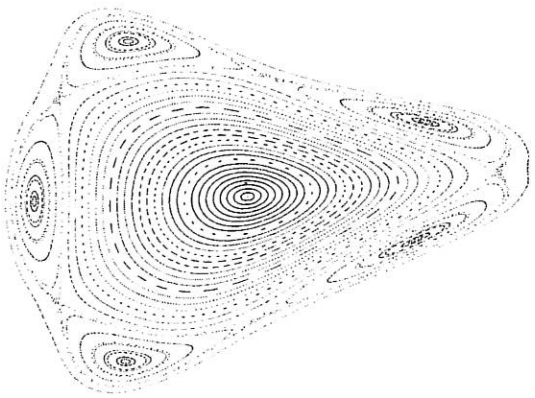

FIG. 1: Flux surfaces of a free-boundary equilibrium for the W7-X coils HS5V10u with $\langle\beta\rangle \approx 1\%$ obtained by FREE-BOUNDARY PIES code (60 radial grid points, $0 \leq m \leq 16$ poloidal and $-16 \leq n \leq 16$ toroidal Fourier modes).

Equilibrium computations for the actual W7-X coils were performed using the FREE-BOUNDARY PIES code. Starting from the vacuum field, about 300 iterations were necessary to obtain an equilibrium with a value of $\langle\beta\rangle$ of 1 %. To improve the performance, it is planned to take NEMEC equilibrium results as initial data for the FREE-BOUNDARY PIES code. The corresponding procedure was already successfully applied to fixed-boundary cases /6, 388/.

3. Quasi-Axially Symmetric Tokamaks

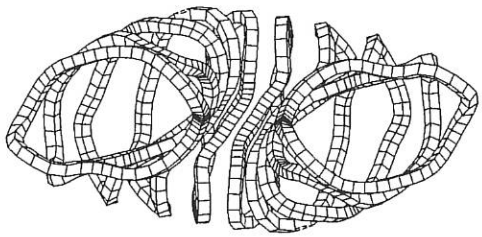

FIG. 2: View of one period of the coil set from the major axis.

Quasi-axially symmetric tokamaks (qa-tokamaks) are 3-d configurations, which exhibit axial symmetry of B in magnetic coordinates. Due to the 3-d shape, part of the rotational transform is created by the external magnetic field.

For a qa configuration investigated in collaboration with NIFS, a coil set (see Fig. 2) was designed /461/ using the extended version of the NESCOIL code by P. Merkel.

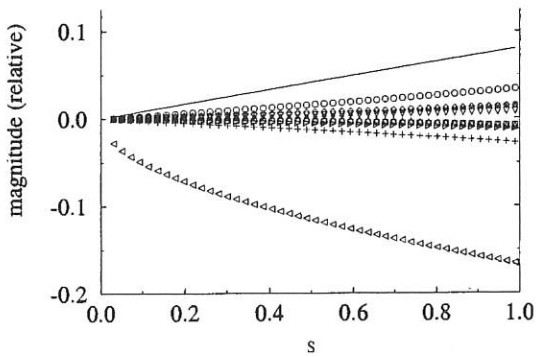

FIG. 3: Fourier decomposition of the magnetic field: — $[B_{0,0} - B_{0,0}(0)]$, ◁ $B_{1,0}$, + $B_{2,0}$, ○ $B_{0,1}$, □ $B_{1,-4}$, ▽ $B_{2,-4}$.

[1] Columbia University, [2] ORNL, [3] EPFL, [4] NIFS, [5] PPPL

Free boundary equilibrium calculations were carried out using the NEMEC code. The effects of free boundary and non-vanishing toroidal plasma current affect integrity of quasi-axisymmetry significantly /461/. However, qa-symmetry can be restored with good precision by application of a vertical magnetic field and individual adjustment of the coil currents. The Fourier spectrum of the magnetic field achieved with these measures is shown in Fig. 3. Monte Carlo simulations of the drift orbits of α particles and of neoclassical transport show that the confinement behaviour retains the qa optimization.

Also, a set of auxiliary coils was designed in order to exert control on the rotational transform. Using fully 3-d shapes for the auxiliary coils, this can be achieved with good efficiency.

4. Finite-β NESCOIL

The NESCOIL code has been extended to determine coils producing the appropriate vacuum field for finite-β 3D MHD equilibria.

Originally, the NESCOIL code was developed to compute external currents for the Helias class of optimized stellarator configurations on which the W7-X device is based. For these equilibria the effect of finite β on the magnetic field structure is small because of the strongly reduced parallel plasma current density. Therefore the coils were designed to produce a field approximating the vacuum solution of the optimized fixed boundary configuration.

However, to treat cases with large plasma currents as quasi axially-symmetric tokamak configurations, the effect of the plasma current cannot be neglected any more.

A fixed-boundary equilibrium magnetic field $\vec{B}_{eq}$ is the sum of a vacuum field $\vec{B}_{vac}$ and the field $\vec{B}_j$ produced by the plasma current with $(\vec{B}_{vac} + \vec{B}_j) \cdot \vec{n} = 0$ on the boundary ($\vec{n}$ = exterior normal).

Because $\vec{B}_{vac}$ is the field to be produced by the coils one needs to know $\vec{B}_{vac}$ for the extended NESCOIL procedure separately. It can be shown that $\vec{B}_{vac}$ in the plasma domain is the field produced by a surface current on the boundary, defined by $\vec{j}_s = \vec{B}_{eq} \times \vec{n}$ (virtual casing principle). Then, the coils are determined by a minimization procedure: $\int \mathrm{d}f[(\vec{B}_{coil} - \vec{B}_{vac}) \cdot \vec{n}]^2 = \min!$ on the plasma boundary.

5. Ideal MHD Stability

In the field of ideal MHD stability /219/, work concentrated on the investigation of quasi-symmetrical configurations, i.e. quasi-helically symmetric (qh), quasi-axisymmetric (qa) and quasi-isodynamic (qi) /518/. Fixed-boundary global-mode studies with the CAS3D stability code and evaluations of the local MHD stability criteria (Mercier, ballooning and resistive interchange) were used. For the qh stellarator the question of ballooning stability is the most challenging, since such equilibria are usually Mercier and resistive interchange stable up to quite large stability-β values. In a case with aspect ratio $\sim$ 12 and six field-periods, which is resistive-interchange stable at $\langle\beta\rangle \approx 0.09$, non-local ballooning modes (CAS3D) occur at $\langle\beta\rangle$-values above 0.06, while local ballooning instability prevails for $\langle\beta\rangle$ above 0.05. From the qa class of configurations two cases with $\iota_{\text{external}} \leq 2/5$ and considerable toroidal current ($\iota > 1/2$), two field periods and aspect ratio $\sim$ 4 were chosen with slightly decreasing and slightly increasing rotational transform profile in order to study their non-local ballooning stability properties at $\langle\beta\rangle \approx 0.02$. Preliminary results indicate the case with positive shear to have a slighly better non-local stability, $\langle\beta\rangle = 0.026$ versus $\langle\beta\rangle = 0.022$. For the qi-class of stellarators simultaneous qi and magnetic well optimization shows that configurations with a very good confinement of core α-particles and a magnetic well exist. At $\langle\beta\rangle \approx 0.05$ the particular qi equilibrium considered (aspect ratio $\sim$ 10 and five field periods, compare Fig. 4) is stable with respect to local as well as non-local ballooning modes.

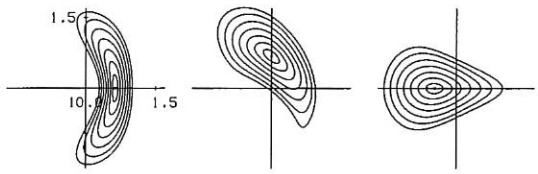

FIG. 4: Flux surface cross-sections for a quasi-isodynamic configuration with five field periods, aspect ratio $A \sim 10$, and a magnetic well of about 0.01.

6. MHD-Stability with Kinetic Effects

Energetic ions in fusion devices may be not only fusion products but also be due to heating techniques as NBI or ICRH. These particles may destabilize Alfvén, ballooning or kink modes.

Therefore, the variational 3D MHD stability code CAS3D has been extended to include kinetic effects in the low frequency limit (CAS3D-K). A kinetic energy principle derived in the limit of low frequency perturbations by Van Dam et al. is employed. In the energy principle for thermal plasmas an average over the change of the particle energy during the bounce motion between the magnetic mirrors replaces the usual MHD fluid compression term. This contribution is stabilizing. For energetic particles the ratio of their diamagnetic and magnetic drift frequencies determines whether they are stabilizing or not. The CAS3D-K stability code /167, 610/ works in a 3D equilibrium (W7-X) as well as in tokamak configurations, classifies the bounce motions and the average magnetic drifts of the energetic particles and solves the resulting eigenvalue problem. The particles reflected between magnetic mirrors have been shown to dominate the stabilizing or destabilizing contribution of the energetic plasma component.

The functional involves field line averages and an additional integration over the pitch angles of the particles, both are done numerically. For the sake of simplicity, the energetic particle distribution function is assumed to be separable in all its variables (pitch angle, energy and flux label) leaving a functional in a 4-D space to be treated.

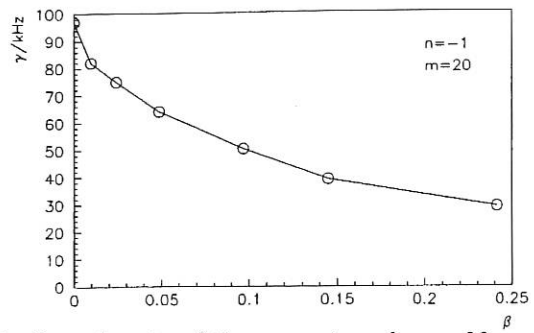

FIG. 5: Growth rate of the $n = -1$ and $m = 20$ mode for a ϑ-pinch in MHD equilibrium as a function of the local β for $\eta \approx 4$ at the point of maximum mode amplitude and a diamagnetic drift $\omega_d \approx 30$kHz.

For a thermal plasma the shift of a point of marginal traditional MHD stability is small. The influence of an energetic particle component is still under investigation.

7. Drift Waves in Stellarators

Resistive drift waves provide a possible mechanism for anomalous transport in the boundary region of stellarators.

In a first step – to gain insight into the structure of linear drift waves in a stellarator – resistivity, which is the necessary ingredient for instability, is neglected. Assuming electrostatic perturbations, adiabatic electrons and cold ions, the linearized two-fluid-equations reduce to a 3-d eigenvalue equation for the perturbed electric potential. In contrast to the ballooning transformation, which can be used to reduce the problem to an ordinary differential equation, the global approach poses no restriction on the perturbation and naturally gives the radial structure of the eigenmodes.

Formulating the problem in magnetic coordinates a Fourier decomposition in the angle-like variables and a finite-difference discretization in the flux label gives a generalized quadratic matrix eigenvalue problem. This is solved by a complex implicitly restarted Arnoldi Method.

For VMEC-generated equilibria and fixed boundary conditions for the perturbation the developed code gives the spectrum of drift waves. A phase factor transformation allows the calculation of modes with a high wave number.

In order to get unstable modes resistivity will be included in a next step.

8. Ion-temperature-gradient-driven (ITG) instabilities

ITG-instabilities are now commonly held responsible for turbulence giving rise to anomalous ion heat transport in the core of tokamaks. Starting from the 2-dimensional GYGLES code by M. Fivaz et al. a linear gyrokinetic simulation code for W7-X is envisaged to be developed.

As a first step the simple case of a ϑ-pinch in MHD equilibrium has been studied. For this purpose it was necessary to rewrite the GYGLES code from Cray Research Adaptive Fortran (CRAFT) to the Shared Memory Library to run the code with 60 Mflop rate per Processor Element (PE) on the T3E of the RZG. Thereby, optimal scaling with the number of the PEs is achieved. Additionally the mesh of the field solver had to be converted from tokamak to ϑ-pinch geometry to give the opportunity to calculate a bumpy cylinder in a subsequent step.

First results show that the magnetic well caused by the MHD equilibrium gives rise to a ∇B drift which has a stabilizing effect on the slab ITG modes (figure 5).

9. PEC3D: First Step Towards a 3-d Plasma Edge Fluid Code

PEC3D is a 3-dimensional plasma fluid code in a slab configuration[1] which solves the standard Braginskii equations for a single plasma species (ions + electrons). In addition the neutrals are treated by a one- or two-group diffusion approximation. The physics employed is rather satisfactory but the geometry is kept simple: a cartesian mesh with one coordinate line taken to be parallel to the magnetic field lines. The parallel direction uses the Braginskii transport coefficients and the two perpendicular directions are treated diffusively in order to account for the anomalous transport.

The highly nonlinear equations are linearized and solved iteratively employing a Newton-Raphson method. The discretization is fully implicit and the Jacobian is computed symbolically.

The slab model approach can be considered as a simple model of a flux tube intersecting the divertor plates and ignoring the actual field structure; consequently the equations are solved for a homogeneous magnetic field.

However the magnetic field in the edge region deviates strongly from homogeneity and this should be accounted for. Therefore, parallel work is in progress to model the other extreme: minimal physics but complex magnetic topology, i.e. to solve the anisotropic Laplace equation for the plasma temperature ($\nabla \bullet (\chi_{\|} \nabla_{\|} T_e + \chi_{\perp} \nabla_{\perp} T_e) = 0$) in one of the island chains existing outside the separatrix of the standard W7-X configuration. Due to the large anisotropy in the thermal transport magnetic coordinates will be used as they are inherently adapted to such a situation.

Eventually the two approaches presented above, realistic physics with simple geometry and simple physics with full geometry, should merge to form the basis for a 3-dimensional plasma edge fluid code adequate for divertor and scrape-off layer modelling in W7-X.

---

[1] S. Weber, in *Plasma Edge Theory, Oxford, 1997*, Contrib. Plasma Phys. **38**, 43 (1998).

IEA IMPLEMENTING AGREEMENT
for Cooperation in Development of the Stellarator Concept
EUROPEAN ATOMIC ENERGY COMMUNITY / US DEPARTMENT OF ENERGY

1. OBJECTIVES OF THE AGREEMENT

The objective of the Implementing Agreement, first concluded in 1985, is to "improve the physics base of the Stellarator concept and to enhance the effectiveness and productivity of research and development efforts related to the Stellarator concept by strengthening co-operation among Agency member countries". To achieve this, it was agreed to exchange information, conduct workshops, exchange scientists, do joint theoretical, design and system studies, coordinate experimental programmes in selected areas, exchange computer codes, and perform joint experiments. In 1995 the Agreement was extended until June 2000. The contracting parties are EURATOM, the U.S. DoE, Japan, and Australia. In September 1994, Russia became an Associate Contracting Party.

2. STATUS OF THE AGREEMENT

In 1997, there were two meetings of the Executive Committee. The 23rd meeting was held at Berchtesgaden, Germany, in conjunction with the EPS Conference on Controlled Fusion and Plasma Physics, which took place from June 9 to 13. The main points were remote participation in experiments, possible association of non-member countries to the IEA Implementing Agreements, increased collaboration when new devices become available, the status of the experiments, and meetings and personnel exchanges. The 24th meeting was held at Toki, Japan, on October 1, in conjunction with the 11th International Stellarator Conference and the 8th International Toki Conference, which took place from September 29 to October 3. It was proposed to intensify collaboration especially for the Large Helical Device (LHD) in Japan, which will be operational in 1998. The Japanese partner has submitted a paper, "Large Helical Device (LHD) International Mutual Experimental Programme (LIME)", which was accepted by the Executive Committee as a good starting paper for setting up the collaboration intended.

3. REPORT ON 1997 ACTIVITIES

In 1997, ten physicists participated in the exchange of scientists. Staying from May 2 to August 18, J.F. Lyon from Oak Ridge conducted experiments with a pellet injector, which he brought from Oak Ridge, as well as in the field of ICRH on W 7-AS. L.P. Ku and D. Monticello, both from Princeton PPL, spent two weeks at IPP (Greifswald) to initiate collaboration with respect to stellarator optimization. S. Hirshman from Oak Ridge discussed stellarator optimization, especially for quasi-isodynamic configurations, and the new version of the NESCOIL code, which is appropriate for given finite-β equilibria, during his visit from November 25 to December 4.

Three scientists from the National Institute for Fusion Science (NIFS), Nagoya, paid short visits to IPP in 1997. During his two stays from February 2 to 7 and March 24 to 27, N. Nakajima intensified the collaboration on MHD modes of two types, ballooning and free-boundary. S. Okamura visited IPP from February 24 to 28, to intensify the cooperation on the physics basis of CHS-qa. A short visit of A. Tiyoshi served the general collaboration between NIFS and W 7-X.

From September 28, 1996, to February 4, 1997, H. Renner from IPP visited NIFS to discuss common issues in the treatment of stellarator divertors. As a result, the cooperation between IPP and NIFS has been strengthened. C.D. Beidler from IPP presented results from the GSRAKE (General Solution of the Ripple-Average Kinetic Equation) neoclassical transport code, and discussed the code´s potential uses for LHD during his 4-week stay in spring at Toki, NIFS; GSRAKE has since been transferred to NIFS. The visit of M. Drevlak from June 16 to July 11, to NIFS served for collaboration on coil design and free-boundary equilibrium calculations.

4. WORKSHOPS

The 11th International Stellarator Conference and the 8th International Toki Conference took place at Toki, Japan, from September 29 to October 3, 1997.

Divisions and Groups

THE SCIENTIFIC DIVISIONS OF IPP

Experimental Plasma Physics Division 1
Director: Prof. M. Kaufmann

ASDEX Upgrade (Divertor Tokamak)
- operation of ASDEX Upgrade
- investigation of ITER plasma boundary in a reactor-relevant divertor, especially under high-confinement conditions
- investigation of energy transport, MHD stability, beta limit, density limit and disruptions in an ITER-type plasma
- advanced tokamak studies

JET collaboration
- operation of special discharge scenarios at JET and general collaboration

Experimental Plasma Physics Division 2
Director: Prof. G. Grieger

WENDELSTEIN 7-X
- divertor development
- contributions to stellarator power plant systems studies

Experimental Plasma Physics Division 3
Director: Prof. F. Wagner

WENDELSTEIN 7-AS (Advanced Stellarator)
- stellarator with improved confinement conditions
- toroidal plasma confinement in the stellarator
- net-current-free plasmas, plasma production and heating by neutral injection, and high-frequency waves
- plasma stability and impurity effects
- development of an island divertor

Preparation of the WENDELSTEIN 7-X diagnostics

Experimental Plasma Physics Division 4
Director: Prof. K. Behringer

Experimental and theoretical investigations of plasma boundary and divertor physics, impurity transport, chemical impurity production and plasma radiation in ASDEX Upgrade and WENDELSTEIN 7-AS
- spectroscopic diagnostics on ASDEX Upgrade
- spectroscopic diagnostics on WENDELSTEIN 7-AS
- laboratory experiments at the University of Augsburg, Department of Experimental Plasma Physics

Surface Physics Division
Directors: Prof. V. Dose, Prof. J. Küppers

Surface physics
- atomistic characterization of surfaces

Plasma-wall interactions (analytical)
- interactions of atoms, ions and electrons with solid surfaces
- wall fluxes in the boundary layer of plasma devices
- limiter and wall analyses

Plasma-wall interaction (preparative) (see also Technology Division)
- preparation and characterization of thin-film coatings for plasma devices

Data analysis
- application of Bayesian techniques to experimental data

WENDELSTEIN 7-X Construction
Director: Dr. M. Wanner

WENDELSTEIN 7-X R&D programme
WENDELSTEIN 7-X Construction
- engineering, construction and installation of the WENDELSTEIN 7-X device incl. plasma heating and in-vessel components
- project control and quality management

Technology Division
Director: Prof. R. Wilhelm

Neutral injection
- development and construction of the injection systems for WENDELSTEIN 7-AS, ASDEX Upgrade and WENDELSTEIN 7-X
- implementation of injection experiments

Electron cyclotron resonance heating
- construction and operation of an ECRH system for ASDEX Upgrade

Ion cyclotron resonance heating
- preparation and implementation of ICRH experiments for WENDELSTEIN 7-AS, ASDEX Upgrade and WENDELSTEIN 7-X

Plasma technology (see also Surface Physics Division)
- development, characterization and modelling of low-pressure plasma processes for thin-film formation

Theory Division
Acting Director: Prof. K. Pinkau

General fusion-oriented plasma theory
- MHD equilibrium and stability
- analytical theory of drift instabilities

Tokamak Physics
Director: Prof. K. Lackner

General tokamak physics
- experiment-oriented theoretical work for the design and interpretation of tokamak experiments

Plasma edge physics
- experimental and theoretical work on plasma edge physics

Nonlinear plasma dynamics
- numerical simulation of turbulent transport and MHD reconnection phenomena

ITER collaboration

Computer Science Division
Director: Prof. F. Hertweck

Development of data acquisition systems for experiments at IPP
Studies in parallel computer architectures
Studies in neural networks
Parallelization of programs

Plasma Diagnostics Division
Director: Prof. G. Fussmann

Edge plasma physics
- experimental and theoretical work relating to fusion devices

Plasma generator PSI-1
- basic plasma physics
- plasma interaction with solid surfaces
- development and testing of plasma diagnostics

Electron Beam Ion Trap (EBIT)
- production of highly charged ions
- X-ray spectroscopy and atomic physics measurements

UHV laboratory, arc physics, ITER collaboration

Greifswald Branch of IPP
Director: Prof. G. Grieger

Construction of institute and infrastructure

Stellarator Theory Division
Director: Prof. J. Nührenberg

Further development of the stellarator concept and numerical and analytical methods to investigate equilibrium, stability and transport problems in three-dimensional toroidal configurations.

EXPERIMENTAL PLASMA PHYSICS DIVISION 1

(Prof. Dr. Michael Kaufmann)

The division E1 comprises

1. Four diagnostic groups
   a. pellet injection, electromagnetic measurements, DCN interferometer, plasma control, MSE, halo current measurements, calorimetry
   b. Thomson scattering, bremsstrahlung, bolometer, SXR
   c. He measurements, neutral gas, neutron measurements, HXR, mass spectrometer
   d. ECE, microwave reflectometry, SABA, charge exchange, LENA

   which are responsible for the development of plasma diagnostics as well as for plasma physics exploitation.

2. Three machine groups
   a. operation
   b. mechanical design
   c. assembly,

   which are concerned with the operation and engineering developments of the tokamak experiment ASDEX Upgrade and its peripheral installation.

3. Two computer groups
   a. real-time control of the ASDEX Upgrade plasma,
   b. data acquisition and data evaluation.

These groups are supported by 3 workshops: mechanical, electrical, and electronical.

Divison E1 is also devoted to support diagnostics on JET and to continue studies for ITER.

WENDELSTEIN 7-X Construction

(Dr. Manfred Wanner)

The work of the division is fully reported in section WENDELSTEIN 7-X Construction.

The members of the division are: R. Bünde, M. Pillsticker, J. Sapper, F. Schauer, I. Schoenewolf, M. Wanner, F. Werner, I. Bojko, J.-H. Feist, H. Grote, B. Hein, G. Krainz, H. Laqua, H. Niedermeyer, A. Nitsche, M. Pieger-Frey, H. Schneider, F. Schneider, F. Werner

The team was supported by contributions from the Central Technical Services of IPP, D. Arz, H. Pirsch, F. Ascher, W. Bitter, B. Fleischer, St. Geißler, R. Goihl, N. Jaksic, R. Holzthüm, O. Jandl, F. Kerl, J. Simon-Weidner, B. Sombach, M. Weißgerber, J. Tretter, A. E. Maier, J. Perchermeier, S. Kötterl, as well as from Forschungszentrum Karlsruhe (FZK) and Institut für Plasmaforschung Stuttgart (IPF)

GREIFSWALD BRANCH OF IPP

(Prof. Dr. Günter Grieger)

The Greifswald Branch of IPP is planned to house practically all the stellarator activities of IPP. At present, the activity is concentrated on the construction of the institute and its infrastructure. Additonally, also the Stellarator Theory Division (see below) under Prof. Dr. J. Nührenberg has moved to Greifswald.

The relevant team is:

G. Grieger, C. Grohrock, J. Junker, W. König, R. Krampitz, G. Mauser, M. Müller, G. Pfeiffer, M. Winkler, H. Zedler.

The team is supported by the construction divisions of IPP and MPG.

STELLARATOR THEORY DIVISION

(Prof. Dr. Jürgen Nührenberg)

The activity of the Stellarator Theory Division is concentrated on further development of the stellarator concept and numerical and analytical methods to investigate equilibrium, stability and transport problems in three-dimensional toroidal configurations.

The relevant team is:

S. Arndt, M.Drevlak, Ch. Hennig, R. Hatzky, R. Kleiber, A. Könies, P. Merkel, C. Nührenberg, J. Nührenberg, S. Weber.

EXPERIMENTAL PLASMA PHYSICS DIVISION 2

(Prof. Dr. Günter Grieger)

The activity of the Experimental Plasma Physics Division 2 is concentrated on the WENDELSTEIN 7-X related work of divertor development and stellarator power plant studies.

The relevant team is:

W 7-X-Team

C.D. Beidler, S. Gori, H. Greuner, G. Grieger, H. Grote*, E. Harmeyer, O. Heinrich, F. Herrnegger, F.-W. Hoffmann, J. Junker, A. Kendl, J. Kißlinger, H. Münch, I. Ott, H. Renner, U. Schwenn, I. Sidorenko, E. Strumberger, H. Wobig, A.V. Zolotukhin.

(*W7-X Construction Division)

Supporting activities by Plasma Diagnostics Division, Berlin (Prof. Dr. Gerd Fußmann)

D. Hildebrandt, P. Bachmann, W. Bohmeyer, B. Jüttner*, M. Laux, D. Naujoks, R. Radtke, J. Sachtleben, D. Sünder, U. Wenzel.

(* Humboldt University, Berlin)

The W7-X team is supported by contributions from Forschungszentrum Karlsruhe (FZK - Institut für Technische Physik), Forschungszentrum Jülich, by the Tore Supra team of CEA, Cadarache, and by the Central Technical Services of IPP.

EXPERIMENTAL PLASMA PHYSICS DIVISION 3 (W7-AS)

(Prof. Dr. Friedrich Wagner)

The W7-AS group comprises Experimental Plasma Physics Division 3. The work is fully reported in the section "STELLARATOR Project", of which the members are as follows:

Experimental Plasma Physics Division 3: P. Amadeo[9], M. Anton, S. Bäumel[22], T. Baloui[21], G. Beikert[21], E. Bellido[22], J. Bleuel[21], R. Brakel, H. Callaghan[2], B. Brotas d.Carvalho[13], G. Cattanei, H. Chatenet[3], Ch. Christou, R. Croci, D. Dorst, O. Dumbrajs[7], K. Dyabilin[16], S. Egorov[15], M. Ellmauer[22], A. Elsner, M. Endler, K. Engelhardt, V. Erckmann, B. Ernst[22], Y. Feng, S. Fiedler, M. Francés[17], C. Fuchs[21], U. Gasparino, A. Geier[22], J. Geiger, T. Geist, L. Giannone, C. Görner[21], P. Grigull, H. Hacker, M. Häse[21], H.J. Hartfuß, G. Herre[21], M. Hirsch, J. Hofmann, F. Hoffmann, E. Holzhauer[6], J.K. Hübner[4], K. Itoh[11], S.-I. Itoh[12], R. Jaenicke, F. Karger, M. Kick, A. Kislyakov[14], T. Klinger[5], J. Knauer, C. Konrad[21], J.P. Koponen[21], H. Kroiss, G. Kühner, A. Kus, H. Laqua, L. Ledl[21], H. Maaßberg, N. Marushchenko[18], K. McCormick, S. Murakami[11], H. Niedermeyer, I. Nomura[11], W. Ohlendorf, W. Pernreiter[21], U. Pfeiffer[22], V. Plyusnin[18], S. Reimbold[21], M. Romé, N. Ruhs, N. Rust[21], J. Saffert, M. Saffmann[1], A. Salat, F. Sardei, Ch. Scheiba[22], S. Schill[22], F. Schneider, V. Sergeev[15], E. Simmet, E. Solano[20], U. Stroth, W. Svendsen[1], J. Tataronis[19], G. Theimer[21], F. Wagner, H. Walter[21], A. Weller, C. Wendland, A. Werner, E. Würsching, P. Zeiler[22], X. Zhang, D. Zimmermann, M. Zippe, S. Zoletnik[8]

1) Guest from RISØ, Roskilde (Denmark)
2) Guest from University of Cork (Eire)
3) Guest from University of Paris-Sud (France)
4) Guest from IAP/University Heidelberg (Germany)
5) Guest from University of Kiel (Germany)
6) Guest from IPF Stuttgart (Germany)
7) Guest from University of Helsinki, Espoo (Helsinki)
8) Guest from KFKI Research Inst., Budapest (Hungary)
9) Guest from ENEA, Frascati (Italy)
11) Guest from NIFS, Toki (Japan)
12) Guest from RIAM, Kyushu (Japan)
13) Guest from IST, Lisbon (Portugal)
14) Guest from IOFFE Institute, St. Petersburg (Russia)
15) Guest from TUAP, St. Petersburg (Russia)
16) Guest from GPI, Moscow (Russia)
17) Guest from CIEMAT, Madrid (Spain)
18) Guest from IPT-NSC Kharkov (Ukraine)
19) Guest from University of Wisconsin (USA)
20) Guest from University of Texas (USA)
21) Doctoral fellow, and
22) Undergraduate

Technical Team W7-AS: G. Abele, W. Andres, S. Bartsch, W. Bendak, M. Bergbauer, P. Böhm, J. Bömerl, K.H. Brumm, H. Czich, S. Eder, A. Eschlwech, J. Fink, M. Fußeder, D. Gonda, H. Greve, G. Grünwald, M. Heckmeier, T. Henningsen, J. Hofner, F.W. Hoffmann, H. Holitzner, R. Horn, G. Hussong, H. Ibbach, K. Iraschko, E. Katzmarek, K.H. Knauer, J. Littwin, R. Mulzer, R. Neuner, F. Offenbächer, J. Prechtl, S. Ravichandran, M. Richter-Glötzl, H. Rixner, H. Schmid, L. Schmid, A. Schmidtmeier, H. Scholz, S. Schraub, R. Semler, H. Speer, J. Stadlbauer, B. Stajminger, M. Steffen, P. Voigt, H. Volkenandt, K.H. Wagner, U. Weber, H. Wolf, C. Wöstmann, G. Zangl, W. v. Zeppelin, Do. Zimmermann, and the workshop of E2/E3.

Experimental Plasma Physics Division 2: C. Beidler, K. Kisslinger, H. Wobig

Experimental Plasma Physics Division 4: J. Baldzuhn, K. Behringer, R. Burhenn, J.V. Hofmann, A. Weghorn

ECRH (Electr. Cycl. Resonance Heating): W. Kasparek, L. Empacher, W. Förster, G. Gantenbein, P.G. Schüller, K. Schwörer (IPF Stuttgart). A. Borshegovsky, V. Ilyin (Kurchatov Inst. Moscow), V. Irkhin, L. Lubyako, S. Malygin V.N. Sigalaev, E. Suvorov (IAP Nizhny Novgorod), V. Malygin (GYCOM Nizhny Novgorod)

ICRH (Ion Cycl. Resonance Heating): W. Becker, F. Braun, H. Faugel, R. Fritsch, D.A. Hartmann, F. Hofmeister, J.M. Noterdaeme, F. Wesner (Technology Division)

NBI (Neutral Beam Injection): W. Ott, F.-P. Penningsfeld, F. Probst, E. Speth, R. Süß (Techn. Div.)

Plasma Surface Interaction Group: R. Behrisch, V. Dose, H. Verbeek, J. Roth, E. Taglauer, P. Zebisch

Plasmadiagnostics (Berlin): A. Herrmann, D. Hildebrandt, B. Jüttner, D. Naujoks

Computer Centre: S. Heinzel, H. Lederer

Central Techn. Services: D. Arz, B. Brucker, H. Eixenberger, E. Grois, F. Gresser, O. Jandl, S. Kötterl, W. Melchior, W. Melkus, J. Perchermeier, M. Weißgerber, G. Wenzel

EXPERIMENTAL PLASMA PHYSICS DIVISION 4

(Head of Division: Prof. Dr. Kurt Behringer)

Experimental Plasma Physics Division 4 (E4) consists of the ASDEX Upgrade, W 7-AS and ITER Diagnostics groups. Their work is described in the ASDEX Upgrade and W 7-AS project reports as well as in the ITER Diagnostics contribution. Experimental Plasma Physics at the University of Augsburg is closely linked to E4, allowing physics students to participate in IPP's scientific programme or do basic research at Augsburg. Recent results are given under University Contributions to IPP Programme.

ASDEX Upgrade: K. Asmussen, A. Bard, H. Bucher, S. De Peña Hempel, R. Dux, B. Endras, W. Engelhardt, J. Fink, J. Gafert, A. Geier, M. Hien, F. Huber, A. Kallenbach, T. Madeira, B. Napiontek, R. Neu, H. Meister, D. Schlögl, G. Schmitt, K. Schmidtmann, A. Thoma, C. Wachter
W 7-AS: J. Baldzuhn, R. Burhenn, J. Hofmann; A. Weghorn
Augsburg: U. Fantz, B. Heger, A. Kottmair, H. Paulin, B. Schalk , ITER Diagnostics: H. Salzmann
Co-operation: IPP Berlin, JET, KFA Jülich, TU München, University of Strathclyde, Scotland, Stuttgart University

The E4 scientific programme deals with plasma boundary and divertor physics, impurity transport and plasma radiation, and low- and high-Z wall materials. Mainly spectroscopic diagnostics and analysis methods are being used in E4. Recent topics in ASDEX Upgrade were CDH mode, parallel flows, and chemical erosion in Divertor II. The interest in W 7-AS is focused on measurements of toroidal rotation, electric fields, and neoclassical impurity transport.

A particular problem in the analysis of plasma radiation is the large amount of atomic data required. This knowledge is being gathered in the international co-operation project, ADAS (Atomic Data Analysis Structure). Present activities deal with advanced methods of measuring hydrogen and hydrocarbon fluxes (chemical erosion studies), opacity problems and metastable resolved ionization, recombination and radiation data. Stepwise ionization through metastable states is particularly important in Be-like ions. Figure 1 shows CIII ionization rate coefficients from the ground state and results including the metastable level. Stepwise ionization is important at all densities and must be included in unresolved modelling calculations. "93" data are also shown (W.J. Dickson, 1993). Another issue is the normalization to either ground state or total ion density.

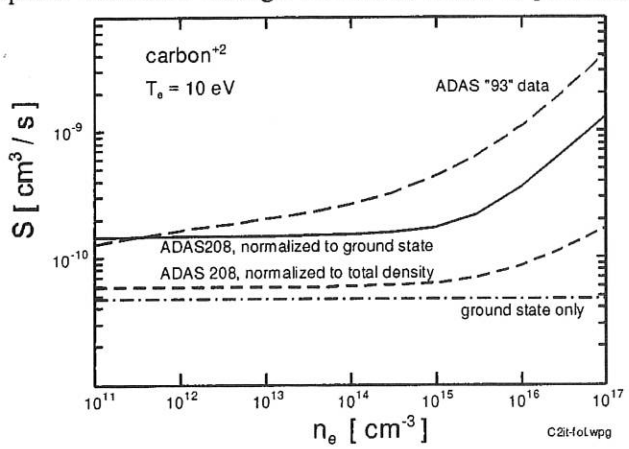

FIG. 1: Various ionization rate coefficients for CIII.

Impurity transport calculations usually assume excited states to be in instantaneous equilibrium with the ground state due to their short lifetime. However, metastable levels are long-lived at low n_e and the influence of transport on their population can be important. A more refined approach solving the coupled transport equations for ground and metastable states of every ionization stage was compared with former results for carbon and oxygen in the main plasma of ASDEX Upgrade. The metastable resolved rate coefficients were taken from ADAS and the transport calculations were performed with a revised STRAHL version. Profiles of n_e and T_e were taken from an L-mode discharge with separatrix density $n_{e,sep}=2.5\ 10^{19}m^{-3}$ and temperature $T_{e,sep}=80eV$. Purely diffusive transport was assumed with a diffusion coefficient $D=2.5m^2/s$. Metastable populations are important for Be-like ($2s2p\ ^3P$) and B-like ions ($2s2p^2\ ^4P$). Figure 2 shows the differences between resolved and unresolved calculations for CIII. For the important emission lines the intensity ratios differ by less than 10%. Thus, for typical ASDEX Upgrade edge densities and transport parameters non-resolved calculations of radial impurity transport yield satisfactory results. However, care must be taken to apply ionization, recombination, and radiation data consistently.

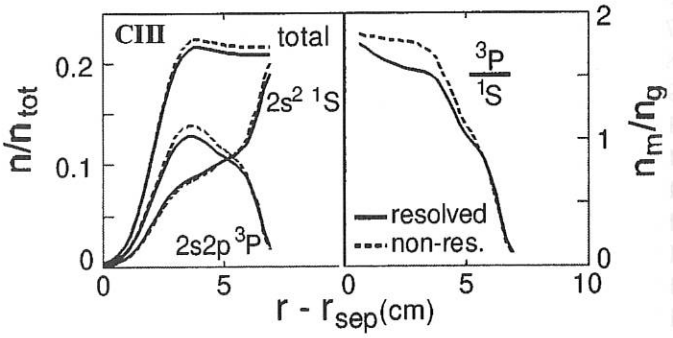

FIG. 2: Population fractions of CIII states for metastable resolved and non-resolved transport calculations.

GENERAL THEORY

(Acting Head: Prof. Dr. Klaus Pinkau)

Contributions by: D. Correa-Restrepo, D.F. Düchs, D. Lortz, R. Meyer-Spasche, F. Pohl, G.O. Spies, and D. Pfirsch (emeritus) (all IPP)
and by O. Dumbrajs (Helsinki Univ. of Technology, Finland), K. Graf Finck von Finckenstein (Techn. Univ. Darmstadt), Satoshi Itoh and K. Sakamura (TRIAM, Kyushu Univ., Japan), G. Kamelander (Österreichisches Forschungszentrum Seibersdorf), A. Reinfelds (Latvian Academy of Sciences, Riga), G.N. Throumoulopoulos (Univ. of Ioannina, Greece), H. Weitzner (Courant Institute, New York University, USA).

1. OVERVIEW

During 1997, the staff of "General Theory" was again substantially reduced by transfers and retirement.
In an attempt to compensate for these losses, the remaining members intensified their collaboration with scientists from outside IPP.
By this means, the research still covered a wide subject spectrum extending from development of new theory (e.g. constants of motion, relaxed equilibrium configurations, resistive instabilities, anomalous transport mechanisms) and new numerical methods to theory-based modelling of specific experiments (e.g. stability and particle balance of LH-driven tokamak plasmas, orbits in a gyrotron resonator).

The various topics are grouped below according to their basic assumptions, which take the plasma either as a macroscopic fluid (Sec. 2) or as a statistical particle ensemble (Sec. 3). The necessary development of mathematical resources (Sec. 4), and basic deliberations on fusion research (Sec. 5) complete this report.
Research activities were complemented by regular teaching at three universities.

2. FLUID PLASMA THEORY

2.1 Relaxed Toroidal Plasma-Vacuum Systems (Lortz, Spies)

Taylor's theory of relaxed toroidal plasmas (states of minimum energy with fixed total helicity) is extended to plasma-vacuum systems. It is shown that an equilibrium (stationary energy) cannot be an energy minimum if the plasma-vacuum interface is smooth. This is consistent with our previous finding that linearized resistive magnetohydrodynamics in a plane plasma-vacuum slab constitutes an ill-posed initial-value problem because Interface Localized Modes (ILMs) are unstable with unbounded growth rates.

2.2 Non-resonant Resistive Instabilities (Lortz, Spies)

Non-resonant resistive modes (no mode-resonant flux surfaces) with small wavelengths are studied in plane slab equilibria. The growth rates are proportional to the maximum resistivity gradient, and the eigenmodes are concentrated where the resistivity gradient is largest. This refutes the common belief that resistive instabilities require mode-resonant surfaces.

2.3 Two-fluid Modes (Pfirsch, Weitzner)

Instabilities and waves in a system of a massless electron fluid coupled to an ionic fluid in slab geometry were studied. Both non-dissipative and dissipative fluids were used, although the dissipation is not the most general needed. Exact solutions in simple cases were found.

2.4 Drift Fluid Modes (Correa-Restrepo, Pfirsch)

Linear, collisional, electrostatic modes were investigated and expressions for the energy balance of general perturbations derived. When expanding in small resistivity around ideal modes, difficulties arise due to the incompleteness of the set of eigenfunctions for the ideal eigenvalue problem.

The consequences of including electromagnetic effects hinge on the ways of describing the low-beta and low-resistivity limit.

3. KINETIC PLASMA THEORY

3.1 Constants of Motion for Particles in Drift Approximation (Pfirsch)

Additional constants of motion for Lagrangian systems can be derived by a modification of Noether's formalism. These constants turn out to be linear combinations of the canonical momenta with coefficients depending only on the generalized coordinates.

This new formalism is then specified for the Littlejohn-Wimmel Lagrangian for drifting particles. When applied to Palumbo equilibria and quasihelical ones, the known constants of motion are immediately obtained.

3.2 Analysis of Electron Trajectories in a Gyrotron Resonator (Meyer-Spasche, Dumbrajs, Reinfelds)

A mathematical analysis of electron interaction with the high-frequency field in a gyrotron resonator is presented. Electron trajectories in the phase space are classified. It is proved that for Gaussian high-frequency fields, the solutions of the gyrotron equation are asymptotically equal to the solutions of the corresponding unforced equation. Chaotic trajectories are thus impossible, except maybe inside the resonator. For parameter values corresponding to the maximum efficiency of the gyrotron, trajectories were numerically computed and displayed.

3.3 Impact of Radial Electric Fields on Negative-Energy Perturbations in Cylindrical Equilibria (Throumoulopoulos, Pfirsch)

For cylindrial tokamak-like and shearless stellarator-like equilibria stabilizing effects of electric fields (E) on negative energy perturbations (NEPs) are found. Under usual conditions such E-fields cannot be neglected, contrary to the customary procedure. Especially in plasma edge regions E reduces the activity of NEPs preferably for electrons.

3.4 Stability of LH-driven Tokamak (Düchs, Satoshi Itoh, Sakamura)

The TRIAM tokamak with driven current runs for very long times without disruption. A model is investigated which combines a run-away current with levitron stability considerations.

For the same experiment multi-ion particle balances and models for plasma-wall interaction in dynamical steady state are developed by analytical and numerical methods.

3.5 Validity of Drift Approximation (Düchs, Kamelander, Pohl)

Fast ions can encounter plasma gradients where gyroradii and gradient lengths are comparable. Through numerical studies the quantitative limits for the drift orbit approximation and possible corrections are derived.

4. DEVELOPMENT OF MATHEMATICAL TOOLS

4.1 Diffusion Equation with Sources (Düchs, Graf Finck von Finckenstein, Pohl)

The long-time behaviour of solutions of diffusion equations with sources were investigated. The conditions for stability or for "blow-up" were delineated by numerical test calculations (also within the frame of a diploma thesis).

4.2 Difference Schemes of Optimum Degree of Implicitness for a Family of Simple ODEs (Meyer-Spasche)

We studied the question of how implicit a scheme should be from several different points of view: we discussed the properties of the linearized trapezoidal and of its discrete blow-up; we gave exact schemes for a family of polynomial ODEs ; we showed that other standard schemes are exact on certain differential equations; we compared leading error terms; and we discussed two ways of adapting the degree of implicitness of a scheme to a given differential equation.

4.3 Numerical Schemes for Resistive MHD (Düchs, Graf Finck von Finckenstein)

Discretization methods for resistive MHD equations (in two and three dimensions) are being reviewed, starting from existing investigations on mixed hyperbolic-parabolic systems of partial differential equations.

5. FOUNDATIONS OF FUSION ENERGY RESEARCH

5.1 Optimization of Nuclear Energy (Düchs)

In the long term (centuries) only solar and nuclear energy will be available to a reasonable extent. The importance of fusion seems to rest on its potential for optimizing the nuclear energy option.

TOKAMAK PHYSICS

(Head of Project: Prof. Dr. Karl Lackner)

The Tokamak Physics Division conducts basic and applied theory in the area of toroidal plasma confinement, with emphasis on application to existing and planned tokamak experiments. The main areas of research are (1) plasma transport, (2) edge plasma physics, (3) MHD studies. Quantitatively smaller effort is dedicated to wave physics and interaction of extremely high heat loads with material surfaces as occurs during pellet ablation and disruptive instabilities. The research on MHD instabilities is mainly described in the frame of the ASDEX Upgrade project, as are the major contributions of the edge physics group (with some contributions described under the JET project). Ablation model development (for pellets and disruption consequence simulations) is described in the ITER section. To allow adequate technical description in the space available, one area of the other scientific work - turbulent transport simulation - was selected for detailed representation in this report, other subjects being treated only in the form of very short summaries

Head: K. Lackner, Deputy: J. Neuhauser
G. Becker, A. Bergmann, D. Biskamp, K. Borrass, M. Brambilla, K. Büchl, A. Carlson, D. Correa-Restrepo, D. Coster, W. Feneberg, S. Günter, K. Hallatschek, J. Janauschek, F. Jenko, O. Kardaun, L. Lengyel, D. Lortz, P. Martin, J. Neuhauser, G. Pautasso, A. Peeters, S. Pinches, K. Reinmüller, W. Sandmann, S. Schade, R. Schneider, W. Schneider, E. Schwarz, J. Schweinzer, B. Scott, H. Tasso, A. Teo, M. Weinlich, R. Wunderlich, H.-P. Zehrfeld, A. Zeiler

Guests: R. Bilato, Instituto Gas Ionizzati, Padova, A. Boozer, Columbia University, New York, B. Braams, New York University, R. Brandenburg, Technische Universität, Wien, J. Drake, Institute of Plasma Research, Maryland, A. Hatayama, Keio University, Japan, S. Khirwadkar, Institute for Plasma Physics, India, G. Petravich, Central Research Institute, Hungary, A. Rogister, Institut für Plasmaphysik, Jülich, N. Tsois, Demokritos, Athens, P. Lalousis, IESF.FORTH, Heraklion, P. McCarthy, H. Callaghan, University of Cork, A. Ushakov, I. Veselova, V. Rozhansky, Technical University, St. Petersburg, H. Weitzner, Courant Institute of Mathematical Sciences, New York

1. ENERGY AND PARTICLE TRANSPORT

1.1 Plasma Edge Turbulence

Previous investigations of plasma edge transport were continued and variously extended to afford a more complete description. Anomalous transport is widely attributed to resistive mechanisms at the plasma edge and ion temperature gradient driven (η_i) modes in the core. Thus, understanding the intermediate regime, in particular the edge pedestal, calls for a model which adequately describes both limits. On the basis of the complete drift-reduced Braginskii equations this regime was investigated linearly and nonlinearly. Linear eigenmode calculations demonstrate that resistive ballooning and toroidal η_i modes can exist as separate roots with similar growth rates but with differing structure along the magnetic field. While the typical transverse scale length of the resistive modes strongly depends on collisionality, the transverse scales of the η_i mode are essentially independent of the collisionality even in the absence of any assumption on the adiabaticity of the electrons. Three-dimensional nonlinear simulations quantitatively describe the transition between the resistivity-dominated outermost edge and regions with moderately higher temperature where resistive modes are stabilized and the collisionless η_i mode dominates. A significant result is that the η_i modes continue to drive significant particle transport even in regimes where the linear stability analysis indicates the electrons are dominantly adiabatic. Though the set of equations underlying these results is substantially more complete than earlier treatments of η_i-mode turbulence, the ion heat flux due to the curvature drift was still neglected in part. The importance of this term is currently under investigation. Preliminary results indicate a significant impact on the η_i-mode threshold.
As a second major topic, the impact of electromagnetic perturbations was investigated. As previously observed [B. N. Rogers, J. F. Drake, Phys. Rev. Lett **79**, 229 (1997)], finite β leads to a strong increase of the transport rates in the resistive ballooning regime. In a more drift-wave-like situation strong poloidal sheared flow is generated as a combined effect of finite ion temperature and magnetic perturbations and consequently the transport rates strongly decreased. As in earlier simulations, self-generated poloidal flows are relatively strong even in the electrostatic limit, much stronger than in cold-ion simulations.

Unlike in the electrostatic limit, where the poloidal flows are unstable, they persist for a long time at sufficiently large β. In these sheared flows the total ion velocity vanishes, as the ion diamagnetic flow and the E × B flow balance each other, which emphasizes the importance of finite ion temperature. Since the formation of the poloidal flows is strongly influenced by damping, ion-ion stress was included to take magnetic pumping into account.

As a major computational improvement, performed in close collaboration with the Computer Science Division, the nonlinear three-dimensional code for simulations of drift-Braginskii turbulence was ported from a vector architecture to the Cray T3E massively parallel system.

The results presented above were all obtained in the local approximation assuming that plasma parameters are constant over the whole computational domain. To overcome this limitation two approaches are followed. A three-dimensional anisotropic multi-grid Poisson solver was developed to treat the parabolic parts of the equations. A particular advantage of this approach is that it can be efficiently implemented on parallel-distributed memory architectures. In the design of the solver considerable effort had to be made to ensure that the presence of anisotropy (e.g., arising from magnetic shear) does not lead to significant degradation of performance. A three-dimensional slab version of the solver was implemented and successfully tested for the nonlocal Hasegawa-Wakatani equations. As a shorter-term activity, a nonlocal code previously developed for cold ions and isothermal electrons, was extended to include the ion temperature dynamics. In this code Fourier transforms are taken in the poloidal direction only, thus taking the important radial variation of the plasma parameters into account. The specific goal is to observe the transition from resistive ballooning to toroidal η_i-mode turbulence, as predicted by the local simulations, within the same simulation due to radial variation mainly of the collisionality, and to study the self-consistent formation of temperature and density profiles which results from the predicted radial variation of the transport rates.

1.2 Advances in Turbulent Drift Wave Studies

The computational model for electron drift dynamics described in previous reports was further extended. The electron drift regime is that in which the E×B flow can be treated as a fluid; scales were of the order of 0.1 to 1 MHz and 0.1 to 1 cm, as found in experimental fluctuation measurements. Extension of the model to collisionless and electromagnetic regimes was completed – the model contains as subsets, for example, reduced MHD, collisional drift waves, and collisionless universal modes. As a result, various mechanisms such as MHD ballooning and drift Alfvén turbulence can be compared by removing the set of terms in the equations representing first one and then the other phenomenon. Both the qualitative properties of the fluctuations and the scaling of the resulting transport can therefore be attributed to a particular subset of phenomena, giving more insight than what one gains simply by comparing undiagnosed transport scalings with experiments. These studies showed that the transport rises sharply with the normalized plasma beta (giving the ratio of drift wave to shear Alfvén frequencies), and that the reason is that magnetic induction (the time dependent part of the electric field) determines the speed of the electrons' response to static forces along the magnetic field. The turbulence is of the drift-Alfvén type, as shown by the insensitivity of the qualitative behaviour or the transport scaling to the presence or absence of terms in the equations representing magnetic curvature or ''magnetic flutter'' (the change in the parallel gradient due to the magnetic fluctuations). We also incorporated self-consistent ion temperature dynamics. This involves several new effects. The best known is the toroidal ion temperature gradient, or η_i turbulence currently receiving most attention in core transport studies. When these two types of dynamics – η_i and drift-Alfvén – act together in the computations, the resulting turbulence is a hybrid of the two. The sensitivity to the plasma β of drift-Alfvén turbulence and that of η_i turbulence to the ion/electron temperature ratio both remain, but this mix of dynamics leaves the turbulence with a qualitative character different to that of either of its constituent ''modes''. An interesting result is marked sensitivity to variations in the gradient scale lengths relative to one another. The turbulence is strongest when all three of $\nabla \log n$, $\nabla \log T_e$, and $\nabla \log T_i$ are similar. In absolute terms, computation in a flux surface geometry similar to ASDEX Upgrade (aspect ratio 3.3, elongation 1.6, triangularity 0.1, near-edge q of 3.5) leads to a total energy transport of 14 MW, as compared with an experimental value of 7. If $\nabla n \approx 0$, the particle flux is slightly negative, reflecting a particle pinch according to the ''ion mixing mode'' mechanism of Coppi and Spight [Phys. Rev. Letters **41**, 551-554.(1978)], although in the present case the η_i mode is of the toroidal variety.

An ongoing parallel study of this same type of turbulence using a drift-kinetic Vlasov model was also extended to include these shear Alfvén effects, and the result is similar behaviour. The kinetic model can treat the nonlinear trapping of electrons in the electric field of the drift waves. When there is no magnetic shear a wave travelling along the magnetic field can persist indefinitely, and trapping is found to be very important in limiting the strength of the turbulence. Tokamak edge relevant values of shear, however, lead to a short correlation length along the magnetic field, and the only remaining role of the parallel dynamics is to provide the channel to dissipation. The drift kinetic results therefore show much less sensitivity to this trapping effect. This lends additional support to the use of extended fluid models in the collisionless regime obtaining over most tokamak parameters. We are extending these models to include the effects of nonlocal profile/turbulence interaction (their scale lengths differ by a factor of only 2 to 3) and limited field lines, as was done (1995) in the electrostatic case. We hope to be able to investigate self-consistency phenomena such as the L-H transition and ELMs, which have not yielded to the more usual ''local'' computations.

1.3 Physics of L-H Mode Transition

To study the L-H transition, a general set of equations describing the evolution of the radial electric field and poloidal rotation was derived. Neutral friction in ASDEX Upgrade was shown to be small compared with neoclassical viscosity. The Stringer spin-up mechanism depends only weakly on the geometry.

2. EDGE PHYSICS STUDIES

2.1 Edge and Divertor Simulation with B2–Eirene Code

B2–Eirene is a code package treating 2–dimensional plasma transport in the scape-off layer with a fluid model, and the neutral particle dynamics by a Monte Carlo model. In addition to ASDEX Upgrade and JET modelling, our group supports the ITER design activities by preparing and providing an up-to-date code version to the Garching Joint Central Team.

2.2 Particle Simulation Studies

Two-dimensional particle simulations of a scrape-off layer (SOL) plasma were made by means of a particle-in-cell code with a Fokker-Planck model of Coulomb collisions. The following issues were studied: 1) Model of a SOL with transport only by Coulomb collisions and drift motion in the oblique magnetic field in order to determine the influence of drift motion on the radial SOL scale lengths. 2) The influence of the E×B drift on the current flow to flat Langmuir probes mounted into a divertor target plate. 3) Formation of hot spots on a target plate with strong thermal electron emission: their characteristic size and their motion in a tilted magnetic field.

3. MHD EQUILIBRIUM AND STABILITY

The advance of ASDEX Upgrade to higher performance levels and the growing interest in tokamak operation scenarios with steady-state potential have led to a strong increase in our effort to understand observed MHD activity and predict future operating limits. Significant effort has also been made in the documentation and analysis of plasma conditions leading to terminal disruptions. Results of all these efforts are described in detail under the ASDEX Upgrade Project.

3.1 Equilibrium Reconstruction for ASDEX Upgrade

On ASDEX Upgrade, the method of equilibrium indentification for both real-time (feedback-control) and post-discharge analysis is the FP algorithm, which uses a statistical fit (via "function parametrization") to a pre-computed database. The transition to Divertor II and the associated changes in the possible PF coil current patterns required substantial extensions to these algorithms, concerning both the input and the desired output information. An equilibrium reconstruction code ("CLISTE") was developed which makes full equilibrium computations by fitting plasma current and pressure profiles to match magnetic measurements. The input is provided by poloidal field and flux measurements outside the plasma and by the MSE (Motional Stark Effect) - diagnostic described in the ASDEX Upgrade section - of poloidal fields inside the plasma region.

3.2 MHD Equilibrium and Ballooning Stability

For the purpose of providing realistic input for stability analysis by the Castor and Garbo codes, extended MHD equilibrium and data modelling studies were performed, offering advanced features such as handling of finite current densities near the separatrix, parametrized pedestal-type pressure profiles and enhanced accuracy near the plasma boundary. On this basis detailed ballooning stability investigations were done for the ASDEX Upgrade and ITER tokamaks and the W7–AS stellarator. By analytical and numerical studies it was shown that, except for extreme interpretation of the experimental observations, ASDEX Upgrade is always below the ideal ballooning limit near the plasma edge. This contrasts to the simplified α-s model evaluations.

3.3 Toroidal Equilibria with Incompressible Flows

Exact equilibria are constructed, including those with nonvanishing poloidal and toroidal flows and differentially varying radial electric fields. Unlike the case in cylindrical equilibria with isothermal surfaces [Throumoulopoulos and Tasso, Phys. Plasmas 4, 1492 (1997)], there is no restriction on the shapes of the magnetic surfaces in the corresponding axisymmetric case, apart from in the vicinity of the magnetic axis. Regarding the stability of mechanical systems, a sufficient stability condition was derived for dissipative mechanical systems having gyroscopic and circulatory forces.

4. HEATING BY PLASMA WAVES

A new version of the FISIC toroidal ion cyclotron waves code takes advantage of the reduced numerical requirements of the Order Reduction Algorithm (ORA) to allow a relatively fast scan of the complete toroidal spectrum launched by the IC antenna. The ORA replaces the excitation of ion Bernstein waves at mode conversion layers by an equivalent power sink; although heuristic, this approach gives excellent results in almost all IC scenarios, while appreciably reducing the execution time. The variational principle for the self-consistent evaluation of antennas for ion cyclotron heating and current drive was extended to the case of arrays of coupled antennas. The generalized principle was implemented in ANTWKB, a code which evaluates the surface impedance matrices of the plasma, assuming that the WKB approximation can already be used at the plasma boundary. This procedure is very fast, so that several hundred Fourier modes can be taken into account in both the toroidal and poloidal directions, as required for the convergence of the reactive part of the antenna loads. ANTWKB evaluates the complex impedance matrix of the array, which allows one to regard the antennas as fully characterized elements of the IC power circuit, and thus to compare the numerical model directly with the experimental measurements.

SURFACE PHYSICS DIVISION

(Prof. Dr. Dr. h.c. Volker Dose
Prof. Dr. Jürgen Küppers)

Scientific activities in the Surface Physics Division proceed via three routes, which we call plasma wall interaction (analytical), plasma wall interaction (preparative) and surface science. Our work on analytical problems of plasma wall interaction is for the purpose of this report further divided into two categories. Those activities which take place in intimate collaboration with fusion devices are included in the respective chapters on tokamaks and stellarators. Additional laboratory work described in this chapter is grouped under the title plasma wall interaction processes. Contributions to the field of plasma wall interaction (preparative) are described in a separate section entitled plasma technology. This project is a joint venture with the IPP Technology Division. More fundamental studies, summarized under the heading of surface science, comprise a continuation of previous activities in magnetism and contributions to the Sonderforschungsbereich 338. The latter concentrates on adsorption at solid surfaces and integrates work at the Munich Universities and IPP and MPQ.

Head: V. Dose, Deputy Head: E. Taglauer

Scientific Staff:

A. Annen[3], A. Atrei[4], M. Balden[3], R. Behrisch, E. Berger[1], E. Bertel, J. Biener[3], M. Donath, W. Eckstein, K. Ertl, R. Fischer, P. Goldstraß[1], Ch. Höfner[3], M. Hohenegger[1], A. Horn[1], L. Houssiau[5], W. Jacob, H. Kang[1], D. Keren[6], A. v. Keudell[3], A. Kohl[2], H. Knözinger[12], K. Krieger, M. Küstner[1], S. Labich[1], B. Landkammer[1], J. Lehmann[1], W. von der Linden, St. Lindig[2], Ch. Linsmeier[3], C. Lutterloh[1], K. Maruyama[7], Ch. Math[1], M. Mayer[3], M. Meier[2], N. Memmel[3], S. Miller[1], W. Möller[13], J. Onsgaard[8], P. Pecher[1], K. Plamann[3], H. Plank[3], J. du Plessis[9], R. Preuss[3], V. Prozesky[10], A. Ramaswami[11], G. Rangelov[3], J. Reinmuth[1], J. Roth, Th. Schwarz-Selinger[1], G. Staudenmaier, A. Steltenpohl[1], K. Swamy[1], U. von Toussaint[1], P. Valášek[3], S. Vasquez[1], G. Venus, H. Verbeek, S. Vetter[1], P. Zebisch[3].

Technical Staff:

S. Bassen, L. Beck, M. Ben Hamdane, S. Figge, Ch. Fritsch, K. Gehringer, R. Hippele, A. Holzer, M. Hunger, P. Matern, J. Mauermair, M. Nagy, W. Ottenberger, M. Roppelt, J. Schäftner, A. Schlamp, H. Schmidl, F. Schuster, I. Zeising.

1 Doctoral Candidate
2 Undergraduate Student
3 Post Doc

Guests:

4 Universität Florenz, Italia
5 Université Catholique, Louvain-la-Neuve, Belgium
6 University of Haifa, Israel
7 Nagaoka University of Technology, Japan
8 Odense Universitet, Denmark
9 University of the Free State, Bloemfontein, SA
10 National Accelerator Center, Faure, SA
11 Washington University, St. Louis, MO, USA

Collaboration with:

12 Ludwig-Maximilians-Universität, Munich, Germany
13 Forschungszentrum Rossendorf, Germany

1. DATA ANALYSIS

Experimental measurements provide only rarely the physical quantities, which the experiment aims at. These are rather deteriorated by finite resolution, corrupted by noise or tied up in correlations. In order to arrive at the quantities sought, inferences must be made. Bayesian probability theory is an axiomatic, simple, but by no means easy approach to data analysis.

The topic of group analysis is the general problem of partitioning large data sets according to nonscalable variables into equivalent subsets. Clearly one wants to find the minimum number of data groups such that the data are explained satisfactorily within their error margins. A computer code has been set up and applied to thin film deposition data classified according to the carrier gas in the plasma reactor.

Deconvolution of experimental data in order to enhance spectral resolution is an evergreen in data analysis. Two equally well performing algorithms based on adaptive cubic spline interpolation and on the adaptive kernel method have been implemented. Application to Cu RBS spectra resulted in resolution enhancements by a factor of six.

Bayesian parameter estimation was applied to dimensionally constrained energy confinement analysis of W7-AS data. Prior information was drawn from the Connor Taylor similarity transformation relations. The model function was a single term power law. The results of this analysis question severely the suitability of the latter assumption.

2. PLASMA-WALL INTERACTION

2.1 Hydrogen Inventory in Plasma-facing Materials (PFM)

In a thermonuclear fusion reactor, such as ITER, plasma-facing materials will be eroded due to plasma ion and neutral bombardment. The present design for ITER uses carbon fibre composites (CFC) for the divertor plates and beryllium for the main plasma chamber walls. Carbon eroded from the divertor plates will be deposited, along with hydrogen isotopes from the plasma, onto less exposed areas, including the Be wall of the main plasma chamber. The inventory of tritium in this codeposited material could become large enough to restrict operation of the machine. Methods to recover tritium from these codeposited layers are therefore of vital interest for the operation of ITER.

2.1.1 Release of deuterium from carbon-deuterium films on beryllium during carbide formation and oxidation

(collaboration with SANDIA Labs, Albuquerque)

The present investigations concern the interaction of Be with a-C:D films, the Be_2C phase formation and the deuterium release. Ion beam analysis is used to follow the evolution of the concentrations of Be, O, C and D and H versus depth in the near-surface region as the a-C:D layer reacts with the Be substrate. In addition, Auger electron spectroscopy (AES) gives information on the composition and chemical state of the surface. The oxidation kinetics of Be and a-C:D layers were also examined.

The present investigations provide in-situ depth analysis of the Be-C reaction and associated D release, combined with chemical phase analysis from AES line shapes, for a-C:D films deposited on Be substrates. With this combination it could be shown that the a-C:D film reacts with the Be substrate to form stoichiometric beryllium carbide, Be_2C. The reaction begins at the interface and progresses through the film at around 800 K until the entire film has reacted. D is absent from the reacted portion of the film but is still present in the unreacted portion. Be is the diffusing species as seen from an oxide marker at the interface. The a-C:D films could be removed from the Be without forming the carbide by heating in oxygen at 700 K.

2.1.2 Deuterium retention in carbides and doped graphites

The retention of 1 keV and 8 keV deuterium implanted in doped graphites (dopants: B, Si and Ti) and the carbides B_4C, SiC and TiC was studied at room temperature by thermal desorption spectroscopy and ion beam analysis. For all graphites the total content of retained deuterium does not saturate up to fluences of 6.7×10^{19} D atoms/cm^2 (FIG. 1). Compared with pyrolytic graphite, all doped graphites showed a tendency to increased retention of deuterium, especially the materials with high porosity. This could be explained by diffusion of deuterium along inner surfaces beyond the implantation zone into the bulk.

For the carbide B_4C the saturation concentration of deuterium in the implantation zone is about 0.4 D per target atom and, therefore, comparable to the saturation concentration of D in graphite. SiC exhibits a significantly higher saturation concentration of 0.6 D per target atom, whereas TiC shows a significantly lower saturation concentration of 0.15 D per target atom.

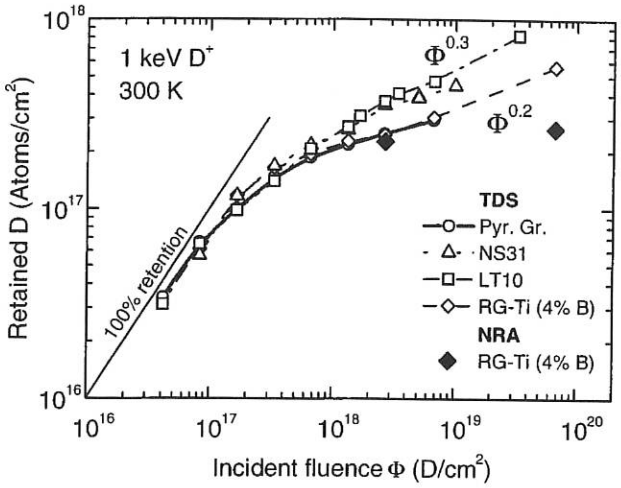

FIG. 1: Fluence dependence of the retained amount of deuterium in pyrolytic graphite, NS31 (10 at.% Si), LT10 (10 at.% Ti) and RG-Ti-91 (1.7 at.% Ti and 4 at.% B) for bombardment with 3 keV D_3^+ at room temperature.

2.1.3 Erosion behaviour of soft a-C:D films by heat treatment in air and under vacuum

Films deposited onto limiters and protective tiles in fusion experiments are often porous, soft a-C:D films. Removal of these films by oxidation has been proposed as in-situ cleaning method. Previously, the erosion of hard a-C:D films by heat treatment was investigated and it was shown that the surface deuterium is quantitatively balanced by oxygen uptake and hydrogen isotope exchanges in the film until deuterium is completely released. The investigations were extended to similar studies of the erosion behaviour by heating soft a-C:D films with a large initial hydrogen content in vacuum and air and changes in the films stoichiometry and structure during heating.

The erosion of soft a-C:D films by heat treatment in air and under vacuum is studied quantitatively by ion-beam compositional analysis. When the film is heated in air at temperatures higher than 500 K, the film thickness and areal densities of carbon and especially deuterium decrease in conjunction with oxygen incorporation. The initial atomic loss rate of carbon and deuterium from the film is 3×10^{17} C atoms cm^{-2}h^{-1} and 6×10^{17} D atoms cm^{-2}h^{-1} at a temperature of 550 K. However, after deuterium depletion the films show a resistivity to further erosion due to heating in air and erosion proceeds similarly to that of the hard films previously investigated. FIG. 2 shows a comparison of film removal in air for hard films and two soft films with different initial hydrogen content. It can

be seen that the film removal at 550 K is the stronger the higher the initial hydrogen content, i.e. the softer the initial film.

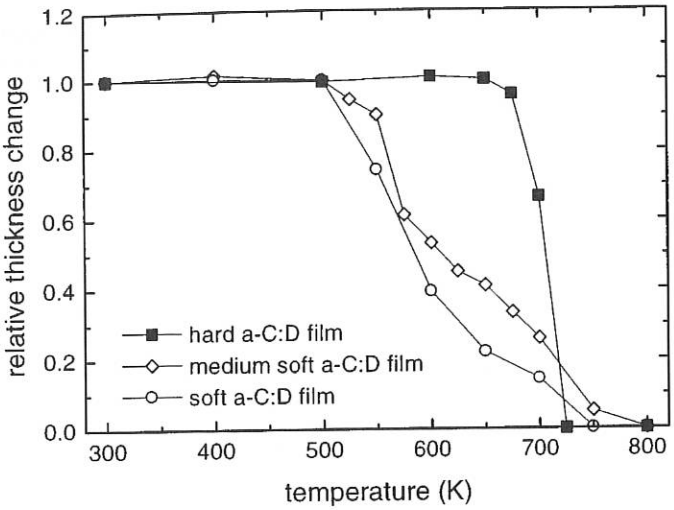

FIG. 2: Comparison of the removal of a-C:D films of different hardness and initial hydrogen content by heating in air for 1 h.

2.2 Erosion and Deposition

The wall material selection for ITER is governed by material properties such as sputtering yield, melting point, thermal conductivity etc. During plasma discharges, the erosion, transport and redeposition of wall material lead to the formation of layers and compounds consisting of a mixture of the wall materials and plasma impurities. These multi-component materials show strongly altered erosion properties compared with the pristine wall materials.

In order to study these mixed phases, a new experimental setup was designed and built. It allows the well-defined formation of mixed phases, their characterization and testing of their erosion and hydrogen interaction properties. The experimental setup consists of a UHV chamber connected to the MeV accelerator beam line, an ion source with magnetic beam separation, an evaporator, sources and analyzer for electron spectroscopies and a mass spectrometer. In 1997, the design was completed and the setup of the experiment started.

2.2.1 *Layer deposition and erosion by C^+ and CO^+ ion bombardment of beryllium*

Beryllium as a potential first-wall material was bombarded with C^+ and CO^+ ions in the energy range between 3 and 12 keV. The implanted amounts of carbon and oxygen were measured by Rutherford backscattering spectroscopy (RBS) and compared with simulations with the TRIDYN Monte Carlo code. For the C^+ bombardment, carbon is deposited at all beam energies. With increasing fluence, net deposition occurs and a carbon layer of increasing thickness is formed. The experimental results are in agreement with the TRIDYN simulations. In the case of the CO^+ bombardment, which can be regarded as co-bombardment with carbon and oxygen, behaviour similar to that for carbon is only found at small fluences. In this regime, a surface layer consisting of both C and O is formed. TRIDYN reproduces this process. After a nominal layer thickness of about 10 atomic layers, however, another process starts which erodes the layer formed and leads to a deposition-erosion equilibrium. With further CO^+ bombardment, the layer thickness reaches a constant value which is dependent on the ion energy. The simulation, which only considers kinetic processes and does not take into account any chemical interactions, fails to reproduce this regime at higher fluences.

2.2.2 *Data sets for sputtering, reflection and ranges*

Data tables of the sputtering yield and sputtered energy are produced with TRIM.SP (trvmcmom version) for H, D, T, ^{4}He, N, Ne, Ar on Be, C, and W and self-bombardment in the energy range from 10 eV to 1 keV (up to 50 keV for He) and 9 incidence angles. The matrices are stored in /afs/ipp/u/wge/trim.data/sputter.data. Similar files for particle and energy reflection coefficients can be found in refl.data, and values of the mean penetration depth in range.data.

2.2.3 *Isotope sputtering*

The TRIM.SP and TRIDYN Monte Carlo programs were adjusted to the new CRAY-T3E parallel computer. The efficiency of TRIM.SP is larger than 90% for 256 processors, whereas for TRIDYN 16 processors are the optimum for most cases.

As an example, sputtering of the natural isotope mixture of molybdenum with 7 isotopes was investigated. As a measure of the preferred emission of light isotopes, the fractionation was determined as a function of the incident energy and angle for all noble gases. The sputtering yield for the lightest isotope with mass 92 and bombardment with 70 eV He is a factor of 2 larger than for the isotope with mass 100. The discrepancy between the analytic theory and experiments as well as computer simulation is due to neglecting primary knock-on atoms in the analytic theory. Calculations with TRIDYN have confirmed Wehner's result that the light isotopes are emitted preferentially in the normal emission direction at steady state (large fluence).

2.2.4 *Time development of sputtering*

The temporal aspects of sputtering of TaC, C and Ta targets by 1 keV Ar at two angles of incidence were compared. The Monte Carlo program was modified to investigate the change of the cascade with time. The time developments of the energy and angular distributions of sputtered Ta and C atoms were determined as well as the sputtering yield and particle reflection coefficient.

2.3 Ion Beam Analysis and Nuclear Reactions

The plasma-wall interaction modifies predominantly the near-surface region of the solids exposed to the plasma by erosion, redeposition and implantation. Ion beam analysis with MeV

ions is an established, powerful tool for quantitative and non-destructive investigation of these near-surface layers.

2.3.1 *Computer simulation of MeV ion beam analysis spectra*

Interpretation of measured back or forward scattering spectra is a complex task calling for simulation programs. A new program (SIMNRA) with full graphical user interface (GUI) for simulation of RBS (including non-Rutherford scattering), ERDA and NRA spectra has been developed. SIMNRA can calculate any ion-target combination, including incident heavy ions, and any geometry, including arbitrary foils in front of the detector. It uses the most recent stopping power (Ziegler-Biersack) and energy loss straggling data, including propagation of straggling in thick layers and geometrical straggling due to finite beam spot size and detector aperture. Effects of plural scattering can be calculated approximately. A data base of about 300 different cross-sections for non-Rutherford backscattering and nuclear reactions has been developed.

2.3.2 *Determination of the $^{11}B(p,\alpha_0)^8Be$ and $^{11}B(p,p)^{11}B$ cross-sections*

Quantitative detection of light elements, such as boron, on substrates composed of heavier atoms with ion beam analysis is an analytical challenge. In many cases light elements can be detected by nuclear reaction analysis (NRA). However, accurate cross-section data are needed for quantitative results. The $^{11}B(p,\alpha_0)^8Be$ nuclear reaction and the $^{11}B(p,p)^{11}B$ backscattering cross-sections were measured in the energy range 1700 - 2700 keV at a scattering angle of 165° with an absolute accuracy of about 7%. Older nuclear physics data from the sixties turned out to be up to 60% too low.

2.3.3 *MeV ion beam analysis of rough surfaces*

For the analysis of surface layers with a rough surface by MeV ion scattering, ion incidence and emergence close to the surface normal should be applied. For ion-implanted surfaces this was shown to give the correct depth distribution with respect to the actual surface. For oblique angles of incidence and emergence, such as used in ERDA measurements, the depth profiles as evaluated assuming a flat surface seem to be shifted to shallower and larger depths, in agreement with results of a computer simulation. However, the total amount of atoms determined in the surface layer analysis is nearly independent of the analysis angles.

2.3.4 *Transmutations in plasma-facing materials due to the neutron flux in a burning D,T fusion reactor*

For the calculated neutron flux at the first wall of a burning D,T fusion reactor the transmutations, gas production and activation of low-Z elements were calculated with the FISPACT computer transport code. For the low-Z elements the hydrogen and He production dominate, being of the order of 10^{-3} per atom and operating year with a neutron wall load corresponding to 1 MW/m^2. The induced radioactivity for the low-Z elements is in the range of 10^{-11} Bq/atom, being governed by the tritium produced.

2.4 Plasma Edge Studies in Fusion Experiments

The investigations of the plasma-wall interaction group in direct collaboration with the ASDEX Upgrade, W 7-AS, JET and NET/ITER plasma experiments are treated in the respective sections.

3. SURFACE SCIENCE

The cooperation of the surface science group within the Sonderforschungsbereich (SFB 338: Adsorption on Solid Surfaces) is continuing. Recent contributions include the structural and concomitant electronic changes induced by adsorbates on metal surfaces, the role of oxygen as a surfactant influencing thin-film growth and the investigation of model catalysts. Additionally, the magnetic properties of thin-film systems are being studied.

3.1 SFB 338

The self-organized formation of quasi-one-dimensional (1-D) surface oxide domains on Cu(110) was used to achieve 1-D confinement of Shockley surface states. High-resolution photoemission spectra show the appearance of singularities in the density of states expected for 1-D electron bands. Due to phase space restrictions for scattering in one dimension the lifetime broadening of the corresponding photoemission peaks is extremely small. The observed features are the sharpest found hitherto in photoemission from solid surfaces.

The etching of a Pt(110) surface by bromine was investigated by atomically resolved scanning tunnelling microscopy. At room temperature Br atoms form an ordinary adlayer. At 450 K the Br atoms attack the surface by replacing Pt atoms in the topmost layers. The expelled Pt atoms in turn react with Br atoms in the adlayer, forming mixed Pt-Br islands. This leads to a highly corrugated, disordered surface. However, if the bromine dose amounts to precisely half a monolayer and the surface is annealed to 800 K, a very stable, well-ordered c(2x2) adlayer is formed which passivates the surface against etching attacks by bromine at all temperatures below 800 K.

Growth of Pd on clean and oxygen-covered Pd(111) was studied for deposition temperatures between 210 K and 420 K by scanning tunnelling microscopy (STM). It was previously shown that energy barriers for step down diffusion depend on step edge orientation and that step edges evolving at a deposition temperature of 400 K have exceptionally high barriers. Now it was found that preadsorption of oxygen enhances interlayer mass transport, thus flattening the film morphology. By evaluating Pd-island densities as a function of deposition temperature it was also found that oxygen increases the diffusion barrier on flat surfaces from 0.34 eV for the clean

surface to 0.49 eV for the oxygen-covered surface, leading to higher island densities. The increase in island density is also partially responsible for a change in island shape (see FIG. 3). The emerging step edges no longer have the exceptionally high energy barriers of the clean film, thus enhancing interlayer mass transport.

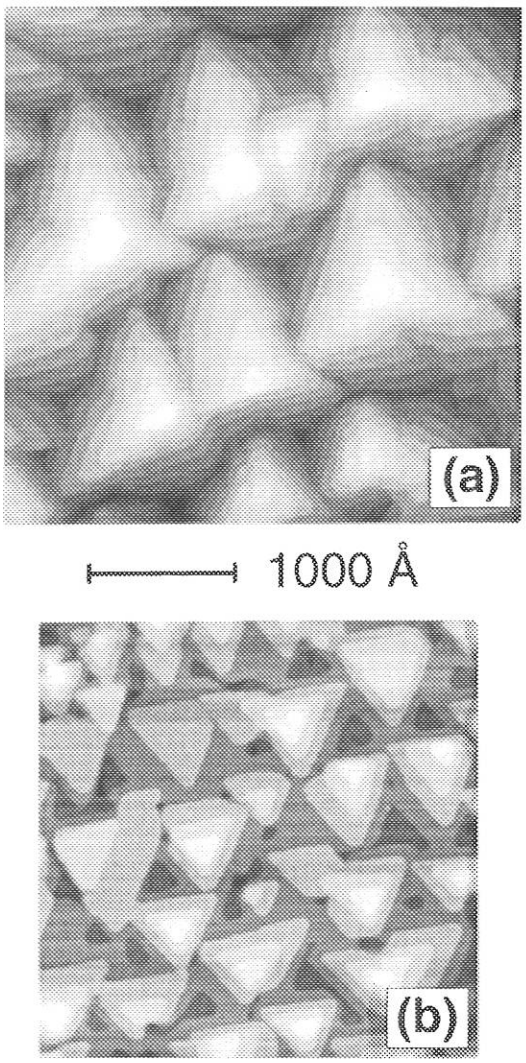

FIG. 3: STM pictures of approximately 5 ML Pd deposited at 400 K on (a) clean and (b) oxygen-precovered Pd(111)

The vicinal Cu(115) surface was investigated by scanning tunnelling microscopy (STM) at 300 K. Regular monoatomic steps are apparently stabilized by their strong repulsive interaction, which leads to a very low kink activity. In addition to the regular steps, the formation of double steps was observed as a particular phenomenon on this surface. These double steps determine the dynamic behaviour at room temperature. By applying known models for the fluctuations of the step positions in space and time, the formation energy for kinks at these double steps was determined to be 0.16 eV. According to this evaluation, diffusion along step edges is the dominating mass transport mechanism. A model for the structure of the double steps and for the atomic displacement processes necessary for kink migration at these steps was developed.

In continuing investigations of metal-support interactions on a microscopic scale appropriate model systems for rhodium catalysts were developed. They were prepared by evaporation of pure titanium or silicon onto a molybdenum foil in oxygen atmosphere and subsequent vapour deposition of about one monolayer of Rh in ultra-high vacuum (UHV). The oxide films had a thickness of 8 - 20 nm. To reach the state of metal-support interaction, the samples were heated stepwise up to 873 K in UHV.

ISS measurements and depth profiling of the system $Rh/TiO_2/Mo$ showed an increasing agglomeration of Rh into clusters after heating to 673 K. This process was finished at 723 K. Above that temperature the Rh particles were encapsulated by about one monolayer of TiO_x. Parallel measurements with thermal desorption spectroscopy corroborated these results. Reoxidation and a subsequent low temperature reduction restore the original state of the model catalyst. X-ray photoelectron spectroscopy (XPS) indicated a small amount of reduced titania above 673 K. A reaction mechanism for these observations was proposed.

On the system $Rh/SiO_2/Mo$ agglomeration already starts at 623 K. Oxidation at 573 K resulted in a redispersion of the Rh clusters. No encapsulation was found in the parameter range tested. XPS measurements gave evidence of a Rh silicide phase Rh_3Si above 850 K. The selectivity of Rh catalysts can be controlled by adding promotor substances such as vanadium oxide. Therefore $Rh/V_2O_5/SiO_2/Mo$ model systems were prepared and analyzed. It was shown that Rh acts as an efficient reduction catalyst for the oxides in these systems. These reactions have important consequences for the surface morphology.

3.2 Surface Magnetism

One focus of interest was the thickness-dependent electronic structure of the thin-film system Gd/W(110). Spin-resolved inverse photoemission was used to monitor the development of surface and bulk electronic states and their spin dependence as a function of film thickness. The results suggest that the exchange interaction at the surface increases with increasing film thickness.

The second major topic was exchange coupling phenomena in layered structures consisting of different magnetic and nonmagnetic materials. The potential of spin-resolved appearance potential spectroscopy as an element-specific technique was demonstrated for a number of systems: Fe/W(110), Fe/Cr/Fe/W(110), Tb/W(110), Tb/Fe/W(110). The following phenomena were detected and investigated: interface effects influencing the magnetic anisotropy, magnetic reorientation transitions as a function of the film thickness and temperature, magnetic order in paramagnetic materials induced by exchange fields from ferromagnets, and interlayer coupling between ferromagnetic layers separated by nonmagnetic spacer layers.

TECHNOLOGY DIVISION

(Prof. Dr. Rolf Wilhelm)

The main task of the Technology Division is the technical development and operation of the various plasma heating systems on the ASDEX Upgrade tokamak (neutral beam injection (NBI), ion cyclotron heating (ICRH), and electron cyclotron heating (ECRH)) and the W7-AS stellarator (NBI and ICRH). Further work includes planning and preparation of heating systems for the W7-X stellarator (NBI, ICRH), and research and development on heating and - specifically - current drive systems for the future tokamak programme at IPP (NBI - including high-energy injection based on negative-ion technology - ICRH/fast wave current drive, and ECRH/ECCD).

For details the reader is referred to the respective sections of this report. The following section gives some additional information on specific technical developments and theoretical work.

1. NEUTRAL INJECTION HEATING

NI Group

1.1 Development of a RF Negative-Ion Source

The collaboration between CEA and IPP is being continued. The aim of this collaboration is to investigate the ability of RF sources to produce negative-ion current densities compatible with ITER NBI requirements. The incentive is the anticipated superiority of RF sources - compared with arc discharge sources - with respect to cost and maintenance.

Work in 1997 concentrated, on the one hand, on upgrading some of the hardware on the small teststand: the separate extraction power supply, which had to be operated at high potential and gave rise to many problems, was replaced by a voltage divider. With the addition of a small snubber, HV operation is now completely satisfactory. The operation and control of the RF generator was also considerably improved by adding a thyrister control for the RF power. 120 kW is now routinely available, the power being limited by the available primary power. It is now being upgraded.

To the source itself a change was made: because it was feared that Cs might destroy the Viton seals of the compact (type III) source, the standard design type II source with internal quartz vessel, Faraday shield and stainless-steel vacuum vessel was re-installed. Furthermore, an optimized set of grids was delivered by CEA; an improved calorimeter was also installed by CEA together with the corresponding data acquisition system. Consequently, a reliable data base for operation of the source in pure volume mode without Cs has now been generated.

The results show negative-ion yields comparable to those of other sources. After a linear rise with RF power the H-current density saturates, the level depending on the gas pressure. Values close to 10 mA/cm^2 have been reached without Cs at 100 kW and 2.4 Pa. A big improvement was achieved by adding small amounts (5%) of argon. This could be interpreted as the effect of a lower electron temperature caused by (among other things) enhanced radiation cooling. Further work is aimed at optimizing this by testing different wall materials and improving magnetic confinement in order to achieve operation at low gas pressures (< 0.5 Pa). Further medium to long-term goals are steady-state operation and demonstration of large-area uniformity.

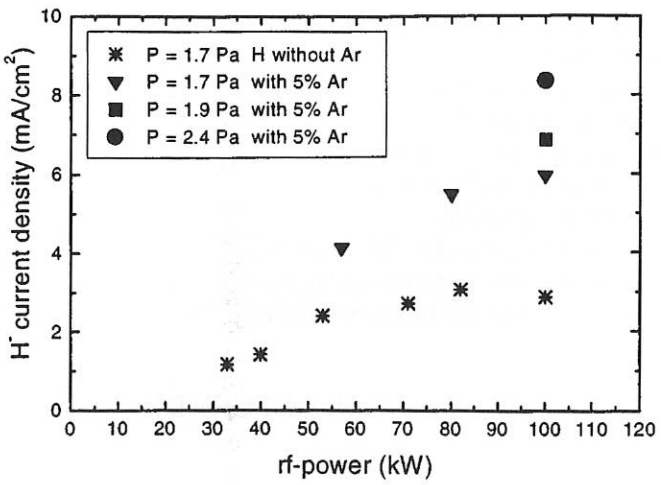

FIG. 1: H-current density versus RF power for different pressures.

1.2 Concept Studies for JENIPHER

Apart from cost and maintenance, further critical areas have been identified by the ITER home/joint central teams in the design and development of ITER NBI: e.g. reliable long-pulse operation of large-area beam sources at low pressure and control of electrons in the source and accelerator at the required negative-ion current density. These requirements have led to a proposal for extended collaboration between CEA and IPP: the development of a large-area source and accelerator unit implementing novel concepts such as the RF source and the SINGAP accelerator. This proposal has been dubbed "JENIPHER" (Joint European Negative-Ion Project for High Energies).

The size of the source and the beam energy have been chosen such as to make maximum use of it for its potential application on medium-size European experiments such as ASDEX Upgrade, Tore Supra, W7-X: 20 A D^-, 350 keV, yielding approximately 3 MW of neutrals. As derived from the physics and technology requirements of these experiments, it is found that injectors with the same specifications can provide central NBCD in T.S., off-axis NBCD in AUG (for $T_e \geq 5$ keV) and central heating at high densities in W7-X.

This "multiple use" aspect would provide "testbed experience" for ITER NBI and simultaneously make negative-ion technology available in Europe. Ideas exist of how to split the development tasks and the effort between CEA and IPP. The final aim would be a full-power demonstration on the neutron-shielded deuterium testbed at Cadarache in the year 2004.

It has not yet been decided whether or not these beams will be applied on the various machines. The funding arrangements and the manpower involved therefore require final decisions by both partners.

2. ION CYCLOTRON RESONANCE HEATING

ICRH Group

After 3-dB couplers were successfully tested on 2 AUG ICRF systems in 1996 and 1997 to reduce the effect of plasma variations (in particular ELMs) on the generators, all systems were equipped with them. The expected increase in availability and reliability was confirmed. Different types of connnections and compensations are now being compared to implement current-drive phasing.

Preparations are under way to modify the antenna to make it compatible with more triangular plasma shapes. The changes will be implemented in the summer of 1998.

3. ECRH ON ASDEX UPGRADE

ECRH Group (AUG)

(in cooperation with IPF Stuttgart and IAP Nizhni Novgorod)

The ECRH system is still under construction and will finally use 4 gyrotrons with 0.5 MW, 2 s each. Two gyrotrons are now in operation, as described in the ASDEX Upgrade section of this report (Sec. 7.6).

The gyrotrons are installed in a rectangular arrangement with distances of 2.8 m and 4 m between the axes of the tubes. During adjustment of the cryomagnet for the second gyrotron with the help of a dummy tube we observed an intolerable distortion of the electron beam deposition in the collector while the magnet of the neighbouring gyrotron was switched on. This magnet is at a distance of 2.8 m. Its stray field at the position of the perturbed gyrotron is only about 3 Gauss (as compared with the 5.5 T in the cryomagnet centre). But its horizontal component, integrated along the beam trajectory, leads to a vertical displacement of the electron beam on the collector surface of ±8 cm, thus reaching uncooled areas. Single-turn coils connected in series to the neighbouring cryomagnets were designed to provide automatic compensation whenever the perturbing fields are present.

The long time intervals between ASDEX Upgrade pulses, and also occasional arcs in the gyrotrons, suggested the installation of switching mirrors and fixed high power loads close to each gyrotron so that they can be reconditioned between shots. Small volume loads, constructed of stone plates (Kalksandstein), with a low reflection coefficient were developed and successfully tested with 2 s pulses at full power.

The pulse shape of the gyrotron output is not constant during a 2 s pulse. The same pulse shape was shown by detector signals of the forward wave from directional couplers inserted in the second mirror of the matching optics unit at the gyrotron output and in the last mitre bend at the end of the transmission line. This shape was independent of the kind of termination (stone loads, calorimeter loads, plasma). Calorimetric measurements of pulses with different pulse lengths proved that the pulse shape indicated by the detector shows the proper power.

Detailed measurements were made to determine the setting of the left or right elliptic polarization of the microwave beam that is necessary to generate a proper O-mode or X-mode at oblique incidence to the plasma. The measurements revealed an unexpected asymmetry with respect to the corrugated mirror rotation which can be quantitatively explained by small deviations of the corrugation depth in the mirrors from their nominal values of $\lambda/8$ and $\lambda/4$.

4. THEORETICAL WORK

S. Puri

4.1 Radiative Transport using the Balescu-Lenard Equation

In the previous year it was shown that the momentum-transfer collisions via Kirchhoff radiation of electrostatic electron and ion-cyclotron-harmonic waves give rise to an enhanced energy and particle transport closely resembling the experimentally observed anomalous transport in toroidal plasmas. Effort is now under way to confirm the above findings using the Balescu-Lenard equation extended to include the static magnetic-field effects. Once again, the high-harmonic cyclotron radiation appears to play an important role in the transport process. An efficient computational scheme has been devised to handle the multi-dimensional integrations involved in the solution of the Balescu-Lenard equation.

PLASMA TECHNOLOGY

(Prof. Dr. Dr. h.c. Volker Dose

Prof. Dr. Rolf Wilhelm)

The Plasma Technology group is concerned with three tasks: Surface coatings are produced by means of plasma chemical vapour deposition (PCVD) for special applications, mainly in fusion plasma devices. New or improved PCVD procedures or devices are being developed for this purpose. As the scientific part of the activity, plasma, plasma edge, and thin-film diagnostics are employed in order to correlate the discharge parameters with the properties of the resulting coatings and improve understanding of the basic mechanisms of plasma deposition. The third goal is a modelling of the deposition process which allows the discharge conditions to be adjusted in a predictable way in order to optimize a desired property of the growing film.

In 1997, main activities were in-situ characterization of the growth and etching of hydrogenated carbon films, measurement of the particles fluxes onto the substrate from a methane ECR plasma, including modelling of the composition of the ion flux, and deposition and characterization of hydrogenated boron and boron-carbon thin films.

A. Annen[1] (until 30.04.97), V. Dose (Division Head)[1], F. Höhn[2] (until 28.02.97), W. Jacob[1], G. Kerkloh[3], A. von Keudell[1], B. Landkammer[1], P. Pecher[1], T. Schwarz-Selinger[1], R. Wilhelm (Division Head)[2].

1 Surface Physics Division
2 Technology Division
3 Technical Staff

1. IN-SITU PLASMA DIAGNOSTICS Charged and Neutral Particle Fluxes from a Methane ECR Plasma

A comprehensive, quantitative study of the particle fluxes impinging on the substrate in an ECR methane plasma has been conducted for the past few years. We quantitatively measured the mass and energy distributions of the ion flux as well as the neutral particle and CH_3 radical fluxes. FIG. 1 shows as an exemplary result the composition of the ion flux as a function of the methane gas flow. With decreasing gas flow, significant consumption of the feed gas methane occurs and the neutral gas in the plasma chamber consists mainly of hydrogen. This was found in neutral gas analyses under equivalent conditions. As a result of the composition of the neutral gas, the ion flux at the lowest methane feed gas flow comprises mainly hydrogen-carrying ions, namely H_2^+ , and at this relatively high total pressure of 1.0 Pa, predominantly H_3^+. Increasing the methane gas flow causes an increase of the methane partial pressure in the neutral gas and, consequently, an increase of the flux of carbon-carrying ions and a sharp decrease of hydrogen ions. At intermediate gas flows, $C_2H_x^+$ ions dominate, while at even higher gas flows $C_3H_x^+$ ions are the most abundant impinging species. At the highest gas flows investigated even $C_4H_x^+$ ions are more frequent than $C_1H_x^+$ ions. Noteworthy is the relative abundance of molecular ions which have no stable neutral counterpart such as H_3^+ and CH_5^+. These results clearly show the importance of ion-molecule reactions for the composition of the bulk plasma and the ion flux to the substrate surface. In methane discharges the ion flux above pressures of about 0.5 Pa is dominated by molecular ions formed by ion-molecule reactions in the bulk plasma.

The measurements made are, on the one hand, important for checking existing plasma models and, on the other, a prerequisite for improving understanding of the interactions of plasmas with surfaces because the interaction of molecular ions with the surface depends not only on the ion energy, but also on the mass and composition of the ion. For example, an H^+ and an H_3^+ ion with the same total energy interact very differently with a surface. The interaction of one H_3^+ ion is comparable to that of three hydrogen ions with one-third of the total energy each. Thus, at the same total energy the H^+ ion has much deeper penetration into the solid.

A critical comparison of the measured ion flux with the predictions of existing plasma models revealed that these models can by no means, not even qualitatively, predict the composition of the ion flux, although neutral gas densities are

simulated satisfactorily. The obvious reason is the neglect of ion-molecule reactions in the bulk plasma and the plasma sheath. To overcome these difficulties, a simple rate-equation model was developed which is capable of modelling the composition of the ion flux as a function of various experimental parameters.

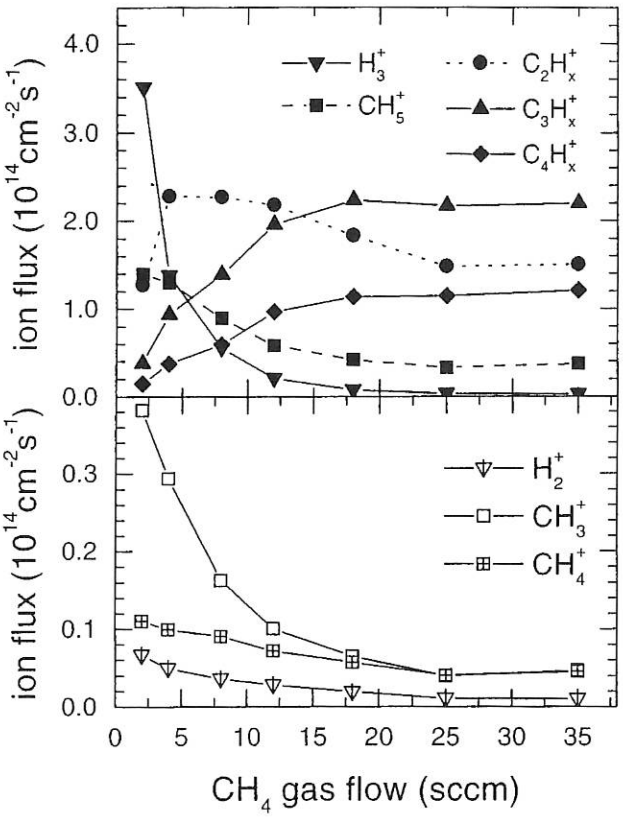

FIG. 1: Composition of the ion flux to the substrate as a function of the methane feed gas flow at a pressure of 1.0 Pa. The lower part of the figure shows minor contributions on an enlarged scale. The $C_xH_y^+$ fluxes shown for x=2,3,4 each represent the sum over all y of each respective molecular ion.

2. THIN FILM DEPOSITION AND EROSION
Glow Discharge removal of C:H Films using different feed gases

The erosion of plasma-deposited hydrogenated carbon (H:C) films by oxygen, hydrogen, and mixed oxygen/hydrogen ECR plasmas was investigated in situ by spectroscopic ellipsometry. Under all plasma conditions applied, oxygen plasmas showed the highest erosion rates. In general, oxygen/hydrogen (1:2) mixtures also show higher erosion rates than water plasmas. The relative rates behave as $O_2 : D_2 : H_2 \approx 10 : 2 : 1$. The erosion rates increase with substrate temperature (for an ion energy of about 10 - 20 eV), ion energy (T = 300 K), and ion flux. However, at an increased ion energy of 100 eV the erosion rate does not increase with temperature as found at 300 K. Energetic ions play an important role in the erosion process. The dominant erosion products are H_2, CO, CO_2, and H_2O.

3. THIN FILM CHARACTERIZATION
Amorphous, Hydrogenated Boron-Carbon Thin Films (a-B:C:H)

Amorphous hydrogenated boron-carbon (a-$B_{1-x}C_x$:H) thin films were prepared by RF plasma deposition using CH_4 and B_2H_6 diluted in H_2 as precursor gases. The composition and density were determined by ion-beam analysis. The results are shown in FIG. 2. The densities of the a-B:H and a-C:H films are similar with $\rho \cong 1.72$ g/cm^3, a value typical of hard and dense a-B:H and a-C:H films. Ternary a-$B_{1-x}C_x$:H films are less dense, having a minimum density of $\rho \cong 1.48$ g/cm^3 at $x = 0.71$. Infrared spectroscopy was used for qualitative and quantitative analysis of the bonding structures. The properties of films up to $x \approx 0.2$ are comparable to those of pure a-B:H films. However, a small carbon content influences the film structure, mainly reducing the number of B-H-B bridge bonds, which are abundant in pure a-B:H films. Modifications of the network are indicated for $x > 0.7$. Below, carbon is predominantly sp^3-hybridized and bonded between boron neighbours. Above $x = 0.7$ the network becomes carbon-dominated with an increasing number of carbon-carbon bonds, and an increasing fraction of sp^2-hybridized carbon was observed.

For pure a-B:H films we found that the hydrogen content and the refractive index are highly correlated to the boron density (correlation coefficient -0.96 and 0.89, respectively) and a-$B_{1-x}C_x$:H films follow a similar trend (although with lower correlation coefficients). This indicates that the determination of the refractive index allows a first estimate of the general properties of these films.

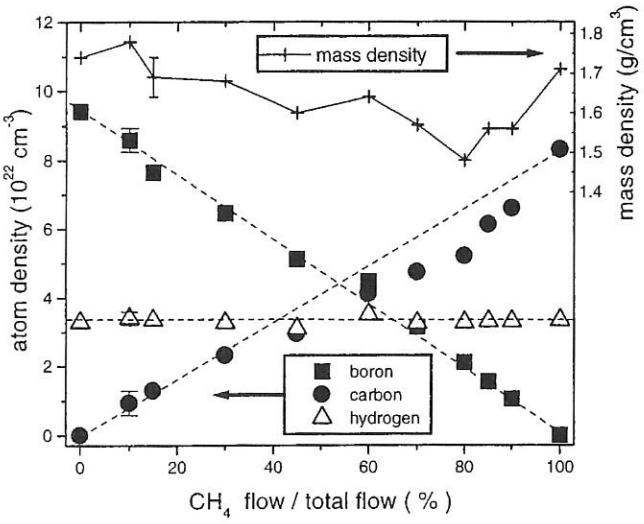

FIG. 2: Dependence of boron, carbon, and hydrogen atom densities (left-hand side) on the relative CH_4 flow (CH_4 flow / total flow). The total gas flow and pressure are kept constant at 10 sccm and 2 Pa, respectively. The mass density ρ is shown on the right-hand scale. A typical error bar is shown for one data point of each curve. Lines are only a guide to the eye.

PLASMA DIAGNOSTICS DIVISION

(Head of Division: Prof. Dr. G. Fussmann)

At the beginning of 1997, the former Berlin Division was integrated in the scientific programme of the Greifswald Branch of IPP and renamed Plasma Diagnostics Division. As a consequence, the activities in Berlin are increasingly devoted to development of the WENDELSTEIN 7-X stellarator project. At present, the Plasma Diagnostics Division is engaged in theoretical investigations of magnetic islands and in the design and development of diagnostics (e.g. IR thermography, spectroscopy, monitoring of target properties). The remaining activities comprise experimental and theoretical investigations in Berlin (PSI plasma generator, UHV laboratory, electron beam ion trap (EBIT) experiment, analytical and computational studies of edge physics problems) and the ASDEX Upgrade and WENDELSTEIN 7-AS fusion experiments at Garching.

For the work on the fusion projects at Garching, the reader is referred to the respective sections of this report. After completing development of the two-photon-induced L_α fluorescence diagnostic, the major area of investigation at the PSI plasma generator concentrated on chemical erosion of graphite in contact with hydrogen plasmas. The EBIT activities are concerned with both improvement of the diagnostic capabilities and spectroscopic measurements of the radiation and recombination properties of highly charged ions.

M. Akbi[1], P. Bachmann, C. Biedermann, W. Bohmeyer, H. Grote, Grützmacher[2], A. Herrmann, D. Hildebrandt, B. Jüttner[3], H. Kastelewicz[3], S. Klose, P. Kornejew, M. Laux, H. Meyer, D. Naujoks, E. Pasch, H. Pursch[3], R. Radtke, H.D. Reiner, V. Rohde, M.I. de la Rosa[2], J. Sachtleben, C. Seiser[2], J. Seidel[2], A. Stareprawo, A. Steiger[2], D. Sünder, U. Wenzel,

1 Guest, University Algier, Algeria

2 Physikalisch-Technische Bundesanstalt, Berlin (PTB)

3 Humboldt-University, Berlin

1. PSI PLASMA GENERATOR

In 1997, chemical erosion measurements were made on carbon fibre composites as a function of the ion flux density. The samples (DUNLOP Concept II and Si-doped SEP NS 31) were heated to temperatures ranging up to 800 K and exposed to hydrogen and deuterium plasmas. The plasma conditions were selected so that physical sputtering and redeposition could be excluded. Optical methods as well as mass spectroscopy and weight loss measurements were employed to obtain chemical erosion yields. These yields were found to be largely independent of the working gas (H_2, D_2). Figure 1 shows a plot of the erosion yield versus flux density. Obviously, there is a drastic decrease of the yield with increasing ion flux, which is of course a highly appreciated property in view of the large fluxes in ITER or in a fusion reactor. Compared with DUNLOP Concept II, the NS 31-samples were found to have slightly smaller erosion yields.

Development of the two-photon-induced L_α fluorescence diagnostic (in cooperation with PTB, Berlin) is now terminated. Conclusive measurements were performed in hydrogen-deuterium plasmas; good signal-to-noise ratios could be obtained for the fluorescence signal. The experience gained in these studies allows the design parameters to be fixed for a first demonstration of this diagnostic at a tokamak aiming for isotope-selective detection sensitivities at densities down to 10^8 cm^{-3}.

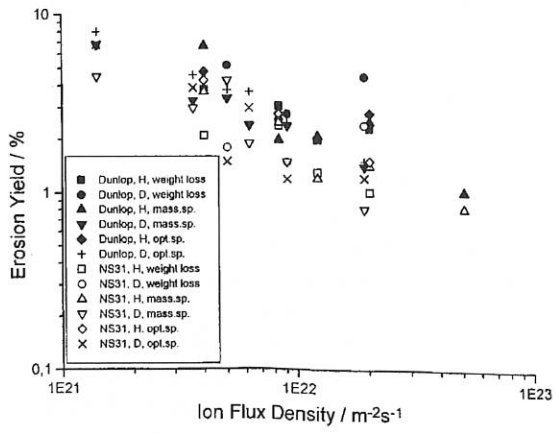

FIG. 1: Chemical erosion yields for carbon fibre composites as a function of the particle flux density (all measurements at $T_{surface} \approx 800$ K).

To improve understanding of specific phenomena in the PSI plasma generator, the investigations of the periodic and turbulent plasma fluctuations were intensified. The fluctuations originate from plasma instabilities, which, in turn, are the result of steep temperature and density gradients. Evidence of the gradients was obtained from measurements of the radial profiles of the electron temperature, electron density, and plasma potential using single and double probes. In addition, the results from the probe measurements were used to deduce the radial electric field. The radial field gives rise to rotation of the plasma column and can be an additional driving force for plasma instabilities. Fourier analysis of the probe signals revealed an extensive spectrum of rotating modes at radial positions where the gradient of the electron pressure is at maximum. This result is in agreement with optical observations where the radiation from the rotating ions was recorded with high temporal and spatial resolution (Fig. 2).

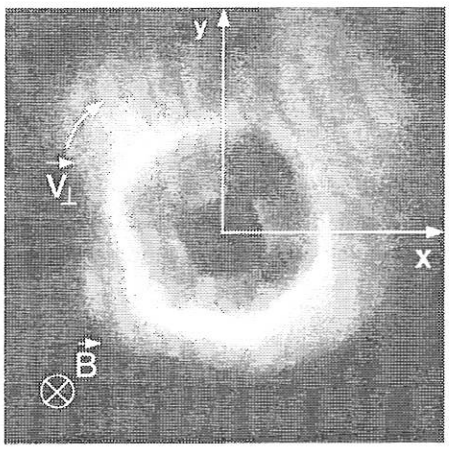

FIG. 2: CCD picture showing the shining plasma cross-section for a discharge in krypton. The plasma is actually a hollow cylinder of pentagonal shape (strong m = 5-mode) rotating with a frequency of 12 kHz.

2. ELECTRON BEAM ION TRAP (EBIT)

The electron beam ion trap (EBIT) has been in operation since 1996. The EBIT technique employs a monoenergetic, magnetically compressed electron beam to produce, confine, and excite highly charged ions. EBIT is intended for general atomic physics measurements and especially for applications to fusion-relevant hot plasmas. The primary goal in 1997 was to check the performance of EBIT and make spectroscopic measurements in the X-ray range. The highest charge state achieved so far is beryllium-like tungsten W^{70+}. A new flexible flat-crystal spectrometer was successfully tested and used to obtain high-resolution X-ray spectra. Linear sweeps of the electron beam energy could be performed over an interval of up to 22 keV, at a rate of 1 keV/ms. This technique was used to make first measurements of excitation functions and dielectronic recombination cross-sections for highly charged krypton. Krypton was chosen since it will probably become important as a coolant for the plasma edge of ITER. In this context, it is highly desirable to have accurate atomic physics data to predict theoretically the effects of the krypton injection on the plasma performance.

In Fig. 3, typical raw data are shown as a scatter plot of X-ray energy versus electron beam energy. The plot was generated by first producing ions at a beam energy of 12 keV and then probing the ions repeatedly by fast scans of the beam energy (here, 8-15 keV scan interval). During the scans, the beam energy and the X-ray energy for each X-ray detected were recorded. Events from bound-state X-ray transitions excited by electron impact are manifested in the form of horizontal lines, while X-rays from radiative recombination (RR) appear as slanted lines. The intense spots in the upper part of the plot are the result of dielectronic recombination (DR) processes. From measurements similar to those illustrated in Fig. 3, channel-specific DR cross-sections were obtained for the KLL, KLM, KLN, and KLO resonances of highly charged krypton. In addition, the ion relaxation process subsequent to dielectronic recombination was analyzed for these resonances (see Annual Report 1996). A new topic is experimental investigation of the radiation and steady-state cooling rates for krypton in helium-, lithium- and beryllium-like charge states. First preliminary results were obtained.

A collaborative research effort between Lawrence Livermore National Laboratory, Racah Institute of Physics (Jerusalem), and the EBIT group was started in 1997.

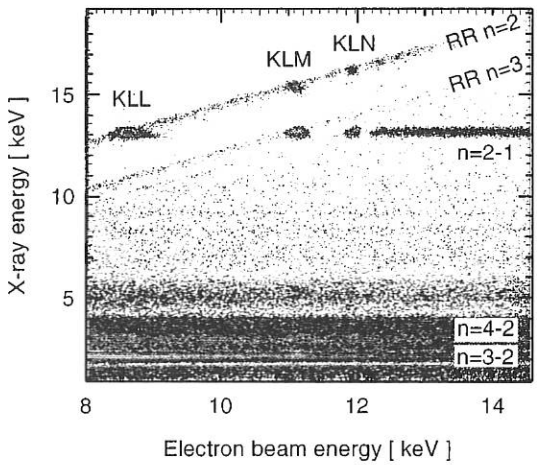

FIG. 3: Scatter plot of X-rays from Kr^{q+} ions (q = 32 - 34) as a function of the electron beam energy.

3. DEUTERIUM TRAPPING IN DIVERTOR TILES OF ASDEX UPGRADE

The gas inventory of divertor target tiles installed at ASDEX Upgrade was analyzed in the UHV laboratory by thermodesorption spectrometry (TDS); in addition, several other surface analysis techniques were used to investigate erosion and deposition phenomena. TDS measurements were made of complete and partial divertor tiles while the samples were heated to temperatures of up to 1500 K. The target tiles consisted of graphite (EK 98) with and without tungsten coatings. The measurements show that the deuterium was largely released as D_2 and HD molecules, with desorption rates peaking at 750 and 1000 K for tungsten-coated and pure graphite tiles, respectively. The samples exhibit significant

differences in the deuterium inventory as well as in the impurity deposition and surface morphology, depending on the location of the tiles in the divertor. For example, the deuterium content in the area of contact with the separatrix is much larger for the inner divertor tiles than for the outer ones (a factor of about 10 and 5 for tiles with and without tungsten coatings, respectively). Depth profiles for carbon, boron, hydrogen, and deuterium revealed several μm thick deposition layers on the inner divertor tiles. More than 10^{24} C atoms/m^2 and $3 \cdot 10^{23}$ B atoms/m^2 were estimated to be deposited on the tiles with tungsten coatings. For the (inner divertor) graphite tiles the findings were quite similar.

In order to have better spatial resolution, TDS measurements were made on pieces of graphite tiles. These showed a strong correlation between the gas inventory and the deposited boron impurities. Both the deuterium inventory and the boron deposition layer minimize in the region of contact with the separatrix. From depth profiles, it was found that deuterium and boron had similar spatial distributions for depths of the order of 10 μm. This is an indication of the high surface roughness of the tiles after plasma exposure, allowing impurities to penetrate into the material. To confirm the findings, similar TDS measurements were made of samples where layers 10, 20, and 30 μm thick were milled off. The results show that most of the deuterium is trapped in the first ten micrometres; the amount of deuterium released from the 30-μm region is less than 7%. Figure 4 is a 2D picture showing the distribution of deuterium and boron at a depth of about 12 μm. One can infer from the almost identical distributions that co-deposition of deuterium and boron during boronization and plasma exposure is the dominant trapping mechanism. Impurity deposits at depths of the order of 10 μm are protected from being eroded by sputtering.

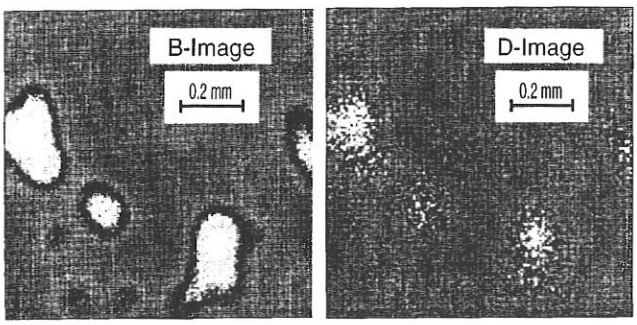

FIG. 4: $^{11}B^+$ and $^2D^+$ distributions obtained from secondary-ion mass spectrometry of an ASDEX Upgrade graphite tile.

4. THEORY AND MODELLING

4.1. Bifurcations of Temperature Profiles

The bifurcation and time evolution of temperature profiles along the magnetic field lines between two target plates were studied. The heat sources were assumed to be localized and the energy to be dissipated by the radiation of sputtered impurities. A major result is that multiple solutions exist for the stationary temperature profiles. If two different impurities species are present, for example, up to seven steady-state solutions exist; however, only four of them are stable. Solutions of the fully time-dependent equations show that the profiles approach their stationary values.

4.2. Multi-fluid Description of Reaction-Diffusion Processes

A system of one-dimensional, time-dependent hydrodynamic equations developed to model the behaviour of impurities in magnetized hydrogen plasmas is being analyzed. The impurity densities are not restricted to being small in relation to the density of the background plasma. Within the framework of the average ion model and in the limit of complete ionization and uniform temperature for all plasma particles, a three-fluid description can be formulated. This was the starting-point to derive a reaction-diffusion equation for the plasma temperature, with different model functions for the impurity densities being taken into consideration.

4.3. Criterion for Zero Net Erosion at Divertor Plates in Fusion Experiments

The erosion of the divertor plates in future fusion experiments such as ITER has to be reduced by redeposition in order to achieve an acceptable lifetime of the plates. The favourable effect of redeposition can be enhanced by exploiting the **ExB** drift motion of the impurity ions in the electric sheath. A suitable choice of the magnetic field direction and geometry can minimize the peak net erosion at the divertor plates. A simple relation was obtained that allowed estimation of the peak net erosion with respect to the following effects: erosion by the plasma ions, selfsputtering, prompt redeposition, and redeposition due to the incident plasma flow.

4.4. Plasma Modelling for the PSI Plasma Generator

B2-EIRENE modelling calculations were performed for the PSI plasma generator, with the cathode-anode region being taken into account. The energy source for the heating of electrons was assumed to be localized to a small concentric layer in the vicinity of the anode surface. Calculated radial distributions for the temperature and density in deuterium discharges show pronounced hollow profiles. In addition, the calculations demonstrate that flow reversal of the plasma back to the anode is possible. Basically, this flow reversal is due to the ionization processes outside the cathode-anode region.

4.5. Collisional Radiative Model for Carbon-Hydrogen Plasmas

A set of rate coefficients is provided to determine the population of ground and metastable states of carbon embedded in a hydrogen plasma. Also included in this data compilation are radiative and electron cooling rates. In addition, appropriate fit formulas derived from a least-squares fit of individual data points are given. The rates are required for the development of realistic models for high-temperature plasmas and for the interpretation of diagnostic observations in such plasmas.

COMPUTER SCIENCE DIVISION

(Prof. Dr. Friedrich Hertweck)

F. Hertweck, G. Czapski, H. Friedrich, K. Hallatschek, P. Heimann, J. Maier, M.-G. Pacco-Düchs, I. Precht, K. Reinmüller, H. Richter, U. Schneider-Maxon, D. Stolz, Ch. Tichmann, R. Tisma, M. Zilker

Part of the activities of the division closely relate to ASDEX Upgrade: the further development and enhancement of hardware and system software for SoftXray, Mirnov and other diagnostics and maintenance of the AMOS/D data acquisition system. Another important area is parallel processing. It is being pursued along several lines: design of a new generation of parallel computers for data acquisition, development of new and porting of existing algorithms to the Cray T3E, and study of neural algorithms.

1. AMOS/D

Part of the work on AMOS/D is described in the section on ASDEX Upgrade data processing. In particular, a new fast PCI bus interface for data acquisition is described there.

1.1 Dependence Data Base

The Dependence Data Base DDB is being regularly used and the number of entries is continually growing. A new version with some extensions was implemented. In particular, the management of the validation indicator was refined.

1.2 Design of a new generation of high-speed/ high-volume data acquisition systems

The very long plasma discharges expected in W7-X and also the growing needs of ASDEX Upgrade call for a new generation of data acquisition systems capable of handling high-volume data streams in real-time (typically a few hundred signals in diagnostics like Mirnov or SoftXray, sampled at rates of a few MHz). This also requires high CPU power to do the analysis. Normally, the I/O bandwidth of a processor is limited and it will therefore be necessary to develop parallel systems that are able to cope with the high influx of data. A fast interconnection network is also required because the state of the plasma at any time as reflected by the diagnostic is spread over the parallel processors of the system.

The hardware will be built from available components, such as CPUs (DEC, IBM powerPC, ultraSPARC, etc.) and interconnection components, such as the SCI (Scalable Coherent Interface). Still, substantial software development in the areas of device drivers, data analysis algorithms, and user interfaces is envisaged.

An experimental system is being built with two Motorola powerPC boards.

1.3 CD ROM archive for ASDEX Upgrade shot files

The archive for storing ASDEX Upgrade raw data on CD ROMs was extended. At present there are about 600 CDs with data; they are stored outside the Computing Center in a fire-proof location. The popular facility is also available for users for keeping their own data safeguarded.

2. PARALLEL COMPUTING ON THE T3E

All the work on parallel programs was done in close cooperation with the owners/users of the programs. Some time was spent on comparing communication performance of the T3E with other parallel systems. Two very successful workshops were organized to exchange experience between the users of the T3E.

2.1 Parallelization of turbulence codes

Two codes for 3D drift resistive ballooning turbulence were parallelized for the T3E: DRB5 and EMHD. They are solvers for partial differential equations, and both good performance and scalability were obtained. One of the programs relies heavily on a 3D FFT (Fast Fourier Transform).

2.2 Parallelization of a Monte Carlo code

A new version of the TRIDYN code (W. Eckstein) was successfully parallelized. The performance problems were solved by introduction of a "dynamic load balancer", which stores the generated secondary particles in a centrally managed but distributed queue. In addition, the former vector techniques of the Cray version were replaced by data structures for the particles and each particle was described by a task descriptor. The program can be interrupted *ad libitum*, to be restarted later.

2.3 Parallelizing the B2 code

This work was done in collaboration with the Tokamak Physics Division and the Computing Center RZG. The B2 code (by S. Braams) is a solver for the time-dependent MHD equations for many-fluid components (typically about 20). Two parallel program libraries were examined: PIM (Parallel Iterative Methods for Systems of Linear Equations) and PETSC (Portable Extensible Toolkit for Scientific Computation). It turned out that only the latter library was suitable. The work is still in progress.

3. NEURAL NETWORK COMPUTING

3.1 Image processing

In ASDEX Upgrade, several video cameras are being used to take pictures of the interior of the vacuum vessel during a discharge in order to register events such as the sputtering of graphite tiles, etc. The system under construction is PC-based, with a CNAPS neuro-computer board and an ELTEC frame grabber for picture input. In a first version, the system will process videos offline. Image processing and neuro-algorithms will be used to detect the events of interest. An online application of the system is planned for the future.

3.2 Development of neural algorithms

After installation of the T3E, this machine became our preferred platform for the development of neural algorithms. A parallel program for Kohonen networks was implemented in Fortran 90 on the T3E. Also, a standard backpropagation code (the version of K. Kutzka) was translated into Fortran 90 and parallelized: both training data and neurons can be treated in parallel. The work is a preliminary study with the goal of detecting oncoming disruptions in ASDEX Upgrade.

4. DATA PROCESSING INFRASTRUCTURE

4.1 Internet

The use of the WWW function of the Internet has been expanded. Announcements and results of workshops and conferences are regularly presented via the WWW.

4.2 Conceptual design for an IPP Workstation Environment

In the past few years, a transition from mainframe computing towards centralized powerful UNIX workstations has taken place at IPP. At the same time, more and more personal computers (IBM compatibles and Apple Macintosh) were introduced. Originally intended for word processing and spreadsheet applications, they can be used today for a wide range of applications, usually run on workstations. At the moment there are about equal numbers of workstations and PCs, with the number of PCs growing faster.

In collaboration with the Computing Center RZG, a survey of existing hardware and applications was conducted with the intention of defining standards for the workstations/PCs to permit centralized management of both hardware and software.

In this framework, a Windows NT network was implemented with several NT 4.0 servers. The System Management Server of Microsoft was evaluated and then installed on the central NT server. The NT servers are the repository for the standard software to be used.

4.3 SAMBA

SAMBA is an SMB server for UNIX and is used to establish the connectivity between central directories (and printers) and PC operating systems. This permits access to the AFS file system and the CD ROMs of the ASDEX Upgrade archive from any Windows 95 or Windows NT client.

CENTRAL TECHNICAL SERVICES

(Dr.-Ing. Harald Rapp)

The Central Technical Services (ZTE) of Max-Planck-Institut für Plasmaphysik support the experimental divisions with the design, construction and operation of experiments and diagnostics. They also provide and run all kinds of utilities for facility operation and employ approximately 160 workers, technicians and engineers. In the course of establishing the new site in Greifswald additional tasks became part of the ZTE charge. Its personnal staff in Garching is going to be decreased continuously. The total costs were 24 mill. DM including facility operation. Creation of value in the workshops added to more than 8 mill. DM.

1. MECHANICAL DESIGN AND CALCULATION (J. Simon-Weidner)

24 technicians and engineers work in the fields of CAD design and FE calculations for all kind of experimental equipment and diagnostics. The department runs the CAD computer network at IPP which now consists of 56 workstations and 4 servers. In the course of the W7-X design the coil support was optimized and the thermodynamics of the cryostat and the divertor target plates was investigated. Call for tender of the magnet coil system was supported and the design of plasma vessel components was continued. An Electronic Product Definition (EPD) system for managing drawings and all kind of project documents has been introduced.

2. ELECTRONICS DEVELOPMENT (D. Arz)

The department consists of 3 groups for developing measurement and control equipment, for high-voltage switching and control and for electronic device maintenance. A wide variety of devices have been developed and delivered to both experiments. Design of new techniques for measurement and control of long pulse plasmas is going on. Construction, commissioning and maintenance of high-voltage modulators were continued providing a high operational reliability of the NBI and ECRH systems.

3. MATERIALS TECHNOLOGY (S. Kötterl)

The department offers technical services for materials analysis and development, vacuum technique and surface processing. Development and tests of plasma facing components have become a major effort. Moreover heavy metal sputtering techniques and production of plastic pellets for plasma injection loaded with distinct materials of specified particle number have been performed. The new laboratory for materials analysis has prepared a lot of probes for plasma diagnostics. Boronization of plasma chambers was supported by toxological investigations. Quality assurance for experiment components is going to become an important task of the department.

4. ELECTRIC POWER SUPPLY (W.R. McGlaun)

The department is responsible for the electric power supply of IPP and the experiments. It operates 4 flywheel generators with a total power of 580 MVA, 20 controlled high current rectifiers (462 MVA in total) and 28 high voltage DC modules up to 140 kV. The renewal of a big flywheel generator has been finished after troublesome commissioning. A thyristor rectifier was blown due to a control fault. Power supply of IPP broke down when a cable failed. A call for tender of 2 additional HV modules for NBI was sent to industry.

5. FACILITY OPERATION (H. Rapp)

The department is charged with planning and supervising of all kind of facility installations like heating and cooling systems. Besides maintenance the commissioning of a new boiler in the heating power station was a main effort.

6. WORKSHOPS (M. Keiner)

About half of the ZTE personnel work in workshops providing the basic manufactoring capacity for experimental components and diagnostic devices. If necessary, additional capacity is purchased from industry. The department consists of mechanical, electrical and sanitary shops as well as joinery, apprentice training and materials stock. The effort is contineously shifted from production to assemblage, coordination and managing of specific technical tasks for the big experiments.

ADMINISTRATION

(Dr. Irmtraud Zilker-Kramer)

The administration and general services of Max-Planck-Institut für Plasmaphysik are organized in six departments:

PERSONNEL DEPARTMENT

The personnel department is responsible for administrative matters relating to personnel. The personnel figures of the institute for 1997 were as follows:

Total personnel (including Greifswald and Berlin)	1006
Scientists	308
Technicians	430
Directorate and Staff Representative Council	29
General Services	45
Administration	77
Other personnel	117
	09.01.98

CONTRACTS AND PURCHASING DEPARTMENT

The contracts and purchasing department is responsible for placing survey and follow-up of all contracts and orders placed by IPP. In 1997, approximately 9.800 orders were made. They include complex contracts, many of which were signed after European-wide calls for tender. Furthermore, all export and import formalities are handled within this department: about 180 international and European shipments were carried out in 1997.

REVISION AND LEGAL DEPARTMENT

In the frame of its internal revision work this department is responsible for the revision of work-flows and proceedings within the IPP.

Concerning patent matters it attends to patent applications and supervision and licensing of patents in cooperation with Garching Innovation GmbH, a subsidiary of the Max Planck Society. In 1997 the division supervised 104 patents and similar rights.

The revision and legal department is further responsible for looking after for committees. Also it works out and controls cooperation contracts with German and European Universities and research institutes.

FINANCE AND ACCOUNTING DEPARTMENT

The finance and accounting department is responsible for the financial planning and all financial transactions and fiscal matters of IPP.

Total expenses in 1997:	197,5 MDM
These expenses were financed as follows:	
Federal Republic of Germany through Federal Ministry of Education, Science, Research and Technology (BMBF)	111,5 MDM
Bavaria	9,3 MDM
Berlin	0,8 MDM
Mecklenburg-Vorpommern	7,9 MDM
EURATOM	43,4 MDM
Other income	24,6 MDM

SITE AND BUILDINGS DEPARTMENT

The site and buildings department is in charge of planning, construction, structural alteration and reconditioning of buildings and main service facilities. Building maintenance is also provided for the neighbouring Max Planck Institutes of Astrophysics and Extraterrestrial Physics, the European Southern Observatory and the Berlin Division of IPP.

SOCIAL DEPARTMENT

The social department gives assistance to employees seeking housing, provides accommodation for guests in IPP residences, and runs the transport pool, bus and cleaning services.

Publications

Publications and Conference Reports

1. *Afanas'ev*, V.P., B. Jüttner, A.A. Logatchev*, H. Pursch et al.:* The Characteristics of Vacuum Arc Discharges and Cathode Processes with Hydrogen-Impregnated Electrodes. In: Proc. 12th Int. Conf. on Gas Discharges and their Applications, Greifswald 1997, (Ed.) G.Babucke. Local Organizing Comm., Greifswald 1997, 30-33.

2. *Annen, A., R. Beckmann and W. Jacob:* Deposition and Characterization of Dense and Stable Amorphous Hydrogenated Boron Films at Low Substrate Temperatures. Journal of Non-Crystalline Solids **209**, 240-246 (1997).

3. *Annen, A. and W. Jacob:* Chemical Erosion of Amorphous Hydrogenated Boron Films. Applied Physics Letters **71**, 1326-1328 (1997).

4. *Annen, A., M. Saß, R. Beckmann and W. Jacob:* Stability of Plasma-Deposited Amorphous Hydrogenated Boron Films. Thin Solid Films **300**, 101-106 (1997).

5. *Anton, M., R. Jaenicke, A. Weller, J. Geiger, W7-AS Team, NI Group and ECRH Group:* Analysis of W7-AS Mirnov Data Using SVD and Correlation Techniques. In: Proc. 24th Conf. on Control. Fusion and Plasma Phys., Berchtesgaden 1997, (Eds.) M.Schittenhelm, R.Bartiromo, F.Wagner. ECA 21A. Europ. Phys. Soc., Geneva 1997, 1645-1648.

6. *Arndt, S., D.A. Monticello* and A.H. Reiman*:* Computation of Stellarator Equilibria with the PIES Code Using Input of VMEC Results. In: Proc. 24th EPS Conf. on Control. Fusion and Plasma Phys., Berchtesgaden 1997, (Eds.) M.Schittenhelm, R.Bartiromo, F.Wagner. ECA 21A. Europ. Phys. Soc., Geneva 1997, 1661-1664.

7. *Asmussen, K., R. Neu, R. Dux, W. Engelhardt, K.B. Fournier*, J.C. Fuchs, K. Krieger, J. Rice*, V. Rohde, D. Schlögl, M. Sokoll, A. Thoma and ASDEX Upgrade Team:* Investigations of Tungsten in the Central Plasma of ASDEX Upgrade. In: Proc. 24th EPS Conf. on Control. Fusion and Plasma Phys., Berchtesgaden 1997, (Eds.) M.Schittenhelm, R.Bartiromo, F.Wagner. ECA 21A. Europ. Phys. Soc., Geneva 1997, 1393-1396.

8. *Bachmann, P., D. Sünder and H. Wobig:* Time Evolution and Bifurcation of Temperature Profiles. In: Proc. 24th EPS Conf. on Control. Fusion and Plasma Physics, Berchtesgaden 1997, (Eds.) M.Schittenhelm, R.Bartiromo, F.Wagner. ECA 21A. Europ. Phys. Soc., Geneva 1997, 1817-1820.

9. *Balbín*, R., C. Hidalgo*, E. Sánchez*, J. Bleuel, H. Niedermeyer et al.:* Sheared Poloidal Flows and Turbulence in the Edge Plasma Region of Stellarator and Tokamak Devices. In: Proc. 24th Conf. on Control. Fusion and Plasma Phys., Berchtesgaden 1997, (Eds.) M.Schittenhelm, R.Bartiromo, F.Wagner. ECA 21A. Europ. Phys. Soc., Geneva 1997, 1665-1668.

10. *Baldzuhn, J., R. Burhenn, O. Heinrich, J.V. Hofmann, M. Kick, H. Maaßberg, W. Ohlendorf and W7-AS Team:* The Role of the Radial Electric Field and Plasma Rotation for the W7-AS Stellarator Confinement. In: Proc. 24th EPS Conf. on Control. Fusion and Plasma Phys., Berchtesgaden 1997, (Eds.) M.Schittenhelm, R.Bartiromo, F.Wagner. ECA 21A. Europ. Phys. Soc., Geneva 1997, 1585-1588.

11. *Baldzuhn, J., W. Ohlendorf and W7-AS Team:* Charge Exchange Recombination Spectroscopy on the Stellarator W7-AS. Review of Scientific Instruments **68**, 1020-1023 (1997).

12. *Becker, G., J. Stober, O. Gehre, H. Murmann, H. Salzmann, J. Schweinzer, K.-H. Steuer, W. Suttrop and ASDEX Upgrade Team:* Transport Analysis of the Edge Plasma in H-Mode Discharges of ASDEX Upgrade. In: Proc. 24th EPS Conf. on Control. Fusion and Plasma Phys., Berchtesgaden 1997, (Eds.) M.Schittenhelm, R.Bartiromo, F.Wagner. ECA 21A. Europ. Phys. Soc., Geneva 1997, 1433-1436.

13. *Beidler, C.D., G. Grieger, E. Harmeyer, F. Herrnegger, J. Kißlinger, J. Nührenberg, F. Rau, J. Sapper, H. Wobig, A.V. Zolotukhin et al.:* The Helias Reactor. In: Proc. 16th Int. Conf. on Fusion Energy, Montreal 1996, IAEA, Vienna 1997, Vol.3, 407-420.

14. *Beidler, C.D., G. Grieger, E. Harmeyer, F. Herrnegger, J. Kißlinger, E. Strumberger, H. Wobig, A.V. Zolotukhin et al.:* Physics and Engineering Studies of a Helias Reactor. In: Proc. 24th EPS Conf. on Control. Fusion and Plasma Phys., Berchtesgaden 1997, (Eds.) M.Schittenhelm, R.Bartiromo, F.Wagner. ECA 21A. Europ. Phys. Soc., Geneva 1997, 1681-1684.

15. *Beidler, C.D. and H. Maaßberg:* Neoclassical Transport in Advanced Stellarators. In: Proc. Joint Varenna-Lausanne Int. Workshop on Theory of Fusion Plasmas, Varenna 1996, (Eds.) J.W.Connor, E.Sindoni, J.Vaclavik. Ed. Compositori, Bologna 1997, 375-380.

16. *Beilis*, I., B.E. Djakov*, B. Jüttner and H. Pursch:* Structure and Dynamics of High Current Arc Cathode Spots in Vacuum. Journal of Physics, D **30**, 119-130 (1997).

17. *Berger, E., P. Valášek and W. von der Linden:* Two-Dimensional Hubbard-Holstein Model. Physical Review, B **52**, 4806-4814 (1997).

18. *Berger, E., W. von der Linden, V. Dose et al.:* Approach for the Evaluation of Speckle Deformation Measurements by Application of the Wavelet Transformation. Applied Optics **36**, 7455-7460 (1997).

19. *Bertel, E.:* Electronic Surface States and the Hydrogen Dissociation Barrier. Physica Status Solidi A **159**, 235-242 (1997).

20. *Biedermann, C., A. Förster*, G. Fußmann and R. Radtke:* First Results from the Berlin EBIT. Physica Scripta **T73**, 360-361 (1997).

21. *Biedermann, C., R. Radtke and G. Fußmann:* Direct Observation of X-Ray Emission from High-n Spectator Electrons Following Radiative Stabilization in Dielectronically Excited Highly Charged Barium. Journal of Physics, A **56**, R2522-R2525 (1997).

22. *Biskamp, D.:* Magnetic Reconnection in Plasmas. Astrophysics and Space Science **242**, 165-207 (1997).

23. *Biskamp, D.:* Nonlinear Magnetohydrodynamics. Cambridge Univ. Press, Cambridge 1997, 378 S.

24. *Biskamp, D. and E. Schwarz:* Scaling Properties of Turbulent Convection in Two-Dimensional Systems. Europhysics Letters **40**, 637-642 (1997).

25. *Biskamp, D., E. Schwarz and J.F.Drake*:* Two-Fluid Theory of Collisionless Magnetic Reconnection. Physics of Plasmas **4**, 1002-1009 (1997).

26. *Bleuel, J., M. Endler, H. Niedermeyer, G. Theimer and W7-AS Team:* Structure of the Edge Fluctuations in the W7-AS Stellarator. In: Proc. 24th Conf. on Control. Fusion and Plasma Phys., Berchtesgaden 1997, (Eds.) M.Schittenhelm, R.Bartiromo, F.Wagner. ECA 21A. Europ. Phys. Soc., Geneva 1997, 1613-1616.

27. *Bonoli*, P., P.J. O'Shea*, M. Brambilla, B. LeBlanc*, R.P. Majeski*, M. Porkolab* et al.:* Theoretical Analysis of Mode Conversion Electron Heating Experiments in Alcator C-Mod. In: Proc. 12th Top. Conf. on Radio Frequency Power in Plasmas, Savannah,GA 1997, (Eds.) P.M.Ryan, T.Intrator. AIP Conf. Proc. 403, AIP Press, New York, NY 1997, 269-272.

28. *Borrass, K., D. Coster, D. Reiter* and R. Schneider:* Study of Recombining Gas Targets. Journal of Nuclear Materials **241-243**, 250-254 (1997).

29. *Borrass, K., D. Coster and R. Schneider:* Numerical Study of the Impact of Divertor Closure on Detachment. In: Proc. 24th EPS Conf. on Control. Fusion and Plasma Phys., Berchtesgaden 1997, (Eds.) M.Schittenhelm, R.Bartiromo, F.Wagner. ECA 21A. Europ. Phys. Soc., Geneva 1997, 1461-1464.

30. *Borrass, K., R. Schneider and R. Farengo*:* A Scrape-off Layer Based Model for Hugill-Greenwald Type Density Limits. Nuclear Fusion **37**, 523-537 (1997).

31. *Bosch, H.-S., D. Coster, R. Dux, C. Fuchs, G. Haas, A. Herrmann, S. Hirsch, A. Kallenbach, J. Neuhauser, R. Schneider, J. Schweinzer, M. Weinlich, ASDEX Upgrade Team and NI Team:* Particle Exhaust in Radiative Divertor Experiments. Journal of Nuclear Materials **241-243**, 82-91 (1997).

32. *Bosch, H.-S., D. Coster, R. Dux, G. Haas, A. Kallenbach, S. De Peña Hempel, K. Lackner, J. Neuhauser, R. Schneider and ASDEX Upgrade Team:* Helium Exhaust and Transport in ASDEX Upgrade. In: Proc. 24th EPS Conf. on Control. Fusion and Plasma Phys., Berchtesgaden 1997, (Eds.) M.Schittenhelm, R.Bartiromo, F.Wagner. ECA 21A. Europ. Phys. Soc., Geneva 1997, 1425-1428.

33. *Bosch, H.-S., D. Coster, R. Dux, G. Haas, A. Kallenbach, M. Kaufmann, K. Lackner, J. Neuhauser, S. De Peña Hempel, W. Poschenrieder, R. Schneider, ASDEX Upgrade Team, NI Team, ICRH Group and ECRH Group:* Particle Exhaust Studies in ASDEX Upgrade. Plasma Physics and Controlled Fusion **39**, 1771-1792 (1997).

34. *Bosch, H.-S., A. Kallenbach, D. Coster, R. Dux, G. Haas, M. Kaufmann, K. Lackner, J. Neuhauser, S. De Peña Hempel, R. Schneider, ASDEX Upgrade Team, NI Team and ICRH Group:* Impurity Transport and Exhaust in Radiative Edge Experiments in ASDEX Upgrade. In: Proc. 16th Int. Conf. on Fusion Energy, Montreal 1996, IAEA, Vienna 1997, Vol.1, 809-815.

35. *Brakel, R., M. Anton, J. Baldzuhn, R. Burhenn, V. Erckmann, S. Fiedler, J. Geiger, H.-J. Hartfuß, O. Heinrich, M. Hirsch, R. Jaenicke, M. Kick, G. Kühner,.H. Maaßberg, U. Stroth, F. Wagner, A. Weller, W7-AS Team, ECRH Group and NI Group:* Confinement in W7-AS and the Role of Radial Electric Field and Magnetic Shear. Plasma Physics and Controlled Fusion **39**, B273-B286 (1997).

36. *Brambilla, M.:* Recent Progress in IC Wave Codes at IPP Garching. In: Proc. 12th Top. Conf. on Radio Frequency Power in Plasmas, Savannah,GA 1997, (Eds.) P.M.Ryan, T.Intrator. AIP Conf. Proc. 403, AIP Press, New York, NY 1997, 257-264.

37. *Brañas*, B., M. Hirsch, V. Zhuravlev*, J. Baldzuhn, J. Sanchez*, T. Estrada*, T. Geist and H.-J. Hartfuß:* Analysis of the Reflectometer Phase Runaway Effect at Wendelstein 7-AS. In: Proc. 3rd Workshop on Microwave Reflectometry for Fusion Plasma Diagnostics, Madrid 1997, (Eds.) J.Sánchez, E.de la Luna. Informes Tecnicos Ciemat 838. Ciemat, Madrid 1997, 169-179.

38. *Brandenburg*, R., S. Fiedler, K. McCormick, G. Petravich*, F. Aumayr*, J. Schweinzer, W7-AS Team et al.:* Extension and Optimization of Lithium Beam Diagnostic Methods. In: Proc. 24th Conf. on Control. Fusion and Plasma Phys., Berchtesgaden 1997, (Eds.) M.Schittenhelm, R.Bartiromo, F.Wagner. ECA 21A. Europ. Phys. Soc., Geneva 1997, 477-480.

39. *Braun, F. and T. Sperger:* An ARC Detection System for ICR-Heating. In: Proc. 19th Symp. Fusion Technol., Lisbon 1996, (Eds.) C.Varandas, F.Serra. North-Holland Publ., Amsterdam 1997, 601-603.

40. *Brinkschulte, H., A. Fix*, W. Förster*, G. Gantenbein*, F. Leuterer, F. Monaco, M. Münich, A.G. Peeters, F. Ryter et al.:* The 140 GHz - 2 MW - 2 s ECRH System for ASDEX Upgrade. In: Proc. 19th Symp. Fusion Technol., Lisbon 1996, (Eds.) C.Varandas, F.Serra. North-Holland Publ., Amsterdam 1997, 537-540.

41. *Burhenn, R., M. Anton, J. Baldzuhn, R. Brakel, L. Giannone, H. Hacker, M. Hirsch, L. Ledl, M. Maaßberg, U. Stroth, A. Weller, W7-AS Team, ECRH Group and NI Group:* Investigation of Impurity Tracer Transport in High Density Plasmas at the Stellarator Wendelstein 7-AS. In: Proc. 24th EPS Conf. on Control. Fusion and Plasma Phys., Berchtesgaden 1997, (Eds.) M.Schittenhelm, R.Bartiromo, F.Wagner. ECA 21A. Europ. Phys. Soc., Geneva 1997, 1609-1612.

42. *Burtseva*, T., V. Barabash*, I. Mazul*, C. Garcia-Rosales*, S. Deschka, R. Behrisch and A. Herrmann:* Performance of the Ti Doped Graphite RG-Ti-91 at the Divertor of the Tokamak ASDEX Upgrade. Journal of Nuclear Materials **241-243**, 716-721 (1997).

43. *Callaghan*, H., J. Geiger, C. Görner, J.V. Hofmann, R. Jaenicke, P. McCarthy* and A. Weller:* Review of 3-D Equilibrium Calculations and Reconstructions for W7-AS. In: Proc. 24th Conf. on Control. Fusion and Plasma Phys., Berchtesgaden 1997, (Eds.) M.Schittenhelm, R.Bartiromo, F.Wagner. ECA 21A. Europ. Phys. Soc., Geneva 1997, 1617-1620.

44. *Carlson, A., V. Rohde, M. Weinlich and ASDEX Upgrade Team:* The Separation of Angle and Size Effects on Langmuir Characteristics. Journal of Nuclear Materials **241-243**, 722-727 (1997).

45. *Castejón*, F., R. Brakel, W7-AS Team and ECRH Group:* Radiative Instabilities in W7-AS Plasmas with Highly Radiating Boundaries. In: Proc. 24th Conf. on Control. Fusion and Plasma Phys., Berchtesgaden 1997, (Eds.) M.Schittenhelm, R.Bartiromo, F.Wagner. ECA 21A. Europ. Phys. Soc., Geneva 1997, 1581-1584.

46. *Cattanei, G.:* ICRF Wave Propagation in a Non-Axisymmetric Geometry. In: Proc. 12th Top. Conf. on Radio Frequency Power in Plasma, Savannah 1997, (Eds.) P.M.Ryan, T.Intrator. AIP Conf. Proc. 403, AIP Press, Woodbury,NY 1997, 343-346.

47. *Cho*, T., M. Hirata*, J. Kohagura*, S. Kanke*, K. Takahashi*, Y. Sakamoto*, M. Bessenrodt-Weberpals et al.:* Characterization of New Semiconductor Detectors for X-Ray Tomography in the ASDEX Upgrade Tokamak and its Generalized Physics Interpretation. Review of Scientific Instruments **68**, 774-777 (1997).

48. *Confinement Modelling and Database Group:* ITER Forecasts. Science **275**, 289-291 (1997).

49. *Connor*, J.W., C. Hidalgo*, A. Jacchia*, U. Stroth et al.:* EU-US Workshop on Transport in Fusion Plasmas. Plasma Physics and Controlled Fusion **39**, 609-620 (1997).

50. *Connor*, J.W. and ITER Confinement Database and Modelling Working Group:* Validation of 1-D Transport and Sawtooth Models for ITER. In: Proc. 16th Int. Conf. on Fusion Energy, Montreal 1996, IAEA, Vienna 1997, Vol.2, 935-944.

51. *Cordey*, J.G. and ITER Confinement Database and Modelling Working Group:* Energy Confinement Scaling and the Extrapolation to ITER. Plasma Physics and Controlled Fusion **39**, B115-B127 (1997).

52. *Correa-Restrepo, D. and D. Pfirsch:* Negative-Energy Perturbations in General Axisymmetric and Helical Maxwell-Vlasov Equilibria. Physical Review E **55**, 7449-7456 (1997).

53. *Coster, D., H. Kastelewicz, R. Schneider and ASDEX Upgrade Team:* Evolution Modelling of ASDEX Upgrade Shots with B2-Eirene. In: Proc. 24th EPS Conf. on Control. Fusion and Plasma Phys., Berchtesgaden 1997, (Eds.) M.Schittenhelm, R.Bartiromo, F.Wagner. ECA 21A, Europ. Phys. Soc., Geneva 1997, 1437-1440.

54. *De Peña Hempel, S., R. Dux, A. Kallenbach, H. Meister and ASDEX Upgrade Team:* Low-Z-Impurity Transport Coefficients at ASDEX Upgrade. In: Proc. 24th EPS Conf. on Control. Fusion and Plasma Phys., Berchtesgaden 1997, (Eds.) M.Schittenhelm, R.Bartiromo, F.Wagner. ECA 21 A. Europ. Phys. Soc., Geneva 1997, 1401-1404.

55. *Deschka, S., S. Schweizer, B. Streibl, ASDEX Upgrade Team, C. Garcia-Rosales*, G. Hofmann* and J. Linke*:* Divertor II Plasma Facing Components for ASDEX Upgrade. In: Proc. 19th Symp. on Fusion Technol., Lisbon 1997, (Eds.) C.Varandas, F.Serra. North-Holland Publ., Amsterdam 1997, 455-458.

56. *Dohmen, R., H. Friedrich and F. Hertweck:* Dynamic Load Balancing Applied to a Fortran 90 Monte-Carlo Code. In: Proc. 3rd Europ. Cray-SGI MPP Workshop, Paris 1997, http://armoise.saclay.cea.fr/~workshop/Documents/Final_Papers/Renate_Dohmen_11-Part-Mont.ps

57. *Dohmen, R., U. Schwenn and T. Hayashi*:* Comparing the Performance of the 3D Plasma Equilibrium Code HINT on Vector and Cray T3D/T3E Systems. In: Proc. Nichtlineare Dynamik, Chaos und Strukturbildung, München 1996, (Eds.) R.Meyer-Spasche, M.Rast, C.Zenger. Spektrum Akad. Verl., München 1997, 125-129.

58. *Donath, M., B. Gubanka and F. Passek:* Temperature-Dependent Spin Polarization of Magnetic Surface State at Gd(0001). Physical Review Letters **77**, 5138-5141 (1997).

59. *Dose, V., G. Venus and H. Zohm*:* Wavelet Analysis of Fusion Plasma Transients. Physics of Plasmas **4**, 323-328 (1997).

60. *Drake, J.F.*, D. Biskamp and A. Zeiler:* Break-up of the Electron Current Layer in 3D Collisionless Magnetic Reconnection. Geophysical Research Letters **24**, 2921-2923 (1997).

61. *Dux, R., K. Asmussen, R. Neu, S. De Peña Hempel, V. Rohde, A. Thoma and ASDEX Upgrade Team:* Modelling of Impurity Transport and Radiation for ASDEX Upgrade Discharges. In: Proc. 24th EPS Conf. on Control. Fusion and Plasma Phys., Berchtesgaden 1997, (Eds.) M.Schittenhelm, R.Bartiromo, F.Wagner. ECA 21A. Europ. Phys. Soc., Geneva 1997, 1405-1408.

62. *Eckstein, W.:* Isotope Sputtering of Molybdenum. Radiation Effects and Defects in Solids **142**, 319-322 (1997).

63. *Eckstein, W.:* Physical Sputtering and Reflection Processes in Plasma-Wall Interactions. Journal of Nuclear Materials **248**, 1-8 (1997).

64. *Eckstein, W. and R. Dohmen:* Isotope Sputtering of Molybdenum. Nuclear Instruments and Methods in Physics Research, B **129**, 327-340 (1997).

65. *Ehrenberg*, J.K., D.J. Campbell*, P.J. Harbour*, K. McCormick et al.:* Neutral Particle Compression in the JET Mk I Divertor. Journal of Nuclear Materials **241-243**, 420-425 (1997).

66. *Empacher*, L., W. Förster*, G. Gantenbein*, V. Erckmann, T. Geist, H. Laqua et al.:* Conceptual Design of the 140 GHz/10 MW CW ECRH System for the Stellarator W7-X. In: Proc. 19th Symp. Fusion Technol., Lisbon 1996, (Eds.) C.Varandas, F.Serra. North-Holland Publ., Amsterdam 1997, 541-544.

67. *Empacher*, L., G. Gantenbein*, W. Kasparek*, V. Erckmann and H.P. Laqua:* Matching of a Non-Gaussian Gyrotron Output Beam to an ECRH Transmission Line Using Thermographic Measurements. In: Proc. 24th Conf. on Control. Fusion and Plasma Phys., Berchtesgaden 1997, (Eds.) M.Schittenhelm, R.Bartiromo, F.Wagner. ECA 21A. Europ. Phys. Soc., Geneva 1997, 1825-1828.

68. *Erckmann, V., H.P. Laqua, U. Gasparino, J. Geiger, H.-J. Hartfuß, R. Jaenicke, G. Kühner, H. Maaßberg, N. Niedermeyer, M. Romé, A. Weller, W7-AS Team and ECRH Group:* High Density ECRH and Shear Related Confinement with ECCD in W7-AS. In: Proc. 16th Int. Conf. on Fusion Energy, Montreal 1996, IAEA, Vienna 1997, Vol.2, 119-126.

69. *Erckmann, V., H.P. Laqua, H. Maaßberg, M. Romé, A. Borschegovsky*, V.I. Il'in*, W7-AS Team and ECRH Group:* Overview on ECRH and ECCD Experiments at the W7-AS Stellarator. In: Proc. 2nd Int. Workshop Strong Microwaves in Plasmas, (Ed.) A.G.Litvak. Russ. Acad. of Sci., Inst. of Appl. Phys., Nizhny Novgorod, 1, 69-88 (1997).

70. *Fahrbach, H.-U., O. Kardaun, J. Stober, Yu.N. Dnestrovskij*, W. Herrmann, A. Khutoretsky* and ASDEX Upgrade Team:* Fast Determination of T_i-Profiles from Analysis of Neutral Flux Measurements In: Proc. 24th EPS Conf. on Control. Fusion and Plasma Phys., Berchtesgaden 1997, (Eds.) M.Schittenhelm, R.Bartiromo, F.Wagner. ECA 21A. Europ. Phys. Soc., Geneva 1997, 1501-1504.

71. *Feng*, X.Y., Z.H. Wang*, E.Y. Wang*, R. Burhenn et al.:* Laser Blow-off Experiment and Study of Impurity Transport on HL-IM Tokamak. In: Proc. 24th EPS Conf. on Control. Fusion and Plasma Phys., Berchtesgaden 1997, (Eds.) M.Schittenhelm, R.Bartiromo, F.Wagner. ECA 21A. Europ. Phys. Soc., Geneva 1997, 657-660.

72. *Feng, Y., G. Herre, P. Grigull, F. Sardei and W7-AS Team:* The Effects of Field Reversal on the W7-AS Island Divertor at Low Densities. In: Proc. 24th Conf. on Control. Fusion and Plasma Phys., Berchtesgaden 1997, (Eds.) M.Schittenhelm, R.Bartiromo, F.Wagner. ECA 21A. Europ. Phys. Soc., Geneva 1997, 1569-1572.

73. *Feng, Y., F. Sardei, J. Kißlinger and P. Grigull:* A 3-D Monte Carlo Code for Plasma Transport in Island Divertors. Journal of Nuclear Materials **241-243**, 930-934 (1997).

74. *Fischer, R., M. Mayer, W. von der Linden and V. Dose:* Enhancement of the Energy Resolution in Ion-Beam Experiments with the Maximum-Entropy Method. Physical Review, E **55**, 6667-6673 (1997).

75. *Francés*, M., M. Hirsch, M. Anton, T. Geist, H.-J. Hartfuß, E. Holzhauer*:* Study of Density Turbulence and Coherent Mode Activity in W7-AS by Microwave Reflectometry. In: Proc. 24th Conf. on Control. Fusion and Plasma Phys., Berchtesgaden 1997, (Eds.) M.Schittenhelm, R.Bartiromo, F.Wagner. ECA 21A. Europ. Phys. Soc., Geneva 1997, 1589-1592.

76. *Franzen, P., R. Behrisch, C. Garcia-Rosales*, ASDEX Upgrade Team et al.:* Hydrogen Isotope Inventory in the Graphite Divertor Tiles of ASDEX Upgrade as Measured by Thermal Desorption Spectroscopy. Nuclear Fusion **37**, 1375-1393 (1997).

77. *Franzen, P., C. García-Rosales*, H. Plank and V.Kh. Alimov*:* Hydrogen Trapping in and Release from Tungsten: Modelling and Comparison with Graphite with Regard to its Use as Fusion Reactor Material. Journal of Nuclear Materials **241-243**, 1082-1086 (1997).

78. *Franzen, P., H. Maier, D. Schleußner, R. Behrisch, M. Balden and ASDEX Upgrade Team:* Hydrogen Isotope Inventories in the ASDEX Upgrade Tungsten Coated Divertor Tiles. In: Proc. 24th EPS Conf. on Control. Fusion and Plasma Phys., Berchtesgaden 1997, (Eds.) M.Schittenhelm, R.Bartiromo, F.Wagner. ECA 21A. Europ. Phys. Soc., Geneva 1997, 1429-1432.

79. *Friedrich*, M., G. Sun*, R. Grötzschel*, R. Behrisch et al.:* Tritium Depth Profiling in Carbon by Accelerator Mass Spectrometry. Nuclear Instruments and Methods in Physics Research, B **123**, 410-413 (1997).

80. *Fuchs, J.C, K.-F. Mast, G. Haas and ASDEX Upgrade Team:* Bolometric Measurements in the ASDEX Upgrade Divertor. In: Proc. 24th EPS Conf. on Control. Fusion and Plasma Phys., Berchtesgaden 1997, (Eds.) M.Schittenhelm, R.Bartiromo, F.Wagner. ECA 21A. Europ. Phys. Soc., Geneva 1997, 1453-1456.

81. *Furno*, I., H. Weisen*, J.M. Moret* and M. Anton:* X-Ray Measurements of MHD Activity in Shaped TCV Plasmas. In: Proc. 24th Conf. on Control. Fusion and Plasma Phys., Berchtesgaden 1997, (Eds.) M.Schittenhelm, R.Bartiromo, F.Wagner. ECA 21A. Europ. Phys. Soc., Geneva 1997, 545-548.

82. *Fußmann, G.:* Cross-Field Diffusion by Charge Changing Processes. Contributions to Plasma Physics **37**, 363-375 (1997).

83. *Fußmann, G.:* Cross-Field Diffusion by Charge Changing Processes. In: Proc. 24th EPS Conf. on Control. Fusion and Plasma Phys., Berchtesgaden 1997, (Eds.) M.Schittenhelm, R.Bartiromo, F.Wagner. ECA 21A. Europ. Phys. Soc., Geneva 1997, 1813-1816.

84. *Gafert, J., K. Behringer, D. Coster, C. Dorn, K. Hirsch, M. Niethammer*, U. Schumacher* and ASDEX Upgrade Team:* First Experimental Determination of Ion Flow Velocities and Temperatures in the ASDEX Upgrade Divertor. Plasma Physics and Controlled Fusion **39**, 1981-1995 (1997).

85. *Gafert, J., D. Coster, C. Dorn, B. Napiontek, U. Schumacher*, NI Team and ASDEX Upgrade Team:* Ion Dynamics Observed by High Resolution Spectroscopy in the ASDEX Upgrade Divertor I and II. In: Proc. 24th EPS Conf. on Control. Fusion and Plasma Phys., Berchtesgaden 1997, (Eds.) M.Schittenhelm, R.Bartiromo, F.Wagner. ECA 21A. Europ. Phys. Soc., Geneva 1997, 1397-1400.

86. *García-Cortés*, I., M. Endler, A. Loarte, S. Davies*, S.K. Erents* et al.:* Turbulence Studies in the JET Scrape-off Layer Plasmas. In: Proc. 24th EPS Conf. on Control. Fusion and Plasma Phys., Berchtesgaden 1997, (Eds.) M.Schittenhelm, R.Bartiromo, F.Wagner. ECA 21A. Europ. Phys. Soc., Geneva 1997, 109–112.

87. *García-Rosales*, C., S. Deschka, W. Hohenauer*, R. Duwe*, E. Gauthier*, J. Linke*, M. Lochter*, W.K.W.M. Malléner*, L. Plöchl*, P. Rödhammer*, A. Salito* and ASDEX Upgrade Team:* High-Heat-Flux Loading of Tungsten Coatings on Graphite Deposited by Plasma Spray and Physical Vapor Deposition. Fusion Technology **32**, 263-276 (1997).

88. *Gasparino, U., H.-J. Hartfuß, H. Maaßberg, N. Marushchenko*, W. Pernreiter and M. Romé:* Energy and Density Inhomogeneities Driven by Toroidally Localized ECRH in W7-AS. In: Proc. 24th Conf. on Control. Fusion and Plasma Phys., Berchtesgaden 1997, (Eds.) M.Schittenhelm, R.Bartiromo, F.Wagner. ECA 21A. Europ. Phys. Soc., Geneva 1997, 1637-1640.

89. *Geist, T., E. Würsching and H.-J. Hartfuß:* Multichannel Millimeter Wave Interferometer for W7-AS. Review of Scientific Instruments **68**, 1162-1167 (1997).

90. *Giannone, L., E. Bellido, R. Brakel, R. Burhenn, R. Dux, A. Elsner, S. Fiedler, T. Geist, P. Grigull, H. Hacker, H.-J. Hartfuß, A. Herrmann, J.P.T. Koponen, F.-P. Penningsfeld, G. Pereverzev, U. Stroth, F. Wagner, NI Group and W7-AS Team:* Bolometer Measurements and Transport Simulations of the Density Limit on the W7-AS Stellarator. In: Proc. 24th Conf. on Control. Fusion and Plasma Phys., Berchtesgaden 1997, (Eds.) M.Schittenhelm, R.Bartiromo, F.Wagner. ECA 21A. Europ. Phys. Soc., Geneva 1997, 1565-1568.

91. *Giannone, L., A. Elsner, O. Heinrich, M. Hirsch and W7-AS Team:* Tomography by the Maximum Entropy Method for the W7-AS and W7-X Multichannel Bolometer Systems. Review of Scientific Instruments **68**, 762-765 (1997).

92. *Gori, S., W. Lotz and J. Nührenberg:* Quasi-Isodynamic Stellarators. In: Proc. Joint Varenna-Lausanne Int. Workshop on Theory of Fusion Plasmas, Varenna 1996, (Eds.) J.W.Connor, E.Sindoni, J.Vaclavik. Ed. Compositori, Bologna 1997, 335-342.

93. *Görner, C., M. Anton, J. Geiger, W. von der Linden, A. Weller, S. Zoletnik* and W7-AS Team:* Tomographic Reconstruction of Plasma Equilibria and MHD-Modes at Wendelstein 7-AS. In: Proc. 24th Conf. on Control. Fusion and Plasma Phys., Berchtesgaden 1997, (Eds.) M.Schittenhelm, R.Bartiromo, F.Wagner. ECA 21A. Europ. Phys. Soc., Geneva 1997, 1625-1628.

94. *Greuner, H., W. Bitter, R. Holzthüm, O. Jandl, F. Kerl, J. Kißlinger and H. Renner:* Divertor Engineering for the Stellarator Wendelstein 7-X. In: Proc. 19th Symp. Fusion Technol., Lisbon 1996, (Eds.) C.Varandas, F.Serra. North-Holland Publ., Amsterdam 1997, 463-466.

95. *Greuner, H., T. Huber*, J. Kißlinger, H. Renner et al.:* Design, Manufacturing and Testing of the W7-X Target Element Prototypes. In: Proc. 19th Symp. Fusion Technol., Lisbon 1996, (Eds.) C.Varandas, F.Serra. North-Holland Publ., Amsterdam 1997, 467-470.

96. *Grieger, G.:* Lunar Mining for He --- Power Generation by Thermonuclear Fusion. In: A Lunar-Based Analytical Laboratory, (Eds.) C.W.Gehrke, M.K.Hobish, R.W.Zumwalt et al. Deepak Publ., Hampton,VA 1997, 276-285.

97. *Grigull, P., R. Brakel, K. Borrass, J. Baldzuhn, A. Elsner, S. Fiedler, H. Hacker, H.-J. Hartfuß, D. Hildebrandt, R. Schneider, U. Stroth, F. Wagner, A. Weller, X.D. Zhang, W7-AS Team and ECRH Group:* Feedback Control. Radiative Edge Cooling Experiments in the Wendelstein 7-AS Stellarator. In: Proc. 24th EPS Conf. on Control. Fusion and Plasma Phys., Berchtesgaden 1997, (Eds.) M.Schittenhelm, R.Bartiromo, F.Wagner. ECA 21A. Europ. Phys. Soc., Geneva 1997, 1573-1576.

98. *Grigull, P., Y. Feng, D. Hildebrandt, F. Sardei, G. Herre, O. Heinrich, A. Elsner, S. Fiedler, J.V. Hofmann, J. Kißlinger, G. Kühner, H. Niedermeyer, R. Schneider, H. Verbeek, F. Wagner, A. Weller, R. Wolf and W7-AS Team:* High Recycling in W7-AS Island Divertor Configurations. In: Proc. 16th Int. Conf. on Fusion Energy, Montreal 1996, IAEA, Vienna 1997, Vol.2, 307-313.

99. *Grigull, P., D. Hildebrandt, F. Sardei, Y. Feng, G. Herre, A. Herrmann, J.V. Hofmann, J. Kißlinger, G. Kühner, H. Niedermeyer, R. Schneider, H. Verbeek, F. Wagner, R. Wolf, X.D. Zhang, W7-AS Team and NI Group:* Experimental Study on High Collisional Edge Plasmas in W7-AS Island Divertor Configurations. Journal of Nuclear Materials **241-243**, 935-940 (1997).

100. *Grigull, S., W. Jacob, D. Henke* et al.:* On the Presence of Molecular Nitrogen in Nitrogen-Implanted Amorphous Carbon. Applied Physics Letters **70**, 1387-1389 (1997).

101. *Grigull, S., U. Kreissig*, H. Huber* and W. Assmann*:* Element-Dependent ERDA Probing Depths Using Different Detection Systems. Nuclear Instruments and Methods in Physics Research, B **132**, 709-717 (1997).

102. *Grossmann*, M.T., E. Holzhauer*, M. Hirsch et al.:* A 2-D Code for the Analysis of Microwave Reflectometry Measurements in Fusion Experiments. In: Proc. 24th EPS Conf. on Control. Fusion and Plasma Phys., Berchtesgaden 1997, (Eds.) M.Schittenhelm, R.Bartiromo, F.Wagner. ECA 21A. Europ. Phys. Soc., Geneva 1997, 1497-1500.

103. *Grossmann*, M.T., E. Holzhauer*, M. Hirsch, F. Serra* et al.:* A 2-D Code for the Analysis of Microwave Reflectometry Measurements in Fusion Experiments. In: Proc. 3rd Workshop Microwave Reflectometry for Fusion Plasma Diagnostics, Madrid 1997, (Eds.) J.Sánchez, E.de la Luna. Informes Tecnicos Ciemat 838. Ciemat, Madrid 1997, 29-38.

104. *Grote, H., W. Bohmeyer, H.-D. Reiner, H. Behrendt, G. Fußmann, H. Meyer, D. Naujoks and E. Pasch:* Comparison of Chemical Sputtering Yields for Different Graphites at High Ion Flux Densities. Journal of Nuclear Materials **241-243**, 1152-1155 (1997).

105. *Grote, K. and R. Meyer-Spasche:* Dynamische Eigenschaften von Differenzenverfahren. In: Proc. Nichtlineare Dynamik, Chaos und Strukturbildung, München 1996, (Eds.) R.Meyer-Spasche, M.Rast, C.Zenger. Akad.Verl., München 1997, 160-180.

106. *Gruber, O., ASDEX Upgrade Team and NI Team:* MHD Stability and Disruption Studies in ASDEX Upgrade In: Proc. 16th Int. Conf. on Fusion Energy, Montreal 1996, IAEA, Vienna 1997, Vol.1, 359-368.

107. *Gruber, O., V. Mertens, J. Neuhauser, F. Ryter, W. Suttrop, M. Albrecht, M. Alexander, K. Asmussen, G. Becker, K. Behler, K. Behringer, A. Bergmann, M. Bessenrodt-Weberpals, K. Borrass, H.-S. Bosch, B. Braams*, M. Brambilla, F. Braun, H. Brinkschulte, K. Büchl, A. Buhler, A. Carlson, R. Chodura, D. Coster, L. Cupido*, H.J. de Blank, S. de Peña Hempel, S. Deschka, C. Dorn, R. Drube, R. Dux, W. Engelhardt, J. Engstler, H.-U. Fahrbach, J.-H. Feist, S. Fiedler, P. Franzen, J.C. Fuchs, G. Fußmann, J. Gafert, O. Gehre, J. Gernhardt, S. Günter, G. Haas, K. Hallatschek, J. Hartmann, B. Heinemann, G. Herppich, A. Herrmann, W. Herrmann, S. Hirsch, M. Hoek*, F. Hoenen*, F. Hofmeister, H. Hohenöcker, E. Holzhauer*, P. Ignacz*, D. Jacobi, W. Junker, M. Kakoulidis*, A. Kallenbach, N. Karakatsanis*, O. Kardaun, T. Kass, M. Kaufmann, A. Khutoretsky*, H. Kollotzek, W. Köppendörfer, W. Kraus, K. Krieger, B. Kurzan, G. Kyriakakis*, K. Lackner, P.T. Lang, R.S. Lang, M. Laux, L. Lengyel, F. Leuterer, M. Maraschek, M. Markoulaki*, K.-F. Mast, P. McCarthy*, D. Meisel, H. Meister, R. Merkel, H.W. Müller, M. Münich, H. Murmann, B. Napiontek, G. Neu, R. Neu, M. Niethammer*, J.-M. Noterdaeme, E. Pasch, G. Pautasso, A.G. Peeters, G. Pereverzev, C.S. Pitcher, W. Poschenrieder, G. Raupp, K. Reinmüller, R. Riedl, V. Rohde, H. Röhr, J. Roth, H. Salzmann, W. Sandmann, H.-B. Schilling, M. Schittenhelm, D. Schlögl, H. Schneider, R. Schneider, W. Schneider, G. Schramm, J. Schweinzer, S. Schweizer, R. Schwörer, B.D. Scott, U. Seidel, F. Serra*, S. Sesnic, A. Silva*, M. Sokoll, E. Speth, A. Stäbler, K.-H. Steuer, J. Stober, B. Streibl, A. Thoma, W. Treutterer, M. Troppmann, N. Tsois*, M. Ulrich, P. Varela*, H. Verbeek, O. Vollmer, H. Wedler, M. Weinlich, U. Wenzel, F. Wesner, R. Wolf, R. Wunderlich, N. Xantopoulus*, Q. Yu*, D. Zasche, T. Zehetbauer, H.-P. Zehrfeld, H. Zohm* and M. Zouhar:* Divertor Tokamak Operation at High Densities in ASDEX Upgrade. Plasma Physics and Controlled Fusion **39**, B19-B38 (1997).

108. *Gude, A., K. Hallatschek, M. Bessenrodt-Weberpals, S. Günter, A. Kallenbach, K. Lackner, S.D. Pinches, S. Sesnic, M. Sokoll and ASDEX Upgrade Team:* Radially Propagating High-n/High-m Mode Cascades during Flattening or Inversion of Central *q*-Profile in ASDEX Upgrade. In: Proc. 24th EPS Conf. on Control. Fusion and Plasma Phys., Berchtesgaden 1997, (Eds.) M.Schittenhelm, R.Bartiromo, F.Wagner. ECA 21A. Europ. Phys. Soc., Geneva 1997, 1513-1516.

109. *Günter, S. and A. Könies:* Shifts and Asymmetry Parameters of Hydrogen Balmer Lines in Dense Plasmas. Physical Review E **55**, 1-5 (1997).

110. *Günter, S. and A. Könies:* Shifted and Asymmetric Profiles of Hydrogen and Hydrogenic Ions. In: Proc. Spectral Line Shapes, Florenz 1996, (Eds.) M.Zoppi, L.Ulivi. AIP, Woodbury,NY 1997, 99-112.

111. *Günter, S., S.D. Pinches, A. Gude, K. Hallatschek, K. Lackner and ASDEX Upgrade Team:* Modified High-n/High-m Tearing Modes in Low Shear Regions with High Pressure Gradients and High Resistivity. In: Proc. 24th EPS Conf. on Control. Fusion and Plasma Phys., Berchtesgaden 1997, (Eds.) M.Schittenhelm, R.Bartiromo, F.Wagner. ECA 21A. Europ. Phys. Soc., Geneva 1997, 1529-1532.

112. *Günther*, S., M. Marsi*, A. Kolmakov*, E. Taglauer et al.:* Photoelectron Spectromicroscopic Study of the Spreading Behavior of MoO_3 on Titania and Alumina Model Supports. Journal of Physical Chemistry, B **101**, 10004-10011 (1997).

113. *Hanesch*, P. and E. Bertel:* Mesoscopic Self-Organization Induced by Intrinsic Surface Stress on Pt(110). Physical Review Letters **79**, 1523-1526 (1997).

114. *Harmeyer, E., N. Jaksic and J. Simon-Weidner:* On Modular Coils of a Helias Reactor. In: Proc. 19th Symp. Fusion Technol., Lisbon 1996, (Eds.) C.Varandas, F.Serra. North-Holland Publ., Amsterdam 1997, 1035-1038.

115. *Hartfuß, H.-J., R. Brakel, M. Endler, T. Geist, P. Grigull, J.V. Hofmann, J. Junker, M. Kick, G. Kühner, H. Niedermeyer, H. Ringler, A. Teubel, F. Wagner and A. Weller:* Diagnostic Strategy of the W7-X Stellarator. Review of Scientific Instruments **68**, 1244-1249 (1997).

116. *Hartfuß, H.-J., T. Geist and M. Hirsch:* Heterodyne Methods in Millimetre Wave Plasma Diagnostics with Applications to ECE, Interferometry and Reflectometry. Plasma Physics and Controlled Fusion **39**, 1693-1769 (1997).

117. *Hartfuß, H.-J., S. Sattler, M. Häse, M. Hirsch, T. Geist and W7-AS Team:* Temperature Fluctuation Measurements with ECE at W7-AS. Fusion Engineering and Design **34-35**, 81-87 (1997).

118. *Hartmann, A.:* Interessenausgleich und Sozialplan in außeruniversitären Forschungseinrichtungen. In: Festschrift für Ernst-Joachim Meusel, (Ed.) M.Winkler. Nomos Verl.Ges., Baden-Baden 1997, 55-63.

119. *Hartmann, D., G. Cattanei, F. Braun, T. Sperger, F. Wesner, S. Fiedler, W7-AS Team et al.:* ICRF Results from W7-AS. In: Proc. 12th Top. Conf. on Radio Frequency Power in Plasmas, Savannah,GA 1997. (Eds.) P.M.Ryan, T.Intrator. AIP Conf. Proc. 403, AIP Press, Woodbury,NJ 1997, 49-56.

120. *Hartmann, D., G. Cattanei, J.F. Lyon*, V. Plyusnin*, ICRH Group and W7-AS Team:* ICRF Experiments on the Stellarator W7-AS. In: Proc. 24th EPS Conf. on Control. Fusion and Plasma Phys., Berchtesgaden 1997, (Eds.) M.Schittenhelm, R.Bartiromo, F.Wagner. ECA 21A. Europ. Phys. Soc., Geneva 1997, 1633-1636.

121. *Heikkinen*, J.A., W. Herrmann and T. Kurki-Suonio*:* The Effect of a Radial Electric Field on Ripple-Trapped Ions Observed by Neutral Particle Fluxes. Physics of Plasmas **4**, 3655-3662 (1997).

122. *Heikkinen*, J.A., W. Herrmann and T. Kurki-Suonio*:* Monte Carlo Simulations of Ripple-Trapped Beam Ions in the Presence of a Non-Uniform Radial Electric Field. In: Proc. 24th EPS Conf. on Control. Fusion and Plasma Phys., Berchtesgaden 1997, (Eds.) M.Schittenhelm, R.Bartiromo, F.Wagner. ECA 21A. Europ. Phys. Soc., Geneva 1997, 1205-1208.

123. *Heikkinen*, J.A., T.P. Kiviniemi*, T. Kurki-Suonio*, W. Herrmann, W. Suttrop et al.:* Ion Orbit Loss Flux in the Presence of a Radial Electric Field. In: Proc. 24th EPS Conf. on Control. Fusion and Plasma Phys., Berchtesgaden 1997, (Eds.) M.Schittenhelm, R.Bartiromo, F.Wagner. ECA 21A. Europ. Phys. Soc., Geneva 1997, 1209-1212.

124. *Heinke, S.:* Forschung und Abfall: Was bringt das Kreislaufwirtschafts- und Abfallgesetz für Forschungseinrichtungen? In: Festschrift für Ernst-Joachim Meusel, (Ed.) M.Winkler. Nomos Verl.Ges., Baden-Baden 1997, 65-74.

125. *Heinrich, O., H. Maaßberg, J. Baldzuhn, S. Fiedler and W7-AS Team:* Role of Recycling to Achieve High $nT\tau_E$ in W7-AS. In: Proc. 24th EPS Conf. on Control. Fusion and Plasma Phys., Berchtesgaden 1997, (Eds.) M.Schittenhelm, R.Bartiromo, F.Wagner. ECA 21A. Europ. Phys. Soc., Geneva 1997, 1593-1596.

126. *Herre, G., R. Schneider, D. Coster, F. Sardei, D. Reiter*, P. Grigull and J. Kißlinger:* A 2-D Approach to Island Divertor Modelling for Wendelstein 7-AS. Journal of Nuclear Materials **241-243**, 941-945 (1997).

127. *Herrmann, A., P. Franzen, W. Herrmann, C. Fuchs, M. Weinlich, ASDEX Upgrade Team, NI Team and ICRH Group:* Energy Deposition at the Divertor Plates during elmy H-Mode and Poloidal and Toroidal Distribution of Heat Load on the Wall in ASDEX Upgrade. In: Proc. 24th EPS Conf. on Control. Fusion and Plasma Phys., Berchtesgaden 1997, (Eds.) M.Schittenhelm, R.Bartiromo, F.Wagner. ECA 21A, Europ. Phys. Soc., Geneva 1997, 1417-1420.

128. *Hidalgo*, C., M.A. Pedrosa*, B. van Milligen*, J. Bleuel, L. Giannone, H. Niedermeyer et al.:* Statistical Properties of Turbulent Transport and Fluctuations in Tokamak and Stellarator Devices. In: Proc. 16th Int. Conf. on Fusion Energy, Montreal 1996, IAEA, Vienna 1997, Vol.1, 617-624.

129. *Hildebrandt, D., R. Brakel, A. Elsner, P. Grigull, R. Burhenn, S. Fiedler, L. Giannone, C. Görner, H. Hacker, H.-J. Hartfuß, A. Herrmann, J.V. Hofmann, G. Kühner, D. Naujoks, F. Sardei, A. Weller, R. Wolf, W7-AS Team, ECRH Group and NI Group:* Plasma Response on Impurity Injection in W7-AS. Journal of Nuclear Materials **241-243**, 950-955 (1997).

130. *Hildebrandt, D., V. Rohde, R. Brakel, A. Elsner, S. Fiedler, J.C. Fuchs, L. Giannone, C. Görner, P. Grigull, H. Hacker, G. Herre, H. Kastelewicz, B. Napiontek, D. Naujoks, R. Neu, W. Suttrop, W7-AS Team and ASDEX Upgrade Team:* Plasma Radiation with Local Impurity Injection into a Magnetic Island of the W7-AS Stellarator and at the Separatrix of AUG Tokamak. In: Proc. 24th EPS Conf. on Control. Fusion and Plasma Phys., Berchtesgaden 1997, (Eds.) M.Schittenhelm, R.Bartiromo, F.Wagner. ECA 21A. Europ. Phys. Soc., Geneva 1997, 1577-1580.

131. *Hirsch, M., E. Holzhauer*, J. Baldzuhn, R. Brakel, S. Fiedler, T. Geist, P. Grigull, H.-J. Hartfuß, J.V. Hofmann, R. Jaenicke, J.P.T. Koponen, F. Wagner, A. Weller, H. Wobig and W7-AS Team:* Dynamic Behaviour of the H-Mode Edge Transport Barrier in the W7-AS Stellarator. In: Proc. 24th Conf. on Control. Fusion and Plasma Phys., Berchtesgaden 1997, (Eds.) M.Schittenhelm, R.Bartiromo, F.Wagner. ECA 21A. Europ. Phys. Soc., Geneva 1997, 1601-1604.

132. *Hirsch, M., E. Holzhauer*, J. Baldzuhn, B. Brañas*, S. Fiedler, J. Geiger, T. Geist, P. Grigull, H.-J. Hartfuß, J.V. Hofmann, R. Jaenicke, J.P.T. Koponen, C. Konrad, J.P.T. Koponen, G. Kühner, W. Pernreiter, F. Wagner, A. Weller, H. Wobig and W7-AS Team:* Edge Transport Barrier and Edge Turbulence during H-Mode Operation in the W7-AS Stellarator. In: Proc. 16th Int. Conf. on Fusion Energy, Montreal 1996, IAEA, Vienna 1997, Vol.2, 315-321.

133. *Hirsch, M., E. Holzhauer*, B. Kurzan, P. Amadeo et al.:* Potential and Limitations of Reflectometry due to Scattering from Density Fluctuations. In: Proc. 3rd Workshop on Microwave Reflectometry for Fusion Plasma Diagnostics, Madrid 1997, (Eds.) J.Sánchez, E.de la Luna. Informes Tecnicos Ciemat 838. Ciemat, Madrid 1997, 21-28.

134. *Hofmeister, F. and ICRH Group:* Matching Fast ICRF Antenna Coupling Variations by Frequency Change. In: Proc. 19th Symp. Fusion Technol., Lisbon 1996, (Eds.) C.Varandas, F.Serra. North-Holland Publ., Amsterdam 1997, 605-608.

135. *Höhn, F., W. Jacob, R. Beckmann and R. Wilhelm:* Transition of a Multipactor to a Low-Pressure Gas Discharge. Physics of Plasmas **4**, 940-944 (1997).

136. *Hu*, G., J.A. Krommes* and J. Bowman:* Statistical Theory of Resistive Drift-Wave Turbulence and Transport. Physics of Plasmas **4**, 2116-2133 (1997).

137. *Inoue*, T., Y. Okumura*, Y. Fujiwara*, B. Heinemann et al.:* Design and R&D of High Power Negative Ion Source/Accelerator for ITER NBI. In: Proc. 19th Symp. Fusion Technol., Lisbon 1996, (Eds.) C.Varandas, F.Serra. North-Holland Publ., Amsterdam 1997, 701-708.

138. *Ishi*, S., J. Biener, C. Lutterloh and J. Küppers:* Applications of H/C Surface Chemistry to Wall Materials in Fusion Devices and Low Pressure Diamond Synthesis. Memoirs of the Tomakomai College of Technology of Japan **32,** 131-139 (1997).

139. *Ishi*, S., A. Horn, K. Pöhlmann*, C. Lutterloh, J. Biener and J. Küppers:* Kinematic Study of Isotope Effect of Erosion Reaction at C: H Film Surfaces. Journal of the Surface Science Society of Japan **18**, 29-32 (1997).

140. *Jacob, W. and P. Pecher:* Quantitative Determination of the Ion- and Neutral Flux to the Substrate in a Methane ECR Plasma. In: Proc. Workshop "Frontiers in Low Temperature Plasma Diagnostics II", Bad Honnef 1997, (Eds.) H.F.Doebele et al. Arbeitsgemein. Plasmaphysik, Bochum 1997, 155-158.

141. *Jahreiß, H.:* ...desto gefälliger und christlicher ist der Kauf. Einkauf einmal anders: als moraltheologisches Problem. In: Festschrift für Ernst-Joachim Meusel, (Ed.) M.Winkler. Nomos Verl.Ges., Baden-Baden 1997, 75-82.

142. *Jaksic, N., J. Simon-Weidner and J. Sapper:* Local Stress Analysis of the W7-X Superconducting Winding Pack. In: Proc. 19th Symp. on Fusion Technolgy, Lisbon 1996, (Eds.) C.Varandas, F.Serra. North-Holland Publ., Amsterdam 1997, 1031-1034.

143. *Jüttner, B.:* Displacement Constants of Arc Cathode Spots in Vacuum at Low and High Currents. In: Proc. 12th Int. Conf. on Gas Discharges and their Applications, Greifswald 1997, (Ed.) G.Babucke. Local Organizing Comm., Greifswald 1997, 18-21.

144. *Jüttner, B.:* The Dynamics of Arc Cathode Spots in Vacuum: New Measurements. Journal of Physics, D **30**, 221-229 (1997).

145. *Kaiser*, R. and A. Salat:* New Classes of Three-Dimensional Ideal-MHD Equilibria. Journal of Plasma Physics **57**, 425-448 (1997).

146. *Kallenbach, A., H.-S. Bosch, S. De Peña Hempel, R. Dux, M. Kaufmann, V. Mertens, J. Neuhauser, W. Suttrop and H. Zohm*:* Possible Divertor Solutions for a Fusion Reactor. Part I: Physical Aspects Based on Present Day Divertor Operation. Fusion Engineering and Design **36**, 101-108 (1997).

147. *Kallenbach, A., R. Dux, A. Bard, S. De Peña Hempel, J.C. Fuchs, A. Gude, H. Salzmann, J. Schweinzer, M. Weinlich and ASDEX Upgrade Team:* Radiative Cooling and Improved Confinement in ASDEX Upgrade. In: Proc. 24th EPS Conf. on Control. Fusion and Plasma Phys., Berchtesgaden 1997, (Eds.) M.Schittenhelm, R.Bartiromo, F.Wagner. ECA 21A. Europ. Phys. Soc., Geneva 1997, 1473-1476.

148. *Kammler*, T. and J. Küppers:* Interaction of Hydrogen Atoms with Coadsorbed D/CH_3I Adlayers on Ni (100) Surfaces: Evidence for Hot Atom Mediated Reactions. Journal of Chemical Physics **107**, 287-290 (1997).

149. *Kammler*, T. and J. Küppers:* Methanation of Carbon on Ni(100) Surfaces at 120 K with Gaseous H Atoms. Chemical Physics Letters **267**, 391-396 (1997).

150. *Kammler*, T., J. Lee* and J. Küppers:* A Kinetic Study of the Interaction of Gaseous H(D) Atoms with D(H) Adsorbed on Ni(100) Surfaces. Journal of Chemical Physics **106**, 7362-7371 (1997).

151. *Kammler*, T., M. Scherl* and J Küppers:* Interaction of H Atoms with Oxygen Adsorbed at Ni(100) Surfaces: Direct Reactions Towards OH and H_2O. Surface Science **382**, 116-126 (1997).

152. *Kappel*, M., M. Steidl*, J. Biener and J. Küppers:* Surface Topography of Low Energy He-Ion-Bombarded Graphite by AFM: Temperature Effects. Surface Science Letters **387**, L1062-L1067 (1997).

153. *Kardaun, O.:* Some Answers to the Questions for Discussion by Prof. D.R. Cox, on Occasion of his Bernoulli Lecture at Groningen, 1997, http://www.ipp.mpg.de/~Otto.Kardaun/rep.html .

154. *Kass, T., S. Günter, M. Maraschek, W. Suttrop, H. Zohm* and ASDEX Upgrade Team:* Characteristics of Type I and Type III ELM Precursors in ASDEX Upgrade. In: Proc. 24th EPS Conf. on Control. Fusion and Plasma Phys., Berchtesgaden 1997, (Eds.) M.Schittenhelm, R.Bartiromo, F.Wagner. ECA 21A. Europ. Phys. Soc., Geneva 1997, 1521-1524.

155. *Kastelewicz, H., D. Reiter*, R. Schneider, D. Coster and H. Meyer:* Plasma Modelling for PSI-1. In: Proc. 24th EPS Conf. on Control. Fusion and Plasma Phys., Berchtesgaden 1997, (Eds.) M.Schittenhelm, R.Bartiromo, F.Wagner. ECA 21A, Europ. Phys. Soc., Geneva 1997, 1805-1808.

156. *Kaufmann, M., J. Schweinzer, M. Albrecht, M. Alexander, K. Asmussen, G. Becker, K. Behler, K. Behringer, R. Behrisch, E. Berger, A. Bergmann, M. Bessenrodt-Weberpals, K. Borrass, H.-S. Bosch, B. Braams*, M. Brambilla, F. Braun, H. Brinkschulte, C. Brosig*, K. Büchl, A. Buhler, H. Callaghan*, A. Carlson, R. Chodura, D. Coster, L. Cupido*, H.J. de Blank, S. de Peña Hempel, S. Deschka, V. Dose, C. Dorn, G. Dodel*, R. Drube, R. Dux, A.S. Egorov*, W. Engelhardt, J. Engstler, H.-U. Fahrbach, U. Fantz*, J.-H. Feist, S. Fiedler, G. Fieg*, A. Field, P. Franzen, J.C. Fuchs, G. Fußmann, J. Gafert, G. Gantenbein*, C. Garcia-Rosales*, O. Gehre, J. Gernhardt, M.T. Grossmann*, O. Gruber, S. Günter, G. Haas, K. Hallatschek, J. Hartmann, B. Heinemann, P. Heimann, A. Herrmann, W. Herrmann, G. Herppich, F. Hertweck, K. Hirsch, S. Hirsch, M. Hoek*, F. Hofmeister, F. Hoenen*, E. Holzhauer*, H. Hohenöcker, P. Ignacz*, D. Jacobi, B. Jüttner, W. Junker, M. Kakoulidis*, A. Kallenbach, V. Kapralov*, N. Karakatsanis*, O. Kardaun, T. Kass, H. Kastelewicz, C.C. Klepper*, H. Kollotzek, W. Köppendörfer, W. Kraus, K. Krieger, B. Kurzan, B.V. Kuteev*, G. Kyriakakis*, K. Lackner, P.T. Lang, R.S. Lang, S. Lashkul*, M. Laux, B. Leblanc*, L. Lengyel, A. Leonard*, F. Leuterer, G. Lieder, C. Loureiro*, J. Maier, R. Maingi*, M.E. Manso*, M. Maraschek, M. Markoulaki*, K.-F. Mast, P. McCarthy*, D. Meisel, H. Meister, R. Merkel, V. Mertens, I. Miroshnikov*, H.W. Müller, F. Münich, H. Murmann, B. Napiontek, D. Naujoks, G. Neu, R. Neu, J. Neuhauser, J.-M. Noterdaeme, M. Niethammer*, L. O'Shea, M.-G. Pacco-Düchs, E. Pasch, G. Pautasso, A.G. Peeters, G. Petravich*, C.S. Pitcher, W. Poschenrieder, I. Precht, F. Puri, G. Raupp, K. Reinmüller, H. Reimerdes, R. Riedl, V. Rohde, H. Röhr, J. Roth, F. Ryter, H. Salzmann, W. Sandmann, J. Santos*, W. Schärich, H.-B. Schilling, M. Schittenhelm, D. Schlögl, H. Schneider, R. Schneider, U. Schneider-Maxon, W. Schneider, K. Schönmann, G. Schramm, U. Schumacher*, T. Schütte, S. Schweizer, R. Schwörer, B. Scott, U. Seidel, S. Sesnic, F. Serra*, A. Silva*, M. Sokoll, P. Spathis*, E. Speth, A. Stäbler, K.-H. Steuer, J. Stober, B. Streibl, W. Suttrop, A. Thoma, C. Tichmann, R. Tisma, W. Treutterer, M. Troppmann, N. Tsois*, M. Ulrich, P. Varela*, I.Y. Veselova*, H. Verbeek, P. Verplancke, O. Vollmer, M.R. Wade*, H. Wedler, U. Wenzel, F. Wesner, M. Weinlich, H. Werthmann, R. Wilhelm, R. Wolf, R. Wunderlich, D. Wutte, N. Xantopoulus*, R. Zanino*, D. Zasche, H.-P. Zehrfeld, T. Zehetbauer, M. Zilker, H. Zohm* and M. Zouhar:* Overview of ASDEX Upgrade Results: In: Proc. 16th Int. Conf. on Fusion Energy, Montreal 1996, IAEA, Vienna 1997, Vol.1, 79-94.

157. *Kaye*, S., M. Greenwald*, U. Stroth, O. Kardaun, A. Kus, D. Schissel* et al.:* ITER L-Mode Confinement Database. Nuclear Fusion **37**, 1303-1328 (1997).

158. *Keudell, A. von:* Surface Reactions during Plasma-Enhanced Chemical Vapor Deposition of Hydrocarbon Films. Nuclear Instruments and Methods in Physics Research, B **125**, 323-327 (1997).

159. *Keudell, A. von, A. Annen and V. Dose:* Multivariate Analysis of Noise Corrupted PECVD Data. Thin Solid Films **307**, 65-70 (1997).

160. *Keudell, A. von and W. Jacob:* Interaction of Hydrogen Plasmas with Hydrocarbon Films, Investigated by Infrared Spectroscopy Using an Optical Cavity Substrate. Journal of Vacuum Science and Technology, A **15**, 402-407 (1997).

161. *Keudell, A. von and W. Jacob:* Surface Relaxation during Plasma-Enhanced Chemical Vapor Deposition of a-C:H Films,

Investigated by in-situ Ellipsometry. Journal of Applied Physics **81**, 1531-1535 (1997).

162. *Keudell, A. von, T. Schwarz-Selinger and W. Jacob:* Surface Relaxation during Plasma Chemical Vapor Deposition of Diamond-Like Carbon Films, Investigated by in-situ Ellipsometry. Thin Solid Films **308-309**, 195-198 (1997).

163. *Khutoretsky*, A., H.-U. Fahrbach, O. Kardaun, J. Stober, Yu.N. Dnestrovskij*, W. Herrmann et al.:* Recovery of Ion Temperature Profiles from the Analysis of Energy-Resolved Neutral-Flux Measurements. Final Report for Grant I/70032 of Volkswagenstiftung, 1-29 (1997).

164. *Kick, M., J. Baldzuhn, J. Geiger, O. Heinrich, R. Jaenicke, A.I. Kislyakov*, G. Kühner, H. Maaßberg, W. Ohlendorf, F.-P. Penningsfeld, N. Rust, A. Weller and W7-AS Team:* High Ion Temperatures and High Beta in W7-AS. In: Proc. 16th Int. Conf. on Fusion Energy, Montreal 1996, IAEA, Vienna 1997, Vol.2, 27-39.

165. *Kick, M., H.-J. Hartfuß, J.V. Hofmann, P. Grigull, H. Ringler, W7-AS Team and W7-X Team:* Overview of W7-X Diagnostics. Fusion Engineering and Design **34-35**, 817-821 (1997).

166. *Knözinger*, H. and E. Taglauer:* Spreading and Wetting. In: Handbook of Heterogeneous Catalysis, (Eds.) G.Ertl, H.Knözinger, J.Weitkamp. VCH Verlagsges., Weinheim 1997, 216-231.

167. *Könies, A.:* Analysis of a Kinetic Energy Principle for a 3D Plasma Equilibrium. In: Proc. 24th EPS Conf. on Control. Fusion and Plasma Phys., Berchtesgaden 1997, (Eds.) M.Schittenhelm, R.Bartiromo, F.Wagner. ECA 21A. Europ. Phys. Soc., Geneva 1997, 1657-1660.

168. *Koponen, J.P.T. and O. Dumbrajs*:* Electron Density Profile Reconstruction from Multichannel Microwave Interferometer Data at W7-AS. Review of Scientific Instruments **68**, 4038-4042 (1997).

169. *Köstlin, T.:* Zur Kompetenzverteilung zwischen Wissenschaft und Verwaltung in der Leitung von Forschungseinrichtungen. In: Festschrift für Ernst-Joachim Meusel, (Ed.) M.Winkler. Nomos Verl.Ges., Baden-Baden 1997, 111-123.

170. *Kraus, W., J.-H. Feist and E. Speth:* Optimization of a Large-Area RF Plasma Generator. In: Proc. 19th Symp. Fusion Technol., Lisbon 1996, (Eds.) C.Varandas, F.Serra. North-Holland Publ., Amsterdam 1997, 649-652.

171. *Krieger, K., K. Asmussen, R. Neu, V. Rohde, J. Roth, R. Schwörer, A. Thoma, ASDEX Upgrade Team, NI Team and ICRH Group:* Erosion and Transport of Tungsten in ASDEX Upgrade. In: Proc. 16th Int. Conf. on Fusion Energy, Montreal 1996, IAEA, Vienna 1997, Vol.1, 817-823.

172. *Krieger, K., H. Maier, V. Rohde, K. Asmussen, M. Balden, D. Coster, J. Roth, R. Schneider, A. Thoma and ASDEX Upgrade Team:* Tungsten Erosion and Migration in ASDEX Upgrade. In: Proc. 24th EPS Conf. on Control. Fusion and Plasma Phys., Berchtesgaden 1997, (Eds.) M.Schittenhelm, R.Bartiromo, F.Wagner. Europ. Phys. Soc., Geneva 1997, 1421-1424.

173. *Krieger, K., V. Rohde, R. Schwörer, K. Asmussen, A. Herrmann, R. Neu, J. Roth, A. Thoma, M. Weinlich and ASDEX Upgrade Team:* Migration of Tungsten Eroded from Divertor Tiles in ASDEX Upgrade. Journal of Nuclear Materials **241-243**, 734-738 (1997).

174. *Krieger, K., J. Roth, A. Annen, W. Jacob, C.S. Pitcher, W. Schneider, A. Thoma, M. Weinlich and ASDEX Upgrade Team:* Study of Gross and Net Erosion in the ASDEX Upgrade Divertor. Journal of Nuclear Materials **241-243**, 684-689 (1997).

175. *Kristof*, G. and L. Lengyel:* Two-Fluid MHD Simulation of Confinement of Pellet-Produced Hydrogen Clouds in Hot Magnetized Plasmas. In: Proc. 24th EPS Conf. on Control. Fusion and Plasma Phys., Berchtesgaden 1997, (Eds.) M.Schittenhelm, R.Bartiromo, F.Wagner. ECA 21A. Europ. Phys. Soc., Geneva 1997, 1553-1556.

176. *Kronhardt*, H., K.-D. Herrmann*, W. Broocks* and M. Pillsticker:* Determination of Compound Properties for Superconducting Magnets by Combined Theoretical and Experimental Methods. In: Proc. 19th Symp. Fusion Technol., Lisbon 1996, (Eds.) C.Varandas, F.Serra. North-Holland Publ., Amsterdam 1997, 1007-1010.

177. *Kubota*, T., T. Iwasaki*, S. Itoh*, U. Stroth et al.:* Avalanche Dynamics of Collapse and Non-Local Model of Transport. In: Proc. 24th EPS Conf. on Control. Fusion and Plasma Phys., Berchtesgaden 1997, (Eds.) M.Schittenhelm, R.Bartiromo, F.Wagner. ECA 21A. Europ. Phys. Soc., Geneva 1997, 1769-1772.

178. *Kühner, G., J.P. Knauer and H. Ringler:* Probing f_e (v) by Thomson Scattering on W7-X. Review of Scientific Instruments **68**, 732-734 (1997).

179. *Kukushkin*, A., H.D. Pacher, V. Abramov*, M. Baelmans*, H.-S. Bosch, D. Boucher*, B. Braams*, D. Coster, J. Neuhauser, R. Schneider et al.:* Analysis of ITER Divertor Performance and ITER Tokamak Edge Parameter Database. In: Proc. 16th Int. Conf. on Fusion Energy, Montreal 1996, IAEA, Vienna 1997, Vol.2, 987-993.

180. *Kukushkin*, A., H.D. Pacher, D. Coster, G. Janeschitz, D. Reiter* and R. Schneider:* Effect of Light Impurities on the Divertor Performance in ITER. In: Proc. 24th EPS Conf. on Control. Fusion and Plasma Phys., Berchtesgaden 1997, (Eds.) M.Schittenhelm, R.Bartiromo, F.Wagner. ECA 21A. Europ. Phys. Soc., Geneva 1997, 1001-1004.

181. *Kupschus*, P., J.C.M. de Haas*, L. Horton*, M. Gadeberg*, P.T. Lang et al.:* Experiments on Plasma Fuelling and ELM Control by Pellet Injection on JET. In: Proc. 24th EPS Conf. on Control. Fusion and Plasma Phys., Berchtesgaden 1997, (Eds.) M.Schittenhelm, R.Bartiromo, F.Wagner. ECA 21A. Europ. Phys. Soc., Geneva 1997, 45-48.

182. *Kurzan, B., T. Kass, M. Maraschek, J. Schweinzer, A. Silva*, W. Suttrop, ASDEX Upgrade Team, ICRH Group and NI Team:* Characterization of EdgeTurbulence in Neutral Beam Injection and Ion Cyclotron Resonance Heated Plasmas in ASDEX Upgrade. In: Proc. 24th EPS Conf. on Control. Fusion and Plasma Phys., Berchtesgaden 1997, (Eds.) M.Schittenhelm, R.Bartiromo, F.Wagner. ECA 21A. Europ. Phys. Soc., Geneva 1997, 1505-1508.

183. *Kurzan, B. and K.-H. Steuer:* Runaway Electrons in a Tokamak: A Free-Electron Maser. Physical Review E **55**, 4608-4616 (1997).

184. *Kurzan, B., K.-H. Steuer and W. Suttrop:* Runaway Electrons in a Tokamak: A Free-Electron Maser. Review of Scientific Instruments **68**, 423-426 (1997).

185. *Kus, A. and O. Kardaun:* SAS in der fusionsorientierten Plasmaphysik. In: Proc. 1. Konferenz der SAS-Benutzer in Forschung und Entwicklung, Berlin 1997, (Ed.) W.F.Lesener. Rechenzentrum Humboldt-Univ. Berlin 1997, 313-325.

186. *Lang, P.T., K. Büchl, M. Kaufmann, R.S. Lang, V. Mertens, H.W. Müller, J. Neuhauser, ASDEX Upgrade Team and NI Team:* High-Efficiency Plasma Refuelling by Pellet Injection from the Magnetic High-Field Side into ASDEX Upgrade. Physical Review Letters **79**, 1487-1490 (1997).

187. *Lang, P.T., K. Büchl, M. Kaufmann, R.S. Lang, V. Mertens, H.W. Müller, J. Neuhauser, F. Ryter and ASDEX Upgrade Team:*

Pellet Refueling from the Magnetic High Field Side. In: Proc. 24th EPS Conf. on Control. Fusion and Plasma Phys., Berchtesgaden 1997, (Eds.) M.Schittenhelm, R.Bartiromo, F.Wagner. ECA 21A. Europ. Phys. Soc., Geneva 1997, 1481-1484.

188. *Lang, P.T., P. Cierpka and P. Kupschus*:* High Repetitive Pellet Injectors for Plasma Density Control. In: Proc. 19th Symp. on Fusion Technol., Lisbon 1997, (Eds.) C.Varandas, F.Serra. North-Holland Publ., Amsterdam 1997, 1129-1132.

189. *Langhoff, M. and B.M.U. Scherzer:* The Hydrogen Inventory in Plasma Exposed Graphite Surfaces. Journal of Nuclear Materials **245**, 60-65 (1997).

190. *Laqua, H.P., V. Erckmann, H.-J. Hartfuß, H. Laqua, W7-AS Team and ECRH Group:* Resonant and Non-Resonant Electron Cyclotron Heating at Densities above the Plasma Cut-off by O-X-B Mode Conversion at the W7-AS Stellarator. Physical Review Letters **78**, 3467-3470 (1997).

191. *Laqua, H.P., V. Erckmann, W7-AS Team and ECRH Group:* Resonant Electron Bernstein Wave Heating via Mode Conversion in W7-AS. In: Proc. 24th EPS Conf. on Control. Fusion and Plasma Phys., Berchtesgaden 1997, (Eds.) M.Schittenhelm, R.Bartiromo, F.Wagner. ECA 21A. Europ. Phys. Soc., Geneva 1997, 1641-1644.

192. *Laux, M., A. Herrmann., V. Rohde and U. Wenzel:* Impurity Concentration as a Critical Parameter in a Diverted Scrape-off Layer. In: Proc. 24th EPS Conf. on Control. Fusion and Plasma Phys., Berchtesgaden 1997, (Eds.) M.Schittenhelm, R.Bartiromo, F.Wagner. ECA 21A. Europ. Phys. Soc., Geneva 1997, 1445-1448.

193. *Lederer, H.:* Hochleistungs-Parallelrechner installiert - Massiv-paralleles Rechnen: vor ein paar Jahren noch unwägbares Risiko, heute schon unverzichtbar für die Grundlagenforschung. MPG-Spiegel 1, 14-19 (1997).

194. *Lederer, H.:* Visuelles Supercomputing über eine 14000 km lange Netzverbindung. MPG-Spiegel 5/6, 54-55 (1997).

195. *Lengyel, L., V.A. Rozhansky* and I.Y. Veselova*:* Drift Motion in the Scrape-off Layer during Hard Disruptions. In: Proc. 24th EPS Conf. on Control. Fusion and Plasma Phys., Berchtesgaden 1997, (Eds.) M.Schittenhelm, R.Bartiromo, F.Wagner. ECA 21A. Europ. Phys. Soc., Geneva 1997, 1549-1552.

196. *Lengyel, L.L., V.A. Rozhansky*, I.Y. Veselova* and P.J. Lalousis*:* Drift Motion in the Scrape-off Layer during Hard Disruptions. Nuclear Fusion **37**, 1245-1253 (1997).

197. *Leuterer F., A.G. Peeters, G. Pereverzev, F. Ryter and ASDEX Upgrade Team:* Localized ECRH Power Deposition in ASDEX Upgrade. In: Proc. 24th EPS Conf. on Control. Fusion and Plasma Phys., Berchtesgaden 1997, (Eds.) M.Schittenhelm, R.Bartiromo, F.Wagner. ECA 21A. Europ. Phys. Soc., Geneva 1997, 1533-1536.

198. *Linden, W. von der, V. Dose, R. Matzdorf* et al.:* Improved Resolution in HREELS Using Maximum-Entropy Deconvolution: CO on $Pt_xNi_{1-x}(111)$. Journal of Electron Spectroscopy and Related Phenomena **83**, 1-7 (1997).

199. *Lingertat*, J., A. Tabasso*, S. Ali-Arshad*, B. Alper*, P. van Belle*, K. Borrass et al.:* Studies of Giant ELM Interaction with the Divertor Target in JET. Journal of Nuclear Materials **241-243**, 402-407 (1997).

200. *Lortz, D.:* Stability of Axisymmetric Modes in Plasma-Vacuum Equilibria. Journal of Plasma Physics **58**, 655-664 (1997).

201. *Lyon*, J.F., L.R. Baylor*, J. Baldzuhn, S. Fiedler, M. Hirsch, G. Kühner and A. Weller:* Analysis of D Pellet Injection Experiments in the W7-AS Stellarator. In: Proc. 24th EPS Conf. on Control. Fusion and Plasma Phys., Berchtesgaden 1997, (Eds.) M.Schittenhelm, R.Bartiromo, F.Wagner. ECA 21A. Europ. Phys. Soc., Geneva 1997, 1629-1632.

202. *Maaßberg, H., J. Baldzuhn, C.D. Beidler, V. Erckmann, U. Gasparino, M. Romé, W7-AS Team et al.:* The Neoclassical "Electron-Root" Feature in W7-AS. In: Proc. 24th EPS Conf. on Control. Fusion and Plasma Phys., Berchtesgaden 1997, (Eds.) M.Schittenhelm, R.Bartiromo, F.Wagner. ECA 21A, Europ. Phys. Soc., Geneva 1997, 1605-1608.

203. *MacFarland T., J. Pichlmeier*, F. Pearce* et al.:* MP Hydra: A Parallel P3M Code for Very Large Scale Cosmological Simulations. In: Proc. 3rd Europ. Cray-SGI MPP Workshop, Paris 1997, http://armoise.saclay.cea.fr/~workshop/Documents/Final_Papers/Tom_MacFarland_12_Best_Paper.ps.

204. *Maingi*, R., B. Terreault*, G. Haas, G.L. Jackson*, W. Zuzak*, P.K. Mioduszewski*, A. Mahdavi*, M.R. Wade*, S. Chiu*, M.J. Schaffer*, J.T. Hogan* and C.C. Klepper*:* Comparison of Wall/Divertor Deuterium Retention and Plasma Fueling Requirements on the DIII-D, TdeV and ASDEX Upgrade Tokamaks. Journal of Nuclear Materials **241-243**, 672-677 (1997).

205. *Manso*, M.E., J. Santos*, I. Nunes*, F. Nunes*, B. Kurzan, F. Serra*, A. Silva*, W. Suttrop et al.:* Broadband Reflectometry to Investigate Profiles and Fluctuations during ELMs on ASDEX Upgrade. In: Proc. 24th EPS Conf. on Control. Fusion and Plasma Phys., Berchtesgaden 1997, (Eds.) M.Schittenhelm, R.Bartiromo, F.Wagner. ECA 21A. Europ. Phys. Soc., Geneva 1997, 1489-1492.

206. *Manso*, M.E., F. Serra*, J. Santos*, B. Kurzan, W. Suttrop et al.:* Density Profile and Fluctuation Measurements with Microwave Reflectometry on ASDEX Upgrade. In: Proc. 3rd Workshop on Microwave Reflectometry for Fusion Plasma Diagnostics, Madrid 1997, (Eds.) J.Sánchez, E.de la Luna. Informes Tecnicos Ciemat 838. Ciemat, Madrid 1997, 65-75.

207. *Maraschek, M., S. Günter, T. Kass, B. Scott and ASDEX Upgrade Team:* Observation of Toroidicity-Induced Alfvén Eigenmodes in Ohmically Heated Plasmas by Drift Wave Excitation. Physical Review Letters **79**, 4186-4189 (1997).

208. *Maraschek, M., S. Günter, T. Kass, B. Scott, H. Zohm* and ASDEX Upgrade Team:* Observation of TAE-Modes in Ohmically Heated Plasmas by Drift Wave Excitation. In: Proc. 24th EPS Conf. on Control. Fusion and Plasma Phys., Berchtesgaden 1997, (Eds.) M.Schittenhelm, R.Bartiromo, F.Wagner. ECA 21A. Europ. Phys. Soc., Geneva 1997, 1525-1528.

209. *Marushchenko*, N., U. Gasparino, H. Maaßberg and M. Romé:* Bounce-Averaged Fokker-Planck Code for the Description of ECRH in a Periodic Magnetic Field. Computer Physics Communications **103**, 145-156 (1997).

210. *Mast, K.-F., J.C. Fuchs, M. Allgäuer, P.T. Lang, M. Münch, R. Reichle*, G. Schramm, G. Weber et al.:* Miniaturisiertes breitbandiges Bolometerarray. Technisches Messen **64**, 164-171 (1997).

211. *Matthews*, G.F., S. Allen*, N. Asakura*, A. Kallenbach, K. McCormick, K-H. Steuer et al.:* Scaling Radiative Plasmas to ITER. Journal of Nuclear Materials **241-243**, 450-455 (1997).

212. *Matthews*, G.F., B. Balet*, J.G. Cordey*, A. Kallenbach et al:* ρ^* Scaling in Radiative Plasma Regimes. In: Proc. 24th EPS Conf. on

Control. Fusion and Plasma Phys., Berchtesgaden 1997, (Eds.) M.Schittenhelm, R.Bartiromo, F.Wagner. ECA 21A. Europ. Phys. Soc., Geneva 1997, 1045-1048.

213. *Mayer, M.:* Codeposition of Deuterium with BeO at Elevated Temperatures. Journal of Nuclear Materials **240**, 164-167 (1997).

214. *Mayer, M., R. Behrisch, P. Andrew* et al.:* Erosion at the Vessel Walls of JET. Journal of Nuclear Materials **241-243**, 469-475 (1997).

215. *McCormick, K., A. Chankin*, S. Clement*, S. Davies* et al.:* Derivation of SOL Transport Coefficients Using 2-D Modelling for Hot-Ion ELM-Free H-Modes in JET. Journal of Nuclear Materials **241-243**, 444-449 (1997).

216. *McCormick, K., S. Fiedler, G. Kocsis*, J. Schweinzer and S. Zoletnik*:* Edge Density Measurements with a Fast Li-Beam Probe in Tokamak and Stellarator Experiments. Fusion Engineering and Design **34-35,** 125-134 (1997).

217. *Memmel, N.:* Magnitude of the sp-Derived Surface-State Contribution to the Magnetic Moment of Ni(111). Physical Review, B **55**, 5634-5635 (1997).

218. *Memmel, N. and E. Bertel:* Elektronische Oberflächenzustände an Metallen - Ursache und Bedeutung. Physikalische Blätter **53**, 323-328 (1997).

219. *Merkel, P., C. Nührenberg and W.A. Cooper*:* Freeboundary Ideal MHD Modes in W7-AS. In: Proc. Joint Varenna-Lausanne Int. Workshop on Theory of Fusion Plasmas, Varenna 1996, (Eds.) J.W.Connor, E.Sindoni, J.Vaclavik. Ed. Compositori, Bologna 1997, 233-240.

220. *Mertens, V., C. Aubanel, O. Gruber, M. Kaufmann, G. Neu, G. Raupp, H. Richter, W. Treutterer, D. Zasche, T. Zehetbauer, ASDEX Upgrade Team, NI Team and ICRH Group:* Plasma Performance Optimization in ASDEX Upgrade. Fusion Technology **32**, 459-467 (1997).

221. *Mertens, V., H.-S. Bosch, M. Kaufmann, M. Maraschek, J. Neuhauser, H. Salzmann, J. Schweinzer, W. Suttrop and ASDEX Upgrade Team:* Edge Profile Investigations Close to the Density Limit of Various Plasma Regimes in ASDEX Upgrade. In: Proc. 24th EPS Conf. on Control. Fusion and Plasma Phys., Berchtesgaden 1997, (Eds.) M.Schittenhelm, R.Bartiromo, F.Wagner. ECA 21A. Europ. Phys. Soc., Geneva 1997, 1389-1392.

222. *Mertens, V., M. Kaufmann, J. Neuhauser, J. Schweinzer, J. Stober, K. Büchl, O. Gruber, G. Haas, A. Herrmann, A. Kallenbach, M. Weinlich and ASDEX Upgrade Team:* High Density Operation Close to Greenwald Limit and H-Mode Limit in ASDEX Upgrade. Nuclear Fusion **37**, 1607-1614 (1997).

223. *Meyer-Spasche, R. and D.F. Düchs:* A General Method for Obtaining Unconventional and Nonstandard Difference Schemes. Dynamics of Continuous, Discrete and Impulsive Systems **3**, 453-467 (1997).

224. *Meyer-Spasche, R. and K. Grote:* Dynamical Properties of a Linearly Implicit Scheme. In: Proc 15th IMACS World Congress on Scientific Computation, Modelling and Applied Mathematics, München 1997, (Ed.) A.Sydow. Verl. Wiss.u.Technik, Berlin 1997, Vol.2, 581-586.

225. *Meyer-Spasche, R., M. Rast and C. Zenger (Eds.):* Nichtlineare Dynamik, Chaos und Strukturbildung. Faktum 13. Akad. Verl., München 1997, 216 S.

226. *Mikhailov*, M.I., V.D. Shafranov* and D. Sünder:* Two Problems of the Plasma Confinement in Stellarators. In: Proc. 24th EPS Conf. on Control. Fusion and Plasma Phys., Berchtesgaden 1997, (Eds.) M.Schittenhelm, R.Bartiromo, F.Wagner. ECA 21A, Europ. Phys. Soc., Geneva 1997, 765-768.

227. *Milch, I.:* Wärmeschub bei Wendelstein. HGF Jahresheft, 9-10 (1997).

228. *Miller, S., G.L.P. Berning*, H. Plank and J. Roth:* X-Ray Photoelectron Spectroscopy Study of TiC Films Grown by Annealing Thin Ti Films on Graphite. Journal of Vacuum Science and Technology, A **15**, 2029-2034 (1997).

229. *Miller, S., R. Fischer, H. Plank, J. Roth and V. Dose:* Characterization of the Temperature Dependent Phase Transition of Evaporated Ti Films on Diamond: Phase Identification Using Maximum Entropy Data Analysis. Journal of Applied Physics **82**, 3314-3320 (1997).

230. *Müller, H.W., P.T. Lang, K. Büchl, M. Kaufmann, B.V. Kuteev*, P. McCarthy*, V. Mertens, I. Miroshnikov*, W. Schneider, H. Zohm* and ASDEX Upgrade Team:* Improvement of q-Profile Measurement by Fast Observation of Pellet Ablation at ASDEX Upgrade. Review of Scientific Instruments **68**, 4051-4060 (1997).

231. *Murakami*, S., N. Nakajima*, U. Gasparino et al.:* Simulation Study of Radial Electric Field in CHS and LHD. Plasma Physics Reports **23**, 512-516 (1997).

232. *Murakami*, S., N. Nakajima*, S. Okamura*, U. Gasparino et al.:* Orbit Effects of Energetic Particles on the Reachable b-Value and the Radial Electric Field in NBI and ECR Heated Heliotron Plasmas. In: Proc. 16th Int. Conf. on Fusion Energy, Montreal 1996, IAEA, Vienna 1997, Vol.2, 157-165.

233. *Nakajima*, N., M. Yokoyama*, M. Okamoto* and J. Nührenberg:* Optimization of M=2 Stellarator. Plasma Physics Reports **23**, 460-471 (1997).

234. *Napiontek, B., U. Wenzel, K. Behringer, D. Coster, J. Gafert, R. Schneider, A. Thoma, M. Weinlich and ASDEX Upgrade Team:* Line and Recombination Emission in the ASDEX Upgrade Divertor at High Density. In: Proc. 24th EPS Conf. on Control. Fusion and Plasma Phys., Berchtesgaden 1997, (Eds.) M.Schittenhelm, R.Bartiromo, F.Wagner. ECA 21A. Europ. Phys. Soc., Geneva 1997, 1413-1416.

235. *Naujoks, D.:* Criterion for Zero NET-Erosion at Divertor Plates in Fusion Experiments. Nuclear Fusion **37**, 1193-1197 (1997).

236. *Naujoks, D., P. Bachmann and D. Sünder:* Monte Carlo Modelling of the Transport in the Stellarator Pheriphery with Magnetic Islands. Journal of Nuclear Materials **241-243,** 925-929 (1997).

237. *Naujoks, D., J. Steinbrink, U. Wenzel and PSI-1 Group:* Spatial Distributions of Neutral Atoms in the Near-Target Plasma: Theory and Experiment. Journal of Nuclear Materials **241-243**, 707-711 (1997).

238. *Neu, R., K. Asmussen, S. Deschka, A. Thoma, M. Bessenrodt-Weberpals, R. Dux, W. Engelhardt, J.C. Fuchs, J. Gafert, A. Herrmann, K. Krieger, K.-F. Mast, J. Roth, V. Rohde, M. Weinlich, U. Wenzel, ASDEX Upgrade Team, NI Team et al.:* The Tungsten Experiment in ASDEX Upgrade. Journal of Nuclear Materials **241-243**, 678-683 (1997).

239. *Neu, R., K.B. Fournier*, D. Schlögl and J. Rice*:* Observation of X-Ray Spectra from Highly Charged Tungsten Ions in Tokamak Plasmas. Journal of Physics, B **30**, 5057-5067 (1997).

240. *Noda*, N., V. Philipps* and R. Neu:* A Review of Recent Experiments on W and High-Z Materials as Plasma-Facing Components in Magnetic Fusion Devices. Journal of Nuclear Materials **241-243**, 227-243 (1997).

241. *Ott, W., F.-P. Penningsfeld, W. Melkus, F. Probst, E. Speth, R. Süss and W7-AS Team:* Upgrading of the Injection Power of the W7-AS Neutral Beam System. In: Proc. 19th Symp. Fusion Technol., Lisbon 1996, (Eds.) C.Varandas, F.Serra. North-Holland Publ., Amsterdam 1997, 641-644.

242. *Peeters, A.G., H. Salzmann, O. Gehre, F. Ryter, W. Suttrop, B. Brüsehaber and ASDEX Upgrade Team:* Particle Transport Determined from Modulated Gas Puff. In: Proc. 24th EPS Conf. on Control. Fusion and Plasma Phys., Berchtesgaden 1997, (Eds.) M.Schittenhelm, R.Bartiromo, F. Wagner. ECA 21A. Europ. Phys. Soc., Geneva 1997, 1469-1472.

243. *Pereverzev, G.:* Beam Tracing of Electromagnetic Waves in Inhomogeneous Plasmas. In: Proc. 24th EPS Conf. on Control. Fusion and Plasma Phys., Berchtesgaden 1997, (Eds.) M.Schittenhelm, R.Bartiromo, F.Wagner. ECA 21A. Europ. Phys. Soc., Geneva 1997, 1801-1804.

244. *Perkins*, F.W., D. Post*, M. Rosenbluth*, O. Sauter*, K. Borrass, D.J. Campbell*, J.G. Cordey*, M. Greenwald*, T.C. Hender*, Y. Kamada*, R. LaHaye*, A. Mahdavi*, A.W. Morris*, V. Mertens, J. Neuhauser, T.S. Taylor*, H.R. Wilson*, R. Yoshino*, H. Zohm* and ITER Joint Central Team:* ITER Operational Limits. In: Proc. 16th Int. Conf. on Fusion Energy, Montreal 1996, IAEA, Vienna 1997, Vol.2, 963-969.

245. *Pfirsch, D. and D. Correa-Restrepo:* Lagrangian for Plasmas in the Drift-Fluid Approximation. Plasma Physics and Controlled Fusion **39**, 555-558 (1997).

246. *Pinches, S.D., S. Günter, M. Maraschek and ASDEX Upgrade Team:* TAE Studies in ASDEX Upgrade. In: Proc. 24th EPS Conf. on Control. Fusion and Plasma Phys., Berchtesgaden 1997, (Eds.) M.Schittenhelm, R.Bartiromo, F.Wagner. ECA 21A. Europ. Phys. Soc., Geneva 1997, 1557-1560.

247. *Pinkau, K.:* Energie aus Kernfusion. Atomwirtschaft, Atomtechnik **42**, 145-216 (1997).

248. *Pinkau, K.:* Internationale Großprojekte, ihre Begründung, Entstehung, Arbeitsweise und ihre Auswirkungen. MPG Berichte und Mitteilungen **1**, 232-246 (1997).

249. *Pinkau, K.:* Neue Energiequellen: Mit Hilfe von Fusionsforschung aus Meerwasser Strom gewinnen. Position 03, Bundesverb. Dt. Ind., Köln 1997, 10-11.

250. *Pinkau, K.:* Die offene Gesellschaft und ihre Wissenschaft. In: Wissenschaft - Staat - Gesellschaft, (Ed.) IPP. Garching 1997, 41-49.

251. *Pinkau, K.:* Von internationalen Forschungszentren (CERN, ILL, JET) zu multinationalen Einrichtungen. In: Wünsche an das künftige Wissenschaftssystem, (Ed.) IPP. Garching 1997, 36-41.

252. *Pitcher, C.S., A.H. Boozer*, H. Murmann, J. Schweinzer, W. Suttrop, H. Salzmann, ASDEX Upgrade Team and NI Group:* The Relation of Edge Confinement to Global Confinement in ASDEX Upgrade (Axially Symmetric Divertor Experiment). Physics of Plasmas **4**, 2577-2583 (1997).

253. *Pitcher, C.S., A. Carlson, C. Fuchs, A. Herrmann, W. Suttrop, J. Schweinzer, M. Weinlich, ASDEX Upgrade Team and NI Group:* Routes to Divertor Detachment in ASDEX Upgrade. Journal of Nuclear Materials **241-243**, 696-700 (1997).

254. *Pitcher, C.S., A. Herrmann, H. Murmann, H. Reimerdes, J. Schweinzer, W. Suttrop, H. Salzmann, ASDEX Upgrade Team and NI Group:* Heat Transport at the Boundary of ASDEX Upgrade. Plasma Physics and Controlled Fusion **39**, 1129-1144 (1997).

255. *Plamann, K. and R. Behrisch:* Elastic Recoil Detection Analysis (ERDA) of Thick Films. Nuclear Instruments and Methods in Physics Research, B **129**, 501-510 (1997).

256. *Plank, H. and W. Eckstein:* Preferential Sputtering of Carbides under Deuterium Irradiation - a Comparison between Experiment and Computer Simulation. Nuclear Instruments and Methods in Physics Research, B **124**, 23-30 (1997).

257. *Prozesky*, V.M., J. Padayachee*, R. Fischer, W. von der Linden, V. Dose et al.:* The Use of Maximum Entropy and Bayesian Statistics in Ion-Beam Applications. In: Application of Accelerators in Research and Industry, (Eds.) J.L.Duggan, I.L.Morgan. AIP Press, New York 1997, 595-598.

258. *Raupp, G., O. Gruber, A. Kallenbach, V. Mertens, G. Neu, B. Streibl, W. Treutterer, T. Zehetbauer, D. Zasche and ASDEX Upgrade Team:* Discharge Supervision Control on ASDEX Upgrade. Fusion Technology **32**, 444-458 (1997).

259. *Raupp, G., K. Lüddecke, G. Neu, W. Treutterer, D. Zasche, T. Zehetbauer and ASDEX Upgrade Team:* Structure for Next Generation Discharge Control Systems. In: Proc. 19th Symp. on Fusion Technol., Lisbon 1997, (Eds.) C.Varandas, F.Serra. North-Holland Publ., Amsterdam 1997, 929-932.

260. *Reichle*, R., J.K. Ehrenberg*, N.A.C. Gottardi*, K. McCormick et al.:* Low Energy Neutral Fluxes in the JET Divertor. Journal of Nuclear Materials **241-243**, 456-461 (1997).

261. *Reiman*, A.H., L.P. Ku*, D.A. Monticello*, C. Nührenberg et al.:* MHD Calculations for MHH2. Plasma Physics Reports **23**, 472-482 (1997).

262. *Reinmüller, K. and A. Bergmann:* 2-D PIC Simulation of Hot Spot Formation on Target Plates and of Current Flow to Flat Langmuir Probes. In: Proc. 24th EPS Conf. on Control. Fusion and Plasma Phys., Berchtesgaden 1997, (Eds.) M.Schittenhelm, R.Bartiromo, F.Wagner. ECA 21A. Europ. Phys. Soc., Geneva 1997, 1441-1444.

263. *Reinmuth, J., F. Passek, V.N. Petrov*, M. Donath et al.:* Spin-Dependent Local Density of Empty Electronic States in $FeNi_3$. Physical Review, B **56**, 12893-12898 (1997).

264. *Renner, H., E. Strumberger, J. Kißlinger, J. Nührenberg and H. Wobig:* Boundary Modelling of the Stellarator Wendelstein 7-X. Journal of Nuclear Materials **241-243**, 946-949 (1997).

265. *Richter, H.:* Verbindungsnetzwerke für parallele und verteilte Systeme. Spektrum Akad. Verl., Heidelberg, 1997, 322 S.

266. *Rogers*, B.N., J.F. Drake*, Y.T. Lau*, P.N. Guzdar*, A.B. Hassam*, S.V. Novakovskii* and A. Zeiler:* Turbulence and the Formation of Transport Barriers in Finite Beta Tokamaks In: Proc. 16th Int. Conf. on Fusion Energy, Montreal 1996, IAEA, Vienna 1997, Vol.2, 361-370.

267. *Rohde, V., M. Laux, P. Bachmann, A. Herrmann, M. Weinlich and ASDEX Upgrade Team:* Direct Measurement of the Plasma Potential in the Edge of ASDEX Upgrade Using a Self Emitting Probe. Journal of Nuclear Materials **241-243**, 712-715 (1997).

268. *Romé, M., V. Erckmann, U. Gasparino, H.-J. Hartfuß, G. Kühner, H. Maaßberg and N. Marushchenko*:* Kinetic Modelling of the ECRH Power Deposition in W7-AS. Plasma Physics and Controlled Fusion **39**, 117-158 (1997).

269. *Romé, M., U. Gasparino, H. Maaßberg, N. Marushchenko*, S. Murakami*, N. Nakajima* et al.:* Kinetic Description of Low Density ECRH Discharges at W7-AS. In: Proc. Joint Varenna-Lausanne Int. Workshop Theory of Fusion Plasmas, Varenna 1996. (Eds.) J.W.Connor, E.Sindoni, J.Vaclavik. Ed. Compositori, Bologna 1997, 315-320.

270. *Roth, J., W. Eckstein and M. Guseva*:* Erosion of Be as Plasma-Facing Material. Fusion Engineering and Design **37**, 465-480 (1997).

271. *Roth, J., W.R. Wampler* and W. Jacob:* Release of Deuterium from Carbon-Deuterium Films on Beryllium during Carbide Formation and Oxidation. Journal of Nuclear Materials **250**, 13-22 (1997).

272. *Rust, N., G. Beikert, K. Hübner*, M. Kick, F.-P. Penningsfeld, U. Stroth and B. Wolle*:* Simulation and Analysis of Neutral Particle Spectra for W7-AS in Combination with Neutron Activation Measurements. In: Proc. 24th EPS Conf. on Control. Fusion and Plasma Phys., Berchtesgaden 1997, (Eds.) M.Schittenhelm, R.Bartiromo, F.Wagner. ECA 21A. Europ. Phys. Soc., Geneva 1997, 1621-1624.

273. *Ryter, F., M. Alexander, O. Gruber, O. Vollmer, G. Becker, O. Gehre, K.W. Gentle*, K. Lackner, F. Leuterer, A.G. Peeters, H. Murmann, S. De Peña Hempel, G. Pereverzev, H. Salzmann, J. Schweinzer, W. Suttrop, ASDEX Upgrade Team, ECRH Group and NI Team:* Confinement and Transport Studies in ASDEX Upgrade. In: Proc. 16th Int. Conf. on Fusion Energy, Montreal 1996, IAEA, Vienna 1997, Vol.1, 625-632.

274. *Ryter, F., F. Leuterer, G. Pereverzev, J.C. Fuchs, J. Schweinzer, W. Suttrop and ASDEX Upgrade Team:* Physics of Perturbative Transport from Sawtooth Propagation and ECRH Modulation in ASDEX Upgrade. In: Proc. 24th EPS Conf. on Control. Fusion and Plasma Phys., Berchtesgaden 1997, (Eds.) M.Schittenhelm, R.Bartiromo and F.Wagner. ECA 21A. Europ. Phys. Soc., Geneva 1997, 1477-1480.

275. *Saibene*, G., B. Balet*, S. Clement*, B. de Esch*, G. Fishpool*, J.C.M. de Haas*, G. Haas et al.:* Steady State H-Modes at High Plasma Density in JET. In: Proc. 24th EPS Conf. on Control. Fusion and Plasma Phys., Berchtesgaden 1997, (Eds.) M.Schittenhelm, R.Bartiromo, F.Wagner. ECA 21A. Europ. Phys. Soc., Geneva 1997, 49-52.

276. *Salat, A. and J.A. Tataronis*:* The Shear Alfvén Continuum in an Asymmetric MHD Equilibrium. Physics of Plasmas **4**, 3770-3782 (1997).

277. *Salat, A. and J.A. Tataronis*:* The Shear Alfvén Continuum of an Ideal MHD Equilibrium without Spatial Symmetry. In: Proc. 24th EPS Conf. on Control. Fusion and Plasma Phys., Berchtesgaden 1997, (Eds.) M.Schittenhelm, R.Bartiromo, F.Wagner. ECA 21A. Europ. Phys. Soc., Geneva 1997, 1653-1656.

278. *Sardei, F., Y. Feng, P. Grigull, G. Herre, D. Hildebrandt, J.V. Hofmann, J. Kißlinger, R. Brakel, J. Das, J. Geiger, O. Heinrich, G. Kühner, H. Niedermeyer, D. Reiter*, M. Richter-Glötzl, A. Runov*, R. Schneider, U. Stroth, H. Verbeek, F. Wagner, R. Wolf, W7-AS Team and NI Group:* Island Divertor Studies on W7-AS. Journal of Nuclear Materials **241-243**, 135-148 (1997).

279. *Saß, M., A. Annen and W. Jacob:* Hydrogen Bonding in Plasma-Deposited Amorphous Hydrogenated Boron Films. Journal of Applied Physics **82**, 1905-1908 (1997).

280. *Schneider, F.:* Real Time Control of the Wendelstein Fusion Experiment W7-AS. In: Proc. Europ. Studies on Norms for Electronics, PC Technology in Real Time and Controls, Geneva 1997, (Eds.) D.Notz, C.Parkman. CERN, Geneva 1997, 31-49.

281. *Schneider, R., H.-S. Bosch, J. Neuhauser, D. Coster, K. Lackner and M. Kaufmann:* Divertor Geometry Optimization for ASDEX Upgrade. Journal of Nuclear Materials **241-243**, 701-706 (1997).

282. *Schneider, R., D. Coster, K. Borrass, H.-S. Bosch, J. Neuhauser, K. Lackner, M. Kaufmann, A. Kallenbach, K. Behringer, K. Büchl, R. Dux, J.C. Fuchs, G. Haas, A. Herrmann, K.-F. Mast, J. Schweinzer, N. Tsois*, B. Braams*, D. Reiter* and ASDEX Upgrade Team:* Modelling of Radiation Distribution and Impurity Divertor Compression in ASDEX Upgrade. In: Proc. 16th Int. Conf. on Fusion Energy, Montreal 1996, IAEA, Vienna 1997, Vol.2, 465-476.

283. *Schömann, S. and E. Taglauer:* Surface Segregation on $Au_3Cu(001)$. Surface Review and Letters **3**, 1823-1829 (1997).

284. *Schweinzer, J., W. Sandmann, G. Haas, J. Neuhauser, H. Murmann, H. Salzmann, ASDEX Upgrade Team and NI Team:* Relation between Neutral Gas Flux Density and Parameters of the Scrape-off Layer. In: Proc. 24th EPS Conf. on Control. Fusion and Plasma Phys., Berchtesgaden 1997, (Eds.) M.Schittenhelm, R.Bartiromo, F.Wagner. ECA 21A. Europ. Phys. Soc., Geneva 1997, 1449-1452.

285. *Schwörer, R., H. Plank and J. Roth:* Reduction of the Chemical Erosion of Doped Graphite due to Surface Modification during Low Energy D^+ Bombardment. Journal of Nuclear Materials **241-243**, 1156-1159 (1997).

286. *Scott, B.:* Three-Dimensional Computation of Collisional Drift Wave Turbulence and Transport in Tokamak Geometry. Plasma Physics and Controlled Fusion **39**, 71-504 (1997).

287. *Scott, B.:* Three-Dimensional Computation of Drift Alfvén Turbulence. Plasma Physics and Controlled Fusion **39**, 1635-1668 (1997).

288. *Scott, B., S. Camargo* and F. Jenko:* Self-Consistent Computation of Transport by Fluid Drift Turbulence in Tokamak Geometry In: Proc. 16th Int. Conf. on Fusion Energy, Montreal 1996, IAEA, Vienna 1997, Vol.2, 649-654.

289. *Scott, B. and F. Jenko:* Three Dimensional Computation of Fluid and Kinetic Drift Alfvén Turbulence in Tokamak Geometry. In: Proc. 24th EPS Conf. on Control. Fusion and Plasma Phys., Berchtesgaden 1997, (Eds.) M.Schittenhelm, R.Bartiromo, F.Wagner. ECA 21A. Europ. Phys. Soc., Geneva 1997, 1545-1548.

290. *Serra*, F., A. Silva*, B. Kurzan, M.E. Manso*, M.T. Grossmann*, J. Santos* and W. Suttrop:* Continuous Tracking of Density Profile Build-up during L-H Transition on ASDEX Upgrade from Microwave Reflectometry. In: Proc. 24th EPS Conf. on Control. Fusion and Plasma Phys., Berchtesgaden 1997, (Eds.) M.Schittenhelm, R.Bartiromo, F.Wagner. ECA 21A. Europ. Phys. Soc., Geneva 1997, 1493-1496.

291. *Silva*, A., L. Cupido*, B. Kurzan, J. Santos* et al.:* New Developments of the ASDEX Upgrade Tokamak Microwave

Reflectometry. In: Proc. 3rd Workshop on Microwave Reflectometry for Fusion Plasma Diagnostics, Madrid 1997, (Eds.) J.Sánchez, E.de la Luna. Informes Tecnicos Ciemat 838. Ciemat, Madrid 1997, 127-132.

292. *Simmet, E.E., C.D. Beidler and H. Maaßberg:* Time-Resolved Transport in W7-X as Predicted by Neoclassical Theory. In: Proc. 24th EPS Conf. on Control. Fusion and Plasma Phys., Berchtesgaden 1997, (Eds.) M.Schittenhelm, R.Bartiromo, F.Wagner. ECA 21A, Europ. Phys. Soc., Geneva 1997, 1673-1676.

293. *Simmet, E.E., H.-U. Fahrbach, W. Herrmann and U. Stroth:* Analysis of Ion Energy Transport in Ohmic Discharges in the ASDEX Tokamak. Plasma Physics and Controlled Fusion **39**, 993-1014 (1997).

294. *Simon-Weidner, J., N. Jaksic and J.Sapper:* Buckling Analysis and Results Post-Processing of the W7-X Inner Vacuum Vessel. Computers and Structures **64**, 1165-1173 (1997).

295. *Simon-Weidner, J., N. Jaksic and J. Sapper:* Buckling Analysis of the W7-X Inner Vacuum Vessel. In: Proc. 19th Symp. on Fusion Technol., Lisbon 1996, Eds. C.Varandas, F.Serra. North-Holland Publ., Amsterdam 1997, 1371-1374.

296. *Smith*, O.R.P., C. Gowers*, P. Nielsen* and H. Salzmann:* A Self-Calibration Technique for a Thomson Scattering System. Review of Scientific Instruments **68**, 725-730 (1997).

297. *Snipes*, J. and ITER H-Mode Threshold Database Working Group:* Threshold Power and Energy Confinement for ITER. In: Proc. 24th EPS Conf. on Control. Fusion and Plasma Phys., Berchtesgaden 1997, (Eds.) M.Schittenhelm, R.Bartiromo, F.Wagner. ECA 21A. Europ. Phys. Soc., Geneva 1997, 961-964.

298. *Sokoll, M., M. Bessenrodt-Weberpals and ASDEX Upgrade Team:* Differential Rotational Soft X-Ray Tomography of Coupled MHD Modes. In: Proc. 24th EPS Conf. on Control. Fusion and Plasma Phys., Berchtesgaden 1997, (Eds.) M.Schittenhelm, R.Bartiromo, F.Wagner. ECA 21A. Europ. Phys. Soc., Geneva 1997, 1517-1520.

299. *Steinbrink, J., U. Wenzel, W. Bohmeyer, G. Fußmann and PSI Team:* Sputtered Tungsten Atoms Investigated in a Linear Plasma Generator. In: Proc. 24th EPS Conf. on Control. Fusion and Plasma Phys., Berchtesgaden 1997, (Eds.) M.Schittenhelm, R.Bartiromo, F.Wagner. ECA 21A. Europ. Phys. Soc., Geneva 1997, 1809-1812.

300. *Steltenpohl, A., N. Memmel, E. Taglauer et al.:* Pd, Au and Codeposited Pd-Au Ultrathin Films on Ru(001). Surface Science **382**, 300-309 (1997).

301. *Streibl, B., S. Deschka, O. Gruber, B. Jüttner, P.T. Lang, K. Mattes, G. Pautasso, J. Perchermeier, K. Schippl*, H. Schneider, U. Seidel, W. Suttrop, G. Teller* and M. Weißgerber:* In-Vessel Cryo Pump for ASDEX Upgrade Divertor II. In: Proc. 19th Symp. on Fusion Technol., Lisbon 1997, (Eds.) C.Varandas, F.Serra. North-Holland Publ., Amsterdam 1997, 427-430.

302. *Stroth, U., M. Anton, J. Baldzuhn, R. Burhenn, M. Francés*, J. Geiger, T. Geist, L. Giannone, H.-J. Hartfuß, M. Hirsch, R. Jaenicke, J.P.T. Koponen, M. Kick, G. Kühner, F.-P. Penningsfeld, F. Wagner and A. Weller:* High-Confinement NBI Discharges in W7-AS. In: Proc. 24th EPS Conf. on Control. Fusion and Plasma Phys., Berchtesgaden 1997, (Eds.) M.Schittenhelm, R.Bartiromo, F.Wagner. ECA 21A. Europ. Phys. Soc., Geneva 1997, 1597-1600.

303. *Stroth, U., R. Burhenn, J. Geiger, L. Giannone, H.-J. Hartfuß, G. Kühner, L. Ledl, E.E. Simmet, H. Walter, ECRH Group and W7-AS Team:* Comparative Studies of Stellarator and Tokamak Transport. In: Proc. 16th Int. Conf. on Fusion Energy, Montreal 1996, IAEA, Vienna 1997, Vol.2, 127-133.

304. *Strumberger, E.:* Finite-β Magnetic Field Line Tracing for Helias Configurations. Nuclear Fusion **37**, 19-27 (1997).

305. *Strumberger, E.:* First Survey of Finite-β Magnetic Fields of W7-X. In: Proc. 24th EPS Conf. on Control. Fusion and Plasma Phys., Berchtesgaden 1997, (Eds.) M.Schittenhelm, R.Bartiromo, F.Wagner. ECA 21A, Europ. Phys. Soc., Geneva 1997, 1677-1680.

306. *Sun*, G., M. Friedrich*, R. Grötzschel*, R. Behrisch et al.:* Quantitative AMS Depth Profiling of the Hydrogen Isotopes Collected in Graphite Divertor and Wall Tiles of the Tokamak ASDEX Upgrade. Journal of Nuclear Materials **246**, 9-16 (1997).

307. *Sünder, D., M.I. Mikhailov* and A.A. Subbotin*:* Distinctive Features of the Stability of Ballooning Modes in Conventional Stellarators. Plasma Physics Reports **23**, 953-958 (1997).

308. *Suttrop, W., K. Büchl, J.C. Fuchs, M. Kaufmann, K. Lackner, M. Maraschek, V. Mertens, R. Neu, M. Schittenhelm, M. Sokoll, ASDEX Upgrade Team et al.:* Tearing Mode Formation and Radiative Edge Cooling Prior to Density Limit Disruptions in ASDEX Upgrade. Nuclear Fusion **37**, 119-125 (1997).

309. *Suttrop, W., M. Kaufmann, H.J. de Blank, B. Brüsehaber, K. Lackner, V. Mertens, H. Murmann, J. Neuhauser, F. Ryter, H. Salzmann, J. Schweinzer, J. Stober, ASDEX Upgrade Team et al.:* Identification of Plasma-Edge-Related Operational Regime Boundaries and the Effect of Edge Instability on Confinement in ASDEX Upgrade. Plasma Physics and Controlled Fusion **39**, 2051-2066 (1997).

310. *Suttrop, W., M. Kaufmann, O. Kardaun, K. Lackner, F. Ryter, H. Salzmann, J. Schweinzer, J. Stober and ASDEX Upgrade Team:* Influence of Plasma Edge Pressure Gradient Limits on H-Mode Confinement in ASDEX Upgrade. In: Proc. 24th EPS Conf. on Control. Fusion and Plasma Phys., Berchtesgaden 1997, (Eds.) M.Schittenhelm, R.Bartiromo, F.Wagner. ECA 21A. Europ. Phys. Soc., Geneva 1997, 1465-1468.

311. *Suvorov*, E.V., E. Holzhauer*, W. Kasparek*, V. Erckmann, T. Geist, M. Kick, H. Laqua, M. Rust, W7-AS Team, ECRH Group, NI Group et al.:* Collective Thomson Scattering at W7-AS. Plasma Physics and Controlled Fusion **39**, B337-B351 (1997).

312. *Taglauer, E.:* Ion Scattering Spectroscopy. In: Surface Characterization, (Eds.) D.Brune, R.Hellborg, H.J.Whithlow et al.. VCH Verlagsges., Weinheim 1997, 190-204.

313. *Taglauer, E.:* Ion Scattering Studies of the Structure and Chemical Composition of Surfaces. Journal of Surface Analysis **3**, 252-258 (1997).

314. *Taglauer, E.:* Low-Energy Ion Scattering and Rutherford Backscattering. In: Surface Analysis - The Principal Techniques, (Ed.) J.C.Vickerman. Wiley, Chichester 1997, 215-266.

315. *Taglauer, E.:* Surface Chemical Composition. In: Handbook of Heterogeneous Catalysis, (Eds.) G.Ertl, H.Knözinger, J.Weitkamp. VCH Verlagsges., Weinheim 1997, 614-626.

316. *Takizuka*, T. and ITER Confinement Database and Modelling Working Group:* Threshold Power and Energy Confinement for ITER. In: Proc. 16th Int. Conf. on Fusion Energy, Montreal 1996, IAEA, Vienna 1997, Vol.2, 795-808.

317. *Tasso, H.:* A Nonlinear Equation for Drift Waves. Physics Letters, A **232**, 247-251 (1997).

318. *Thannhäuser, G.:* Anforderungen an eine moderne Interne Revision. In: Festschrift für Ernst-Joachim Meusel, (Ed.) M.Winkler. Nomos Verl.Ges., Baden-Baden 1997, 295-300.

319. *Thoma, A., K. Asmussen, R. Dux, K. Krieger, A. Herrmann, B. Napiontek, R. Neu, J. Steinbrink, M. Weinlich, U. Wenzel and ASDEX Upgrade Team:* Spectroscopic Measurements of the Tungsten Erosion in the ASDEX Upgrade Divertor. In: Proc. 24th EPS Conf. on Control. Fusion and Plasma Phys., Berchtesgaden 1997, (Eds.) M.Schittenhelm, R.Bartiromo, F.Wagner. ECA 21A. Europ. Phys. Soc., Geneva 1997, 1409-1412.

320. *Thoma, A., K. Asmussen, R. Dux, K. Krieger, A. Herrmann, B. Napiontek, R. Neu, J. Steinbrink, M. Weinlich, U. Wenzel and ASDEX Upgrade Team:* Spectroscopic Measurements of Tungsten Erosion in the ASDEX Upgrade Divertor. Plasma Physics and Controlled Fusion **39,** 1487-1499 (1997).

321. *Throumoulopoulos, G.N. and D. Pfirsch:* Negative-Energy Perturbations in Cylindrical Equilibria with a Radial Electric Field. Physical Review, E **56**, 5979-5989 (1997).

322. *Throumoulopoulos, G.N. and H. Tasso:* Cylindrical Ideal Magnetohydrodynamic Equilibria with Incompressible Flows. Physics of Plasmas **4**, 1492-1494 (1997).

323. *Toussaint, U. von, T. Schimmel* and J. Küppers:* Computer Simulation of the AFM/LFM Imaging Process: Hexagonal versus Honeycomb Structure on Graphite. Surface and Interface Analysis **25**, 620-625 (1997).

324. *Treutterer, W., J. Gernhardt, O. Gruber, P. McCarthy*, G. Raupp, U. Seidel and ASDEX Upgrade Team:* Plasma Shape Control Design in ASDEX Upgrade. In: Proc. 24th EPS Conf. on Control. Fusion and Plasma Phys., Berchtesgaden 1997, (Eds.) M.Schittenhelm, R.Bartiromo, F.Wagner. ECA 21A. Europ. Phys. Soc., Geneva 1997, 933-936.

325. *Ullrich, W., H.-S. Bosch, F. Hoenen* and ASDEX Upgrade Team:* Application of a Si-Diode Detector for Fusion Product Measurements in ASDEX Upgrade. Review of Scientific Instruments **68**, 4434-4438 (1997).

326. *Verbeek, H., J. Stober, D. Coster and R. Schneider:* Erosion of the Main Chamber Walls of Tokamaks by CX-Neutrals. In: Proc. 24th EPS Conf. on Control. Fusion and Plasma Phys., Berchtesgaden 1997, (Eds.) M.Schittenhelm, R.Bartiromo, F.Wagner. ECA 21A. Europ. Phys. Soc., Geneva 1997, 1457-1460.

327. *Vichev*, R.G. and W. Eckstein:* Temporal Aspects of Sputtering of TaC, C and Ta Targets. Nuclear Instruments and Methods in Physics Research, B **122**, 215-223 (1997).

328. *Vollmer, O., F. Ryter, A. Stäbler, P. McCarthy* and ASDEX Upgrade Team:* Scaling of Thermal Energy Confinement in ASDEX Upgrade. In: Proc. 24th EPS Conf. on Control. Fusion and Plasma Phys., Berchtesgaden 1997, (Eds.) M.Schittenhelm, R.Bartiromo and F.Wagner. ECA 21A. Europ. Phys. Soc., Geneva 1997, 1485-1488.

329. *Wagner, F.:* Topics in Toroidal Confinement. Plasma Physics and Controlled Fusion **39**, A23-A50 (1997).

330. *Wang*, W., J. Roth, W. Eckstein, R. Schwörer, H. Plank et al.:* Deposition of Amorphous Hydrogenated Carbon Films due to Hydrocarbon Molecule Ion-Beam Bombardment. Nuclear Instruments and Methods in Physics Research, B **129**, 210-216 (1997).

331. *Wang*, W., V.Kh. Alimov*, B.M.U. Scherzer and J. Roth:* Deuterium Trapping in and Release from Tungsten Carbide. Journal of Nuclear Materials **241-243**, 1087-1092 (1997).

332. *Wang*, W., W. Jacob and J. Roth:* Oxidation and Hydrogen Isotope Exchange in Amorphous Deuterated Carbon Films. Journal of Nuclear Materials **245**, 66-71 (1997).

333. *Watari*, T., R. Kumazawa*, K. Nishimura*, J.-M. Noterdaeme et al.:* RF Heating Experiments in CHS and RF Development for LHD. In: Proc. 12th Top. Conf. on Radio Frequency Power in Plasmas, Savannah,GA 1997. (Eds.) P.M.Ryan, T.Intrator. AIP Conf. Proc. 403, AIP Press, Woodbury,NJ 1997, 57-64.

334. *Weinlich, M. and A. Carlson:* Flush Mounted Langmuir Probes in an Oblique Magnetic Field. Physics of Plasmas **4**, 2151-2160 (1997).

335. *Weinlich, M., A. Carlson, V. Rohde, ASDEX Upgrade Team and NI Team:* Scale Lengths of Current Flow in Magnetized Plasmas. In: Proc. 24th EPS Conf. on Control. Fusion and Plasma Phys., Berchtesgaden 1997, (Eds.) M.Schittenhelm, R.Bartiromo, F.Wagner. ECA 21A. Europ. Phys. Soc., Geneva 1997, 1537-1540.

336. *Weller, A., M. Anton, J. Geiger, C. Görner, R. Jaenicke, C. Konrad, F.-P. Penningsfeld, N. Rust, D.A. Spong*, C.Y. Teo, W7-AS Team, NI Group and ECRH Group:* Correlation between MHD-Activity, Energetic Particle Behaviour and Anomalous Transport Phenomena in WENDELSTEIN 7-AS. In: Proc. 24th EPS Conf. on Control. Fusion and Plasma Phys., Berchtesgaden 1997, (Eds.) M.Schittenhelm, R.Bartiromo, F.Wagner. ECA 21A, Europ. Phys. Soc., Geneva 1997, 1649-1652.

337. *Weller, A., J. Baldzuhn, R. Brakel, R. Burhenn, V. Erckmann, Y. Feng, S. Fiedler, J. Geiger, L. Giannone, P. Grigull, H.-J. Hartfuß, M. Hirsch, J.V. Hofmann, M. Kick, C. Konrad, H. Maaßberg, N. Rust, F. Sardei and E.V. Suvorov*:* Plasma Diagnostics and Physics in the W7-AS Stellarator. Fusion Engineering and Design **34-35**, 17-24 (1997).

338. *Wenzel, U., A. Thoma, R. Dux, C. Fuchs, A. Herrmann, S. Hirsch, A. Kallenbach, H. Kastelewicz, M. Laux, K.-F. Mast and B. Napiontek:* Spatial Radiation Profiles in the ASDEX Upgrade Divertor for Detached Plasmas. Journal of Nuclear Materials **241-243**, 728-733 (1997).

339. *Wenzel, U., P. Bachmann, A. Carlson, M. Laux, B. Napiontek and M. Weinlich:* Relaxation Oscallations in the Divertor of the ASDEX Upgrade Tokamak. Nuclear Fusion **37**, 1343-1347 (1997).

340. *Wesner, F., W. Becker, M. Brambilla, F. Braun, H. Faugel, D. Hartmann, F. Hofmeister, J.-M. Noterdaeme, T. Sperger, S. Wukitch*, ASDEX Upgrade Team and NI Team:* Experimental Results from ICRF on ASDEX Upgrade. In: Proc. 12th Top. Conf. on Radio Frequency Power in Plasmas, Savannah,GA 1997. (Eds.) P.M.Ryan, T.Intrator. AIP Conf. Proc. 403, AIP Press, Woodbury,NJ 1997, 101-104.

341. *Wesner, F., W. Becker, F. Braun, H. Faugel, R. Fritsch, F. Hofmeister, J.-M. Noterdaeme and T. Sperger:* ICRF Operation during H-Mode with ELMs Development Status at ASDEX Upgrade. In: Proc. 19th Symp. Fusion Technol., Lisbon 1996, (Eds.) C.Varandas, F.Serra. North-Holland Publ., Amsterdam 1997, 597-600.

342. *Wielunski, M., M. Mayer, R. Behrisch, J. Roth and B.M.U. Scherzer:* Simultaneous Profiling of Hydrogen and Deuterium by 2.6 MeV ^{4}He ERDA Using a ΔE-E Telescope Detector. Nuclear Instruments and Methods in Physics Research, B **122**, 113-120 (1997).

343. *Winkler, M.(Ed.):* Festschrift für Ernst-Joachim Meusel. Nomos Verl.Ges., Baden-Baden 1997, 350 S.

344. *Wobig, H.:* Der Stellarator als Fusionskraftwerk. Atomwirtschaft, Atomtechnik **42**, 162-166 (1997).

345. *Wolf, R., P. McCarthy*, F. Mast, H.-P. Zehrfeld and ASDEX Upgrade Team:* Motional Stark Effect Polarimetry for the Determination of the ASDEX Upgrade Current Density Profile. In: Proc. 24th EPS Conf. on Control. Fusion and Plasma Phys., Berchtesgaden 1997, (Eds.) M.Schittenhelm, R.Bartiromo, F.Wagner. ECA 21A. Europ. Phys. Soc., Geneva 1997, 1509-1512.

346. *Wutte*, D., R.K. Janev*, F. Aumayr*, M. Schneider*, J. Schweinzer, J. Smith* and H.P. Winter*:* Cross Sections for Collision Processes of Li Atoms Interacting with Electrons, Protons, Multiply Charged Ions and Hydrogen Molecules. Atomic Data and Nuclear Data Tables **65**, 155-180 (1997).

347. *Zebisch, P., P. Grigull, V. Dose, E. Taglauer and W7-AS Team:* Mass Spectroscopic Measurements in the Plasma Edge of the W7-AS Stellarator and their Statistical Analysis. Journal of Nuclear Materials **241-243**, 919-924 (1997).

348. *Zehetbauer, T., P. Franzen, G. Neu, V. Mertens, G. Raupp, W. Treutterer, D. Zasche and ASDEX Upgrade Team:* Plasma Regime Guided Discharge Control at ASDEX Upgrade. In: Proc. 19th Symp. on Fusion Technol., Lisbon 1997, (Eds.) C.Varandas, F.Serra. North-Holland Publ., Amsterdam 1997, 925-928.

349. *Zehrfeld, H.-P. and J. Geiger:* Growth Rates of Resistive Ballooning Modes in ASDEX Upgrade and W7-AS. In: Proc. 24th EPS Conf. on Control. Fusion and Plasma Phys., Berchtesgaden 1997, (Eds.) M.Schittenhelm, R.Bartiromo, F.Wagner. ECA 21A. Europ. Phys. Soc., Geneva 1997, 1561-1564.

350. *Zeiler, A., D. Biskamp, J.F. Drake* and B.N. Rogers*:* Three-Dimensional Plasma Edge Turbulence Including Electron and Ion Temperature Fluctuations. In: Proc. 16th Int. Conf. on Fusion Energy, Montreal 1996, IAEA, Vienna 1997, Vol.2, 657-663.

351. *Zeiler, A., J. Bowman and D. Biskamp:* Three-Dimensional Simulations of Two-Fluid Drift-Braginskii Turbulence. In: Proc. 24th EPS Conf. on Control. Fusion and Plasma Phys., Berchtesgaden 1997, (Eds.) M.Schittenhelm, R.Bartiromo, F.Wagner. ECA 21A. Europ. Phys. Soc., Geneva 1997, 1541-1544.

352. *Zeiler, A., J.F. Drake* and D. Biskamp:* Electron Temperature Fluctuations in Drift-Resistive Ballooning Turbulence. Physics of Plasmas **4**, 991-1001 (1997).

353. *Zeiler, A., J.F. Drake* and B.N. Rogers*:* Nonlinear Reduced Braginskii Equations with Ion Thermal Dynamics in Toroidal Plasmas. Physics of Plasmas **4**, 2134-2138 (1997).

354. *Zohm*, H., D. Gates*, H.R. Wilson*, G. Gantenbein*, O. Gruber, S. Günter, M. Maraschek, A.W. Morris*, M. Sokoll, D. Wagner*, ASDEX Upgrade Team and COMPASS-D Team:* Neoclassical MHD in ASDEX Upgrade and COMPASS-D. Plasma Physics and Controlled Fusion **39**, B237-B246 (1997).

355. *Zohm*, H., W. Suttrop, H.J. de Blank, R.J. Buttery*, D. Gates*, J.A. Heikkinen*, W. Herrmann, A. Kallenbach, T. Kass, M. Kaufmann, T. Kurki-Suonio*, B. Kurzan, M. Maraschek, H. Reimerdes, F. Ryter, H. Salzmann, J. Schweinzer, J. Stober, ASDEX Upgrade Team, ECRH Group, ICRH Group and NI Team:* Study of H-Mode Physics in ASDEX Upgrade. In: Proc. 16th Int. Conf. on Fusion Energy, Montreal 1996, IAEA, Vienna 1997, Vol.1, 439-451.

Diploma Theses

356. *Bellido, E.:* Betrieb einer neuen Bolometerkamera und Berechnung der Emmisivität am Stellarator W7-AS. Techn. Univ. München 1997.

357. *Ellmauer, M.:* Aufbau und Optimierung eines Vielkanal-Spektrometersystems zur Messung radialer Verunreinigungsprofile, Driftgeschwindigkeit und Ionentemperaturen in W7-AS Plasmen. Univ. Regensburg 1997.

358. *Endras, B.:* Aufbau und Test einer Pulshöhen-Analyse-Diagnostik für den Tokamak ASDEX Upgrade. Univ. Augsburg 1997.

359. *Ernst, B.:* Untersuchung des Ionentemperaturprofils am Plasmarand des Stellarators W7-AS. Techn. Univ. München 1997.

360. *Geier, A.:* Transientes Verhalten von Langmuirsonden in einem magnetischen Plasma. Techn. Univ. München 1997.

361. *Kleberg, I.:* Brennfleckphänomene auf Graphitmaterialien. Humboldt-Univ. Berlin 1997.

362. *Mayer, R.P.:* Optische Untersuchungen von Kathodenbrennfleckplasmen. Humboldt-Univ. Berlin 1997.

363. *Meister, H.:* Untersuchungen zu Plasmarotationen und Impulstransport in ASDEX Upgrade. Univ. Augsburg 1997.

364. *Pfeiffer, U.:* Messung von Elektronentemperatur, Potential und Dichte in einem Plasma mit hoher Zeitauflösung mittels Langmuirsonde. Techn. Univ. München 1997.

365. *Schmidtmann, K.:* Messungen der Temperaturen und Driften angeregter Argonatome mittels LIF am Plasmagenerator PSI-1. Humboldt-Univ. Berlin 1997.

366. *Steinbrink, J.:* Spektroskopische Untersuchungen von zerstäubtem Wolfram in einer Plasmaentladung. Humboldt-Univ. Berlin 1997.

Doctoral Theses

367. *Annen, A.:* Amorphe hydrogenisierte Bor-Kohlenstoff-Filme: Herstellung, Charakterisierung und Untersuchung des Erosionsverhaltens. Univ. Bayreuth 1997.

368. *De Peña Hempel, S.:* Untersuchungen zum Transport leichter Verunreinigungen an ASDEX Upgrade. Techn. Univ. München 1997.

369. *Höhn, F.:* Untersuchung von Multipaktorentladungen und deren Wechselwirkung mit Oberflächen. Techn. Univ. München 1997.

370. *Krainz, G.:* Quench Protection and Powering in a String of Superconducting Magnets for the Large Hadron Collider. Techn. Univ. Graz 1997.

371. *Küstner, M.:* Zerstäubung rauher Oberflächen. Univ. Bayreuth 1997.

372. *Labich, S.:* Untersuchungen zur Metall-Träger-Wechselwirkung an Rhodium-Modellkatalysatoren. Univ. München 1997.

373. *Lutterloh, C.:* Reaktionen thermischer Wasserstoffatome: Adsorption, Austausch und Wechselwirkung mit physisorbierten Kohlenwasserstoffen auf Pt(111) und Graphit/Pt(111). Univ. Bayreuth 1997.

374. *Maraschek, M.:* Alfvénwellen in toroidaler Geometrie am Tokamak ASDEX Upgrade. Techn. Univ. München 1997.

375. *Miller, S.:* Untersuchung der chemischen Wechselwirkung von Titan und Kohlenstoff mittels Röntgen-Photoelektronen-Spektroskopie. Univ. Bayreuth 1997.

376. *Pecher, P.:* Quantitative Bestimmung der Teilchenflüsse aus Methan-ECR-Plasmen. Univ. Bayreuth 1997.

377. *Reinmuth, J.:* Auftrittspotentialspektroskopie (APS) mit spinpolarisierten Elektronen an Mehrkomponentensystemen. Univ. Bayreuth 1997.

378. *Sokoll, M.:* MHD-Instabilitäten in magnetisch eingeschlossenen Plasmen und ihre tomographische Rekonstruktion im Röntgenlicht. Techn. Univ. München 1997.

379. *Theimer, G.:* Charakterisierung transportrelevanter turbulenter elektrostatischer Fluktuationen in der Abschälschicht des Tokamaks ASDEX mittels Darstellung als Superposition von raum-zeitlich lokalisierten Ereignissen. Techn. Univ. München 1997.

380. *Verplancke, P.:* Langmuir Probes at High Frequencies in a Magnetized Plasma: A Theoretical and Experimental Study. Ghent Rijksuniversiteit 1997.

Patents

381. *Heinemann, B.; R. Riedl, W. Kraus et al.:* Vakuumgefäß. Europ. Patentanmeldung 97710016.3: 16.8.1997 EP(DE, GB, FR, IT, ES, NL, CH, AU)

382. *Mast, K.-F., G. Schramm and M. Münch:* Folienmanometer. Deutschland 19711874.7: Patentanmeldung 21.3.1997

383. *Probst, F.:* Dichtung für ein Hochvakuumgefäß Deutschland 19713975.2: Patentanmeldung 04.04.1997

Lectures

384. *Annen, A.:* Eigenschaften und Erosionsverhalten amorpher hydrogenisierter Bor (a-B:H) - und Bor-Kohlenstoff (a-C:H) Filme. Seminarvortrag, FZK, Jülich 1997.

385. *Annen, A., A. von Keudell, M. Saß and W. Jacob:* Zusammensetzung, Struktur und Erosionsverhalten amorpher hydrogenisierter Bor-Kohlenstoff (a-B/C:H) Schichten. Verhandl. DPG (VI) **32**, 622, DS18.4 (1997).

386. *Annen, A., M. Saß and W. Jacob:* Eigenschaften amorpher hydrogenisierter Bor (a-B:H) Schichten. Verhandl. DPG (VI) **32**, 622, DS18.3 (1997).

387. *Anton, M., T. Klinger*, M. Häse, J. Geiger, C. Görner, H.-J. Hartfuß, R. Jaenicke, A. Weller, W7-AS Team, NI Group, ECRH Group et al.:* Recent Observations of MHD Instabilities on W7-AS. Joint Conf. of 11th Int. Stellarator Conf. and 8th Int. Toki Conf. on Plasma Phys. and Control. Nucl. Fusion, Toki 1997.

388. *Arndt, S.:* W7-X Equilibria with Magnetic Islands Using the PIES Code. Int. Sherwood Fusion Theory Conf., Madison,WI 1997.

389. *Asmussen, K., W. Engelhardt, K. Krieger, R. Neu, J. Roth, V. Rohde, A. Thoma, ASDEX-Upgrade Team, NI Team, ICRH Group and ECRH Group:* Zentrale Wolfram-Konzentrationen und $W(CO)_6$-Divertor Experimente an ASDEX Upgrade. Verhandl. DPG (VI) **32**, 294, P16.3 (1997).

390. *Bachmann, P. and D. Sünder:* Multi-Fluid Plasma Description of Reaction-Diffusion Processes. 6th PET-Workshop, Oxford 1997.

391. *Bachmann, P., D. Sünder and H. Wobig:* On Bifurcation of Temperature Profiles. 6th PET-Workshop, Oxford 1997.

392. *Balden, M.:* Thermal Stability and Chemical Erosion of Silicon Doped Graphite (NS31). NET/ITER Meeting on Chemical Erosion, Kloster Seeon 1997.

393. *Balden, M. and J. Roth:* Erosionsverhalten und Siliziumverteilung des Si-dotierten CFC-Materials NS31. Verhandl. DPG (VI) **32**, 299, P20.6 (1997).

394. *Balden, M., J. Roth and C.H. Wu*:* Thermal Stability and Chemical Erosion of the Silicon Doped CFC Material NS31. 8th Int. Conf. on Fusion Reactor Materials, Sendai 1997.

395. *Balzer*, D., W. Bohmeyer, H. Grote, B. Gusovius*, P. Kornejev, H.-D. Kronfeldt*, V.V. Pustugow*, J. Rutkowsky* and B. Sumpf*:* Anwendung eines Bleisalzdiodenlaserspektrometers zur Konzentrationsbestimmung von Methan in Wasserstoffplasmen über Graphitoberflächen. Verhandl. DPG (VI) **32**, 238, MO8.25 (1997).

396. *Barabash*, V., M. Akiba*, J.P. Bonal*, W. Jacob et al.:* Carbon Fiber Composites Application in ITER Plasma Facing Components. 8th Int. Conf. on Fusion Reactor Materials, Sendai 1997.

397. *Becker, G.:* Confinement Times in ITER. 7th Meeting of the ITER Confinement Database and Modelling Working Group, Garching 1997.

398. *Behler, K., H. Blank, A. Buhler, R. Drube, H. Friedrich, K. Förster, K. Hallatschek, P. Heimann, F. Hertweck, J. Maier, R. Merkel, M.-G. Pacco-Düchs, G. Raupp, H. Reuter, U. Schneider-Maxon, R. Tisma, M. Zilker, Computer Science Division, Computer Centre and ASDEX Upgrade Team:* Review of the ASDEX Upgrade Data Acquisition Environment - Present Operation and Future Requirements. IAEA Techn. Comm. Meeting on Data Acquisition and Management for Fusion Research, IPP, Garching 1997.

399. *Behringer, K.:* Der aktuelle Stand der Fusionsforschung. MNU-Fortbildungsseminar für Lehrer, Univ. Augsburg 1997.

400. *Behringer, K.:* Einführung in die Plasmaspektroskopie. Vorlesung, Univ. Augsburg, WS 1997/98.

401. *Behringer, K.:* Seminar über aktuelle Fragen der Plasmaphysik. Vorlesung, Univ. Augsburg, SS 1997, WS 1997/98.

402. *Behringer, K.:* Spektroskopie von Nichtgleichgewichtsplasmen. Vorlesung, Univ. Augsburg, SS 1997.

403. *Behringer, K. et al.:* Seminar über Anwendungen und Diagnostik von Niederdruckplasmen. Vorlesung, Univ. Augsburg, SS 1997, WS 1997/98.

404. *Behringer, K. and U. Fantz*:* Physik III (Atom- und Molekülphysik). Vorlesung, Univ. Augsburg, WS 1997/98.

405. *Behringer, K. and U. Fantz*:* Physikalisches Praktikum für Fortgeschrittene. Univ. Augsburg, SS 1997, WS 1997/98.

406. *Behrisch, R.:* Analysen von Oberflächenschichten von Festkörpern mit MeV Ionenstrahlen über den Nachweis der energetischen Rückstoßatome (ERDA). Kolloquiumsvortrag, Univ. Jena 1997.

407. *Behrisch, R.:* Materialien für die erste Wand bei Fusionsapparaturen. Kolloquiumsvortrag, IPP, Garching 1997.

408. *Behrisch, R.:* Das Problem des Plasma-Festkörperübergangs bei den Versuchen zur kontrollierten thermonuklearen Fusion - „wo Festes sich mit Feuer mischt". Kolloquiumsvortrag, Univ. Augsburg 1997.

409. *Behrisch, R.:* Transmutation of Plasmafacing Materials by the Neutron Flux in a D7 Fusion Reactor. 8th Int. Conf. on Fusion Reactor Materials, Sendai 1997.

410. *Behrisch, R., P. Franzen, C. Garcia-Rosales*, M. Mayer, C. Plamann, ASDEX Upgrade Team et al.:* Measurement of the D and H Retention at the Different Areas of the Vessel Walls of JET and ASDEX Upgrade. ITER Task Related Meeting, JET, Abingdon 1997.

411. *Behrisch, R., S. Grigull and U. Kreissig*:* Influence of Surface Roughness on Measuring Depth Profiles of Implanted Ions by ERDA. 13th Int. Conf. on Ion Beam Analysis, Lisbon 1997.

412. *Behrisch, R. and M. Mayer:* D-Content of JET Long Term Samples. NET/ITER Meeting on Chemical Erosion, Kloster Seeon 1997.

413. *Behrisch, R., M. Mayer, P. Andrew* et al.:* Measurements of the D and H Trapped in the Different Areas of the Vessel Wall of JET during the Be Phases. ITER Task Related Meeting, JET, Abingdon 1997.

414. *Beidler, C.D., G. Grieger, E. Harmeyer, F. Herrnegger, J. Kißlinger, E. Strumberger, H. Wobig, A.V. Zolotukhin et al.:* Physics and Engineering Studies of a Helias Reactor. Joint Conf. of 11th Int. Stellarator Conf. and 8th Int. Toki Conf. on Plasma Phys. and Control. Nucl. Fusion, Toki 1997.

415. *Bergmann, A.:* Kinetic Modelling of a 'Classical' Scrape-off Layer. 6th Int. Workshop on Plasma Edge Theory in Fusion Devices, Oxford 1997.

416. *Bergmann, A.:* Teilchen-Simulation von Plasmen in starken Magnetfeldern. Techn. Univ. Darmstadt 1997.

417. *Bertel, E.:* Low-Dimensional Electron States on Metal Surfaces. 16th General Conf. of the Condensed Matter Division, EPS, Leuven 1997.

418. *Bertel, E.:* Promotoren, Inhibitoren und Surfactants: Oberflächendotierung von Metallen in Katalyse und Epitaxie. Seminar, Univ. Essen 1997.

419. *Bertel, E.:* Streß und mesoskopische Oberflächenmorphologie von Pt(110). Elektronische Anregungen an Oberflächen. DFG-Rundgespräch, Univ. Erlangen-Nürnberg 1997.

420. *Bertel, E.:* Surface Science - Faszination der Oberfläche. Kolloquiumsvortrag, Univ. Innsbruck 1997.

421. *Bessenrodt-Weberpals, M.:* Diagnostik heißer Laborplasmen. Vorlesung, Univ. Düsseldorf, SS 1997.

422. *Bessenrodt-Weberpals, M.:* Diagnostik der Verunreinigungsdynamik in Tokamakplasmen. Kolloquium, Univ. Kiel 1997.

423. *Bessenrodt-Weberpals, M.:* Einführung in die Astrophysik. Vorlesung, Univ. Düsseldorf, WS 1997/98.

424. *Bessenrodt-Weberpals, M.:* Experimental Results in Tokamak Physics. Summer Univ. for Plasma Physics, Greifswald 1997.

425. *Bessenrodt-Weberpals, M.:* Verunreinigungsdynamik und Instabilitäten in Tokamakplasmen. Jülich 1997.

426. *Bessenrodt-Weberpals, M., H.J. de Blank, M. Maraschek, P. McCarthy*, M. Sokoll and ASDEX Upgrade Team:* Zentrale Bestimmung des Stromprofiles in Tokamaks. Verhandl. DPG (VI) **32**, 266, P3.1 (1997).

427. *Biedermann, C., G. Fußmann and R. Radtke:* Dielektronische Rekombination von Barium in einer Elektronenstrahl-Ionenfalle. Verhandl. DPG (VI) **32**, 210, A25.1 (1997).

428. *Biedermann, C., G. Fußmann and R. Radtke:* EBIT - Eine Elektronenstrahl-Ionenfalle zur Untersuchung hochgeladener Ionen. Verhandl. DPG (VI) **32**, 267, P4.1 (1997).

429. *Bilato*, R. and M. Brambilla:* Feasibility Study of Lower Hybrid Current Drive to Sustain the Reversed Field Pinch Configuration. Bull. Am. Phys. Soc. **42**, 1933 (1997).

430. *Biskamp, D.:* Computer Simulation von Plasmaturbulenz. Verhandl. DPG (VI) **32**, 263, PIV (1997).

431. *Biskamp, D.:* MHD Theory. 4 Vorträge. Summer School on Turbulence, Saint-Oyen 1997.

432. *Bleuel, J., M. Endler, H. Niedermeyer and G. Theimer:* Die Randschicht-Fluktuationen am Stellarator Wendelstein 7-AS. Verhandl. DPG (VI) **32**, 267, P3.3 (1997).

433. *Bleuel, J., M. Endler, H. Niedermeyer and G. Theimer:* Structure of the Edge Fluctuations in the W7-AS Stellarator. TTF Turbulence Working Group Meeting, Cadarache 1997.

434. *Bohmeyer, W.:* Stationärer Plasmagenerator. Verhandl. DPG (VI) **32**, 263, PII (1997).

435. *Bosch, H.-S.:* Basic Nuclear Fusion. Summer Univ. for Plasma Physics, Greifswald 1997.

436. *Bosch, H.-S.:* Diagnostics of Fusion Plasmas. Summer Univ. for Plasma Physics, Greifswald 1997.

437. *Bosch, H.-S.:* Was haben die Sterne mit unserer Energieversorgung zu tun? 3 Schulvorträge, MPG Hauptversammlung, Bremen 1997.

438. *Bosch, H.-S., D. Coster, R. Dux, G. Haas, A. Kallenbach, M. Kaufmann, K. Lackner, J. Neuhauser, S. de Peña Hempel, W. Poschenrieder, R. Schneider and ASDEX Upgrade Team:* Heliumtransport and Heliumpumping in ASDEX Upgrade. DIII-D Seminar, General Atomics, San Diego,CA 1997.

439. *Bosch, H.-S., D. Coster, S. de Peña Hempel, R. Dux, G. Haas, A. Kallenbach, K. Lackner, W. Poschenrieder, R. Schneider and W. Ullrich:* Heliumtransport und Heliumpumpen in ASDEX Upgrade. Verhandl. DPG (VI) **32**, 303, P25.1 (1997).

440. *Bosch, H.-S., J. Neuhauser, W. Sandmann, J. Schweinzer, R. Wunderlich, H. Salzmann and ASDEX Upgrade Team:* Scrape-off Layer Data from ASDEX Upgrade. ITER Divertor Database Subgroup Meeting, San Diego,CA 1997.

441. *Brakel, R.:* The Influence of Magnetic Shear on Confinement in Stellarators. 5th Europ. Fusion Physics Workshop, Sesimbra 1997.

442. *Brakel, R.:* W7-X: Concepts for Machine Operation. LHD/ W7-X Diagnostic Workshop, Toki 1997.

443. *Brakel, R., M. Anton, V. Erckmann, S. Fiedler, J. Geiger, H.-J. Hartfuß, M. Hirsch, R. Jaenicke, G. Kühner, H. Maaßberg, U. Stroth, F. Wagner, A. Weller, W7-AS Team, ECRH Group and NI Group:* The Role of Magnetic Shear in the Confinement of W7-AS Plasmas. Joint Conf. of 11th Int. Stellarator Conf. and 8th Int. Toki Conf. on Plasma Phys. and Control. Nucl. Fusion, Toki 1997.

444. *Brandenburg*, R., S. Fiedler, J. Schweinzer, W7-AS Team, ASDEX Upgrade Team et al.:* Fast Lithium Beam Edge Plasma Spectroscopy - Status and Recent Developments. IAEA Techn. Comm. Meeting on Research Using Small Fusion Devices, Kairo 1997.

445. *Burhenn, R.:* Spectroscopy W7-X (X-Ray and VUV). LHD/ W7-X Diagnostics Workshop, Toki 1997.

446. *Burhenn, R., M. Anton, J. Baldzuhn, R. Brakel, L. Giannone, H. Hacker, M. Hirsch, L. Ledl, H. Maaßberg, E. Unger, A. Weller, W7-AS Team, ECRH Group and NI Group:* Impurity Transport Investigation at W7-AS. Joint Conf. of 11th Int. Stellarator Conf. and 8th Int. Toki Conf. on Plasma Phys. and Control. Nucl. Fusion, Toki 1997.

447. *Carlson, A.:* MHD on Scales between the Fluctuations and the Gyroradius: Why Langmuir Probes Work even at Low Temperatures. 3rd Workshop on Electrical Probes in Magnetized Plasmas, Berlin 1997.

448. *De Blank, H.J.:* Basic Plasma Physics. Summer Univ. for Plasma Physics, Greifswald 1997.

449. *De Peña Hempel, S., R. Dux, A. Kallenbach and ASDEX Upgrade Team:* Untersuchungen zum Transport leichter Verunreinigungen an ASDEX Upgrade. Verhandl. DPG (VI) **32**, 274, P13.2 (1997).

450. *Dinger*, A., C. Lutterloh, J. Biener and J. Küppers:* H/D Austausch an einer Monolage Graphit auf Pt(111) mit Atomen. Verhandl. DPG (VI) **32**, 927, O35.3 (1997).

451. *Dohmen, R., U. Schwenn and T. Hayashi*:* Performance and Load Balancing of Diverse Parallel Implementations of the Plasma Code HINT. Parallel Computing 1997, Bonn 1997.

452. *Donath, M.:* Magnetic Surface States in Thin-Film Systems: Studies with Spin-Resolved Inverse Photoemission. Univ. Tokyo 1997.

453. *Donath, M.:* Magnetische Oberflächeneffekte in Dünnschichtsystemen. DFG-Rundgespräch, Univ. Erlangen-Nürnberg 1997.

454. *Donath, M.:* Magnetische Ordnung und elektronische Struktur in Dünnschichtsystemen. Phys. Kolloquium, Techn. Univ. Darmstadt 1997.

455. *Donath, M.:* Magnetische Ordnung und elektronische Struktur in niedrigdimensionalen Systemen. Univ. Marburg 1997.

456. *Donath, M.:* Magnetismus an Oberflächen und in dünnen Schichten: Experimente mit spinpolarisierten Elektronen I. Univ. Göttingen 1997.

457. *Donath, M.:* Magnetismus: Phänomene - Meßmethoden - Anwendungen. Vorlesung, Univ. Bayreuth, WS 1997/98.

458. *Donath, M., B. Gubanka and F. Passek:* Temperaturabhängige Spinpolarisation des magnetischen Oberflächenzustands von Gd(0001). Verhandl. DPG (VI) **32**, 925, O34.6 (1997).

459. *Donath, M., B. Gubanka and F. Passek:* Temperaturverhalten des magnetischen Oberflächenzustands auf Gd(0001). 168. WE-Heraeus- Seminar, Bad Honnef 1997.

460. *Donath, M., J. Reinmuth and F. Passek:* Local Magnetic Information from Appearance Potential Spectroscopy. 7th Int. Conf. on Electron Spectroscopy, Univ. of Chiba 1997.

461. *Drevlak, M.:* Coil Design and Equilibrium Studies for a Quasi-Axially Symmetric Tokamak. Joint Conf. of 11th Int. Stellarator Conf. and 8th Int. Toki Conf. on Plasma Phys. and Control. Nucl. Fusion, Toki 1997.

462. *Drevlak, M., P. Merkel, J. Nührenberg, S. Okamura* et al.:* Conceptual Design of a Quasi-Axisymmetric Stellarator (CHS-qa). Joint Conf. of 11th Int. Stellarator Conf. and 8th Int. Toki Conf. on Plasma Phys. and Control. Nucl. Fusion, Toki 1997.

463. *Düchs, D.F.:* 'Anomalous' Pinch Effect for Large Ion Gyroradii and Steep Gradients. NIFS, Nagoya 1997.

464. *Düchs, D.F.:* Consistent and Quantitative Global Description of Tokamak Plasmas by Computer Codes. Kyushu Univ., Fukuoka 1997.

465. *Düchs, D.F.:* Critical Remarks on the Present Status of, and the Present Program (ITER) for Thermonuclear Fusion Research. Kyushu Univ., Fukuoka 1997.

466. *Düchs, D.F.:* Gleichgewichte magnetisierter Plasmen und deren Berechnung. Vorlesung, Univ. Bochum, SS 1997.

467. *Düchs, D.F.:* Zur Theorie der Diagnostiken und Datenauswertung bei Fusionsplasmen. Vorlesung, Univ. Bochum, WS 1996/97.

468. *Düchs, D.F.:* Theorie von Stoßwechselwirkungen in heißen Plasmen. Vorlesung, Univ. Bochum, WS 1997/98.

469. *Dux, R.:* ADAS - Progress and New Directions. ADAS Workshop, Abingdon 1997.

470. *Dux, R.:* Plasmaphysik und Fusionsforschung I. Vorlesung, Univ. Augsburg, WS 1997/98.

471. *Dux, R.:* Plasmaphysik und Fusionsforschung II. Vorlesung, Univ. Augsburg, SS 1997.

472. *Eckstein, W.:* Computer Simulation of Ion-Solid Interactions. Chungbuk Nat. Univ., Cheougju 1997.

473. *Eckstein, W.:* Interaction of Ions with Materials. 1st TESLA Workshop, Belgrad 1997.

474. *Eckstein, W.:* Isotope Sputtering. Sichuan Univ., Chengdu 1997.

475. *Eckstein, W.:* Isotope Sputtering of Molybdenum. Korea Research Inst. for Standard and Science, Taduk Science Town 1997.

476. *Eckstein, W.:* Reflection from and Sputtering of Tungsten. W-Workshop, Sendai 1997.

477. *Eckstein, W.:* Target Composition Changes due to Ion Bombardment. Korea Basic Science Inst., Taduk Science Town 1997.

478. *Eckstein, W.:* Target Composition Changes due to Ion Bombardment. South Western Inst., Leshou 1997.

479. *Eckstein, W.:* Target Composition Changes due to Ion Bombardment. Yousei-Univ., Seoul 1997.

480. *Eckstein, W., P. Goldstraß and C. Linsmeier:* Erosion of Be and Deposition of C and O due to Bombardment of C^+ and CO^+. Be-Workshop, Mito 1997.

481. *Empacher*, L., W. Förster*, G. Gantenbein*, V. Erckmann et al.:* The ECRH Transmission System for W7-X. 9th Joint Russian-German Meeting on ECRH and Gyrotrons. Karlsruhe/Stuttgart/Garching 1997.

482. *Endler, M.:* Turbulenz im Tokamak – wie entkommt das Plasma aus dem magnetischen Käfig? Journal-Klub des Physik-Dept., Techn. Univ. München, Garching 1997.

483. *Endler, M., I. García-Cortés*, S. Davies* et al.:* Observation of Electrostatic Fluctuations and ELMs and of the Induced Radial Particle Transport in the SOL of JET. TTF Turbulence Working Group Meeting, Cadarache 1997.

484. *Endler, M., U. Pfeiffer, J. Bleuel, H. Niedermeyer and G. Theimer:* Density, Temperature and Potential Fluctuation Measurements with Multiple Fast Swept Langmuir Probes on W7-AS. 3rd Int. Workshop on Langmuir Probes in Magnetized Plasmas, Berlin 1997.

485. *Endler, M., U. Pfeiffer, J. Bleuel, H. Niedermeyer and G. Theimer:* Density, Temperature and Potential Fluctuation Measurements with Multiple Fast Swept Langmuir Probes on W7-AS. JET Divertor Physics Topic Group Meeting, Abingdon 1997.

486. *Erckmann, V.:* The W7-X Project: Scientific Basis and Technical Realization. 17th IEEE/NPSS Symp. on Fusion Engineering, San Diego,CA 1997.

487. *Erckmann, V., U. Gasparino, M. Romé and N. Karulin*:* ECRH and ECCD in W7-X. 9th Joint Russian-German Meeting on ECRH and Gyrotrons, Karlsruhe/Stuttgart/Garching 1997.

488. *Erckmann, V., W7-AS Team, ECRH Group and Gyrotron Group:* ECRH at W7-AS and W7-X. 9th Joint Russian-German Meeting on ECRH and Gyrotrons, Karlsruhe/Stuttgart/Garching 1997.

489. *Ernst, B.:* Untersuchungen der Neutralteilchenflüsse an der verbesserten LENA-Diagnostik am W7-AS. Verhandl. DPG (VI) **32**, 291, P14.55 (1997).

490. *Ernst, B., H. Verbeek and O. Heinrich:* Untersuchung der Neutralteilchenflüsse mit der verbesserten LENA-Diagnostik an W7-AS. Verhandl. DPG (VI) **32**, 291, P14.55 (1997).

491. *Fantz*, U. and K. Behringer:* Chemische Erosion von Kohlenstoffschichten in H_2- und D_2-Plasmen. Verhandl. DPG (VI) **32**, 276, P13.17 (1997).

492. *Feist, J.-H., P. Frank, W. Kraus and E. Speth:* First Results from BATMAN. Joint Development Comm. Meeting, Naka 1997.

493. *Feng, Y.:* Modellierung des Plasmatransports in der Randschicht von W7-AS. Theorie Workshop, Zinnowitz 1997.

494. *Feng, Y., F. Sardei, P. Grigull and W7-AS Team:* Modelling Drift Effects on the Limiter SOL of Low Density Plasmas in W7-AS. 6th Int. Workshop on Plasma Edge Theory in Fusion Devices, Oxford 1997.

495. *Fiedler, S., R. Brandenburg*, J. Baldzuhn, K. McCormick, J. Schweinzer, W7-AS Team et al.:* Impurity Investigations by Means of Li-Beam Induced Charge Exchange Spectroscopy on W7-AS. Joint Conf. of 11th Int. Stellarator Conf. and 8th Int. Toki Conf. on Plasma Phys. and Control. Nucl. Fusion, Toki 1997.

496. *Fischer, R., M. Mayer, W. von der Linden and V. Dose:* Energy Resolution Enhancement in Ion Beam Experiments with Bayesian Probability Theory. 13th Int. Conf. on Ion Beam Analysis, Lisbon 1997.

497. *Förster, A.*, C. Biedermann, G. Fußmann and R. Radtke:* Working Regime Limits for the EBIT Originating from the Two-Stream Rotational Instability. Workshop on Nonneutral Plasmas, Boulder 1997.

498. *Frank P., J.-H. Feist, W. Kraus, E. Speth et al.:* BATMAN Status. JDC Meeting, Jülich 1997.

499. *Frank, P., J.-H. Feist, W. Kraus, E. Speth, B. Heinemann, F. Probst et al.:* A Large-Area RF Source for Negative Hydrogen Ions. Joint Meeting 8th Int. Symp. on the Production and Neutralization of Negative Ions and Beams, Villagium of Giens 1997.

500. *Franzen, P.:* Measurement of the H, D, and T Collected at Different Areas of the Carbon Tiles from the Vessel Walls of ASDEX Upgrade. EU Meeting on 'Removal of Tritium from Co-Deposited Layers', Garching 1997.

501. *Franzen, P., R. Behrisch, D. Schleußner* et al.:* Measurement of the H, D, and T Collected at Different Areas of the Carbon Tiles from the Vessel Walls of ASDEX Upgrade. ITER Task Related Meeting, JET, Abingdon 1997.

502. *Franzen, P., W. Herrmann and J.C. Fuchs:* Thermische Belastungen der Gefäßeinbauten bei zusatzgeheizten Entladungen in ASDEX Upgrade. Verhandl. DPG (VI) **32**, 274, P13.4 (1997).

503. *Freed, N., C. Linsmeier and I.S.T. Tsong:* Deposition of GaN Thin Films by Dual Low-Energy Ion Beams. 13th Int. Conf. on Ion Beam Analysis, Lisbon 1997.

504. *Fuchs, C. and H.-J. Hartfuß:* Line-Integrated Density Measurements Using the Cotton-Mouton-Effect. 9th Joint Russian-German Meeting on ECRH and Gyrotrons, Karlsruhe/Stuttgart/Garching 1997.

505. *Fuchs, C. und H.-J. Hartfuß:* Messung der Liniendichte am W7-AS über den Cotton-Mouton-Effekt. Verhandl. DPG (VI) **32**, 297, P19.3 (1997).

506. *Fußmann, G.:* Atom-und Molekülphysik. Vorlesung, Humboldt-Univ. Berlin, WS 1997/98.

507. *Fußmann, G.:* Plasmaanalyse unter Verwendung eines thermischen Heliumstrahls. Vortrag, INP, Greifswald 1997.

508. *Fußmann, G.:* Stand und Aussichten der kontrollierten Kernfusion. Novembervorlesungen, Humboldt-Univ. Berlin 1997.

509. *Fußmann, G.:* Teilchentransport in Magnetoplasmen durch ladungsändernde Prozesse. Verhandl. DPG (VI) **32**, 270, P7.2 (1997).

510. *Gafert, J., D. Coster, C. Dorn, ASDEX Upgrade Team et al.:* Erste Ergebnisse zur Ionendynamik im ASDEX Upgrade Divertor. Verhandl. DPG (VI) **32**, 297, P19.4 (1997).

511. *Gafert, J., D. Coster, C. Dorn, ASDEX Upgrade Team et al.:* Meßsystem zur hochauflösenden Spektroskopie am ASDEX Upgrade Divertor. Verhandl. DPG (VI) **32**, 290, P14.45 (1997).

512. *Gasparino, U., V. Erckmann, H.-J. Hartfuß, H. Maaßberg and M. Romé:* On- and Off-Axis Modulation: 'Obscure' Transport or ECRH Deposition Effect? 9th Joint Russian-German Meeting on ECRH and Gyrotrons, Karlsruhe/Stuttgart/Garching 1997.

513. *Gasparino, U., H. Maaßberg, M. Romé, N. Marushchenko* and S. Murakami*:* ECRH Kinetic Modelling. 9th Joint Russian-German Meeting on ECRH and Gyrotrons, Karlsruhe/Stuttgart/Garching 1997.

514. *Geier, A. and H. Niedermeyer:* Transient Behaviour of Langmuir Probes in a Magnetized Plasma. 3rd Int. Workshop on Langmuir Probes in Magnetized Plasmas, Berlin 1997.

515. *Geier, A. und H. Niedermeyer:* Transientes Verhalten von Langmuirsonden in einem magnetischen Plasma. Verhandl. DPG (VI) **32**, 268, P4.4 (1997).

516. *Geist, T.:* Dichtemessung in Plasmaexperimenten mittels Millimeter- und Submillimeter-Interferometrie. Informationstechn. Kolloquium, Univ. Braunschweig 1997.

517. *Geist, T. and U. Siart:* A Band-Splitting Filter for ECE Radiometers. 9th Joint Russian-German Meeting on ECRH and Gyrotrons, Karlsruhe/Stuttgart/Garching 1997.

518. *Gori, S., C. Nührenberg, J. Nührenberg and R. Zille:* Beta Studies in Quasi-Symmetric Configurations. Joint Conf. of 11th Int. Stellarator Conf. and 8th Int. Toki Conf. on Plasma Phys. and Control. Nucl. Fusion, Toki 1997.

519. *Görner, C., A. Weller, M. Anton, J. Geiger, W. von der Linden, C.Y. Teo, W7-AS Team et al.:* MHD-Moden und Gleichgewichte am W7-AS in tomographischen Rekonstruktionen. Verhandl. DPG (VI) **32**, 267, P3.5 (1997).

520. *Grieger, G.:* Fusion - Option for an Environmentally Acceptable and Powerful Energy Source. IEA CERT Workshop on Energy Technology R & D Trends, Rome 1997.

521. *Grieger, G.:* Impact of ITER Construction on the European Fusion Laboratories. Statement of the Association Euratom-IPP. Programme Comm. of the CCFP, Brussels 1997.

522. *Grieger, G.:* Stand der Kernfusion. Parlamentarischer Abend der VDI Landesvertretung Bayern und des VDE Bezirksvereins Südbayern mit der Landtagsfraktion der CSU, München 1997.

523. *Grieger, G.:* Der Wendelstein 7-X in Greifswald. Kolloquium, Techn. Univ. Berlin 1997.

524. *Grieger, G. and W7-X Team:* The Wendelstein 7-X Project. Joint Conf. of 11th Int. Stellarator Conf. and 8th Int. Toki Conf. on Plasma Phys. and Control. Nucl. Fusion, Toki 1997.

525. *Grigull, P.:* Edge and Divertor Diagnostics for W7-X. LHD/W7-X Meeting on Divertors, Toki 1997.

526. *Grigull, P., L. Giannone, U. Stroth, R. Brakel, R. Burhenn, A. Elsner, S. Fiedler, T. Geist, H. Hacker, H.-J. Hartfuß, A. Herrmann, D. Hildebrandt, F. Wagner and W7-AS Team:* Density Limit Study on the W7-AS Stellarator. Joint Conf. of 11th Int. Stellarator Conf. and 8th Int. Toki Conf. on Plasma Phys. and Control. Nucl. Fusion, Toki 1997.

527. *Grigull, P., L. Giannone, U. Stroth, K. Borrass, R. Brakel, R. Burhenn, A. Elsner, S. Fiedler, H. Hacker, H.-J. Hartfuß, A. Herrmann, D. Hildebrandt, G. Kühner, R. Schneider, F. Wagner, A. Weller, X.D. Zhang and W7-AS Team:* Density Limit Study on the W7-AS Stellarator. Joint Conf. of 11th Int. Stellarator Conf. and 8th Int. Toki Conf. on Plasma Phys. and Control. Nucl. Fusion, Toki 1997.

528. *Gruber, O.:* Introduction and Summary: Integrated Control and Control Diagnostics for Fusion Devices. 5th Europ. Fusion Physics Workshop, Sesimbra 1997.

529. *Gruber, O.:* ITER Physics Basis, Ch.III.D.3: Kinetic Control and Divertor Control. 7th Disruption, Plasma Control and MHD ITER Expert Group Meeting, Lausanne 1997.

530. *Gruber, O. and ASDEX Upgrade Team:* ASDEX Upgrade: Technical Status and Experimental Results. 12th Executive Comm. Meeting, IEA Implementing Agreement for Investigation of Physics of Tokamaks with Poloidal Divertors, Kloster Seeon 1997.

531. *Gruber, O. and ASDEX Upgrade Team:* ELM and ELM Control Characteristics in ASDEX Upgrade. 6th Disruption, Plasma Control and MHD ITER Expert Group Meeting, Moscow 1997.

532. *Gruber, O. and ASDEX Upgrade Team:* Experimental Results from Divertor II on ASDEX Upgrade. 7th Disruption, Plasma Control and MHD ITER Expert Group Meeting, Lausanne 1997.

533. *Gruber, O. and M. Schittenhelm:* Ripple Effect on Runaway Generation. 6th Disruption, Plasma Control and MHD ITER Expert Group Meeting, Moscow 1997.

534. *Gruber, O. and H. Zohm*:* Stabilization of Neoclassical Modes with ECRH/CD. 6th Disruption, Plasma Control and MHD ITER Expert Group Meeting, Moscow 1997.

535. *Günter, S.:* Cascading High-n Tearing Modes in Flat Shear Regions. 5th Europ. Fusion Physics Workshop, Sesimbra 1997.

536. *Günter, S.:* Dichtebestimmung von Divertorplasmen aus dem Profil von Wasserstofflinien. Seminar, Univ. Rostock 1997.

537. *Günter, S.:* Zur Physik von astrophysikalischen- und Fusionsplasmen. Vorlesung, Univ. Rostock, SS 1997.

538. *Günter, S., A. Könies and G. Röpke*:* Zur Zeitentwicklung des elektrischen Mikrofeldes in Plasmen. Verhandl. DPG (VI) **32**, 293, P14.67 (1997).

539. *Günter, S. and Q. Yu*:* Cascading High-n Tearing Modes in Flat Shear Regions. 5th Europ. Fusion Physics Workshop, Sesimbra 1997.

540. *Haas, G. and H.-S. Bosch:* In-Vessel Pressure Measurements in Nuclear Fusion Experiments with ASDEX Upgrade. 2nd Otto-von-Guericke Workshop on Problems of Vacuum Measurements, Magdeburg 1997.

541. *Haas, G., H.-S. Bosch, D. Coster, L. de Kock*, R. Maingi*, J. Neuhauser and R. Schneider:* Pressure Gauges and Neutral Pressure Measurements in ITER. 2nd Int. Workshop on Diagnostics for Experimental Fusion Reactors, Varenna 1997.

542. *Hallatschek, K., M. Bessenrodt-Weberpals, M. Sokoll and ASDEX Upgrade Team:* Waveletartige Zeit-/Frequenztransformationen zur automatischen Erkennung von Plasmaereignissen. Verhandl. DPG (VI) **32**, 298, P19.7 (1997).

543. *Hallatschek, K. and M. Zilker:* Real Time Data Acquisition with Transputers and Power PCs Using the Wavelet Transform for Event Detection. Realtime 97 Conf., Beaune 1997.

544. *Hanesch, P. and E. Bertel:* Streß und mesoskopische Oberflächenmorphologie von Pt(110). Verhandl. DPG (VI) **32**, 930, O37.1 (1997).

545. *Hartfuß, H.-J.:* Core Fluctuations and Non-Thermal Electron Distributions in W7-AS Joint Conf. of 11th Int. Stellarator Conf. and 8th Int. Toki Conf. on Plasma Phys. and Control. Nucl. Fusion, Toki 1997.

546. *Hartfuß, H.-J.:* Detektion von Millimeter- und Submillimeter-Wellen. Vorlesung, Univ. Regensburg, WS 1997/98.

547. *Hartfuß, H.-J.:* Electron Temperature Fluctuation Measurements. 10th Joint Workshop on Electron Cyclotron Emission and Electron Cyclotron Resonance Heating, Ameland 1997.

548. *Hartfuß, H.-J.:* HF-Methoden in der Diagnostik von Hochtemperaturplasmen. Verhandl. DPG (VI) **32**, 263, PIV (1997).

549. *Hartfuß, H.-J.:* Microwave Diagnostics for Fusion Plasmas. 9th Joint Russian-German Meeting on ECRH and Gyrotrons, Karlsruhe/Stuttgart/Garching 1997.

550. *Hartfuß, H.-J.:* Mikrowellenradiometrie mit Anwendungen in Fernerkundung und Astronomie. Vorlesung, Univ. Regensburg, SS 1997.

551. *Hartfuß, H.-J.:* Non-Thermal Electron Energy Distribution from Vertical ECE-Measurements at the W7-AS Stellarator. 10th Joint Workshop on Electron Cyclotron Emission and Electron Cyclotron Resonance Heating, Ameland 1997.

552. *Hartfuß, H.-J., P. Buratti* and M. Zerbini*:* The Non-Imaging Flux Collector as an ECE-Antenna for ITER. Varenna Workshop on ITER Diagnostics, Varenna 1997.

553. *Häse, M. and H.-J. Hartfuß:* Fluktuationen der Elektronentemperatur an Wendelstein 7-AS. Verhandl. DPG (VI) **32**, 298, P19.6 (1997).

554. *Häse, M., H.-J. Hartfuß and M. Hirsch:* Correlation of Temperature and Density Fluctuations on W7-AS. 10th Joint Workshop on Electron Cyclotron Emission and Electron Cyclotron Resonance Heating, Ameland 1997.

555. *Häse, M., H.-J. Hartfuß, M. Hirsch, T. Geist and W7-AS Team:* Electron Temperature Fluctuation Measurements at W7-AS. 9th Joint Russian-German Meeting on ECRH and Gyrotrons, Karlsruhe/Stuttgart/Garching 1997.

556. *Häse, M., H.-J. Hartfuß and C. Watts*:* ECE Fluctuation Measurements on the W7-AS Stellarator. 10th Joint Workshop on Electron Cyclotron Emission and Electron Cyclotron Resonance Heating, Ameland 1997.

557. *Häse, M., W. Pernreiter and H.-J. Hartfuß:* Core Fluctuations and Non-Thermal Electron Distributions at W7-AS. Joint Conf. of 11th Int. Stellarator Conf. and 8th Int. Toki Conf. on Plasma Phys. and Control. Nucl. Fusion, Toki 1997.

558. *Heinrich, O.:* Stand der Fusionsforschung und Ziele von Wendelstein 7-X. Amt für Arbeitsschutz und techn. Sicherheit, Stralsund/Rügen 1997.

559. *Herrmann, W.:* Aussagen über das radiale elektrische Feld beim L-H-Übergang mittels Ladungsaustausch-Diagnostik. Kolloqiumsvortrag, Univ. Stuttgart 1997.

560. *Herrmann, A., H. Greuner, H. Renner and H.-J. Kutsch:* Thermografische Charakterisierung von Strukturfehlern in Divertorelementen des Stellarators W7-X. Verhandl. DPG (VI) **32**, 291, P14.57 (1997).

561. *Herrmann, W., J.A. Heikkinen*, T. Kurki-Suonio* and ASDEX Upgrade Team:* The Time Behaviour of Radial Electric Fields at the L/H-Transition from the Observation of Ripple-Trapped Ions. 6th IAEA Techn. Comm. Meeting on H-Mode Physics, Kloster Seeon 1997.

562. *Herrmann, A. and H. Salzmann:* High Resolution IR Temperature Monitoring System for the ITER Target Plates. 2nd Int. Workshop on Diagnostics for Experimental Nuclear Fusion Reactors, Varenna 1997.

563. *Hildebrandt, D., R. Brakel, A. Elsner, S. Fiedler, L. Giannone, C. Görner, P. Grigull, H. Hacker, D. Naujoks, D. Sünder and W7-AS Team:* Plasma Radiation with Impurity Injection into the Edge Plasma of the Stellarator W7-AS. Joint Conf. of 11th Int. Stellarator Conf. and 8th Int. Toki Conf. on Plasma Phys. and Control. Nucl. Fusion, Toki 1997.

564. *Hirsch, M., B. Kurzan, H.-J. Hartfuß, T. Geist, P. Amadeo, E. Holzhauer*, B. Brañas*, M. Francés* et al.:* Quantitative Density Fluctuation Measurements from Reflectometry. 9th Joint Russian-German Meeting on ECRH and Gyrotrons, Karlsruhe/Stuttgart/ Garching 1997.

565. *Höhn, F., R. Beckmann, W. Jacob and R. Wilhelm:* Die Potentialverteilung einer Multipaktor-Entladung im Übergangsbereich zur HF-Gasentladung. Verhandl. DPG (VI) **32**, 281, P13.51 (1997).

566. *Horn*, A., J. Biener and J. Küppers:* Reaction of Gaseous H Atoms with Physisorbed Trimethylboron: Dimerization to Tetramethyldiboron. 44th AVS Nat. Symp., San Jose,CA 1997.

567. *Horn*, A., T. Zecho*, J. Biener and J. Küppers:* Wechselwirkung von Bortrimethyl mit thermischen Wasserstoffatomen. Verhandl. DPG (VI) **32**, 927, O35.4 (1997).

568. *Iwasaki*, T., S. Itoh*, M. Yagi*, U. Stroth et al.:* Non-Local Model Analysis of Heat Pulse Propagation. 2nd Asian Pasific Plasma Theory Conf., Toki 1997.

569. *Jacob, W.:* Deposition Mechanisms, a-C:H Deposition. Course on Low Temperature Plasma Physics and Applications, Techn. Univ. Eindhoven 1997.

570. *Jacob, W.:* Oberflächenmechanismen bei Deposition und Erosion. Kolloquiumsvortrag, Univ. Gesamthochschule Essen 1997.

571. *Jacob, W.:* Oberflächenmechanismen bei Deposition und Erosion. Univ. Greifswald 1997.

572. *Jacob, W., F.-P. Bach* and R. Beckmann:* Thermisch-induzierte, strukturelle Änderungen an plasmadeponierten Kohlenwasserstoffschichten. Verhandl. DPG (VI) **32**, 622, DS18.1 (1997).

573. *Jacob, W., B. Landkammer and A. von Keudell:* Erosion plasmadeponierter C:H-Schichten in O_2, H_2O und O_2/H_2 Plasmen. Verhandl. DPG (VI) **32**, 301, P23.4 (1997).

574. *Jacob, W., B. Landkammer, K. Maruyama*, W. Wang* and J. Roth:* Erosion of a-C:D Layers in Oxygen and Hydrogen Plasmas and through Annealing in Air. ITER EU Meeting on Co-Deposition, Garching 1997.

575. *Jacob, W., B. Landkammer, K. Maruyama*, J. Roth et al.:* Erosion of a-C:D Layers in Oxygen and Hydrogen Plasmas and through Annealing in Air. ITER Task Related Meeting, JET, Abingdon 1997.

576. *Jacob, W. and P. Pecher:* Quantitative Determination of the Ion- and Neutral Flux to the Substrate in a Methane ECR Plasma. 170. WE-Heraeus-Seminar, Bad Honnef 1997.

577. *Jacob, W. and P. Pecher:* Quantitative Determination of the Ion- and Neutral Flux to the Substrate in a Methane ECR Plasma. Workshop 'Frontiers in Low Temperature Plasma Diagnostics II', Bad Honnef 1997.

578. *Jacob, W. and T. Schwarz-Selinger:* Einfluß der Quellgase auf die Schichteigenschaften bei der Plasmadeposition von wasserstoffhaltigen Kohlenstoffschichten. 8. Bundesdt. Fachtagung Plasmatechnologie, Dresden 1997.

579. *Jacob, W., W. Wang*, K. Maruyama* and J. Roth:* Oxidation und Wasserstoffisotopenaustausch in amorphen deuterierten Kohlenstoffschichten. Verhandl. DPG (VI) **32**, 301, P23.3 (1997).

580. *Jaenicke, R., J. Baldzuhn, R. Brakel, V. Erckmann, J. Geiger, P. Grigull, H.-J. Hartfuß, M. Kick, F. Wagner, A. Weller, W7-AS Team, W7-X Team, NI Group and ECRH Group:* W7-AS as a Proof of Principle of a Optimized Stellarator. Int. Symp. of IAE on Plasma Dynamics in Complex Electromagnetic Fields, Uji 1997.

581. *Jandl, O. and G. Krainz:* Temperaturverteilung im 80 K Kälteschild eines Kryostaten. Int. Conf. on Computational Mechanics, Pernink 1997.

582. *Jenko, F. and B.D Scott:* Driftwellenturbulenz im Hauptplasma. Verhandl. DPG (VI) **32**, 271, P7.6 (1997).

583. *Junker, J.:* Energieversorgung mittels Kernfusion; Das Fusionsexperiment Wendelstein 7-X. VDE Bezirksverein Dresden, Lubmin 1997.

584. *Junker, J.:* The Fusion Experiment Wendelstein 7-X. - Heating, Confinement and Wall Interaction -. Inst. for Reference Materials and Measurements, Geel 1997.

585. *Jüttner, B.:* Properties of Arc Cathode Spots. General Invited Lecture, 23th Int. Conf. Phen. Ionized Gases, Toulouse 1997.

586. *Kallenbach, A.:* Chemical Erosion and Carbon Content in ASDEX Upgrade. NET/ITER Meeting on Chemical Erosion, Kloster Seeon 1997.

587. *Kallenbach, A.:* Plasmadiagnostik. Vorlesung, Univ. Hannover, WS 1997/98.

588. *Kammler*, T. and J. Küppers:* Reactions of Gaseous H Atoms with Coadsorbed D/Methyliodine on Ni(100) Surfaces: Coverage Dependence. 44th AVS Nat. Symp., San Jose,CA 1997.

589. *Kammler*, T. and J. Küppers:* Wechselwirkung thermischer Wasserstoffatome mit carbidischem Kohlenstoff auf Ni(100) Oberflächen. Verhandl. DPG (VI) **32**, 926, O35.2 (1997).

590. *Kappel*, M., M. Steidl*, J. Biener and J. Küppers:* Ionenstrahl-induzierte Gitterschädigung und He-Implantation in Graphit. Verhandl. DPG (VI) **32**, 927, O35.6 (1997).

591. *Kardaun*, J. and O. Kardaun:* Aspects of Parallel Computation and a Flavour of Catastrophe Fitting. Kyushu Univ., Kasuga 1997.

592. *Kardaun, O.:* Confinement Time and Threshold Power Analysis for High Temperature Plasmas - A Unified Approach. Kyushu Univ., Kasuga 1997.

593. *Kardaun, O.:* Generalising Regression and Discriminant Analysis - An Approach towards Combining Confinement and Threshold Analysis. Naka-machi 1997.

594. *Kardaun, O.:* On Interval Prediction for ITER Confinement. 7th Meeting of the ITER Confinement Database and Modelling Working Group, Garching 1997.

595. *Kardaun, O.:* On ITER Confinement Prediction and Some Points Illuminated by the Objections from Dorland and Kotschenreuther. 6th Meeting of the ITER Confinement Database and Modelling Working Group, San Diego,CA 1997.

596. *Kardaun, O.:* A Meta-Analysis of Data from Various Tokamaks for the Purpose of Designing the Next One. Symposium, Univ. Groningen 1997.

597. *Kardaun, O.:* Predicting the Performance of Future Plasma Fusion Devices - A Case for Complex Regression Modelling. Tokyo 1997.

598. *Kardaun, O.:* Towards Reducing Prediction Uncertainties for ITER Confinment. 7th Meeting of the ITER Confinement Database and Modelling Working Group, Garching 1997.

599. *Kass, T., M. Maraschek, W. Suttrop, H. Zohm* and ASDEX Upgrade Team:* Beobachtung und Charakterisierung von Typ I und Typ III ELM-Precursorn am Tokamakexperiment ASDEX Upgrade. Verhandl. DPG (VI) **32**, 294, P16.2 (1997).

600. *Kastelewicz, H., D. Reiter*, R. Schneider, D. Coster and H. Meyer:* Plasmamodellierung für den PSI 1. Verhandl. DPG (VI) **32**, 275, P13.10 (1997).

601. *Kaufmann, M.:* Aktuelle Themen der Fusionsforschung. Kolloquium, Univ. Erlangen 1997.

602. *Kaufmann, M.:* ASDEX Upgrade: Ziele und Ergebnisse. Kolloquium, KFA, Jülich 1997.

603. *Kaufmann, M.:* Einführung in die Plasmaphysik. Vorlesung, Univ. Bayreuth, SS 1997.

604. *Kaufmann, M.:* The European Fusion Programme. 1st Techn. Workshop on SERF, Garching 1997.

605. *Kaufmann, M.:* Spezielle Themen der Plasmaphysik. Vorlesung, Univ. Bayreuth, WS 1997/98.

606. *Kick, M. and F. Wagner:* W7-AS, Programme and Recent Results. Joint Conf. of 11th Int. Stellarator Conf. and 8th Int. Toki Conf. on Plasma Phys. and Control. Nucl. Fusion, Toki 1997.

607. *Kladny*, R., V. Popp*, T. Schimmel* and J. Küppers:* Reibungsuntersuchungen an dünnen, organischen Filmen auf Au(111) Oberflächen mit AFM/LFM. Verhandl. DPG (VI) **32**, 881, O9.7 (1997).

608. *Klose, S., H. Meyer and M. Laux:* Asymmetries of Double Probe Characteristics Observed in the PSI-1. 3rd Workshop on Electrical Probes in Magnetized Plasmas, Berlin 1997.

609. *Klose, S., H. Meyer, K. Schmidtmann, W. Bohmeyer and G. Fußmann:* Fluktuationsmessungen am Plasmagenerator PSI-1. Verhandl. DPG (VI) **32**, 287, P14.28 (1997).

610. *Könies, A.:* Contribution of Reflected and Passing Particles to the MHD Mode Energy in a Guiding Center Stability Analysis of a Stellarator Plasma. Verhandl. DPG (VI) **32**, 271, P7.7 (1997).

611. *Koponen, J.P.T., O. Dumbrajs*, T. Geist, S. Fiedler, H.-J. Hartfuß, O. Heinrich, M. Hirsch, W. Pernreiter, U. Stroth and H. Walter:* Gas Feed Modulation Experiments at W7-AS. 9th Joint Russian-German Meeting on ECRH and Gyrotrons, Karlsruhe/ Stuttgart/Garching 1997.

612. *Koponen, J.P.T., T. Geist, O. Dumbrajs* and U. Stroth:* Perturbative Particle Transport Studies in Wendelstein 7-AS. Verhandl. DPG (VI) **32**, 295, P16.5 (1997).

613. *Kraus, W., E. Speth, J.-H. Feist, P. Frank, B. Heinemann, R. Riedl et al.:* Large-Area RF Plasma Sources for Fusion Applications. ICIS '97, Taormina 1997.

614. *Krieger, K.:* Plasma Surface Interaction. Summer Univ. for Plasma Physics, Greifswald 1997.

615. *Krieger, K.:* Plasma-Wand-Wechselwirkung in ASDEX Upgrade. Seminar, Univ. Bayreuth 1997.

616. *Küppers, J.:* Abstraction of Adsorbates from Metal Surfaces with H Atoms. Rutgers Univ., New Brunswick,NJ 1997.

617. *Küppers, J.:* Die Wechselwirkung von H Atomen mit Oberflächen von C und C:H. Vom Fusionsreaktor zur Niederdruck-diamantsynthese. Arbeitskreis Kohlenstoff, Giessen 1997.

618. *Kurzan, B.:* Millimeter Wave Reflectometry at ASDEX Upgrade. 9th Joint Russian-German Meet. on ECRH and Gyrotrons, Karlsruhe/Stuttgart/Garching 1997.

619. *Kurzan, B., W. Suttrop, A. Silva*, M.E. Manso*, F. Serra* and ASDEX Upgrade Team:* Messung von Turbulenz am äußeren Plasmarand an ASDEX Upgrade. Verhandl. DPG (VI) **32**, 274, P13.3 (1997).

620. *Kus, A. and O. Kardaun:* Working with SAS and S-Plus. Combined Workshop of the Confinement and Transport Expert Group and Confinement Database and Modelling Expert Group, Garching 1997.

621. *Landkammer, B., A. von Keudell and W. Jacob:* Erosion von a-C:H-Schichten in O_2, H_2O und O_2/H_2 Plasmen: Erosions-messungen, Massenspektrometrie und Oberflächenanalytik. Verhandl. DPG (VI) **32**, 622, DS18.2 (1997).

622. *Lang, P.T.:* Efficient Plasma Refuelling by Pellet Injection from the Magnetic High Field Side on ASDEX Upgrade. Seminar, Cadarache 1997.

623. *Lang, P.T.:* Pellet Fuelling on ASDEX Upgrade. Symp. JS(96)A15 JET, Abingdon 1997.

624. *Lang, P.T.:* Pellet Injection from the Magnetic High-Field Side. US/Japan Workshop on Advanced Fueling, Livermore,CA 1997.

625. *Lang, R.S., P.T. Lang and P. Kupschus*:* Pellet Fuelling System Technology at IPP and JET. Verhandl. DPG (VI) **32**, 289, P14.41 (1997).

626. *Laqua, H.P., V. Erckmann, W7-AS Team and ECRH Group:* ECRH and ECE with Electron Bernstein-Waves at W7-AS. 9th Joint Russian-German Meeting on ECRH and Gyrotrons, Karlsruhe/ Stuttgart/Garching 1997.

627. *Laqua, H.P., V. Erckmann, W7-AS Team and ECRH Group:* Recent ECRH and ECCD Experiments at W7-AS. 10th Joint Workshop on Electron Cyclotron Emission and Electron Cyclotron Resonance Heating, Ameland 1997.

628. *Laux, M., A. Herrmann, H. Kastelewicz, V. Rohde and U. Wenzel:* Entwicklung des Divertorplasmas während einer Dichterampe im Tokamak. (Fachvortrag). Verhandl. DPG (VI) **32**, 294, P16.1 (1997).

629. *Ledl, L., R. Burhenn, G. Kocsis*, W7-AS Team et al.:* Verunreinigungspelletinjektion mittels Pelletinjektor und Laser-Blow-off am Stellarator W7-AS. Verhandl. Verhandl. DPG (VI) **32**, 292, P14.58 (1997).

630. *Lehmann, J. and E. Bertel:* Quantum-Size Effekte auf dem Weg von der 2- zur 1-Dimensionalität. Verhandl. DPG (VI) **32**, 892, O18.4 (1997).

631. *Leuterer, F.:* Elektron Zyklotron Heizung für das Fusionsexperiment ASDEX Upgrade. Univ. Stuttgart 1977.

632. *Leuterer, F.:* Plasma Waves. Summer Univ. for Plasma Physics, Greifswald 1997.

633. *Leuterer F., A.G. Peeters, G. Pereverzev and F. Ryter:* ECRH Deposition Studies in ASDEX Upgrade. 10th Joint Workshop on Electron Cyclotron Emission and Electron Cyclotron Resonance Heating, Ameland 1997.

634. *Leuterer, F., A.G. Peeters, G. Pereverzev and R. Ryter:* Electron Temperature Rise inside the ECRH Power Depositon Region. 9th Joint Russian-German Meeting on ECRH and Gyrotrons, Karlsruhe/ Stuttgart/Garching 1997.

635. *Loarte, A., N. Asakura*, H.-S. Bosch, A. Herrmann, G. Janeschitz, K. McCormick, H.D. Pacher, J. Schweinzer, W. Suttrop et al.:* Experimental Edge Results and Multimachine Comparisons. 6th Int. Workshop on Plasma Edge Theory in Fusion Devices, Oxford 1997.

636. *Lortz, D.:* Hydrodynamik. Vorlesung und Übungen, Univ. München, WS 1997/98.

637. *Maaßberg, H., C.D. Beidler, U. Gasparino, M. Romé, U. Stroth, W7-AS Team et al.:* Transport Analysis in Low-Collisionality W7-AS Plasmas. Joint Conf. of 11th Int. Stellarator Conf. and 8th Int. Toki Conf. on Plasma Phys. and Control. Nucl. Fusion, Toki 1997.

638. *Maaßberg, H., C.D. Beidler and E.E. Simmet:* Density Control Problems in Large Stellarators with Neoclassical Particle Transport. Joint Conf. of 11th Int. Stellarator Conf. and 8th Int. Toki Conf. on Plasma Phys. and Control. Nucl. Fusion, Toki 1997.

639. *Maier, H., S. Kötterl, K. Krieger, R. Neu, M. Balden and ASDEX Upgrade Team:* Performance of Tungsten Coatings as Plasma Facing Components in ASDEX Upgrade. 8th Int. Conf. on Fusion Reactor Materials, Sendai 1997.

640. *Maier, J., F. Hertweck, M.-G. Pacco-Düchs et al.:* Data Files and their Interdependences: A Data Base for the Tokamak Fusion Experiment ASDEX Upgrade. Poster, IAEA Techn. Comm. Meeting on Data Acquisition and Management for Fusion Research, IPP, Garching 1997.

641. *Manso*, M.E., F. Serra*, I. Nunes*, B. Kurzan, W. Suttrop et al.:* H-Mode Studies with Microwave Reflectometry on ASDEX Upgrade. 6th IAEA Techn. Comm. Meeting on H-Mode Physics, Kloster Seeon 1997.

642. *Maraschek, M., S. Günter, T. Kass, B. Scott, H. Zohm* and ASDEX Upgrade Team:* Beobachtung von TAE Moden in ohmsch geheizten Plasmen. Verhandl. DPG (VI) **32**, 270, P7.4 (1997).

643. *Mayer, M. and M. Balden:* Codeposition of Deuterium with Doped Graphites. NET/ITER Meeting on Chemical Erosion, Kloster Seeon 1997.

644. *Mayer, M. and M. Balden:* Retention and Codeposition of Hydrogen with Beryllium and Doped Graphites. ITER EU Meeting on Co-Deposition, Garching 1997.

645. *Mayer, M. and M. Balden:* Retention and Codeposition of Hydrogen with Beryllium and Doped Graphites. ITER Task Related Meeting, JET, Abingdon 1997.

646. *Mayer, M., R. Behrisch, C. Gowers* et al.:* Change of the Optical Reflectivity of Mirror Surfaces Exposed to JET Plasmas. 2nd Int. Workshop on Diagnostics for Experimental Thermonuclear Fusion Reactors, Varenna 1997.

647. *McCormick, K.:* Individual Machine Behavior within the ITER SOL Database, and Interpolation to ITER. 7th Joint ITER Divertor Physics and Divertor Modelling and Database Expert Group Workshop, Naka 1997.

648. *McCormick, K.:* New Results from the ITER SOL Database. 6th Joint ITER Divertor Physics and Divertor Modelling and Database Expert Group Workshop, Garching 1997.

649. *McCormick, K.:* SOL Widths - Trends, and Compatibility of SOL Theories with Experimental Results. JET Divertor Physics Topic Group Meeting, Abingdon 1997.

650. *McCormick, K.:* Status, New Results and Necessary Expansions of the ITER SOL Database. ITER Edge Database Expert Group Workshop, San Diego,CA 1997.

651. *Meister, H., S. de Peña Hempel, A. Kallenbach, M. Alexander and ASDEX Upgrade Team:* Untersuchungen zu Plasmarotation und Impulstransport in ASDEX Upgrade. Verhandl. DPG (VI) **32**, 274, P13.1 (1997).

652. *Mertens, V.:* Core and Divertor Performance Control. 5th Europ. Fusion Physics Workshop, Sesimbra 1997.

653. *Mertens, V.:* High Density Operation in ASDEX Upgrade. JET/ASDEX Upgrade Edge Physics Meeting, Abingdon 1997.

654. *Mertens, V.:* Recent Experiences from Existing Experiments and Recommendations to ITER. 4th ITER PCTF Meeting, Garching 1997.

655. *Meyer, H., W. Bohmeyer, E. Pasch, K. Schmidtmann and G. Fußmann:* Messung der Temperaturen und Strömungsgeschwindigkeit angeregter Argonionen im Plasmagenerator PSI-1. Verhandl. DPG (VI) **32**, 287, P14.29 (1997).

656. *Meyer-Spasche, R.:* Bifurkationsprobleme in Anwendungen. Vorlesung, Techn. Univ. München, WS 1996/97.

657. *Meyer-Spasche, R.:* Dynamische Eigenschaften von linear impliziten Differenzenverfahren. 10. Sitzung u. Workshop, GAMM, Dynamik und Regelungstheorie, Berlin 1997.

658. *Meyer-Spasche, R.:* Dynamische Systeme und Numerische Analysis. Vorlesung, Techn. Univ. München, SS 1997.

659. *Meyer-Spasche, R.:* Nichtlineare Dynamik, numerisch betrachtet. Vorlesung, Techn. Univ. München, WS 1997/98.

660. *Meyer-Spasche, R.:* Secondary Bifurcations of Convection Rolls and Taylor Vortex Flows. Symp. on Stability for Classical and Non-Newtonian Fluids, Oberwolfach 1997.

661. *Meyer-Spasche, R.:* Untersuchungen zur Strukturbildung in Strömungen zwischen rotierenden Zylindern. Kolloquium, Techn. Univ. München 1997.

662. *Müller, H.W., P.T. Lang, K. Büchl, M. Kaufmann, R.S. Lang , V. Mertens, J. Neuhauser, ASDEX Upgrade Team and NI Team:* Effiziente Plasmanachfüllung mittels Pelletinjektion von der magnetischen Hochfeldseite. Verhandl. DPG (VI) **32**, 267, P3.2 (1997).

663. *Münther, C., W. Beck, P. Cierpka, P.T. Lang and G. Weber:* Repetierender Kompakt Li-Injektor. Verhandl. DPG (VI) **32**, 279, P13.42 (1997).

664. *Napiontek, B., K. Behringer and M. Weinlich:* Rekombinationsstrahlung als Plasmadiagnostik im Divertor von ASDEX Upgrade. Verhandl. DPG (VI) **32**, 290, P14.44 (1997).

665. *Naujoks, D., G. Fußmann and H. Meyer:* IU-Characteristics of the Plasma Generator PSI-1. 3rd Workshop on Electrical Probes in Magnetized Plasmas, Berlin 1997.

666. *Neu, R. and ASDEX Upgrade Team:* High-Z Experiments at ASDEX Upgrade. Symp. on Plasma Materials Interactions in Fusion Devices, Nagoya 1997.

667. *Neu, R., K. Asmussen and R. Dux:* Behaviour of Tungsten in ASDEX Upgrade Discharges. Satellite Workshop of ICFRM-8 on High-Z Materials, Sendai 1997.

668. *Neu, R., K. Asmussen, J.C. Fuchs, R. Dux, A. Thoma, ALCATOR C-MOD Group, ASDEX Upgrade Team et al.:* Comparison of High-Z Operation in ASDEX Upgrade and ALCATOR C-Mod. Verhandl. DPG (VI) **32**, 274, P13.5 (1997).

669. *Neu, R., K. Asmussen, K. Krieger, H. Maier, V. Rohde, A. Thoma and ASDEX Upgrade Team:* High-Z Experiments at ASDEX Upgrade. IEA Workshop, Garching/Jülich 1997.

670. *Noterdaeme, J.-M.:* He^3 in H-Mode Conversion Heating Experiments on ASDEX Upgrade. Nagoya Univ. 1997.

671. *Noterdaeme, J.-M.:* H-Minority Heating on W7-AS. Nat. Inst. for Fusion Science. Toki-Shi 1997.

672. *Noterdaeme, J.-M.:* Long Pulse Components Developments in Nagoya. Frascati 1997.

673. *Noterdaeme, J.-M.:* Results of ICRF Heating Experiments on W7-AS and ASDEX Upgrade. Workshop on High Power Heating of Plasmas, Nat. Inst. for Fusion Science, Toki-Shi 1997.

674. *Noterdaeme, J.-M.:* Status of ICRF on ASDEX Upgrade and Calculations for Antenna Modfications. Europ. Coordinating Comm. on Fast Wave, CEA, Cadarache 1997.

675. *Nührenberg, C.:* Curvature and Local Shear Characteristics in Optimized Stellarators. Verhandl. DPG (VI) **32**, 275, P13.11 (1997).

676. *Nührenberg, J.:* The Optimized Stellarator Wendelstein 7-X. 24th Zvenigorod Conf., Zvenigorod 1997.

677. *Nührenberg, J.:* Quasi-Symmetries in Toroidal Confinement. Int. Sherwood Fusion Theory Conf., Madison,WI 1997.

678. *Pacco-Düchs, M.-G., F. Hertweck, J. Maier et al.:* Data Files and their Interdependence: A Data Base for the Fusion Experiment ASDEX Upgrade. Advanced Fusion Research Center, RIAM, Univ. of Kyushu 1997.

679. *Pecher, P.:* Kalibrierte Ionen-, CH_3-Radikalen- und Neutralgasflüsse aus Methan-ECR-Plasmen. 8. Bundesdt. Fachtagung Plasmatechnologie, Dresden 1997.

680. *Pecher, P. and W. Jacob:* Massenspektrometrische Bestimmung der Neutralgaszusammensetzung in einem Methan-ECR-Plasma. Verhandl. DPG (VI) **32**, 266, P2.3 (1997).

681. *Pecher, P. and W. Jacob:* Messungen zum Ionenfluß aus einem Methan-ECR-Plasma. Verhandl. DPG (VI) **32**, 266, P2.4 (1997).

682. *Peeters, A.G., G. Pereverzev and E. Westerhof**: Comparison of Methods for Description of Diffraction in an Anisotropic Plasma. 9th Joint Russian-German Meeting on ECRH and Gyrotrons, Karlsruhe/Stuttgart/Garching 1997.

683. *Peeters A.G., G. Pereverzev, E. Westerhof* and ECRH Group:* Comparison of Methods to Include Diffraction Effects in the Description of the Wave Propagation in an Anisotropic Plasma. 10th Joint Workshop on Electron Cyclotron Emission and Electron Cyclotron Resonance Heating, Ameland 1997.

684. *Peeters A.G. and W. Suttrop:* Nonthermal ECE at the Plasma Edge during the H-Mode. 10th Joint Workshop on Electron Cyclotron Emission and Electron Cyclotron Resonance Heating, Ameland 1997

685. *Pfeiffer, U. und H. Niedermeyer:* Bestimmung fluktuierender Plasmagrößen mittels schnell gesweepter Langmuirsonden. Verhandl. DPG (VI) **32**, 268, P4.3 (1997).

686. *Pfirsch, D.:* Constants of Motion for Drifting Particles. Courant Inst., New York,NY 1997.

687. *Pfirsch, D.:* Lagrangians for Plasmas in Drift-Fluid Approximation. Courant Inst., New York,NY 1997.

688. *Plamann, K., M. Mayer, R. Behrisch et al.:* Erosion und Redeponierung an den Gefäßwänden und dem MKI-Divertor von JET. Verhandl. DPG (VI) **32**, 299, P20.5 (1997).

689. *Puri, S.:* Anomalous Transport via Radiative Collisonality. 7th Europ. Fusion Theory Conf., Jülich 1997.

690. *Puri, S.:* Toroidal Transport via Radiative Collisionality. Int. Sherwood Fusion Theory Conf., Madison,WI 1997.

691. *Radtke, R., C. Biedermann and G. Fußmann:* Relaxation of Dielectronically Excited Ions Observed in an EBIT. Electron Beam Ion Sources and Traps, Gelnhausen 1997.

692. *Rangelov, G. and V. Dose:* Untersuchung von Diamantschichten mit Auftrittspotential-Spektroskopie. Verhandl. DPG (VI) **32**, 878, O8.1 (1997).

693. *Raupp, G., K. Behler, G. Neu, W. Treutterer, D. Zasche, T. Zehetbauer and ASDEX Upgrade Team:* Experience from ASDEX Upgrade Discharge Control Management for Long Pulse Operation. IAEA Techn. Comm. Meeting on Data Acquisition and Management for Fusion Research, IPP, Garching 1997.

694. *Raupp, G., K. Lüddecke*, G. Neu, W. Treutterer, D. Zasche, T. Zehetbauer and ASDEX Upgrade Team:* Evolution Path for the ASDEX Upgrade Real-Time Control System. Int. Conf. on Accelerator and Large Experimental Physics Control System, Beijing 1997.

695. *Raupp, G., O. Gruber, W. Treutterer and ASDEX Upgrade Team:* Advanced Control Concepts Implemented in ASDEX Upgrade. ITER Design Task D324 Review Meeting, Garching 1997.

696. *Reinmüller, K. and A. Bergmann:* Simulation emittierender Langmuir-Sonden. Verhandl. DPG (VI) **32**, 289, P14.38 (1997).

697. *Reinmuth, J., M. Donath, V. Popescu* et al.:* Magnetische Eigenschaften von $FeNi_3$: Untersuchungen mit spinaufgelöster Appearance Potential Spectroscopy. Verhandl. DPG (VI) **32**, 926, O34.11 (1997).

698. *Reinmuth, J., F. Passek and M. Donath:* Magnetic Properties and Electronic Structure of $FeNi_3$. Poster, 17th Europ. Conf. on Surface Science, Enschede 1997.

699. *Renner, H.:* Materials and Engineering of the W7-X Divertor for Stationary Operation. LHD-W7-X Divertor Workshop, NIFS, Toki 1997.

700. *Renner, H.:* Prospects of the W7-X Stellarator as Part of the European Fusion Programme. Colloquium, Kyoto Univ. 1997.

701. *Renner, H., J. Kißlinger, E. Strumberger, H. Greuner and F.-W. Hoffmann:* Divertor Development for Wendelstein 7-X. Joint Conf. of 11th Int. Stellarator Conf. and 8th Int. Toki Conf. on Plasma Phys. and Control. Nucl. Fusion, Toki 1997.

702. *Richter. H. and M. Liebhart*:* Performance Optimizations of Switched SCI-Rings. 11th Annual Int. Symp. on High Performance Computing Systems, Winnipeg 1997.

703. *Richter, H. and M. Ohlenroth*:* Data Acquisition with the SCINET, a Scalable-Coherent-Interface Network. Poster, IAEA Techn. Comm. Meeting on Data Acquisition and Management for Fusion Research, IPP, Garching 1997.

704. *Rodrigues*, A.P., F. Schneider, C.M.B. Correia* et al.:* Multiple DSP System for Real Time Parallel Processing and Feedback Control on Fusion Experiments. IAEA Techn. Comm. Meeting on Data Acquisition and Management for Fusion Research, IPP, Garching 1997.

705. *Roth, J.:* Chemical Sputtering of Graphite and Low Ion Energies. NET/ITER Meeting on Chemical Erosion, Kloster Seeon 1997.

706. *Roth, J.:* Hoch-Z Materialien - eine Alternative für die erste Wand? Verhandl. DPG (VI) **32**, 264, PVII (1997).

707. *Roth, J.:* Hoch-Z Materialien in Fusionsexperimenten. Seminarvortrag, Univ. Stuttgart 1997.

708. *Roth, J.:* Mechanisms and Analytic Description of Chemical Sputtering. Seminarvortrag, Univ. Toronto 1997.

709. *Roth, J. and W. Eckstein:* Erosion of Mixed C/W Materials. IAEA Consultants Meeting on Status of Plasma Induced Erosion Data for Fusion Reactor Materials, IAEA, Wien 1997.

710. *Roth, J., S. Miller, H. Plank and C. Linsmeier:* Dynamics of the Ion Induced Carbide Phase Formation in the Interaction of Metal Layers on Carbon Substrates. 10th Int. Conf. on Surface Modification of Metals by Ion Beams, Gatlinburg 1997.

711. *Roth, J., D. Walsh*, W.R. Wampler* and M. Mayer:* Ion Beam Analysis of Oxidised a-C:D Layers on Be - A Comparison of ^{4}He RBS and ^{28}Si ERD Analysis. 13th Int. Conf. on Ion Beam Analysis, Lisbon 1997.

712. *Roth, J., W.R. Wampler* and W. Jacob:* Deuterium Release from a-C:D Films on Be during Carbide Formation and Oxidation. ITER Task Related Meeting, JET, Abingdon 1997.

713. *Ryter, F.:* ASDEX Upgrade Contribution to ITER Confinement DB3. Combined Workshop of the ITER Expert Groups on Confinement, San Diego,CA 1997.

714. *Ryter, F.:* Rapporteur Summary on ITER Tasks on Threshold. Combined Workshop of the ITER Expert Groups on Confinement, Garching 1997.

715. *Ryter, F.:* Wall Conditioning in ASDEX Upgrade and ASDEX. Combined Workshop of the ITER Expert Groups on Confinement, San Diego,CA 1997.

716. *Ryter, F., F. Leuterer, A.G. Peeters, G. Pereverzev, W. Suttrop and ASDEX Upgrade Team:* Transient Transport from Sawteeth and ECRH Modulation in ASDEX Upgrade. Ist. di Fisica del Plasma, Milano 1997.

717. *Ryter, F., F. Leuterer, A.G. Peeters, G. Pereverzev, W. Suttrop, ECRH Group and ASDEX Upgrade Team:* Modulation der Elektron-Zyklotron-Resonanz-Heizleistung zur Untersuchung des Energietransports im Tokamak ASDEX Upgrade. Plasma-Kolloquium, IPF, Stuttgart 1997.

718. *Ryter, F., F. Leuterer, A.G. Peeters, G. Pereverzev, W. Suttrop, ECRH Group and ASDEX Upgrade Team:* Transient Transport from Sawteeth and ECRH Modulation in ASDEX Upgrade. 9th Joint Russian-German Meeting on ECRH and Gyrotrons, Karlsruhe/ Stuttgart/Garching 1997.

719. *Ryter, F., F. Leuterer, G. Pereverzev, ECRH Group and ASDEX Upgrade Team:* Exploratory on/off Axis ECRH Heating Experiments in ASDEX Upgrade. 9th Joint Russian-German Meeting on ECRH and Gyrotrons, Karlsruhe/Stuttgart/Garching 1997.

720. *Ryter, F., W. Suttrop and ASDEX Upgrade Team:* ASDEX Upgrade Contribution to ITER Confinement DB2. Combined Workshop of the ITER Expert Groups on Confinement, San Diego,CA 1997.

721. *Ryter, F., W. Suttrop, B. Brüsehaber, M. Kaufmann, V. Mertens, H. Murmann, A.G. Peeters, J. Stober, J. Schweinzer, H. Zohm* and ASDEX Upgrade Team:* H-Mode Power Threshold and Transition in ASDEX Upgrade. 6th IAEA Techn. Comm. Meeting on H-Mode Physics, Kloster Seeon 1997.

722. *Sardei, F.:* Kernfusion durch toroidalen Einschluß: Stand und Perspektiven. Univ. der Bundeswehr München, Neubiberg 1997.

723. *Sardei, F.:* La Fusione e il suo Ruolo nel Problema Energetico. Assessorato alla Cultura, Thiene 1997.

724. *Sardei, F.:* Magnetohydrodynamik. Vorlesung Frühjahrs-Trimester, Univ. der Bundeswehr München, Neubiberg 1997.

725. *Sardei, F.:* Rechneranwendungen in der Fluiddynamik. Vorlesung und Praktikum Winter-Trimester, Univ. der Bundeswehr München, Neubiberg 1997.

726. *Schauer, F.:* Kälteversorgungssystem des Kernfusions-experimentes Wendelstein 7-X. Dt. Kälte-Klima-Tagung, Hamburg 1997.

727. *Schimmel*, T., M. Müller* and J. Küppers:* Sub-Einheitszellen-Auflösung per AFM unter Flüssigkeit - Experimentelle Untersuchungen an der Calcit-(1,0,-1,1)-Oberfläche. Verhandl. DPG (VI) **32**, 907, O22.62 (1997).

728. *Schleußner, D., M. Ehrt*, C. Edelmann*, R. Behrisch and P. Franzen:* Wasserstoffinventare in den Divertorkacheln von ASDEX Upgrade. Verhandl. DPG (VI) **32**, 301, P23.2 (1997).

729. *Schneider, R.:* Tree Code - Simulationen zur Plasmabildung mittels ultrakurzer Laserpulse. Verhandl. DPG (VI) **32**, 265, P1.3 (1997).

730. *Schwarz-Selinger, T., A. von Keudell and W. Jacob:* Einfluß der Quellgase auf die Eigenschaften von a-:H-Schichten. Verhandl. DPG (VI) **32**, 620, DS15.4 (1997).

731. *Schweinzer, J.:* Plasma Edge Parameters and Neutral Gas Density in ASDEX Upgrade. JET/ASDEX Upgrade Edge Physics Meeting, Abingdon 1997.

732. *Schweinzer, J., H.-S. Bosch, G. Haas, A. Herrmann, A. Kallenbach, M. Kaufmann, P.T. Lang, V. Mertens, J. Neuhauser, H. Salzmann, W. Sandmann, J. Stober, W. Suttrop, M. Weinlich, ASDEX Upgrade Team and NI Group:* Optimierung der Tokamak-Randschicht auf dem Weg zu ITER. Verhandl. DPG (VI) **32**, 263, PV (1997).

733. *Scott, B.D.:* Computation of Drift-Alfvén Turbulence in Tokamak Geometry and its Role in the L-H Transition. 6th IAEA Techn. Comm. Meeting on H-Mode Physics, Kloster Seeon 1997.

734. *Scott, B.D.:* Computation of Drift-Alfvén Turbulence in Tokamak Geometry and its Role in the L-H Transition. 6th Int. Workshop on Plasma Edge Theory in Fusion Devices, Oxford 1997.

735. *Scott, B.D.:* An Introduction to MHD. Summer Univ. for Plasma Physics, Greifswald 1997.

736. *Scott, B.D.:* A Possible Role for Electromagnetic Drift-Alfvén Microturbulence in the Tokamak L-H Transition. Verhandl. DPG (VI) **32**, 271, P7.5 (1997).

737. *Scott, B.D.:* A Simple Model for Two-Temperature Landau Damping, Applied to Drift-Alfvén Turbulence. Extended MHD Workshop, Madison,WI 1997.

738. *Scott, B.D.:* Theory and Technique for Transport Modelling in a Confined Plasma. Course on Numerical Plasma Physics, Helsinki 1997.

739. *Scott, B.D.:* Three-Dimensional Computation of Drift-Alfvén Turbulence. Int. Sherwood Fusion Theory Conf., Madison,WI 1997.

740. *Scott, B.D.:* Three-Dimensional Computation of Drift-Alfvén Turbulence. Joint US-Europ. Transport Task Force Workshop, Madison,WI 1997.

741. *Shishkin*, A.A., I.N. Sidorenko and H. Wobig:* Magnetic Islands and Drift Resonances in Helias Configurations. Joint Conf. of 11th Int. Stellarator Conf. and 8th Int. Toki Conf. on Plasma Phys. and Control. Nucl. Fusion, Toki 1997.

742. *Sokoll, M., M. Bessenrodt-Weberpals, H. Zohm* and ASDEX Upgrade Team:* MHD-Instabilitäten in β-Limit-Entladungen am Tokamak ASDEX Upgrade. Verhandl. DPG (VI) **32**, 295, P16.4 (1997).

743. *Sorge*, S., G. Röpke*, S. Günter and A. Könies:* Linienverbreiterung durch ein ionisches Mikrofeld. Verhandl. DPG (VI) **32**, 294, P15.2 (1997).

744. *Speth, E., J.-H. Feist, W. Kraus, F.-P. Penningsfeld et al.:* JENIPHER, a European Vision. Joint Development Comm. Meeting, Naka 1997.

745. *Speth, E., B. Heinemann, J.-H. Feist, W. Kraus and R. Riedl:* A Large-Area RF Source for AUG and W7-X NBI. Joint Development Comm. Meeting, Naka 1997.

746. *Stäbler, A.:* Off-Axis NBCD in ASDEX Upgrade - a Proposal. JDC Meeting, Jülich 1997.

747. *Steinbrink, J., U. Wenzel, W. Bohmeyer and G. Fußmann:* Untersuchung von physikalisch zerstäubtem Wolfram in einer linearen Plasmaanlage (PSI-1). Jahrestagung der DPG, Mainz 1997.

748. *Steltenpohl, A. and N. Memmel:* Homoepitaxial Growth of Pd on Pd(111). 17th Europ. Conf. on Surface Science, Enschede 1997.

749. *Steuer, K.-H.:* Fusionsreaktoren, schnelle Brüter und Sonnenkraftwerke - Stand und Perspektiven bei der Erschließung neuer Energiequellen. 4 Schulvorträge, MPG Hauptversammlung, Bremen 1997.

750. *Steuer, K.-H.:* Introduction to Magnetic Fusion. 1st Techn. Workshop on SERF, Garching 1997.

751. *Steuer, K.-H.:* Tokamaks towards Thermonuclear Fusion. Wissenschaftsforum, Demokritos Inst., Athen 1997.

752. *Stroth, U.:* Basic Plasma Physics. Summer Univ. for Plasma Physics, Greifswald 1997.

753. *Stroth, U.:* Confinement Modes in W7-AS. NIFS, Nagoya 1997.

754. *Stroth, U.:* Einführung in die Plasmaphysik I. Vorlesung, Univ. Heidelberg, SS 1997.

755. *Stroth, U.:* Einführung in die Plasmaphysik II. Vorlesung, Univ. Heidelberg, WS 1997/98.

756. *Stroth, U.:* Experimental Results from Stellarators. Summer Univ. for Plasma Physics, Greifswald 1997.

757. *Stroth, U.:* Making Non-Local Transport Visible. Transient Transport Meeting during 24th EPS Conference, Berchtesgaden 1997.

758. *Stroth, U.:* Modelle und Diagnostik zur Untersuchung des Transports in Hochtemperaturplasmen. Kolloquium, Univ. Kiel 1997.

759. *Stroth, U.:* Untersuchungen zu nichtlokalen Transportprozessen am W7-AS Stellarator. Fachvortrag, Verhandl. DPG (VI) **32**, 270, P7.1 (1997).

760. *Stroth, U. and F. Wagner:* Experimental Results from Stellarators with Respect to an Optimization Procedure. 3rd Carolus Magnus Summer School on Plasma Phys., Spa 1997.

761. *Strumberger, E.:* Stochastic Magnetic Field Structure in the Edge Region of W7-X. 6th Int. Workshop on Plasma Edge Theory in Fusion Devices, Oxford 1997.

762. *Strumberger, E. and J. Nührenberg:* Overview W7-X Related Divertor Theory. LHD-W7-X Divertor Workshop, NIFS, Toki 1997.

763. *Suttrop, W.:* Effects of Type I Edge Localized Modes on Transport in ASDEX Upgrade. 6th IAEA Techn. Comm. Meeting on H-Mode Physics, Kloster Seeon 1997.

764. *Suttrop, W.:* Electron Temperature Diagnostics by Electron Emission. Seminar EPFL-CRPP, Lausanne 1997.

765. *Suttrop, W.:* Forschung im IPP - Grundlagen und Beispiele. Techn. Univ. München 1997.

766. *Suttrop, W.:* Identification of H-Mode Operational Limits in ASDEX Upgrade. Trilateral Workshop on High Performance Regimes, Abingdon 1997.

767. *Suttrop, W.:* Influence of Plasma Edge Pressure Gradient Limits on H-Mode Confinement in ASDEX Upgrade. Joint US-Europ. Transport Task Force Workshop, Madison,WI 1997.

768. *Suttrop, W.:* Local Edge Parameter Threshold of the H-Mode Transition in ASDEX Upgrade. Joint US-Europ. Transport Task Force Workshop, Madison,WI 1997.

769. *Suttrop, W., M. Kaufmann, V. Mertens, J. Schweinzer, H. Salzmann, H. Zohm*, ASDEX Upgrade Team and NI Group:* Identifikation Plasmarand-bedingter Operationsgrenzen in ASDEX Upgrade. Verhandl. DPG (VI) **32**, 303, P25.2 (1997).

770. *Taglauer, E.:* The Fusion Reactor. Symp. on Surface Science, Univ. Osnabrück 1997

771. *Taglauer, E.:* Investigations of Surface Structure and Composition by Low-Energy Ion Scattering and Scanning Tunnelling Microscopy. Lawrence Livermore Nat. Lab.,CA 1997.

772. *Taglauer, E.:* Investigations of Surface Structure and Composition by Low-Energy Ion Scattering and Scanning Tunneling Microscopy. Seminar, Sandia Nat. Lab., Livermore,CA 1997.

773. *Taglauer, E.:* Ion Scattering Studies of the Structure and Chemical Composition of Surfaces. 2nd Int. Symp. on Advanced Physical Fields, Tsukuba 1997.

774. *Taglauer, E.:* Ion Scattering Studies of the Structure and Chemical Composition of Surfaces. Nat. Inst. for Research in Inorganic Materials, Tsukuba 1997.

775. *Taglauer, E.:* Oberflächensegregation, Schichtaufbau und Bestrahlungseffekte an metallischen Legierungen: Untersuchungen mit Ionenstreuung. Kolloquiumsvortrag, MPI Metallforschung, Stuttgart 1997.

776. *Taglauer, E.:* Surface Structure and Composition Studies by Low-Energy Ion Scattering. 20th Surface/Interface Research Meeting of the NCCAVS, Livermore,CA 1997.

777. *Taglauer, E.:* Untersuchungen zur Struktur und Zusammensetzung von Metalloberflächen mittels Ionenstreuung. Seminar, Univ. Würzburg 1997.

778. *Taglauer, E. and L. Houssiau*:* Surface Segregation on Binary Alloys Studied by Low-Energy Ion Scattering. Int. Workshop on Surface and Grain Boundary Segregation, Balatonföldvár 1997.

779. *Tasso, H.:* Linear and Nonlinear Stability in Magnetohydrodynamics. Groupe Physique et Statistique des Plasmas, ULB, Brussels 1997.

780. *Tasso, H.:* Lyapunov Stability in Magnetohydrodynamics. Math. Inst., Oberwolfach 1997.

781. *Thoma, A., K. Asmussen, R. Dux, W. Engelhardt, K. Krieger, R. Neu, M. Weinlich, U. Wenzel and ASDEX Upgrade Team, NI Team, ICRH Team and ECRH Group:* Spektroskopische Untersuchung der Wolfram-Erosion in ASDEX Upgrade. Verhandl. DPG (VI) **32**, 276, P13.16 (1997).

782. *Toussaint, U. von, T. Schimmel* and J. Küppers:* Zweidimensionale Computersimulation des AFM-Abbildungsprozesses: Einfluß atomarer stick-slips auf die laterale Auflösung. Verhandl. DPG (VI) **32**, 907, O22.61 (1997).

783. *Vollmer, O. and NI Team*: The Status of the Second ASDEX Upgrade Injector. JDC-Meeting, Jülich 1997.

784. *Wagner, F.:* Aktuelle physikalische Probleme beim magnetischen Einschluß. Kolloquium, Univ. Bremen 1997.

785. *Wagner, F.:* Experimentelle Plasmaphysik I. Vorlesung, Techn. Univ. München, WS 1997/98.

786. *Wagner, F.:* Experimentelle Plasmaphysik II. Vorlesung, Techn. Univ. München, SS 1997.

787. *Wagner, F.:* Fusionsforschung - eine Energiequelle für die Zukunft? MPI Aeronomie, Katlenburg-Lindau 1997.

788. *Wagner, F.:* Major Results from W7-AS with Relevance for W7-X. Kolloquium, Plasma Phys. Lab., Princeton,NJ 1997.

789. *Wagner, F.:* Recent Results from W7-AS Stellarator. APS Meeting, Pittsburgh,PA 1997.

790. *Wagner, F.:* Die Rolle des elektrischen Feldes bei magnetischem Einschluß. Univ. Greifswald 1997.

791. *Wagner, F., H. Niedermeyer and R. Brakel:* Control Requirements in Stellarators. 5th Europ. Fusion Physics Workshop, Sesimbra 1997.

792. *Walter, H., R. Burhenn, L. Giannone, H.-J. Hartfuß, L. Ledl and U. Stroth:* Störexperimente zur Bestimmung des Energietransports im Stellarator W7-AS. Verhandl. DPG (VI) **32**, 267, P3.6 (1997).

793. *Walter, H., R. Burhenn, L. Giannone, H.-J. Hartfuß, L. Ledl and U. Stroth:* Transient Transport Phenomena at W7-AS. Transient Transport Meeting during 24th EPS Conference, Berchtesgaden 1997.

794. *Wanner, M.:* Das Stellarator-Projekt Wendelstein 7-X. Plasmakolloquium, IPF, Stuttgart 1997.

795. *Wanner, M., V. Erckmann, J.-H. Feist, J. Sapper and F. Schauer:* Technical Challenges of the Wendelstein 7-X Stellarator. Joint Conf. of 11th Int. Stellarator Conf. and 8th Int. Toki Conf. on Plasma Phys. and Control. Nucl. Fusion, Toki 1997.

796. *Weinlich, M., A. Carlson and V. Rohde:* Einfluß von Magnetfeldwinkel und Sondengröße auf den Stromfluß zu einer elektrisch geladenen Oberfläche. Verhandl. DPG (VI) **32**, 289, P14.37 (1997).

797. *Weller, A.:* Effect of Shear on Alfvén Eigenmodes in WENDELSTEIN 7-AS. 5th Europ. Fusion Physics Workshop, Sesimbra 1997.

798. *Weller, A., M. Anton, J. Geiger, C. Görner, R. Jaenicke, C. Konrad, C.Y. Teo, W7-AS Team, NI Group et al.:* Global Alfvén Eigenmodes in WENDELSTEIN 7-AS. Proc. 5th IAEA Techn. Comm. Meeting on Alpha Particle Physics, Abingdon 1997.

799. *Weller, A., C. Görner, C.Y. Teo, M. Anton, J. Geiger, R. Jaenicke, C. Konrad, F.-P. Penningsfeld, W7-AS Team, NI Group et al.:* Alfvén Instabilities in WENDELSTEIN 7-AS. Joint Conf. of 11th Int. Stellarator Conf. and 8th Int. Toki Conf. on Plasma Phys. and Control. Nucl. Fusion, Toki 1997.

800. *Wenzel, U. and A. Thoma:* Messung der Strahlungsverluste im Divertor von AUG durch VUV-Spektroskopie. Verhandl. DPG (VI) **32**, 267, P3.4 (1997).

801. *Wesner, F.:* Plasma Heating. Summer Univ. for Plasma Physics, Greifswald 1997.

802. *Wilhelm, R.:* Heating and Current Drive on ITER. 9th Joint Russian-German Meeting on ECRH and Gyrotrons, Karlsruhe/ Stuttgart/Garching 1997.

803. *Wilhelm, R.:* Microwave Plasma Sources and their Applications in Plasmatechnology. Univ. Essen 1997.

804. *Wilhelm, R.:* Microwave Plasma Sources and Applications in Plasma Technology. Workshop Frontiers in Low Temperature Plasma Diagnostics II, Bad Honnef 1997.

805. *Wilhelm, R.:* Mikrowellen-Laufentladung zur Innenbeschichtung von Metallrohren. 8. Bundesdt. Fachtagung Plasmatechnologie, Dresden 1997.

806. *Wilhelm, R.:* Plasma Technology. Summer Univ. for Plasma Physics, Greifswald 1997.

807. *Wilhelm, R.:* Plasma Technology in Germany: Status and Perspectives. Dt.-Japan. Industrieseminar, Bad Honnef 1997.

808. *Wobig, H.:* Der Stellarator als Fusionsreaktor. Seminarvortrag, Berlin 1997.

809. *Wobig, H.:* Theoretische Plasmaphysik I. Vorlesung, Techn. Univ. München, WS 1997/98.

810. *Wobig, H.:* Theoretische Plasmaphysik II. Vorlesung, Techn. Univ. München, SS 1997.

811. *Wobig, H. and J. Kißlinger:* Plasma Equilibrium and Rotation in Stellarators. Joint Conf. of 11th Int. Stellarator Conf. and 8th Int. Toki Conf. on Plasma Phys. and Control. Nucl. Fusion, Toki 1997.

812. *Zecho*, T., A. Horn*, J. Biener and J. Küppers:* Wechselwirkung von atomarem Wasserstoff mit einer Monolage Graphit auf Pt(100). Verhandl. DPG (VI) **32**, 927, O35.5 (1997).

813. *Zehrfeld, H.-P.:* Ideal Modes near the Plasma Edge of ASDEX Upgrade. Informal Meeting on Edge H-Mode Physics for ITER, Garching 1997.

814. *Zehrfeld, H.-P., Yu. Igitkhanov, A.S. Kukushkin, M.I. Mikhailov* and G. Janeschitz:* Effects of Separatrix on MHD Ballooning Mode Stability. 6th Int. Workshop on Plasma Edge Theory in Fusion Devices, Oxford 1997.

815. *Zeiler, A.:* Tokamak Edge Turbulence. 3 Vorträge, Autumn College on Plasma Physics, Trieste 1997.

816. *Zeiler, A., D. Biskamp, J.F. Drake* et al.:* Three-Dimensional Simulations of Tokamak Edge Turbulence. 7th Europ. Fusion Theory Conf., Jülich 1997.

817. *Zilker, M., K. Hallatschek, P. Heimann et al.:* Multiprocessor Systems for Real-Time Data Acquisition on the ASDEX Upgrade and Future Plasma Experiments. Poster, IAEA Techn. Comm. Meeting on Data Acquisition and Management for Fusion Research, IPP, Garching 1997.

818. *Zolotukhin, A.V., C.D. Beidler, F. Herrnegger, J. Kißlinger and H. Wobig:* Effect of Coil Ripple on α-Particle Trajectories in the Helias Reactor. Verhandl. DPG (VI) **32**, 275, P13.12 (1997).

Internal Laboratory Reports

IPP 1/295 *Pitcher, C.S., A. Herrmann, H. Murmann, H. Reimerdes, J. Schweinzer, W. Suttrop, H. Salzmann, ASDEX Upgrade Team and NBI Team:* Heat Transport at the Boundary of ASDEX Upgrade.

IPP 1/308 *Maraschek, M.:* Alfvenwellen in toroidaler Geometrie am Tokamak ASDEX Upgrade.

IPP 1/309 *Sokoll, M.:* MHD-Instabilitäten in magnetisch eingeschlossenen Plasmen und ihre tomographische Rekonstruktion im Röntgenlicht.

IPP 1/310 *Sokoll, M.:* Interpretation and Tomography of SXR Data with the Codes VISO and DIRO.

IPP 1/311 *Neuhauser, J. and ASDEX Upgrade Team:* Report on First Results of ASDEX Upgrade Operations with the LYRA Divertor.

IPP 2/334 *Wobig, H. and J. Kißlinger:* The Effect of Magnetic Field Geometry on Viscous Damping of Rotation in Stellarators.

IPP 2/335 *Drevlak, M.:* Automatic Optimization Procedure for Stellarator Coils.

IPP 2/336 *Werner, F.:* Netzrückwirkungen hervorgerufen durch den Betrieb der Stromversorgungsanlagen für Plasmaheizung und Magnetfeld des Kernfusionsexperiments W7-X.

IPP 2/337 *Karulin*, N.:* Start-up Scenario in a Helias Reactor.

IPP 2/338 *Beidler, C., U. Stroth and H. Wobig:* Empirical Scaling Laws and Extrapolation to Helias Reactors.

IPP 2/339 *Strumberger, E.:* First Survey of Finite-Beta Magnetic Fields of W7-X.

IPP III/217 *Elevant*, T., B. Wolle* and A. Weller:* Neutron Diagnostics for W7-X: A Long Term Plan for the Period 1996-2005.

IPP III/218 *Croci, R.:* Cut-offs and Mode Conversations in a Vlasov Plasma.

IPP III/219 *Salat, A. and J.A. Tataronis*:* The Shear Alfvén Continuum in an Asymmetric MHD Equilibrium.

IPP III/220 *Ellmauer, M.:* Aufbau und Optimierung eines Vielkanal-Spektrometersystems zur Messung radialer Verunreinigungsprofile, Driftgeschwindigkeit und Ionentemperaturen in W7-AS Plasmen.

IPP III/221 *Geist, T., E. Würsching and H.-J. Hartfuß:* Handbuch zum 160 GHZ Interferometer an W7-AS.

IPP III/222 *Wolle*, B.:* Numerical Simulation of Measured Neutron Signals for Plasma Diagnostics on Tokamaks.

IPP III/223 *Theimer, G.:* Charakterisierung transportrelevanter turbulenter elektrostatischer Fluktuationen in der Abschälschicht des Tokamaks ASDEX mittels Darstellung als Superposition von raum-zeitlich lokalisierten Ereignissen.

IPP III/224 *Geier, A.:* Transientes Verhalten von Langmuirsonden in einem magnetischen Plasma.

IPP III/225 W7-AS Contributions to the 24th EPS Conf. on Contr. Fus. a. Pl. Phys. (24-28 June, Kiev, Ukraine). W7-AS Contributions to the Joint Conference of the 11th International Stellarator Conference & 8th International Toki Conference (ITC-8), 29 Sept - 3 Oct 97, Toki-city, Japan.

IPP III/226 *Pfeiffer, U.:* Messung von Elektronentemperatur, Potential und Dichte in einem Plasma mit hoher Zeitauflösung mittels Langmuirsonde.

IPP III/227 *Ernst, B.:* Ionentemperaturen aus niederenergetischen CX-Messungen an W7-AS.

IPP III/228 *Bellido, E.:* Betrieb einer neuen Bolometerkamera und Berechnung der Emmisivität am Stellarator W7-AS.

IPP 4/275 *Verplancke, P.:* Langmuir Probes at High Frequencies in a Magnetized Plasma: A Theoretical and Experimental Study.

IPP 4/276 *Ott, W.:* Neutral-Beam Modulation for Heating Profile Measurements?

IPP 4/277 *Höhn, F.:* Untersuchung von Multipaktorentladungen und deren Wechselwirkung mit Oberflächen.

IPP 5/74 *Scott, B.D.:* Three-Dimensional Computation of Drift-Alfven Turbulence.

IPP 5/75 *Borrass, K., J. Lingertat* and R. Schneider:* A Scrape-off Layer Based Density Limit for JET ELMy H-Modes.

IPP 5/76 *Tasso, H. and G.N. Throumoulopoulos*:* Axissymmetric Ideal Magnetohydrodynamic Equilibria with Incompressible Flows.

IPP 6/347 *Unverzagt, M.:* Energy Related Conservation Law for Fluids and Multi-Fluid Plasmas with Equilibrium Flow.

IPP 8/11 *Napiontek, B., P. Bachmann and H.J. Belitz*:* Collisional-Radiative Model for a Carbon-Hydrogen Plasma, Part 1.

IPP 8/12 *Hantzsche, E.:* Plasma-Randschicht mit aktiver Oberfläche, Teil 2.

IPP 9/112 *Balden, M.:* Thermal Stability and Erosion of the Silicon Doped CFC Material NS31.

IPP 9/113 *Mayer, M.:* SIMNRA User's Guide.

IPP 9/114 *Annen, A.:* Amorphous Hydrogenated Boron-Carbon Films: Deposition, Characterization and Investigation of the Erosion Behaviour.

IPP 9/115 *Labich, S.:* Investigations of the Metal Support Interaction on Rhodium Model Catalysts.

IPP 9/116 *Miller, S.:* Untersuchung der chemischen Wechselwirkung von Titan und Kohlenstoff mittels Röntgen-Photoelektronen-Spektroskopie.

IPP 10/5 *Behringer, K.:* The Influence of Opacity on Hydrogen Line Emission and Ionisation Balance in High Density Divertor Plasmas.

IPP 10/6 *Meister, H.:* Untersuchungen zu Plasmarotationen und Impulstransport in ASDEX-Upgrade.

IPP 10/7 *Neu R., K.B. Fournier*, D. Schlögl et al.:* Observation of X-Ray Spectra from Highly Charged Tungsten Ions in Tokamak Plasmas.

IPP 10/8 *De Peña Hempel, S.:* Untersuchungen zum Transport leichter Verunreinigungen an ASDEX Upgrade.

IPP 10/9 *Asmussen, K., K.B. Fournier*, J.M. Laming*, R. Neu, J.F. Seely*, R. Dux, W. Engelhardt, J.C. Fuchs and ASDEX Upgrade Team:* Spectroscopic Investigations of Tungsten in the EUV Region and the Determination of its Concentration in Tokamaks.

IPP Z/2 *Weißgerber, M. and J. Simon-Weidner:* Analysen zur thermischen und mechanischen Belastung der Targetplatten des AUG - Divertors II.

IPP Z/3 *Jaksic, N.:* Definition der Randbedingungen bei einer Fe-Strukturanalyse durch Nutzung der Symmetriebedingungen einer Stellaratoranordnung.

External Laboratory Reports

FTSC-P(97)P-33.6 *Cordey*, J.G. and O. Kardaun:* Response to M. Kotschenreuther and W. Dorland's Comments Concerning the Prediction of the Performance of ITER. Europ. Domestic Assessment of the ITER Detailed Design Report, S. 66-69.

ITER DDD 5.5.C.01 *Salzmann, H., C. Gowers*, L. de Kock* et al.:* Thomson Scattering Core. ITER Final Design Report.

ITER DDD 5.5.G.06 *Salzmann, H. and L. de Kock*:* ITER Thermography Divertor. ITER Final Design Report.

JET-P(97)39 *Davies*, S.J., M. Endler, S.K. Erents*, K. McCormick et al.:* Overview of Probe Measurements at JET. JET Joint Europ. Torus, Abingdon.

NIFS-470 *Nakajima*, N., M. Yokoyama*, M. Okamoto* and J. Nührenberg:* Optimization of M=2 Stellarator. Nat. Inst. for Fusion Sciences, Nagoya.

UW-CPTC 97-5 *Günter, S.:* MHD Penomena at ASDEX Upgrade. Univ. of Wisconsin,WI.

Index

Teams

ASDEX Upgrade-Team:, M.Albrecht, M.Alexander, K.Asmussen, G.Becker, K.Behler, K.Behringer, A.Bergmann, M.Bessenrodt-Weberpals, K.Borrass, H.-S.Bosch, M.Brambilla, F.Braun, H.Brinkschulte, K.Büchl, A.Buhler, A.Carlson, R.Chodura, D.Coster, L.Cupidol*, H.-J.De Blank, S.De Peña Hempel, S.Deschka, C.Dorn, R.Drube, R.Dux, W.Engelhardt, J.Engstler, H.-U.Fahrbach, S.Fiedler, P.Franzen, J.C.Fuchs, G.Fußmann, J.Gafert, O.Gehre, J.Gernhardt, O.Gruber, S.Günter, G.Haas, K.Hallatschek, D.Hartmann, , B.Heinemann, G.Herppich, A.Herrmann, W.Herrmann, S.Hirsch, M.Hoek, F.Hofmeister, F.Hoenen*, H.Hohenöcker, P.Ignacz, D.Jacobi, W.Junker, A.Kallenbach, O.Kardaun, T.Kass, M.Kaufmann, A.Khutoretski*, H.Kollotzek, W.Köppendörfer, W.Kraus, K.Krieger, B.Kurzan, B.Kuteev*, K.Lackner, P.T.Lang, R.S.Lang, M.Laux, L.L.Lengyel, F.Leuterer, M.Maraschek, M.Markoulaki*, K.-F.Mast, P.McCarthy*, D.Meisel, R.Merkel, V.Mertens, H.W.Müller, F.Münich, H.Murmann, B.Napiontek, G.Neu, R.Neu, J.Neuhauser, J.-M.Noterdaeme, E.Pasch, G.Pautasso, A.G.Peeters, G.Pereverzev, G.Petravich*, C.S.Pitcher, W.Poschenrieder, G.Raupp, K.Reinmüller, R.Riedl, V.Rohde, H.Röhr, J.Roth, F.Ryter, H.Salzmann, W.Sandmann, H.-B.Schilling, M.Schittenhelm, D.Schlögl, H.Schneider, R.Schneider, W.Schneider, G.Schramm, S.Schweizer, J.Schweinzer, R.Schwörer, B.D.Scott, U.Seidel, S.Sesnic, I.Shustov*, C.Sihler, A.Silva*, M.Sokoll, E.Speth, A.Stäbler, K.-H.Steuer, J.Stober, B.Streibl, W.Suttrop, A.Thoma, W.Treutterer, M.Troppmann, N.Tsois*, M.Ulrich, P.Varela*, H.Verbeek, O.Vollmer, Z.Wang*, M.Weinlich, U.Wenzel, F.Wesner, R.Wolf, R.Wunderlich, N.Xantopoulus*, Q.Yu*, D.Zasche, H.-P.Zehrfeld, T.Zehetbauer, H.Zohm.

Confinement Modelling and Database Group: D.Boucher*, A.N.Chudnovskij*, J.W.Connor*, J.G.Cordey*, J.C.DeBoo*, W.Houlberg*, O.Kardaun, S.M.Kaye*, D.R.Mikkelsen*, Y.Miura*, Y.Ogawa*, M.Ossipenko*, F.Ryter, D.P.Schissel*, T.Takizuka*, A.Taroni*, K.Thomsen*, M.F.Turner*, R.E.Waltz*.

ECRH Group (AUG): F.Leuterer, M.Beckmann, H.Brinkschulte, F.Monaco, M.Münich, F.Ryter.

ECRH Group (W7-AS): V.Erckmann, T.Geist, G.Grünwald, J.Hofner, H.Laqua, U.Weber.

ICRH-Group: W.Becker, F.Braun, H.Faugel, R.Fritsch, D.Hartmann, F.Hofmeister, J.-M.Noterdaeme, S.Puri, F.Wesner.

ITER Confinement Database and Modelling Working Group: M.Alexander*, S.E.Attenberger*, G.Bateman*, G.Becker, D.Boucher*, G.Bracco*, T.N.Carlstrom*, J.G.Cordey*, J.W.Connor*, A.N.Chudnovskij*, Yu.N.Dnestrowskij*, J.C.DeBoo*, W.Dorland*, Yu.V.Esipchuck*, S.J.Fielding*, A.Fukuyama*, T.Fukuda*, R.S.Granetz*, M.Greenwald*, G.Hammet*, T.Hirayama*, G.T.Hoang*, D.M.G.Hogeweij*, W.Houlberg*, A.E.Hubbard*, Y.Kamada*, O.Kardaun, S.M.Kaye*, M.Kikuchi*, J.E.Kinsey*, J.A.Konings*, M.Kotschenreuther*, A.H.Kritz*, A Kus, V.M.Leonov*, M.Marinucci*, D.R.Mikkelsen*, Y Martin*, T.Matsuda*, Y.Miura*, O.Naito*, Y.Ogawa*, J.Ongena*, M.Ossipenko*, F.Perkins*, A.R.Polevoi*, E.Righi*, F.Romanelli*, F.Ryter, D.P.Schissel*, H.Shirai*, J.A.Snipes*, P.M.Stubberfield*, U.Stroth, A.Taroni*, T.Takizuka*, H.Tamai*, K.Thomsen*, M.F.Turner*, K.Tsuchiya*, M.Valovic*, G.Vlad*, M.Wakatani*, R.E.Waltz*, J.Weiland*.

NI Group: M.Ciric, P.Frank, P.Franzen, B.Heinemann, W.Kraus, W.Melkus, S.Obermayer; W.Ott, F.-P.Penningsfeld, F.Probst, R.Riedl, W.Schärich, E.Speth, A.Stäbler, R.Süß, O.Vollmer, K.Wittenbecher.

NI Team(W7-AS): W.Melkus, W.Ott, F.-P.Penningsfeld, F.Probst, E.Speth, R.Süß.

PSI Group: W. Bohmeyer, H. Grote, P. Kornejew, H.-D. Reiner.

W7-AS Team: P.Amadeo, M.Anton, S.Baeumel*, T.Baloui*, G.Beikert, E.Bellido, J.Bleuel, R.Brakel, H.Callaghan*, B.Brotas d. Carvalho*, G.Cattanei, H.Chatenet, C.Christou, R.Croci, D.Dorst, O.Dumbrajs*, K.Dyabilin, A.S.Egorov*, M.Ellmauer, A.Elsner, M.Endler, K.Engelhardt, V.Erckmann, B.Ernst, Y.Feng, S.Fiedler, M.Francés, C.Fuchs, U.Gasparino, A.Geier, J.Geiger, T.Geist, L.Giannone, C.Görner, P.Grigull, H.Hacker, M.Häse, H.-J.Hartfuß, G.Herre, M.Hirsch, J.Hofmann, F.Hoffmann, E.Holzhauer, J.K.Hübner, K.Itoh*, S.-I.Itoh*, R.Jaenicke, F.Karger, M.Kick, A.Kislyakov*, T.Klinger*, J.Knauer, C.Konrad, J.P.Koponen, H.Kroiss, G.Kühner, A.Kus, H.Laqua, L.Ledl, H.Maaßberg, N.Marushchenko, M.Mizuuchi, K.McCormick, S.Murakami*, H.Niedermeyer, I.Nomura, W.Ohlendorf, W.Pernreiter, U.Pfeiffer, V.Plyusnin*, S.Reimbold*, M.Romé, N.Ruhs, N.Rust, J.Saffert, M.Saffmann*, A.Salat, F.Sardei, C.Scheiba, S.Schill*, F.Schneider, V.Sergeev*, E.Simmet, E.Solano, U.Stroth, W.Svendsen*, J.A.Tataronis*, G.Theimer, F.Wagner, H.Walter, A.Weller, C.Wendland*, A.Werner*, E.Würsching, P.Zeiler, X.D.Zhang, D.Zimmermann, M.Zippe, S.Zoletnik.

W7-X Team: S.Arndt, C.D.Beidler, R.Bünde, M.Drevlak, S.Gori, H.Greuner, G.Grieger, E.Harmeyer, C.Henning, F.Herrnegger, F.-W.Hoffmann, J.Junker, J.Kißlinger, A.Könies, P.Merkel, H.Münch, A.Nitsche, C.Nührenberg, J.Nührenberg, I.Ott, M.Pillsticker, F.Rau, H.Renner, J.Sapper, F.Schauer, I.Schönewolf, U.Schwenn, H.Strobel, E.Strumberger, M.Wanner, S.Weber, H.Wobig, R.Zille, A.V.Zolotukhin.

Author Index

University Contributions to IPP Programme

LEHRSTUHL FÜR EXPERIMENTELLE PLASMAPHYSIK DER UNIVERSITÄT AUGSBURG

(Prof. Dr. Kurt Behringer)

PLASMA EDGE DIAGNOSTICS

(K. Behringer, U. Fantz, H. Paulin, B. Heger, A. Kottmair and B. Schalk)

1 Molecular Spectroscopy

Knowledge of the ground state vibrational population of molecular hydrogen or deuterium is required for a better understanding of the role of these molecules in the recombination of divertor plasmas. A spectroscopic diagnostic method for measuring this population has been developed in microwave discharges. Using the relevant transition probabilities, analysis of the diagonal Fulcher band (d-a triplet) yields the vibrational population in the upper state. The vibrational temperature in the ground state (X singlet) is correlated with the vibrational population in the upper state via the Franck-Condon principle (see Annual Report 1996). Franck-Condon factors for the three transitions involved have been calculated from RKR potential curves using Telle's *FCFRKR* code (H. Telle, U. Telle, Comput. Phys. Com. **28**, 1982, 1). Vibrational temperatures of H_2 and D_2 range from 2000K to 8500K in the investigated plasmas and show a decrease in T_{vib} with increasing T_e (Fig. 1). The lower T_{vib} in D_2 is due to the greater mass, resulting in lower energy separation of the vibrational levels, while the population is very similar.

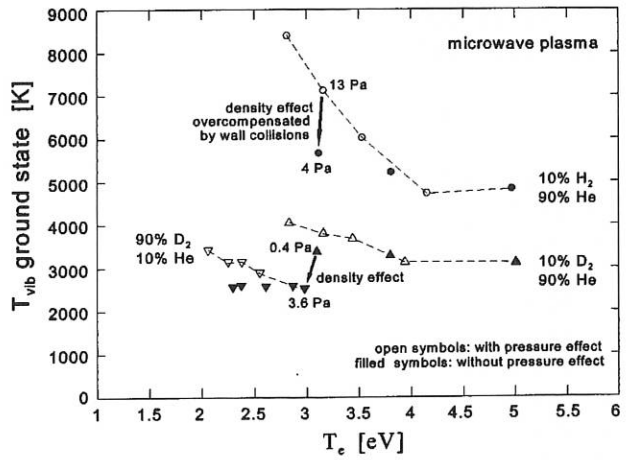

FIG .1: Vibrational population in the ground state of hydrogen and deuterium in low pressure plasmas.

In the investigated microwave discharges an increase in T_e is correlated with a decrease in pressure. The pure effect of T_e is shown by the filled symbols resulting from space resolved measurements. At higher molecular density, the de-exciting heavy particle collisons lead to a decrease in T_{vib}. This process becomes less important at lower densities, but is overcompensated by wall collisions. Measurements of the Fulcher band in the divertor region of ASDEX Upgrade show vibrational temperatures $T_{vib} \approx 4000\text{-}8500$ K ± 500 K in the H_2 ground state depending on line-of-sight and time (i.e. on T_e and n_e). Because of the wide spectral range of the emission bands only two vibrational transitions have been measured resulting in higher error bars for T_{vib}. Together with the rotational temperature in the excited state ($T_{rot} \approx 1000$ - 7000 K ± 50 K) the integral radiance of the bands have been determined. For detailed interpretation of the measurements a collisional radiative model for H_2 and H has been implemented in Augsburg (K. Sawada, T. Fujimoto, J. Appl. Phys. **78**, 1995, 2913, extended by D. Reiter and T. Greenland). In the modelling of H_2, ground state vibrational levels are included as well as electronic states in the united-atom limit. The relevant reactions are selected for a description of fusion plasmas in the limiter/divertor region. The results are e.g. effective ionisation and dissociation rate coefficients, S/XB of Balmer lines and the vibrational population of the H_2 ground state. According to the model, T_{vib} decreases with increasing T_e and is predicted to be 4000K at 10eV. A comparison with experimental data is underway.

2 Chemical Erosion

In low pressure plasmas (microwave plasmas) chemical erosion of carbon by H_2 and D_2 plasmas shows a constant yield of the order of 1 % in the temperature range 300 - 800 K which decreases by a factor of 2 up to 1000 K. A strong isotope effect (factor 3.5) was observed (see Annual Report 1996). This behaviour can be explained by the synergistic effect between hydrogen atoms ($\Gamma_H=\Gamma_D \approx 10^{21} m^{-2}s^{-1}$) and low energy ions (≈10 eV). For a more detailed investigation, a planar inductively coupled RF plasma (27.12 MHz) has been set up. A bias voltage can be applied to the substrate holder. The first experimental results are as follows: The temperature dependence is very similar to the dependence described above. Negative voltage leads to an increased isotope effect (Fig. 2) due to an acceleration of the ions. With positive voltage the isotope effect vanishes above sheath potential and the chemical erosion of cold atoms is being measured. For determination of the atom and ion fluxes to the surface, the plasma parameters must be further investigated.

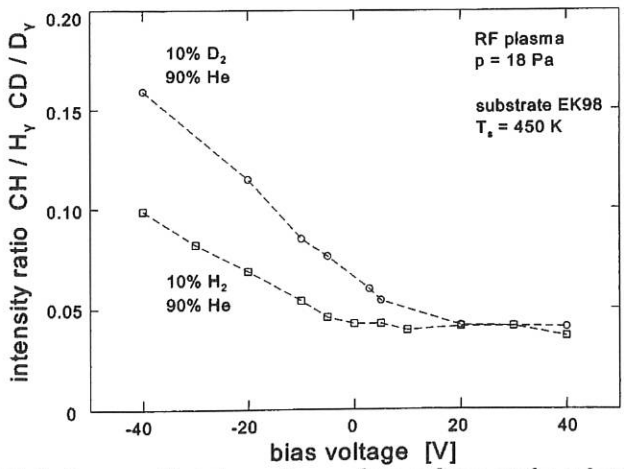

FIG. 2: Isotope effect depending on bias voltage at the substrate holder measured at a temperature of 450 K.

LEHRSTUHL FÜR EXPERIMENTALPHYSIK VI DER UNIVERSITÄT BAYREUTH

(Prof. Dr. Jürgen Küppers)

ELEMENTARY REACTIONS OF HYDROGEN ATOMS WITH ADSORBATES AND SOLID SURFACES

(C. Lutterloh, M. Kappel, A. Horn, T. Zecho)

IPP - University of Bayreuth cooperation is concentrated on investigating fusion-relevant plasma-wall interaction processes. Accordingly, the hydrogen atom surface chemistry on possible wall reactor materials is the primary research topic.

In order to study specifics of boron in H atom/substrate interaction, the reaction of thermal (2000 K) H atoms with adsorbed $B(CH_3)_3$ was investigated. The reaction product $(CH_3)_2B_2H_2(CH_3)_2$ was identified, from which two possible reaction pathways are suggested:

1. abstraction of CH_3 $\quad H + B(CH_3)_3 \rightarrow B(CH_3)_2 + CH_4$
2. H addition $\quad H + B(CH_3)_2 \rightarrow BH(CH_3)_2$
3. dimerization $\quad BH(CH_3)_2 + BH(CH_3)_2 \rightarrow (CH_3)_2B_2H_2(CH_3)_2$

Alternatively,

1. abstraction of CH_3 $\quad H + B(CH_3)_3 \rightarrow HB(CH_3)_2 + CH_3$
2. dimerization $\quad BH(CH_3)_2 + BH(CH_3)_2 \rightarrow (CH_3)_2B_2H_2(CH_3)_2$

The second pathway needs only one H atom induced step, but this step has to release a CH_3 radical. The first pathway needs two H atom steps, but is energetically favourable since the release of methane exhibits considerable exothermicity. At present, it is not possible to decide which pathway is the correct description.

Both reaction schemes involve dimerization of the borane molecule as the final step. This feature is known from borane chemistry as a speciality of B compounds.

The cross-section for the above reactions is a fraction of an $Å^2$. This number identifies the reaction as a direct reaction, as expressed in the Eley-Rideal reaction scheme.

Another molecule tested in reactions with H atoms was propylene oxide, CH_3CHOCH_2. It turned out that H atoms are capable of breaking the C-O-C ring in this molecule on either side, forming an intermediate radical $CH_3CHOHCH_2$, and accordingly n-propanol (CH_3CH_2CHOH) and i-propanol ($CH_3CHOHCH_3$) are reaction products after H atom addition to the radical. The product distribution suggests that n-propanol is the preferential product. The reaction cross-section is in line with the operation of a direct Eley-Rideal process.

As metals are candidates for wall materials, the interaction of H atoms with D-covered surfaces was studied. It was commonly believed that the simple reaction (D abstraction)

$$H + D_{ad}/Ni(100) \rightarrow HD$$

proceeds via an Eley-Rideal step, i.e. hit and react. The fact that the H is not accommodated at the surface prior to reaction has the consequence that the HD product molecule must carry the reaction energy, ca. 2.5 eV, in internal degrees of freedom. In accordance with this expectation, laser spectroscopic measurements have shown that in the $H + D_{ad}/Cu(111)$ reaction the HD products contain ca. 2.5 eV in translational, rotational and vibrational excitation. The hit and react reaction scheme also has the consequence that the kinetics of product formation must be a pure exponential decay of the product rate with time.

The kinetics of D abstraction was measured and found to contradict expectation. Therefore, the description of abstraction of D from metals by H through an Eley-Rideal mechanism (accepted at the textbook level) is wrong. The correct description is a hot atom mechanism in which a hot atom species H* is formed upon H impact on the surface. This hot atom species reacts with the adsorbed D.

Publications and Conference Reports:

Ishi, S., A. Horn, K. Pöhlmann, C. Lutterloh, J. Biener and J. Küppers: Kinematic Study of Isotope Effect of Erosion Reaction at C:H Film Surfaces. Journal of The Surface Science Society of Japan **18 (2)**, 29-32 (1997).

Ishi, S., J. Biener, C. Lutterloh and J. Küppers: Applications of H/C Surface Chemistry to Wall Materials in Fusion Devices and Low Pressure Diamond Synthesis. Memoirs of the Tomakomai College of Technology, Japan, **32**, 131-139 (1997).

Kammler, Th. and J. Küppers: Interaction of Hydrogen Atoms with Coadsorbed D/CH_3I Adlayers on Ni(100) Surfaces: Evidence for Hot Atom Mediated Reactions. Journal of Chemical Physics **107 (1)**, 287-290 (1997).

Kammler, Th. and J. Küppers: Methanation of Carbon on Ni(100) Surfaces at 120 K with Gaseous H Atoms. Chemical Physics Letters **267**, 391-396 (1997).

Kammler, Th., J. Lee and J. Küppers: A Kinetic Study of the Interaction of Gaseous H(D) Atoms with D(H) Adsorbed on Ni(100) Surfaces. Journal of Chemical Physics **106**, 7362-7371 (1997).

Kammler, Th., M. Scherl and J. Küppers: Interaction of H Atoms with Oxygen Adsorbed at Ni(100) Surfaces: Direct Reactions Towards OH and H_2O. Surface Science **382**, 116-126 (1997).

Kappel, M., M. Steidl, J. Biener and J. Küppers: Surface Topography of Low Energy He-Ion-Bombarded Graphite by AFM: Temperature Effects. Surface Science Letters **387**, L1062-L1067 (1997).

Toussaint, U. von, Th. Schimmel and J. Küppers: Computer Simulation of the AFM/LFM Imaging Process: Hexagonal versus Honeycomb Structure on Graphite. Surface and Interface Analysis **25**, 620-625 (1997).

Oral Presentations:

Dinger, A., C. Lutterloh, J. Biener and J. Küppers: H/D Austausch an einer Monolage Graphit auf Pt(111) mit Atomen. Verhandl. DPG (VI) **32**, 927, O 35.3 (1997).

Horn, A., J. Biener and J. Küppers: Reaction of Gaseous H Atoms with Physisorbed Trimethylboron: Dimerization to Tetramethyldiboron. 44th AVS National Symposium, San Jose, CA 1997.

Horn, A., Th. Zecho, J. Biener and J. Küppers: Wechselwirkung von Bortrimethyl mit thermischen Wasserstoffatomen. Verhandl. DPG (VI) **32**, 927, O 35.4 (1997).

Kammler, Th. and J. Küppers: Reactions of Gaseous H Atoms with Coadsorbed D/Methyliodine on Ni(100) Surfaces: Coverage Dependence. 44th AVS National Symposium, San Jose, CA 1997.

Kammler, Th. and J. Küppers: Wechselwirkung thermischer Wasserstoffatome mit carbidischem Kohlenstoff auf Ni(100) Oberflächen. Verhandl. DPG (VI) **32**, 926, O 35.2 (1997).

Kappel, M., M. Steidl, J. Biener and J. Küppers: Ionenstrahl-induzierte Gitterschädigung und He-Implantation in Graphit. Verhandl. DPG (VI) **32**, 927, O 35.6 (1997).

Kladny, R., V. Popp, Th. Schimmel and J. Küppers: Reibungsuntersuchungen an dünnen, organischen Filmen auf Au(111) Oberflächen mit AFM/LFM. Verhandl. DPG (VI) **32**, 881, O 9.7 (1997).

Küppers, J.: Abstraction of Adsorbates from Metal Surfaces with H Atoms. Physics Dept., Rutgers University, NJ 1997.

Küppers, J.: Die Wechselwirkung von H Atomen mit Oberflächen von C und C:H. Vom Fusionsreaktor zur Niederdruckdiamantsynthese. Arbeitskreis Kohlenstoff, Giessen, 1997.

Schimmel, Th., M. Müller and J. Küppers: Sub-Einheitszellen-Auflösung per AFM unter Flüssigkeit - Experimentelle Untersuchungen an der Calcit-(1,0,-1,1)-Oberfläche. Verhandl. DPG (VI) **32**, 907, O 22.62 (1997).

Toussaint, U. von, Th. Schimmel and J. Küppers: Zweidimensionale Computersimulation des AFM-Abbildungsprozesses: Einfluß atomarer stick-slips auf die laterale Auflösung. Verhandl. DPG (VI) **32**, 907, O 22.61 (1997).

Zecho, Th., A. Horn, J. Biener and J. Küppers: Wechselwirkung von atomarem Wasserstoff mit einer Monolage Graphit auf Pt(100), Verhandl. DPG (VI) **32**, 927, O 35.5 (1997).

Diploma Theses:

Dinger, A.: Wechselwirkungen thermischer Wasserstoffatome mit einer Monolage Graphit auf Pt(111) und physisorbierten Kohlenwasserstoffen. Univ. Bayreuth 1997.

Fischer, R.: Aufbau und Test eines UHV-Systems zur Erosion von C-basierten Materialien. Univ. Bayreuth 1997.

Steidl, M.: Die Wechselwirkung von thermischen Wasserstoff-Atomen und mittelenergetischen Helium-Ionen mit Graphit-Oberflächen. Univ. Bayreuth 1997.

Doctoral Thesis:

Lutterloh, C.: Reaktionen thermischer Wasserstoffatome: Adsorption, Austausch und Wechselwirkung mit physisorbierten Kohlenwasserstoffen auf Pt(111) und Graphit/Pt(111). Univ. Bayreuth 1997.

INSTITUT FÜR ANGEWANDTE PHYSIK DER UNIVERSITÄT HEIDELBERG

(Prof. Dr. Klaus Hübner)

Cooperation with IPP in the fields of CX and neutron diagnostics and transport studies was continued in 1997. This comprises CX and neutron measurements at W7-AS, numerical simulation of neutron transport as well as neutron diagnostics for W7-X and investigations of radial heat conduction.

1. SANDMAN - A NEW DETECTOR SYSTEM FOR COLLIMATED D-D NEUTRON FLUX MEASUREMENTS ON W7-X

(T. Baloui, B. Wolle)

A new detector system has been developed for time resolved flux measurements of collimated D-D neutrons in fusion experiments. The novel detection concept, called SANDMAN (special absorber neutron detector moderator assembly), is to place a scatterer behind a collimator and to detect the scattered neutrons in a small Bonner sphere. The system has been optimised by means of MCNP simulations and is capable to be extended for a neutron profile camera. First tests and calibration measurements have been carried out in the 2.5 MeV neutron field at the accelerator facility of PTB. FIG.1 shows the calculated and measured detection probability as a function of the angle of incident neutrons relative to the collimator axis.

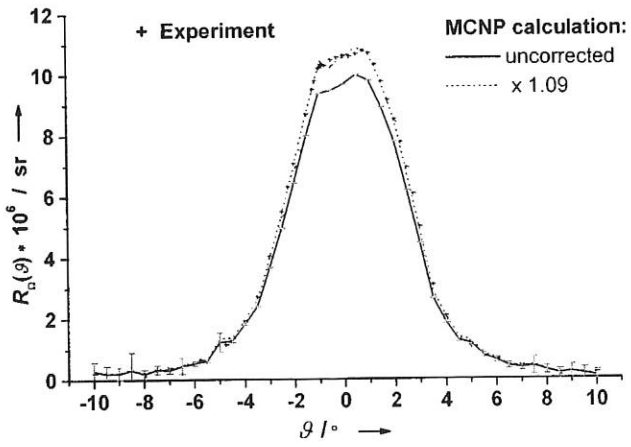

FIG.1: Comparison of measured and simulated angular detection probability

The numerical and experimental results agree well. However, the numerical results are about 9% lower than the experimental ones. This could be due to the neglect of the low-energy scattering background in the simulation of the accelerator neutron source.

2. NEUTRON YIELD MEASUREMENTS BY SAMPLE ACTIVATION ON W7- AS

(S. Schill, T. Baloui, F. Gadelmeier)

Sample activation is considered to be the standard technique for absolute determination of neutron yields from fusion devices. This technique requires a measurement of the sample activation and a Monte Carlo calculation of the ratio of sample activation and neutron yield. On W7-AS it has now also been used to determine the total neutron yields and, thus, to provide a calibration factor for the neutron counters.

Information on the neutron fluence near fusion experiments and near the biological shield is of importance for radiological safety and neutronic compatibility of various plasma diagnostics. On W7-AS, activation measurements have been used to measure the fluence of fast and thermal neutrons at various positions in the diagnostic hall. Neutron transport calculations have been performed using the MCNP code in order to determine the neutron fluence and energy distribution at the irradiation positions. By combining measurements and simulation results, information on the necessary degree of refinement in the geometry modelling and the attainable accuracy in the transport simulations can be obtained. It turns out that the accuracy of the neutronics simulations strongly depends on the quality of the geometric model and the material composition of major structural components. For sufficiently detailed simulation calculations good agreement between experimental and numerical results can be obtained.

LEHRSTUHL FÜR MESSTECHNIK (LMT) DER UNIVERSITÄT DES SAARLANDES

(Prof. Dr. Alexander W. Koch)

The cooperation between IPP and the University of Saarland is concentrated on the development of speckle-measurement techniques to detect arc traces, deformation, erosion, surface roughness, surface structure and surface shape in the divertor region of experimental fusion reactors. The optical method is superior to any mechanical method with respect to data acquisition time and non-perturbing measurement.

1. MEASUREMENT

M. Jakobi, T. Krivosic, M. Ruprecht

The use of phase-shifting methods in speckle interferometry allows calculation of the surface contour of rough objects with three-dimensional information and detection of arc traces. Figure 1a shows a surface deformation measurement of a graphite tile performed with an argon-ion laser and a CCD camera. The detected image corresponds to a measurement area of 10 x 10 mm² and is perturbed by the change of the surface structure caused by two electric arcs on the left side.

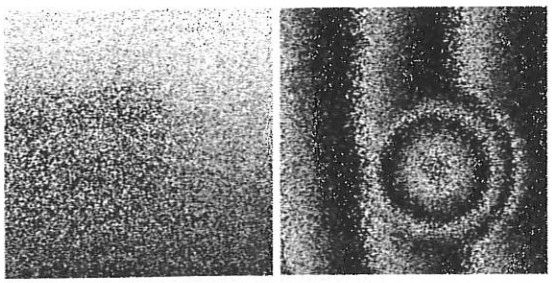

FIG. 1: a) detection of arc traces (left);
b) surface contour measurement (right).

Figure 1b shows a surface contour measurement with a measured area of 5 x 5 mm² tilted 70 µm relatively to an even reference surface and a hole with a depth of 50 µm.

These sample measurements show the ability of the speckle measurement technique to detect arc traces and calculate three-dimensional surface contours of rough objects.

2. SIMULATION

P. Evanschitzky

During a speckle experiment it is very difficult to change the experimental parameters and study their influences separately one after the other. The speckle image simulation presented as a new cooperation project therefore provides a method that can check the practicability of the speckle method for new measurement needs.

The simulation is based on coherent ray tracing allowing image evaluation with conventional personal computers (486 and above). The results of the simulations were compared with theoretical results. We find good agreement between theory and simulation (≈6 %) in the case of, for example, roughness measurements.

At present we are able to simulate the following speckle techniques :

- measurement of surface roughness by spectral speckle correlation (SSC), angular speckle correlation (ASC) and speckle contrast,
- measurement of surface contour and deformation by difference images in speckle interferometry, and
- influence of different parameters such as surface displacement and spectrum of illumination.

Future simulation work will focus on :

- simulation of phase-shifting methods and
- refinement of the simulation model.

INSTITUT FÜR PLASMAFORSCHUNG (IPF) DER UNIVERSITÄT STUTTGART

(Prof. Dr. U. Schumacher)

The long lasting close collaboration of Institute for Plasma Research (IPF) at Stuttgart with MPI of Plasma Physics at Garching is concentrated on the developments, measurements, and interpretation of heating and diagnostic systems. The application of the electron cyclotron resonance heating (ECRH) for W7-X - besides that at the other machines - is of increasing importance, while the diagnostic contributions are in the fields of microwave and high resolution spectroscopy for bulk and divertor plasma diagnostics.

1. PLASMA HEATING AND MILLIMETRE WAVE DIAGNOSTICS

(H. Z o h m , L. Empacher, W. Förster, G. Gantenbein, H. Hailer, E. Holzhauer, W. Kasparek, H. Kumric, G.A. Müller, B. Plaum, P.G. Schüller, K. Schwörer, D. Wagner)

In collaboration with IPP Garching and IAP Nizhny Novgorod.

1.1 Electron cyclotron resonance heating (ECRH)

The studies on ECRH in fusion plasmas were continued. In addition to the contributions to the ECRH systems on the two fusion experiments W7-AS and ASDEX Upgrade in Garching, the design work for the ECRH system of the new stellarator W7-X was a major issue. In addition, different studies for ECRH on ITER were performed. An activity towards the investigation of MHD stability of fusion plasmas using ECRH was started. Accompanying the work for the heating systems, basic research on transmission of high power millimetre waves as well as on power electronics for gyrotrons continued.

1.1.1 ECRH on W7-AS

In 1997 two new 140 GHz long-pulse gyrotrons were put into operation. After commissioning of the gyrotron ECHO, which replaced a defect tube, thermographic measurements were performed, and the beam characteristics (amplitude and phase pattern) were deduced from the data. In collaboration with IAP Nizhny Novgorod, the mirrors needed to match the gyrotron output to the corrugated transmission line were designed, manufactured, and successfully aligned. The ECHO system again delivers 450 kW at the torus window.

The old ALPHA gyrotron was replaced by a new prototype built by Gycom NN (formerly Salut), which delivers 850 kW in 1.5 s pulse-duration. This tube operates with a collector depression of up to 22 kV, resulting in an efficiency of about 50 %. For the operation of the tube, a switched solid-state power supply for the depression voltage with a feed-back control was used, which eliminates noise on the main supply (see also Section *1.1.6*). The optical transmission line was adapted to the output beam for the gyrotron by new matching mirrors, and after alignment is working satisfactorily.

The remotely controlled setting of antenna mirrors and polarisers for the 140 GHz lines is operating now, and work is under way to automatize the polariser setting as a function of the direction of the launched beams, the magnetic field and the operating mode.

In 1998 the two former 70 GHz / 200 kW systems will be replaced by two 500 kW installations, one operating at 70 GHz, the other at 140 GHz. Within the gyrotron building (L3), the transmission of the power will be performed by corrugated waveguides; in the stellarator hall (L7), optical transmission is planned, where both beams share a common mirror system. The design of the transmission was finished, and the waveguide and most of the optical components were fabricated.

1.1.2 ECRH system for ASDEX Upgrade

In 1997 design and construction of the 2 MW, 140 GHz ECRH system for ASDEX Upgrade was continued in collaboration with the ECRH group of ASDEX Upgrade. In its final stage this system will consist of four gyrotrons with individual transmission lines which are a combination of beam waveguide and corrugated HE_{11} waveguide sections.

The transmission lines No. 1 (Sector 8) and No. 2 (Sector 6) were tested with the gyrotrons from GYCOM (Zodiac 3, Zodiac 2). These lines use in their optical part a common pair of mirrors where the two beams overlap. During simultaneous operation of both gyrotrons no problem with arcing occurred in that area. Both transmission lines were aligned carefully by observing the power distribution of the beam on thermosensitive liquid crystal foil at the position of the mirrors and in the waveguide. A circular symmetric power distribution of the mm-wave beam was obtained for the transmission line 2 at the torus window. In the case of line 1, a slightly asymmetric pattern was observed at the torus window which is believed to be due to a small amount of spurious modes from the gyrotron.

A power of about 425 kW in long pulse operation (200 ms) and about 640 kW in short pulse operation (50 ms) was measured calorimetrically at the torus ports.

The beam parameters for the transmission lines No. 3 and 4 were fixed. The manufacture of the optical and waveguide

components was completed. Both lines were assembled and installed partially, including in-vessel components.

1.1.3 *ECRH system for W7-X*

In 1997 the design for the transmission system of the ECRH facility on W7-X was continued in cooperation with the IPP team planning the building. The ECRH system will consist of 10 gyrotrons operating at 140 GHz with 10 MW of RF power in total. Since the system is designed for CW operation, a cooling system for all heat loaded components is required. Transmission of the RF power from the gyrotrons to the stellarator, which is typically over a distance of 60 m, will be performed with mirrors. All five beams of the gyrotrons will be combined and use a common mirror system (so-called Multi Beam Wave Guide, MBWG) installed in the beam duct connecting the ECRH hall to the torus hall. Close to the gyrotrons individual mirrors will be installed to condition the gyrotron beams. Near to the stellarator the beams are split again and guided to the ports of the torus. In total some 150 mirrors, which are remotely controlled (where necessary) are required for this transmission system.

A prototype transmission line of this system is being built up at IPF Stuttgart and will be used to measure beam propagation characteristics with low power equipment at 140 GHz for comparison with the numerical simulations. In a later phase, it can be used as a test-bed for the W7-X components. First parts of this system were manufactured.

3-D diffraction calculations for MBWGs consisting of four mirrors were performed. The mirrors are ellipsoids designed for an axial 140 GHz beam with the geometry of the W7-X system. Although there is some slight astigmatism after two mirrors the distribution of the input beams is correctly reproduced at the output. To check the calculations and to illustrate the behaviour of MBWGs, a small-scale 4-mirror MBWG was constructed. Mirrors with strong curvature were chosen to get strong mode conversion effects. Calculations of amplitude and phase distributions for co- and cross-polarisation were performed and compared with corresponding measurements. In **Fig. 1.1**, various power distributions calculated and measured at the output plane after four mirrors are shown. Generally, good agreement is found for both the central beam and the off-axis beams. The extrapolation of these results to the geometry of the W7-X mirrors shows very little deformation of the beams and very low losses of the fundamental gaussian mode.

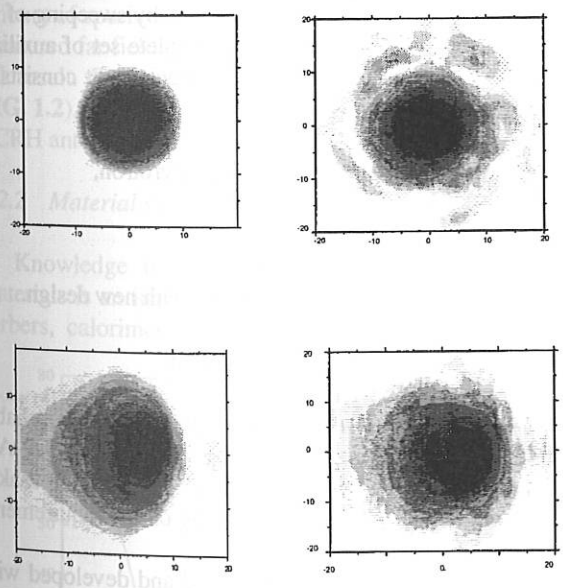

FIG. 1.1: Amplitude patterns for a 140 GHz MBWG with parameters showing mode conversion (f = 120 mm, w_0 = 4.5 mm), calculated (left) and measured (right) after 4 mirrors. Top: central beam; bottom: beam shifted by x = 30 mm.

As the performance of transmission systems strongly depends on the alignment of the mirrors, one focus will be on the development of advanced techniques for precise and reliable adjustment of the beam line. First experiments were performed with diffraction gratings in first order Littrow arrangement. The gratings reflect a small amount of an incident test radiation back into itself. By coupling this beam into the line under test and detecting the reflected power with a directional coupler, the transmission efficiency up to the reflecting device can be monitored. A proof-of-principle experiment for this scheme was carried out using a simple beam waveguide including three mirrors with a grating structure designed for 140 GHz.

A design of the mirrors of the MBWG and their support structure was made. At present it is planned to use a stable Al-framework for the mirrors with an explosion-bonded Cu plate on one side.

The cooling channels will be milled into this Cu plate. A thin Cu layer, made by galvano-technical methods will cover this structure. After final mechanical treatment this layer will serve as the reflecting surface of the mirror. Two small scale prototype mirrors with different cooling channel geometry were manufactured already and will be tested with respect to cooling capabilities and possible deformations.

1.1.4 *ITER contributions*

The work for the EC heating, current drive and start-up systems envisaged on ITER continued. Contributions to ITER R&D work were performed under the ITER task agreement on two parts of the task 'Support for ITER ECRF Design'. Additional work on the properties of microwave transmission elements relevant to ITER diagnostics can be found in Section 1.2.

The conceptual design of a start-up system operating in the range 90 GHz - 140 GHz was finished, the results were summarised in a report.

A costing study for the total ECW system (50 MW port-through power for heating and current drive at 170 GHz plus 6 MW for start-up at 110 GHz and 140 GHz) was performed yielding 94 MECU for the generator (without main power supply) and 92 MECU for the transmission system with two steerable launchers. The main power supply is estimated to cost 31 MECU.

A study for optimisation of the launcher was started. Owing to movements of the vacuum vessel with respect to the cryostat, the antenna waveguides in ITER will be deformed leading to some mode conversion. The goal of the task is to optimise the antenna geometry such that only a low level of spurious modes is excited. Measurements on a slightly scaled launcher model with different waveguide length were performed. Currently, a code to calculate the theoretical mode conversion is set-up which will be

cross-checked with the measurements and then used for the optimisation (see also Section *1.2.1*).

The present concept of the ITER ECRF mirror allows toroidal steering in order to accommodate the various requirements of heating and current drive, both, on- and off-axis and for the full range of toroidal fields. It involves steerable parts close to the plasma which is considered a technical challenge. Thus, the objective of another task was to study alternate concepts that do not have movable parts close to the plasma, but still can fulfil the tasks required.

In the technical part alternative launcher concepts are discussed, e.g. the quasi-optical design which was worked out in 1994. It allows the choice of two injection angles, and a modification of the launcher with an ellipsoidal mirror integrated into the port. The promising concept using corrugated waveguides with square cross-section proposed by GA, San Diego, is now investigated, too. The manufacturing of a 7.8 m long test waveguide was started, and experiments in collaboration with colleagues from IAP Nizhny Novgorod are planned soon. The idea of this concept is to couple the RF power into the waveguide under an angle which, for optimised geometry, is reproduced at the other end. Our investigation will focus on the range of angles for which this transformation leads to acceptable beam quality at the output.

The physics part of the study of alternate concepts focuses on the possibility of using one or two fixed angles for the launcher. This would remove the necessity for steerable parts close to the plasma. It can be shown that, for a frequency of 170 GHz, a choice of 20° and 40° in the toroidal direction does not lead to significant degradation of performance in the standard ignited regime, but shows limited performance for the advanced tokamak regime and only poor performance for the control of MHD modes. This can be improved assuming that step-tunable gyrotrons are available. Then, with two fixed angles the performance of the present system is recovered and even better MHD mode control is possible.

1.1.5 MHD studies using ECRH

Due to its localised deposition ECRH/ECCD has been envisaged as the most promising heating scheme for the control of MHD modes. So far, however, this possibility has not been fully exploited in tokamaks. An activity was started at IPF Stuttgart to investigate this subject in collaboration with the ASDEX Upgrade team.

The steady state β-limit in present day low collisionality tokamaks is given by resistive instabilities, i.e. islands that grow due to the lack of bootstrap current in a once established island (neoclassical tearing modes).

Theoretical studies on the stabilisation of the neoclassical tearing mode by ECCD were performed by considering the generalised Rutherford equation for the island growth. It is found that it is required to drive a helical current of the order of 1 % of the total plasma current in the island for stabilisation. In ITER, this would lead to acceptable power requirements of 20-30 MW of ECRH power.

Applying this theory to ASDEX Upgrade led to the conclusion that stabilisation should be possible with the installed ECRH system. A system for triggering phased ECCD injection into the island was developed and commissioned at IPP Garching. First experiments are planned for early 1998.

1.1.6 Electronic Equipment for ECRH

For the operation of the new gyrotron ALPHA on W7-AS it was necessary to prepare a new power supply adapted to the requirements of depressed collector operation. In detail the gyrotron requires a body to gun (cathode) voltage, i.e. an acceleration voltage of +74 kV and a voltage suppression, i.e. a body to collector voltage of about +24 kV. This could be realised by connecting the gun to a stabilised -50 kV power supply U_b and the body to a +24 kV supply.

To achieve high accuracy of output voltage a modulator was connected between a body-supply U_{body} and the body of the gyrotron. It consists of an old series modulator (tube 1,2) which was formerly built up as a gun anode power supply for the old ALPHA tube. The polarity of this equipment was negative so that a correction was necessary.

With regard to W7-X, in a first stage, a new solid state switched mode power supply developed at IPF was adapted to the requirements of the body-supply. Due to the very low amount of stored energy there was no need of additional crowbar protection units.

In operation difficulties arose due to erosion of the transformer ferrite materials and changed specifications resulting from the first tests. So a second supply in 50 Hz technique was built up. This was operated at +50 kV output voltage. In this arrangement it was possible to demonstrate the operation of the gyrotron in depressed mode with an output RF-power of about 700 kW and a pulse length of 1 s. The achieved efficiency of the gyrotron was 50 %.

The ECRH planned on W7-X is designed for 10 MW output power and requires about 20 MW to 30 MW high voltage electrical power, depending on the efficiency of the gyrotrons. There are efforts to use depressed collector gyrotrons because of the higher efficiency. It is possible that these tubes are equipped with a gun anode for flexible operation and with a collector coil for reduction of ohmic losses at the collector by sweeping of the electron beam. The developments of a complete set of auxiliary supplies has begun at IPF Stuttgart. This equipment consists of the following components:

a) High voltage supply for the body of the gyrotron,
b) high voltage supply for the gun anode,
c) supply for the heater of the gun,
d) current source for collector coils,
e) snubber circuits for gyrotron protection with new design.

(The beam supply is not part of the IPF task.)

The new design will be based on improvements of reliable components already working on ASDEX Upgrade and W7-AS. The components have to be developed in a way which makes individual arrangements possible, depending on the requirements of the gyrotrons.

All equipment is and will be designed and developed with regard to remote operation of the ECRH system on W7-X. This means that there is need of some „intelligence". This will be supplied by implementation of microcontroller circuits. The interface to the W7-X control and supervision system is planned in close contact with the responsible groups at IPP Greifswald and FZK Karlsruhe.

New snubber circuits simplify the crowbar system and improve the reliability.

1.2 General developments in millimetre wave technology

1.2.1 Mode conversion in curved HE_{11} waveguides

Movements of the vacuum vessel of large fusion devices like ITER, e.g. by thermal expansion, can strongly affect the transmission efficiency as well as the radiation pattern of connected oversized HE_{11} waveguide antennas, both, for ECRH and microwave diagnostics. Vertical displacement of the vacuum vessel window leads to an s-bend type deformation of the waveguide.

To analyse the influence of such distortions on the mode purity of oversized corrugated or dielectrically coated waveguides (propagating the low loss HE_{11} hybrid mode), a numerical code based on the coupled mode theory was set up. The code enables also to calculate the far field pattern radiated from the open ended waveguide taking all excited parasitic modes into account. **Figure 1.2** shows the amount of power of spurious modes excited in an s-bend type deformed HE_{11} waveguide with I.D. = 70 mm at 140 GHz as a function of the total length. In this case a vertical displacement d = 28 mm is assumed at the right end of the waveguide, which corresponds to the expected maximum movement of the ITER vacuum vessel during operation.

It can be seen from **Fig. 1.2** that the spurious modes at the waveguide output almost vanish for certain lengths of the s-bend due to reconversion to the main HE_{11} mode. Therefore the excited parasitic mode level can be minimised at certain frequencies by setting the distance of the waveguide supports equal to this length or, if the length is essentially fixed as in the ITER design, by chosing the proper diameter. To verify these numerical results, dielectrically coated HE_{11} waveguides were deformed and the far field radiation patterns measured.

Figure 1.3 shows a comparison between measured and calculated far field radiation pattern of the s-bend with maximum amount of spurious modes (length = 3.3 m, offset = 28 mm). The measured far field pattern is in good agreement with the theoretical result. For a proper design (i.e. in the first minimum of **FIG. 1.2**), practically no mode conversion is expected for the ECRH antenna geometry foreseen in ITER.

1.2.2 Material studies

Knowledge of microwave absorption of suited dielectric materials is an important issue for the design of high power absorbers, calorimetric loads and dummy loads used in ECRH

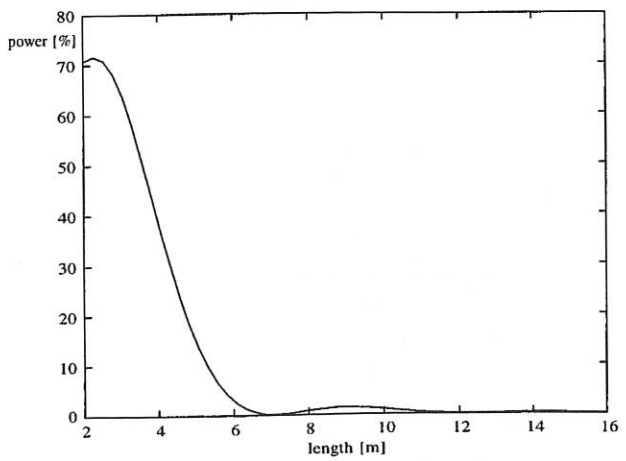

FIG. 1.2: Power converted to spurious modes in an s-bend with I.D. = 70 mm, d = 28 mm, and f = 140 GHz.

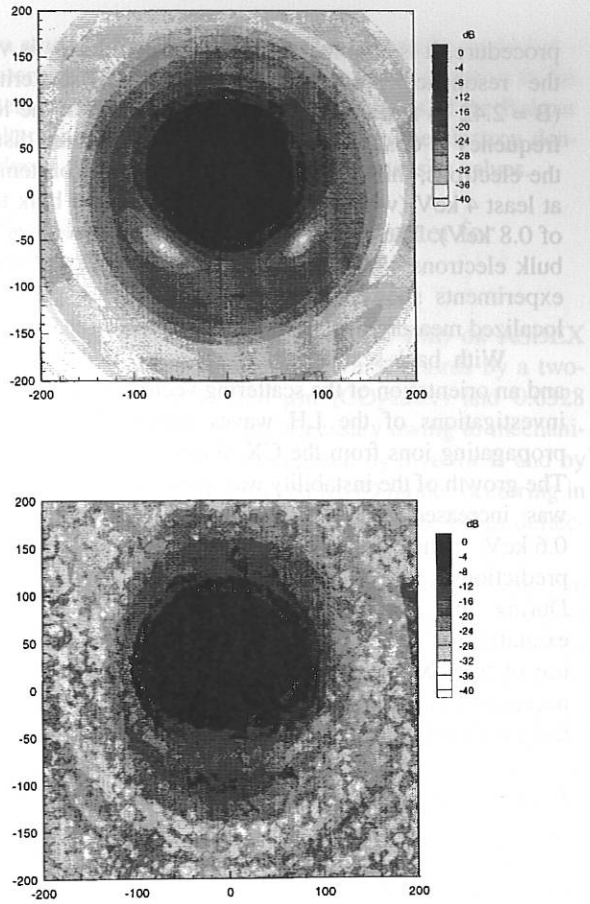

FIG. 1.3: Calculated (top) and measured (bottom) far field radiation pattern of an s-bend with I.D. = 70 mm, L = 3.3 m, d = 28 mm, and f = 140 GHz.

systems for plasma heating. Data of millimetre-wave dielectric properties particularly their dependence on temperature are not available for most materials. Therefore a measuring system is in preparation which consists of an open resonant cavity integrated in a vacuum vessel with a vacuum oven with temperatures up to 1800 °C and a vector-network-analyser measuring amplitude and phase of the wave field in the resonant cavity with and without sample. Since the geometry of the resonator is fixed within narrow limits by the dimensions of the oven, a hemispherical Fabry-Perot resonator about 900 mm long and with beam width w_0 = 17 mm was chosen for measurements at 140 GHz. First test measurements at room temperature were performed and high temperature measurements will be carried out after completion of the resonator device.

1.3 Millimetre wave diagnostics

1.3.1 Collective Thomson scattering on W7-AS

In continuation of the „proof-of-principle" experiments on collective Thomson scattering with powerful gyrotron radiation, experiments in the 90° scattering geometry were performed in collaboration with IAP Nizhny Novgorod. In some shots the EC resonance zone was shifted through the scattering volume by varying the magnetic field B. If the absorbing resonance is behind the scattering volume, a thermal ion feature is measured. The calculated ion temperature is in accordance with the value measured by independent diagnostics. In the evaluation

procedure, it is assumed that cold plasma theory is valid. When the resonance zone is shifted into the scattering volume (B = 2.42 T) strong peaking of the spectrum at the ion acoustic frequency is observed. If we assume Maxwellian distribution of the electrons, this peak indicates a local electron temperature of at least 4 keV (which is to be compared to the bulk temperature of 0.8 keV). The discrepancy can be explained by adding to the bulk electrons 4% of electrons with an energy of 40 keV. The experiments showed, that the 90° scattering geometry allows localized measurements with a spatial resolution of ≤ 4 cm.

With back-scattering experiments (angle about 160 deg) and an orientation of the scattering vector perpendicular to B, the investigations of the LH waves excited by fast transversely propagating ions from the CX diagnostic beam were continued. The growth of the instability was quenched if the ion temperature was increased above a threshold ion temperature of about 0.6 keV. This finding is in agreement with theoretical predictions.
During this experimental campaign, for the first time an excitation of these waves with strong NBI heating without the use of the CX injector was observed. Further investigations are necessary to decide whether this feature can be used to diagnose fast ion distributions.

1.3.2 Microwave reflectometry

The line of sight of the antenna system in the W7-AS stellarator is slightly tilted with respect to the normal onto the cutoff layer. The reflectometer therefore selects density fluctuations with a finite poloidal wavenumber. The poloidal propagation velocity can be calculated from the measured frequency shift together with the poloidal wavenumber. A two-dimensional full-wave code developed in co-operation with the IST (Lisbon) is used to simulate the phase response of the reflectometer. With a simple numerical model for the edge density turbulence good agreement is obtained with the frequency shift measured during an ELM event.

An electronic circuit (frequency tracker) was developed which produces an analogue output signal proportional to the frequency shift in the input signal from the reflectometer. With this device changes in the Doppler shift due to poloidally propagating density fluctuations can now be monitored during a plasma shot without need of recording the original frequency spectrum which can have a width of several MHz.

2. PLASMA EDGE DIAGNOSTICS

(U. Schumacher, G. Dodel, J. Gafert, K. Hirsch, E. Holzhauer, H. Jentschke, S. Klenge, H. Schmidt, K. Schmidtmann)

2.1 High resolution spectroscopy in the divertor of ASDEX Upgrade

The optical system with high spectral, temporal, and spatial resolution applied for the analysis of the ion dynamics in the divertor I of ASDEX Upgrade was used to determine the ion temperature and flow velocity distributions in order to study the specific behaviour of the divertor plasma. As an example the differences of the divertor plasma parameters between L-mode and ELMy H-mode phases and the influence of the ELMs were investigated in more detail. For this reason the intense C III triplet line at 465 nm was recorded for four spatial chords in discharges with hydrogen, for which well defined L-H transitions were performed for nearly constant electron temperature. These mode phases are indicated in **Fig. 2.1** together with the parameters obtained from the numerical fits to the measured C III spectra. The

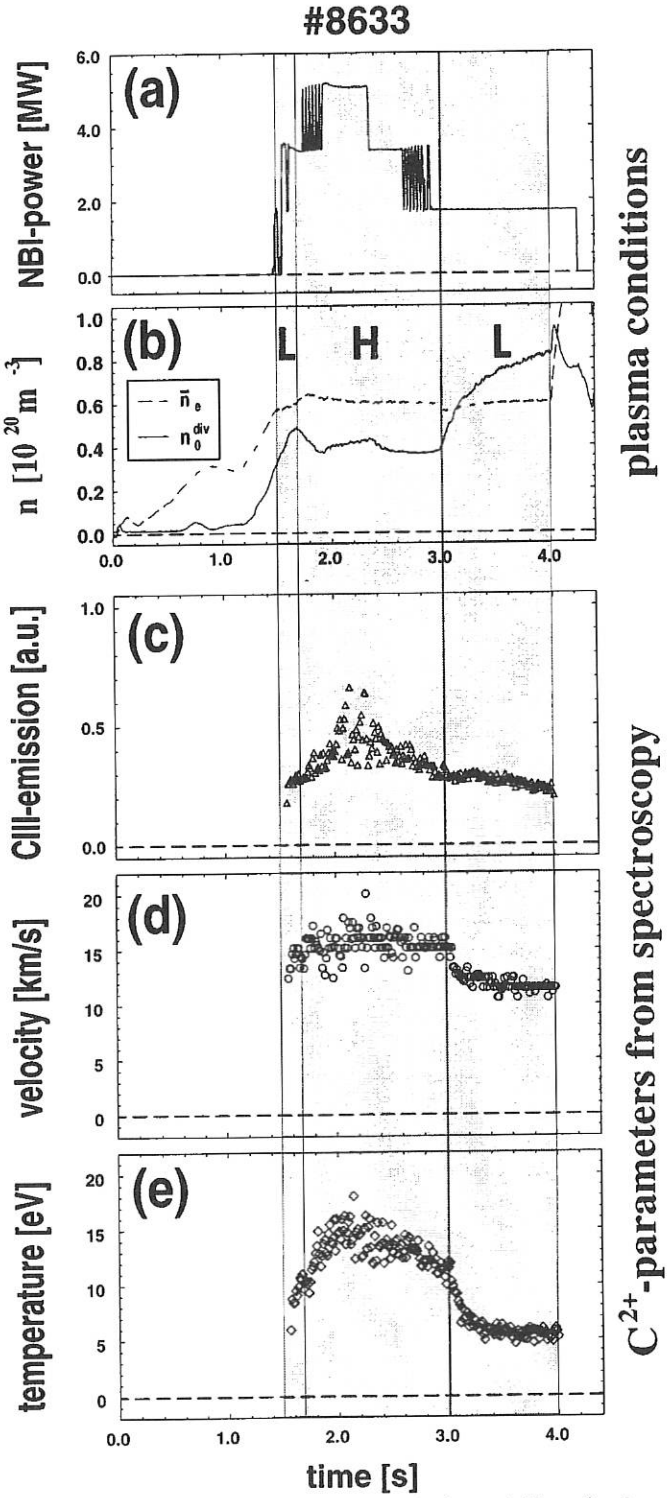

FIG. 2.1: Velocities and temperatures in L- and H-mode phases from C III triplet line spectra, (a) neutral beam injection power, (b) neutral density in divertor and line averaged midplane electron density, (c) C III relative intensity, (d) C^{2+} flow velocities towards the outer divertor plates, (e) C^{2+}-temperatures as function of time.

higher velocity and temperature values during H-mode are due to the ELMs.

The replacement of the ASDEX Upgrade divertor I by the new divertor II led to the reconstruction of the entire divertor spectroscopy. The line of sight arrangement was adapted to the new geometry of the divertor plates, which allows the investigation of the inner and outer divertor region separately. A complete glass fiber coupling system offers the flexibility of connecting each line of sight to any of the spectrometers available providing various temporal, spectral, and spatial resolutions.

The overall number of 160 lines of sight used to investigate the divertor plasma can be divided into the poloidal (for detailed description see the ASDEX Upgrade chapter) and toroidal groups (see **Fig. 2.2**). The toroidal system is designed to measure velocities of ions and neutrals via the Doppler shift of their emission lines. It can be subdivided into chords viewing along the mathematically positive („P") and negative („N") direction. The projections are shown in **Fig. 2.2.** The Doppler shifts measured in lines of sight along the magnetic field lines and those against them are opposite to each other. In order to obtain as much information as possible on the spatial distribution of ion and neutral flows, there are two sets of chords ending on the upper („POU") and lower („POL") part of the outer divertor as well as on the inner divertor („PIL"). Using an appropriate experimental setup and a careful data analysis, flow velocities in the outer and partly in the inner divertor region can be determined reliably. Hence this arrangement allows for the first time a spatially resolved experimental comparison of particle dynamics and spatial emissivity profiles in the outer and inner divertor of ASDEX Upgrade.

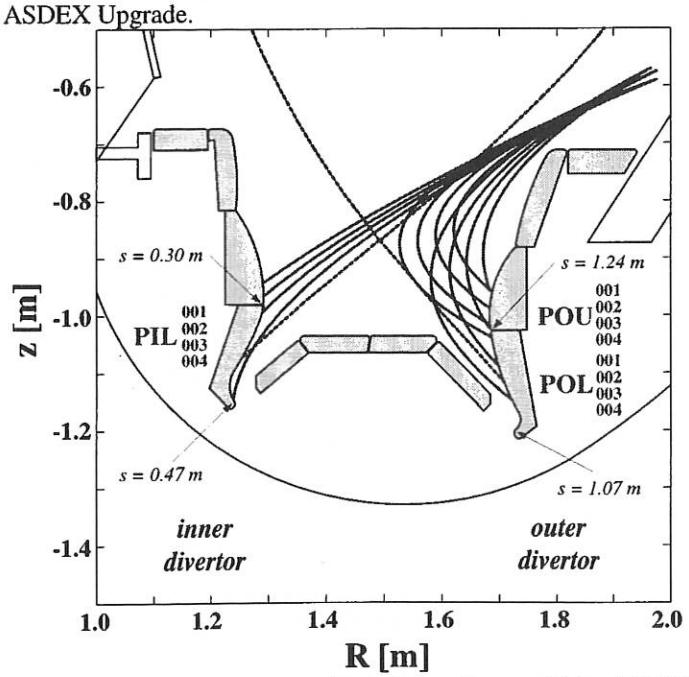

FIG: 2.2: Poloidal cross section of the divertor II in ASDEX Upgrade together with the projections of the toroidal lines of sight.

For specific divertor operations as the detachment phases very strong recombination is observed. This leads to very intense Balmer line and recombination continuum radiation as well. The characteristic features of this radiation can directly be applied for the parameter determination in these dense divertor plasmas. For low electron temperatures (much smaller than about 4 eV) the frequency dependence of the continuum spectrum - if contributions from atomic or molecular line radiation can be neglected - and the intensity step at the Balmer edge are very sensitive to the electron temperature as well as the intensity ratios of the Balmer lines (Boltzmann plot). Using this temperature the electron density is deduced from the absolute continuum intensity values.

2.2 CO_2-laser / HeNe-laser interferometer for ASDEX Upgrade

The DCN-laser interferometer (λ = 195 µm) on ASDEX Upgrade is being replaced in its three vertical chords by a two-wavelength-interferometer at 10.6 µm (CO_2-laser) and 0.6328 µm (HeNe-laser). This change was necessary owing to mechanical constraints (smaller apertures) imposed by divertor II and by physical constraints imposed by locked MHD modes occurring in certain discharges and causing unacceptably large beam deflection at 195 µm.

In collaboration with O. Gehre from IPP Garching the two wavelength interferometer was tested in a laboratory set-up in which the essential beam properties were the same as they will be on the ASDEX Upgrade machine. It is a heterodyne interferometer with a 40 MHz frequency difference between the probing beams and the reference beams generated by acousto-optic modulators. Using phase comparators the interferometer was successfully operated simulating the plasma and its temporal change by rotating a BaF_2-plate in the probing beam and the mechanical vibrations by an oscillating mirror. At present a new electronic data acquisition system developed by G. Schramm from IPP Garching is being tested. It automatically eliminates the contribution of the vibrations to the phase shift yielding an electrical signal from which the line integral of the electron density can be directly deduced.

Before ASDEX Upgrade was closed after installation of divertor II all essential beam positions where marked so that the interferometer can be put into operation on the machine without opening.

2.3 Erosion Studies from Emission and Absorption Spectroscopy

The measurement of erosion products and erosion rates as function of the plasma parameters is of major importance for the tests of thermal protection materials on reusable space transportation systems and on plasma facing walls in thermonuclear fusion devices. The measurements and material tests are performed in plasma wind tunnels, i.e. with plasma jets interacting with targets of the material in question. One of the methods is to study the erosion of a C/C-SiC target of circular cross section in such a plasma jet spectroscopically by high resolution emission and absorption spectroscopy of Si I resonance spectral lines at 251 nm and 288 nm, respectively. The silicon is eroded from the target surface by the plasma jet and forms a radiating cloud in front of the target. The high spectral resolution is obtained applying an Echelle spectrometer.

One method to determine the silicon neutral density from the absorption measurements is to study the branching ratios of the spectral lines in the Si I $3p^2\ ^3P$ - $3p4s\ ^3P^o$ multiplet, an example of which is given in **Fig. 2.3** for different plasma parameters that lead to different optical depths. From this figure the change of the relative line intensities and thus the branching ratios is obvious.

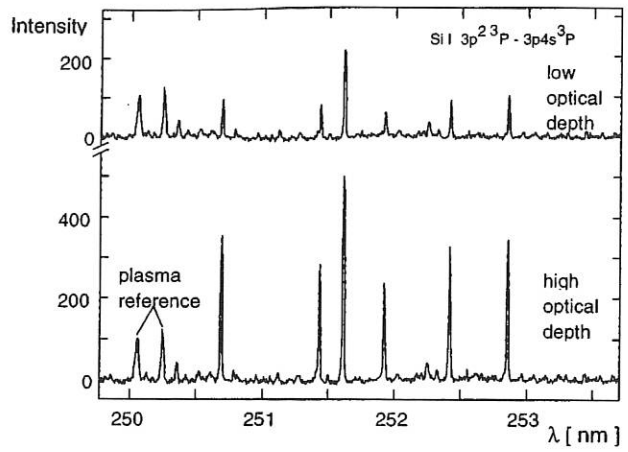

FIG.2.3: An example of the Si I multiplet around 251 nm for different plasma parameters resulting in low optical thickness (top) and higher optical depth (bottom).

Since the optical depths of the different lines of this multiplet are proportional to the silicon ground state line density N_I, the branching ratios allow to determine this line density and hence - with the plasma diameter - the neutral silicon density. Although the line centre intensity ratios are most sensitive to the ground state line density, we applied the less sensitive total spectral line intensity ratios because the complete spectra as shown in **Fig. 2.3** could only be taken with a spectrometer of limited spectral resolution.

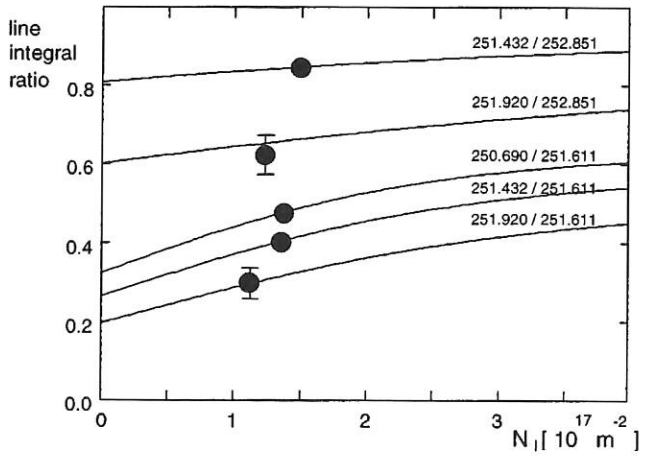

FIG. 2.4: Si I total line intensity ratios versus the silicon line density and experimental results (dots).

An example of the branching ratios and of some other total line intensity ratios of the Si I multiplet around 251 nm plotted versus the silicon ground state line density N_I is given in **Fig. 2.4**. The ratios from the measured spectrum in the lower part of **Fig. 2.3** are included as dots in this figure. In relatively good agreement to each other they result in a silicon line density of about 1.4×10^{17} m^{-2} and hence a silicon ground state density of about 3.5×10^{18} m^{-3}, which, moreover, is in good agreement with other experimental results.

PUBLICATIONS, CONFERENCE REPORTS, DOCTORAL THESES, DIPLOMA THESES, LABORATORY REPORTS, AND LECTURES

PUBLICATIONS

Dose, V., G. Venus, and H. Zohm:
"Wavelet analysis of fusion plasma transients".
Phys. Plasmas **4** (1997) 332-338.

Gafert, J., K. Behringer, D. Coster, C. Dorn, K. Hirsch, M. Niethammer, U. Schumacher, and the ASDEX Upgrade Team:
"First experimental determination of ion flow velocities and temperatures in the ASDEX Upgrade divertor".
Plasma Phys. Control. Fusion **39** (1997) 1981-1995.

Maraschek, M., S. Günter, T. Kass, B. Scott, and H. Zohm:
"Observation of toroidicity induced Alfvén eigenmodes in ohmically heated plasmas".
Phys. Rev. Lett. **79** (1997) 4186-4189.

Müller, H.W., P.T. Lang, K. Büchl, M. Kaufmann, B.V. Kuteev, P.J. McCarthy, V. Mertens, I. Miroshnikov, W. Schneider, and H. Zohm:
"Improvement of q-profile measurement by fast observation of pellet ablation at ASDEX Upgrade".
Rev. Sci. Instrum. **68** (1997) 4051-4060.

Ogawa, I., A. Sakai, T. Idehara, K. Kawahata, and W. Kasparek,:
"A quasi-optical transmission line for plasma scattering measurements using a submillimetre wave gyrotron".
Int. J. Electronics **83** (1997) 635-644.

Sauter, O., R.J. La Haye, Z. Chang, D.A. Gates, Y. Kamada, H. Zohm et al.:
"Beta limits in long-pulse tokamak discharges".
Phys. Plasmas **4** (1997) 1654-1664.

Schittenhelm, M., and H. Zohm:
"Analysis of coupled MHD modes with Mirnov probes in ASDEX Upgrade".
Nucl. Fusion **37** (1997) 1255-1270.

Suvorov, E.V., E. Holzhauer, W. Kasparek et al.:
"Collective Thomson Scattering at W7-AS".
Plasma Phys. Control. Fusion **39** (1997) B337-B351.

Wagner, D., W. Kasparek, G. Gantenbein, M.E. Manso, J. Sanchez, and A.J.H. Donné:
"Transmission line studies for ITER compatible reflectometers".
Rev. Sci. Instrum. **68** (1997) 431-434.

Zohm, H.:
'Stabilization of neoclassical tearing modes by electron cyclotron current drive".
Phys. Plasmas **4** (1997) 3433-3435.

Zohm, H., D.A. Gates, H.R. Wilson, G. Gantenbein, O. Gruber, S. Günther, M. Maraschek, A.W. Morris, M. Sokoll, D. Wagner, ASDEX Upgrade Team, and COMPASS-D Team:
"Neoclassical MHD in ASDEX Upgrade and COMPASS D"
Plasma Phys. Control. Fusion **39** (1997) B237-B246.

CONFERENCE REPORTS

Frühjahrstagung der Deutschen Physikalischen Gesellschaft, Fachausschuß Plasmaphysik, Mainz, March 3 - 6, 1997

Gafert, J., D. Coster, C. Dorn, K. Hirsch, M. Niethammer, U. Schumacher und ASDEX Upgrade Team:
"Meßsystem zur hochauflösenden Spektroskopie am ASDEX Upgrade Divertor"
Verhandl. DPG (VI) **32** (1997) P14.45

Gafert, J., D. Coster, C. Dorn, K. Hirsch, U. Schumacher und ASDEX Upgrade Team:
"Erste Ergebnisse zur Ionendynamik im ASDEX Upgrade Divertor I"
Verhandl. DPG (VI) **32** (1997) P19.4

Schinköth, D., M. Kock, E. Schulz-Gulde:
"Experimentelle Starkkonstanten nahinfraroter Edelgaslinien"
Verhandl. DPG (VI) **32** (1997) P 14.6.

10th Joint Workshop on Electron Cyclotron Emission and Electron Cyclotron Heating, Ameland, The Netherlands, April 7 - 11, 1997

Empacher, L., W. Förster, G. Gantenbein, W. Kasparek, H. Kumric, G.A. Müller, P.G. Schüller, K Schwörer, U. Schumacher, D. Wagner, and H. Zohm:
"Calculations and experiments on multi-beam transmission for the 140 GHz/10 MW CW ECRH system on W7-X".
Proc. EC-**10**.

Kasparek, W., G. Gantenbein, and D. Wagner:
"Application notes for oversized waveguides".
Proc. EC-**10**.

Kumric, H., and H. Zohm:
"The ITER Start-up system".
Proc. EC-**10.**

III. Reflectometry Workshop for Fusion Plasmas, CIEMAT, Madrid, Spain, May 5 - 7, 1997

Grossmann, M.T., E. Holzhauer, M. Hirsch, F. Serra, M .Manso, and I. Nunes:
"A 2-D code for the analysis of microwave reflectometry measurements in fusion experiments".

24th European Physical Society Conference (EPS), Berchtesgaden, Germany, June 9 - 13, 1997

Empacher, L., G. Gantenbein, W. Kasparek, V. Erckmann, and H. Laqua:
"Matching a non-gaussian gyrotron output beam to an ECRH transmission line using thermographic measurements".
Proc. ECA **21A,** 1825-1828.

Gafert, J., D. Coster, C. Dorn, B. Napiontek, U. Schumacher, NBI-Team, and ASDEX Upgrade Team:
"Ion dynamics observed by high resolution spectroscopy in the ASDEX Upgrade divertor I and II".
Proc. ECA **21A,** 1397-1400.

Grossmann, M.T., E. Holzhauer, M. Hirsch, M. Manso, I. Nunes F. Serra, M. Serra:
"A 2-D code for the analysis of microwave reflectometry measurements in fusion experiments".
Proc. ECA **21A,** 475 - 478.

Hirsch, M., J. Baldzuhn, S. Fiedler, T. Geist, P. Grigull, H.J. Hartfuss, J. Hofmann, E. Holzhauer, R. Jaenicke, J.Koponen, F. Wagner, A. Weller, H. Wobig, and the W7-AS Team:
„Dynamic behaviour of the H-mode edge transport barrier in the W7-AS stellarator".
Proc. ECA **21A,** 485 - 488.

Suvorov, E.V., L.V. Lubyako, V. Erckmann, W. Kasparek, E. Holzhauer, S.E. Filchenko, and N.K. Skalyga:
"Spatially resolved measurements of the ion temperature via collective Thomson scattering at W7-AS".
Proc. ECA **21A,** 495 -498.

Zohm, H., G. Gantenbein, D.A. Gates, O. Gruber, S. Günter, K. Hallatschek, T. Kass, M. Maraschek, A.W. Morris, M. Sokoll, D. Wagner, H.R. Wilson, ASDEX Upgrade Team, and COMPASS-D Team:
"Neoclassical MHD in ASDEX Upgrade and COMPASS D".
Proc. ECA **21A,** 156 -159.

International Symposium PLASMA `97, Jarnoltowek near Opole, Poland, June 10 -12, 1997

Hirsch, K., M. Bross, H. Jentschke, and U. Schumacher:
"High resolution emission and absorption spectroscopy for temperature and density determination of erosion products in plasma-target interaction"
Proc. Vol.1, 453-456.

4th International Workshop on Electron Cyclotron Resonance Heating Systems, Germantown, MD, USA, July 16 - 18, 1997

Wagner, D., W. Kasparek, G. Gantenbein, H. Zohm, and M. Thumm:
"Broadband characteristics of HE_{11} transmission lines".

22th International Conference on Infrared and Millimeter Waves, Wintergreen, Virginia, USA, 19 - 24 July, 1997

Michel, G., M. Thumm, and D. Wagner:
"Design of a quasi-optical mode converter for a coaxial 165 GHz $TE_{31,17}$ gyrotron".
Conf. Digest, 25.

Wagner, D., G. Gantenbein, W. Kasparek, M. Thumm, and T. Idehara:
"Scattering matrix description of complete gyrotron oscillators".
Conf. Digest, 156.

2nd International Workshop on Diagnostics for ITER, Varenna, Italy, September 4 - 12, 1997

Manso, M., L. Cupido, G. Leclert, D. Wagner, G. Vayakis, A.J.H. Donné, deKock, C. Laviron, J. Sanchez, F. Serra, A. Silva, C.I. Walker, and the ITER Joint Central Team and Home Teams:
"Reflectometry in the ITER divertor".

Vayakis, G., D. Bartlett, P. Edmonds, H. Hartfuß D. Wagner, C.I. Walker, and the ITER Joint Central Home Teams:
"The ITER ECE diagnostic front end design".

Vayakis, G., T. Ando, N. Bretz, L. deKock, A.J.H. Donné, E .Doyle, J. Irby, E. Martin, M. Manso, A. Mase, J. Sanchez, V. Vershkov, D. Wagner, C.I. Walker, and the ITER Joint Central Team and Home Teams:
"Overview of the ITER reflectometry diagnostic system".

Vershkov, V., M. Manso, G. Vayakis, J. Sanchez, D. Wagner, C.I. Walker, S. Soldatov, L. Kuznetsova, V. Zhuravlev, B. Sestrretskii, and the ITER Joint Central and Home Teams:
"ITER reflectometry diagnostics for the main plasma".

Wagner, D., W. Kasparek, M. Thumm, G. Gantenbein, H. Zohm:
"Transmission line design for broadband microwave diagnostic systems".

5 th European Fusion Physics Workshop, Lisbon, Portugal

Zohm, H.:
„Overview on Experiments on neoclassical tearing modes",

Forschungsforum 1997, Sonderforschungsbereich 259 an der Universität Stuttgart, Leipzig, Germany, September 16 - 20, 1997

Jentschke, H.,I. Dieringer, G. Neuer:
"Hochtemperaturprobleme rückkehrfähiger Raumtransportsysteme"

DOCTORAL THESES

Baumgärtner, K.M.:
„Ramanspektroskopische und morphologische Untersuchungen an Diamantschichten aus plasmatechnischer und thermischer Abscheidung".
(Raman spectroscopic and morphological investigations on diamond layers deposited by plasma technological and thermal techniques.)

Rohrbach, G.:
„Untersuchung der Geschwindigkeitsverteilungsfunktion der Elektronen im Plasma eines Hohlkatodenbogens":
(Investigation of the electron velocity distribution function in the plasma of a hollow cathode arc.)

LECTURES

Jentschke, H.:
"Emissionsspektroskopie am Plasmawindkanal PWK2".
Institut für Niedertemperatur-Plasmaphysik e.V., Greifswald,
February 20, 1997

Schumacher, U.:
„Aufheizung und Analyse magnetisch eingeschlossener Fusionsplasmen".
Physikalisches Kolloquium der Friedrich-Schiller-Universität Jena,
January 20, 1997

Schumacher, U.:
„Das globale Energieproblem"
Sommerakademie der Studienstiftung, Olang (Südtirol), September 9, 1997

Wagner; D.:
"Scattering matrix description of complete gyrotron oscillators". Department of Applied Physics, Faculty of Engineering,
Fukui University, Japan, March 3, 1997.

Wagner, D,:
"Application of oversized HE11 waveguides in broadband plasma diagnostic transmission lines", Centro de Fusao Nuclear, Instituto Superior Technico, Lisboa, Portugal, May 13, 1997.

Zohm, H.:
„MHD-wie sich ein Plasma bewegt",
Elektrotechnisches Kolloquium, Universität Stuttgart ,
Antrittsvorlesung, June 3, 1997

Zohm, H.:
„MHD-Instabilitäten in heißen Fusionsplasmen",
Kolloquium Theoretische Physik, Universität Karlsruhe

Zohm, H.:
"MHD-Instabilitäten in heißen Fusionsplasmen",
Kolloquium Plasmaphysik, MPI für Plasmaphysik, Berlin

How to reach
Max-Planck-Institut für Plasmaphysik (IPP)

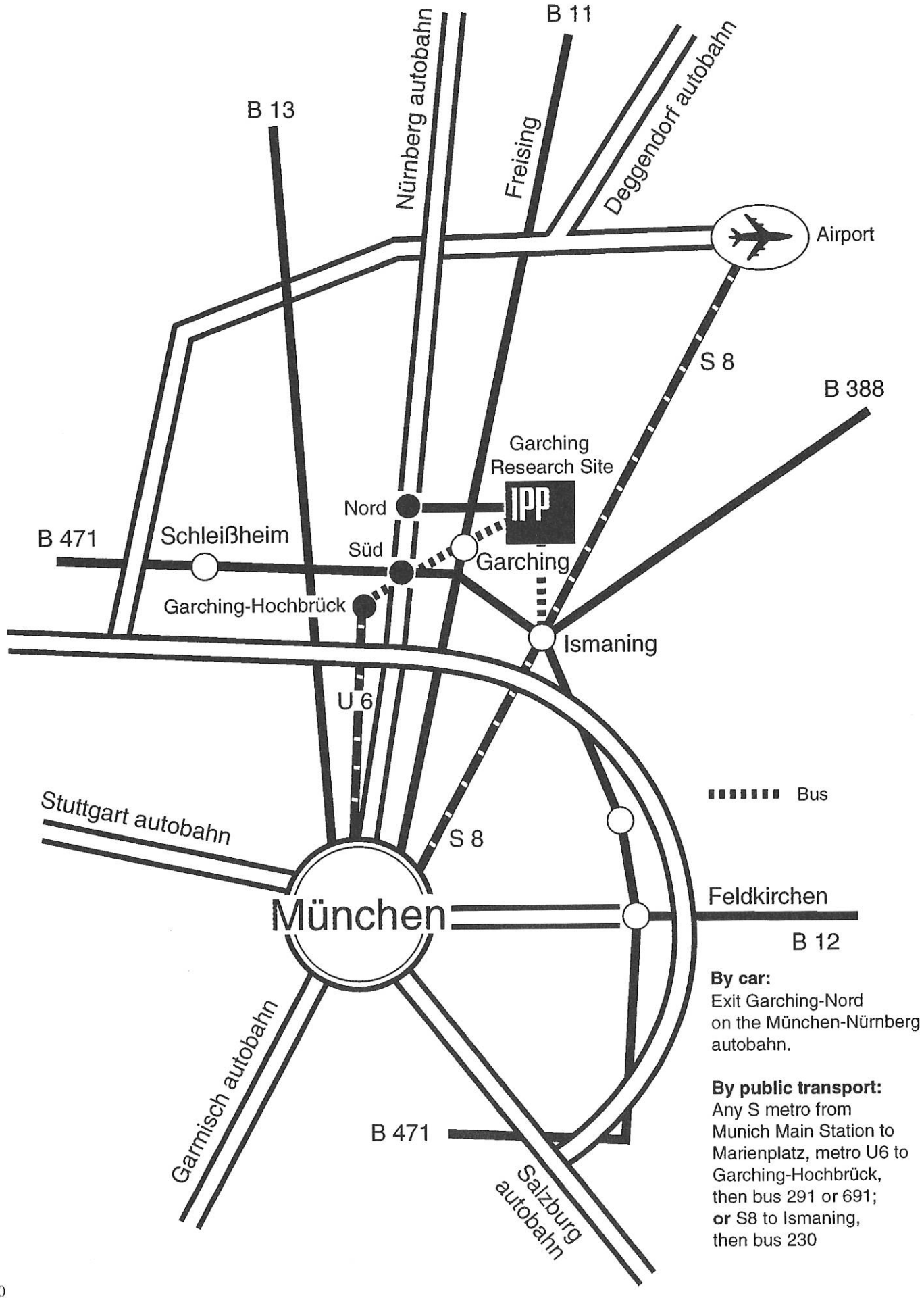

By car:
Exit Garching-Nord
on the München-Nürnberg
autobahn.

By public transport:
Any S metro from
Munich Main Station to
Marienplatz, metro U6 to
Garching-Hochbrück,
then bus 291 or 691;
or S8 to Ismaning,
then bus 230

How to reach Greifswald Branch Institute of Max-Planck-Institut für Plasmaphysik

Greifswald Branch Institute of
Max-Planck-Institut für Plasmaphysik
Walther-Rathenau-Strasse 49a
("Biotechnikum")
D-17489 Greifswald

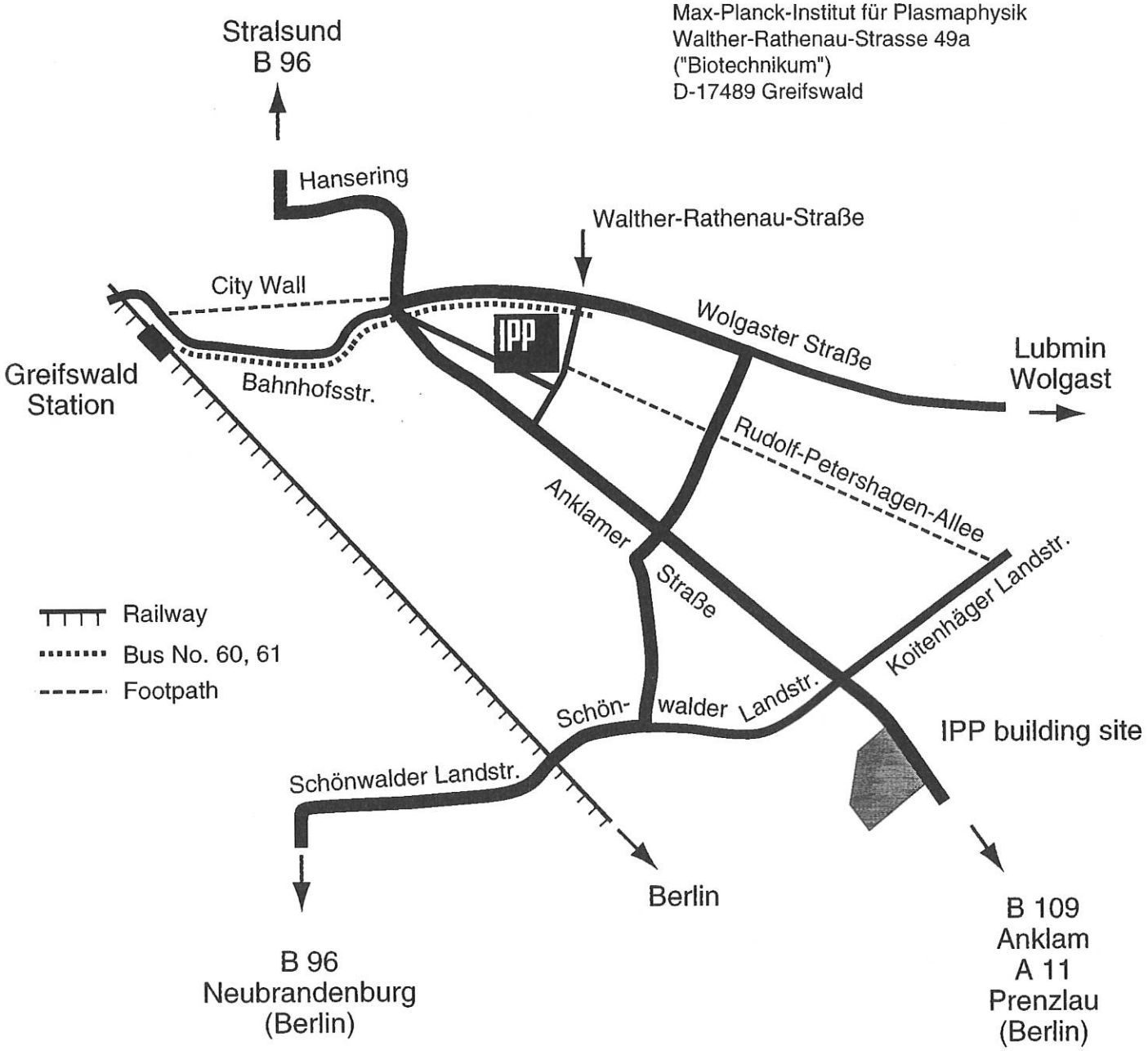

By air:
Via Berlin: from Berlin Tegel Airport by bus No. X9 to Zoologischer Garten, S-Bahn to Lichtenberg Station, by train to Greifswald **or**
Via Hamburg: from the airport to Main Railway Station, by train to Greifswald.

By car:
Via Berlin, Neubrandenburg to Greifswald **or** via Hamburg, Lübeck, Stralsund to Greifswald, in Greifswald follow the "Biotechnikum" signs.

By bus:
From Greifswald Railway Station by bus No. 60 or 61 to the "Am St. Georgsfeld"s stop.

On foot:
From Greifswald Railway Station 30 min by footpath on the City Wall (Stadtwall).

ANNUAL REPORT 1997

Max-Planck-Institut für Plasmaphysik (IPP) • 85748 Garching bei München
Telephone (0 89) 32 99-01 • Telefax (0 89) 32 99-22 00

Printing: Oldenbourg Graphische Betriebe GmbH, Kirchheim

Printed in Germany
ISSN 0179-9347

This work was performed under the terms of the agreement between Max-Planck-Institut für Plasmaphysik and the European Atomic Energy Community to conduct joint research in the field of plasma physics.

Max-Planck-Institut
für Plasmaphysik